DESIGN AND EVALUATION OF CAD-CAM CUSTOM-MADE HIP PROSTHESIS

by

JIA HUA

SUBMITTED FOR THE DEGREE OF DOCTOR
OF PHILOSOPHY IN THE UNIVERSITY OF LONDON

JUNE 1994

DEPT. BIOMEDICAL ENGINEERING, INSTITUTE OF ORTHOPAEDICS
UNIVERSITY COLLEGE LONDON
STANMORE
U.K.

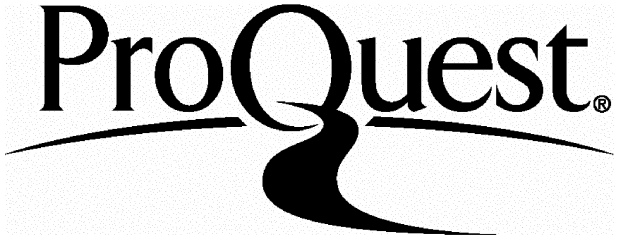

CONTENTS Page

ABSTRACT

The clinical results of uncemented total hip replacement are strongly influenced by the geometry of the stem and its fit within the femoral canal. Particularly where the femoral canals are severely distorted such as in CDH or JRA, the femoral canal can not be accurately fitted by conventional hip stems. The condition of the femur on revision is highly variable, making it difficult to achieve consistently satisfactory constructs in each case. Therefore, there is a strong case for suggesting that custom-designed stems should play an important role in hip reconstruction. For this purpose, a Hip Design Workstation was developed, with the ability to design and manufacture custom femoral intramedullary stems for both primary and revision cases by using the technique of Computer-Aided-Design (CAD) and Computer-Aided-Manufacture (CAM). This system can three dimensionally reconstruct the femoral canal by digitizing A-P and M-L views of the femoral contour from plain radiographic images. In addition, the femoral canal can be reconstructed from CT scans. During reconstructing the femoral canal from plain X-ray films, special software was developed which can correct rotations of radiographs up to 30 degrees in the lateral view and 60 degrees in the frontal view. After the canal was reconstructed, the software then designed the stem for the individual canal with optimal design algorithms, allowing for multiple design options to be specified by the user.

In order to evaluate the custom stems, several comparative studies with standard stems were carried out. The hypotheses for these studies were that custom femoral stems would produce a closer fit in critical regions, would be more stable on stem-bone interface motion, and would produce

closer-to-normal stress distributions. In addition, the advantages of the custom stems would be reflected on the clinical results and radiographic appearances. The stem-canal fit study was conducted by analysing the gaps between stems and canals in four quadrants. Strains on the surface of a femoral bone before and after stem insertion was measured by using a photoelastic coating technique. Stem-bone interface motion under cyclic loading were quantified in four axes by using Linearly Variable Differential Transducers (LVDT). The data from six channels were simultaneously recorded by a linked computer. Radiographic studies including measurement of stem migration and bone density changes were conducted by using a newly developed technique and DEXA scan. In addition, a biological study of tissue osseointegration with titanium stems of different stiffness was carried out on rat femurs.

The results from the studies showed that the custom stems were superior to the standard stems in terms of canal fit, strain distribution and interface motions. For the radiographic follow up, the results showed that 79% of custom stems were stable from zero to six months and 96% from six to twelve months, which was comparable with cemented stems. Bone mineral density changes were found to be less than 10% from zero to six months and from six to twelve months. In the biological study, the results showed that less stiffness of the implant could enhance the osseointegration onto the stems. This provides useful information for hip stem design.

This study demonstrated that custom stems provide a better solution for uncemented total hip replacement. The CAD-CAM technique offers great accuracy and flexibility in designing and manufacturing individual stems. The method does however require additional time and expense

compared with using an off-the-shelf stem. Nevertheless it is fully justified for many cases at this time, while a further reduction in cost will extend the indications to the more standard cases.

ACKNOWLEDGEMENTS

I wish to express my most profound gratitude to my supervisor, Professor Peter S Walker Ph.D, for allowing me the opportunity to study in the Department of Biomedical Engineering, and for his enthusiastic supervision, consistent support and tireless guidance throughout the course of my study. Without his invaluable advice and encouragment, the completion of my thesis would not have been possible.

I am grateful to Professor Geoge Bentley for allowing me to attend surgery in the Professorial Unit during the first year of my study, and for his consistent support and encouragement.

A special note of gratitude is to be extended to Dr. Gordon W Blunn for his support, encouragement, friendship, and for his supervision in animal study as well as meticulously reviewing Chapter nine of the thesis. I would also like to thank Mr. Jay Maswania for his excellent "problem-shooting" advice and I really appreciate his friendship.

My sincere thanks is extended to many other colleagues and friends within the department for their cordial and intellectually stimulating friendship, and with whom I have spent a most enjoyable time during the past and present.

A very special thanks to my wife, Aiqin, for her genuine love, understanding and unfailing commitment, to my parents and my sister for their deep love and consistent support, and to my baby son, Yinglun, for all the happiness he has given me.

This study is funded by Sino-British Friendship Scholarship and thanks are due to the British Council for their excellent arrangement and help throughout the study.

LIST OF FIGURES PAGE

LIST OF TABLES

CHAPTER ONE

INTRODUCTION (I) HISTORY OF TOTAL HIP ARTHROPLASTY

1.1 Evolution of the hip arthroplasty

1.1.1 Historical review

Total hip arthroplasty was started one and half centuries ago. Its revolutionary advance has led the way to the arthroplasty of other joints. Hips are the most important joints in the human body for load bearing and movement. Arthritis and deformity have always been the main causes for the patients seeking a total hip arthroplasty. It was found that as early as half a million years ago, hip osteoarthritis had already tortured the "Java" man, the Ancient Egyptians, and the Romans (Jayson 1971). But little could be done until, in 1822, White in Westminster Hospital of London, excised the upper end of a femur in a nine-year-old boy for sepsis and deformity. In 1826, another surgery was carried out by J R Barton of Lancaster, Pennsylvania, who performed an intertrochanteric osteotomy on a twenty-one years old sailor with severely deformed and ankylosed hip (Barton, 1827). Both operations relieved the pain and obtained a reasonable range of movement. Since then it has started an era of total hip arthroplasty.

Osteotomy arthroplasty was the first step to make an ankylosed hip mobile, although several years later the hip could lose its range of motion again. **Interpositional arthroplasty** followed this in a hope that it would prevent recurrence of ankylosis. Many kinds of interpositional materials had been tried such as wooden blocks (Carnochan, 1940), rubber sheets, celluloid and silver plates. Ollier (1885), Murphy (1905), Lexer (1908) and Payr (1910) placed muscles for interpositioning arthroplasty. Later, pig's bladder, skin and gold foil had also been tried. These interpositioning materials maintained motion at the site of

osteotomy and prevented recurrence of bone growth. However they could not last long enough before the materials were worn off.

Harder materials had therefore been used. Gluck (1891) of Germany constructed an ivory ball and socket joint with nickel plated steel screws and glue for fixation. This probably was the original prototype of total hip replacement. In 1923 Smith-Petersen of Boston used viscaloid material as a cup which was proved to be too fragile as well as producing a marked foreign body reaction. Bakelite and pyrex materials had also been tried but with no success. In 1938, a vitallium mold had been used which remains as today's material for the standard cup. From many years of experiences, it has been understood that the interpositioning material must be hard enough to resist wear, durable to avoid breakage and biologically inert to prevent tissue reaction.

Roughly during the same period, the **reconstructive arthroplasty** was introduced by Whitman (1904) and was followed by other surgeons notably Sir Robert Jones (1921), Brackett (1925), Girdlestone (1928), and Charnley (1953). Reconstructive arthroplasty is still of value particularly as a salvage procedure where other methods have failed. The initial prosthetic replacement of the femoral head was made of ivory (Gluch 1891, Groves 1927) and rubber (Delbet 1919) but with limited success. In 1940, Drs. Austin Moore and Harold Bohlman used the first known metallic femoral prosthesis to replace the upper end of femur. In 1946, the Judet brothers of Paris employed an acrylic prosthesis (methyl methacrylate) for replacing the femoral head, proving that mechanical replacement of hips utilizing plastic material can be tolerated in the human body with minimum tissue reaction. However those acrylic prostheses were eventually broken, worn and loosened, suggesting that

acrylic could not withstand the wear and the prosthesis was not strong enough to absorb the stresses.

In the stem geometry side, it also clearly demonstrated that the straight and short stem was liable to loosen in the canal. Therefore, many types of stems had been designed with different geometries and materials. The short-stems were replaced by the intramedullary long-stems which were more stable. The non-metallic stems had given way to the metallic stems which provided greater durability. During this time, Thompson (1950) and Moore (1952) femoral prostheses were the main representatives which were extensively used for femoral neck fracture and capital ischaemic necrosis. However most of these prostheses eventually failed because they had a "defective load bearing capacity" (Charnley 1982).

The first **total hip arthroplasty** was performed (Wiles 1948) at Middlesex Hospital in London with ball-and-socket stainless steel prosthesis. The femoral component was secured to the neck of the femur by a bolt. The results were unsatisfactory because of mechanical failure, but it paved the way to the development of total hip replacement. Designs were changed in the stem geometry, fixation and materials. Combinations of metal-to-metal and metal-to-plastic contact of ball-socket were also investigated.

In the early 1950's, Austin-Moore developed a prosthesis which had a wedge-shaped, quadrilateral stem with fenestrations in the proximal stem for stem lightness and bone grafts. This design produced the "self-locking" device. About the same time, the Thompson femoral prosthesis was introduced with ideas similar to the Moore's but without fenestrations in the proximal part of the stem. However, the latter stem showed a

higher incidence of sinkage due to calcar resorption, particularly in osteoporotic patients (Anderson et al., 1964). Mckee-Farrar's (1951) initially used stainless-steel for both femoral and acetabular components, later changing to chrome-cobalt. Muller (1957) developed a plastic acetabular cup against chromium-cobalt-molybdenum in the femoral head. In 1958, Charnley introduced the concept of low friction total hip replacement. In the beginning, it was a stainless steel femoral head and a polytetrafluorethylene acetabular cup. Because of the unacceptable wear rates, the high-density polyethylene cup was used, which proved to be a very successful material for the acetabular cup. Since these revolutionary development, clinical results have significantly improved.

1.1.2 Cemented stems

In the early stages, femoral stems were poorly fitted in the canal. Instability and toggling of the prostheses often occurred after weight bearing. Early stem loosening was thus inevitable. In an attempt to tightly fix the femoral component within the canal, Gluck (1890) firstly suggested using bone glue or cement to fasten ivory devices. It was failed because at that time cement was composed of colophony, pumice powder, and plaster of Paris, which was not well tolerated and became walled off in the cavity. Methyl methacrylate, a well-known dental cement, was firstly used in hip replacement by Kiaer and Jansen of Copenhagen. In 1951, Haboush (1951) reported his experiences with self-curing acrylic cement in total hip arthroplasty at the Hospital for Joint Diseases in New York City. However, because at that time the cement was used only for filling, not for creating a secure fixation of the stems and transferring the load, the results were also not satisfactory. In 1957, Wiltse et al introduced self-polymerizing polymethyl methacrylate to orthopaedic surgery. The idea

was soon followed by Charnley (1958), who successfully applied a large volume of methyl methacrylate to cement the femoral and acetabular components. He reported its practical use for increasing stability of the femoral stems, and pointed out that cement had no binding property with the bone, but gave mechanical stability by accurate filling within an irregular cavity.

In general, short term results of cemented stems are excellent due to the initial stability of the stem, but they deteriorate with time. Kavanagh et al (1989) reported a fifteen-year follow up of Charnley prosthesis, which showed a probability of 3% loosening at one year, 13% at five years, 19% at ten years and 32% at fifteen years after the operation. Schurman et al (1989) investigated the risk factors associated with mechanical loosening of cemented stems by using survivorship analysis on the patients with two to twelve years follow up. They found that the failure rate was approximately 1.7% per year in the first several years, and 20% at twelve years. Among those risk factors, weight and age were the most important determinants. The heavier and younger patients were at greater risk of stem loosening. Chandler et al (1981) reported a 53% incidence of actual or potential radiographic loosening in patients less than thirty years old after follow-up for five years or more. Dorr et al (1983) showed similar results of 45% with the cemented stem in patients less than forty-five years old. On the other hand, Collis (1991) demonstrated a better performance on his younger patients with cemented total hip replacement. However, the activities of all his patients were strictly limited.

The high rate loosening of the cemented stems after long-term follow-up has been disappointing. This could be associated with the cement itself

and cementing technique. Therefore, for a long periods, studies have been focused on the nature of acrylic cement and the cementing technique.

The original work of investigating the potential value of acrylic cement in orthopaedic surgery was carried out by Wiltse (1957). The experiments on rabbit and monkey suggested that methyl methacrylate cement caused little tissue reaction, and its strength was adequate to withstand most compression stresses in the body but not transverse stress without reinforcement. However, the study of Heman et al (1989) showed that polymethyl methacrylate detritus was capable of inducing a foreign-body reaction and causing resorption of bone at sites of stem loosening. A recent histopathological study showed that the cement fragmentation might be the major cause for late aseptic stem loosening (Williams et al 1992). It was also found that local defect in the cement mantle surrounding the stem could lead to localised bone lysis (Anthony et al 1990). Jasty et al (1991) defined an initial sign of failure was debonding at the cement-implant interface which could further develop to a fracture in the cement mantle. In general, Jones and Hungerford (1991) attributed the unsatisfactory long-term results of the cemented stem to the inherent biologic and biomechanical properties of methyl methacrylate itself, and called it a "cement disearse".

Thermotoxicity of the cement to the bone was investigated by Euler et al (1989) in a retrospective basis. They found that the majority of total hip replacements which effected on the systemic and the pulmonary circulation were associated with the placement of the cement. The fall in blood pressure was greater after femoral shaft implantation than acetabular replacement (Amaranath et al 1975). During polymerization,

the cement can reach to the temperatures of 63°C, which can lead to a permanent damage of the endosteum and the adjacent bone tissue after only 10 second (Bauer 1988).

Laboratory studies on cadaveric femurs and clinical retrieved specimens showed that the cemented stem could obtain better initial stabilities (Maloney 1989, Schneider 1989 and Phillips 1990), but produce remarkable stress shielding. This stress and strain alteration can exaggerate the process of bone remodelling and bone resorption (Maloney 1989). Bone remodelling may eventually lead to stem loosening and failure, for which revision surgery are usually necessary.

Some poor results of the cemented stem could also be associated with the cementing technique. Therefore, the improvements on cementing techniques have been carried out and this led to the 'second generation cementing technique". Cleaning cancellous bed with a brush or water-lavage device prior to input bone cement will improve the strength of bone-cement interface. Using of medullary plug and the cement gun will increase intrusion pressure and provide a more uniform cement mantle that extends beyond the prosthetic tip with fewer lamination and voids (Harris et al, 1982). Further pressurization of bone cement in the proximal femur by using a femoral cement compacter were reported by Oh et al (1983), which the pressure could be increased by 71%. In addition, there were several reports on the techniques of reducing porosity of cement and improving fatigue life by using centrifugation or vacuum-mixing during preparation (Alkire et al 1987, Burke et al 1984, Davies et al 1987, Jasty et al 1985 and Wixson et al 1987). After using of these cementing technique, long-term clinical and radiographic results have been improved both on primary cemented THR (Mulroy Jr and Harris, 1990,

Barrack et al 1992) and revision cemented THR (Pierson and Harris, 1994, Izquierdo and Northmore-Ball, 1994). However, the clinical results were not always promising. Bosco et al (1993) reported a less satisfactory result of cemented stems with an average of 6.7 years follow-up by using the same improved cementing technique.

Although radiographic loosening, even with complete radiolucent line round interface, does not necessarily require revision, some other radiographic failures for the cemented stems are more serious, which have been classified and analysed (Gruen 1979). The acrylic cement embedded stem pistoning within the medullary canal was the most common failure mode (mode 1b). Stem fracture caused by stem medial migration due to loss of proximal support, while the distal end still rigidly fixed in acrylic cement was the most serious failure mode (mode 4).

Furthermore, once the cemented stem become failure, revision surgery is the most difficult and destructive procedure. The cement particles can destroy the surrounding bone and create large bony defects that may require extensive bone grafting. The removal of cement from femoral canal is a difficult task which may cause such complications as shaft fractures and perforations. Of the most importance is that the results of the revision hip arthroplasty using cement are worse than that of the primary, especially in younger patients (Callaghan et al 1985, Kavanagh et al 1985, Stromberg et al 1988). A failure rates of 29% after three years follow-up had been reported (Carlsson 1979, Hunter 1979).

There is no question that using self-polymerizing polymethyl methacrylate cement has enabled total hip replacement to be practiced on the wide scale. However, the disadvantages for using bone cement

are the reduction of strains transmission and the inability to ensure long-term stabilities of femoral stems. This problem has led to a reawakening of interest in cementless femoral prosthesis. At the present time, general view is that cemented total hip replacement can still remain the choice for the older and less active patients, whereas cementless stems should be considered in younger, heavier and active patients.

1.1.3 Cementless stems

The main difference of the cementless stem with the cemented stem is that the cementless stem requires more accurate and precise fit with the femoral canal. It has been demonstrated that bone ingrowth and attachment strength have significantly increased when bone-stem gap is less than 1 mm (Armstrong et al 1993). If the gap exceeds 1 mm, fibrous tissue interposition may occur, which then prevents bone ingrowth (Bauer et al 1991). It has also been observed that bone ingrowth occurred in a variable percentage of the stem surface, which depend on stem-canal contact and stem surface treatment. If the bone ingrowth does occur, it appears to significantly improve stem fixation.

In the early times, most of the cementless stems did not anatomically match with the femoral canal. Stem fit was poor and a large gap was left. Initial mechanical stability of the stem was not achieved, thus affecting later biological fixation. In addition, non-anatomical shaped stems often produced three-point loading, which could generate local stress concentration in the femur and result in bone hypertrophy (Zhou and Walker 1990). It is believed that the shape of the cementless stem is critical in order to obtain stem fit, close to normal strain distribution and initial stability.

In an attempt to achieve permanent stability of the stem, osseointegration between stem and bone is regarded as a prequisite. Stem stability is achieved in two stages: mechanical stability and biological stability. Mechanical stability depends on stem geometry and stem fit with the canal, while biological stability depends on amount of bone upgrowth onto the stem. Later biological fixation relies on initial mechanical stability. However, early attempts in biological fixation were not entirely successful. This was partially because the mismatch between stem and bone in dimension and geometry, which led to stem unstable (Letournel 1986). A study conducted by Cameron et al (1973) showed that bone could only ingrowth into the pore of porous Vitallium when stem-bone interface motion was less than 150 μm. Therefore, it is clear that initial stability of cementless stem is vital important for long-term fixation of stem. In order to achieve initial stability, design of stem which can optimally fit with the canal become primary objective.

A number of studies have emphasized the substantial variability in the anatomy of the proximal femur (Dai et al 1985, Harper and Carson 1987). In addition, there is poor correlation between the different dimensions of the proximal femur. For this reason, off-the-shelf stems, even an increase in the number of stem sizes, can not provide optimal fit for each case, especially for those very deformed canal geometries. In order to design a cementless stem which can constantly produce optimal fit with each canal, custom design becomes neccesary.

1.1.4 Custom stems

The technique of computer-aid-design (CAD) and computer-aid-manufacture (CAM) has made it possible to design and manufacture a custom femoral stem which can produce line-to-line fit with individual femur. Since 1980's, individually designed CAD-CAM stems for cementless application had been receiving increasingly interest. A number of stem design rationales and stem evaluation criteria were proposed by many investigators. Among these rationales, the stem fit in proximal-medial and proximal-anterior regions have been regarded as priority. Custom design and manufacture offer more accuracy and optimal fit for individual cases. Therefore, it was proposed that custom stems could be superior to conventional stems with respect to stem fit, strain distributions and stem stability.

In order to design a custom stem, canal geometry has to be accurately reconstructed. CT scans can produce three dimensional images with high resolution and a precise definition of cortical boundary (Bargar 1989, Stulberg 1989), and this method has therefore been frequently used to reconstruct femoral canals. However, an error of 1-3 mm of CT scans has been reported for three-dimensional reconstructed models (Vannier 1985, Woolson 1986). In addition, the CT scan has disadvantages of higher radiation exposure, higher cost and limited facilities available in some hospitals. Therefore, in order to find an additional method to reconstruct femoral canals and design custom stems, a research project was conducted to develop a system which could use routine radiography.

1.2 Aim of the study

The aim of the study was to develop a Hip Design Workstation which could design and manufacture primary and revision custom femoral stems. The software in the Hip Design Workstation included three parts. Part 1 — Reconstruction of femoral canals, which included the technique of correction of X-ray rotation; Part 2 — Design of custom stems, which included many design options such as CDH stem design; Part 3 — Manufacture of custom stems, which included many manufacturing options such as proximal grooves and distal cutting flutes.

Another area of the study was to evaluate the reconstructed canals and the custom stems. Laboratory evaluation included comparison of the reconstructed canal with the actual canal, stem fit with the canal, bone surface strain distribution and stem-bone relative motion. Clinical radiographic evaluation included measurement of stem migration by using computer digitising method, and analysis of bone mineral density changes by using DEXA scanning. In addition, a biological study of stem stiffness was conducted in the rat femur. These studies should provide valuable information to the stem design and to the understanding of total hip replacement.

The particular purposes of the Hip Design Workstation are to design stems for the extremely deformed femoral canals, such as CDH, Perthes' disease, fracture and osteotomy, and for revision cases. The custom stems should be accurate and versatile which can be extensively applied to the younger, heavier and active patients, with superior results to standard hip designs.

CHAPTER TWO

INTRODUCTION (II) ANATOMY, PATHOLOGY AND RADIOLOGY OF THE HIP JOINT

2.1. Osteology of the hip and femur

The hip is a synovial joint of ball-socket configuration, formed by a femoral head cupped into an acetabulum, reinforced by strong ligaments, muscles, and tendons. It plays a major role in the static and dynamic physiology of the locomotor system, which include supporting body weight and retaining range of motion. Active movements of the hip are flexion, extension, adduction, abduction, internal and external rotations.

The femoral bone is the longest and strongest bone in the human skeletal system. It is articulated with the pelvic bone to form the hip joint and the tibia to form the knee joint where it carries the patella in front. The proximal end of the femur includes the head, neck, lesser and greater trochanters. Two-thirds of the femoral head is a sphere, its diameter averaging 46 mm with a range of 35-58 mm (Averill 1980, Clark 1987 and Noble 1988). The neck-shaft angle varies from 106 to 155 degrees with an average of 125 degree. Most of the standard femoral prostheses have a neck-shaft angle from 125 to 135 degrees, which correlates with the horizontal (offset) and vertical (height) location of the femoral head. As the neck-shaft angle increases into valgus, the height of the femoral head increases while the offset decreases. These relationships change conversely as the neck-shaft angle decreases into varus. The anteversion of the femoral neck is determined by the angle between the plane of the femoral condyles and the axis of the femoral neck, which decreases from childhood to adult, with an average of 12-15 degrees of anteversion ranging from 33 degrees of anteversion to 16 degrees of retroversion (Kingsley 1948, Fabry 1973 and Reickeras 1983). Total hip replacement has to take neck torsion into account in order to retain the original acetabular position and restore normal gait. The width of the

neck is three-fourths of the equatorial diameter of the head, which allows the hip having a wide range of motion before the neck impinges on the pliable labrum of the acetabulum (Last 1959). The greater trochanter is an important landmark on the femur which provides an extensive area for musculotendinous insertion. The lower trochanteric ridge is the origin of the glutei medius and minimus which pass from the dorsum ilii. The functions of these two muscles are to abduct the thigh and balance the abductors and the adductors, which maintains the pelvis on a relatively level plane during locomotion. The lesser trochanter lies posteromedially and provides for insertion of the iliopsoas tendon.

Only a few of the dimensions of the proximal femoral metaphysis are closely correlated with each other. The canal width in the vicinity of the lesser trochanter is correlated with some other proximal femoral dimensions (Dai 1985, Noble 1988 and Smith 1964). For example, in the A-P view, the canal width measured 20 mm distal to the lesser trochanter was found to be correlated with the canal size (Dai 1985, Noble 1988). The proximal femoral endosteal geometry is generally grouped into three types by Noble et al (1988), based on the canal flare index. The canal flare index is a ratio between the intracortical width 20 mm proximal to the lesser trochanter and the width of the canal isthmus. The "stovepipe" canal shape is described when the canal flare index is less than 3.0, while the "champagne-fluted" canal shape is defined when the value is greater than 4.7. In between a "normal" canal shape is indicated. A general trend was that bones with small canals were likely to have a champagne-fluted shape, and bones with large canals were likely to have a stovepipe shape. It was also found that the canal flare index was age related. Most of younger femurs (< 55 years) showed an index greater than 4.0, whereas most of older femurs (> 80 years) were less

than 4.0. This is because of the expansion of the endosteal at the isthmus with an average of 1.3 mm per decade (Noble 1984). Endosteal expansion occurs at a greater rate than periosteal apposition resulting in cortical thinning, which was most apparent in bones older than 60 years (Noble 1984, Martin et al 1980, Ruff and Hayes 1988, and Thompson 1980).

Extensive studies on the dimensions of the proximal femur (Noble et al 1988, Rubin et al 1992) showed that wide variations occurred in the sizes of femoral bones. Such variations can not be covered by number of sizes of standard stems, as most of the cementless stems only have 7-8 sizes. For example PCA stem system, the variation between one size and the next is from 0.8 to 2.2 mm. This indicates that some standard stems may not provide a good fit with the canal.

Standard stems usually have constant geometry ratios between the proximal and the distal parts of the stem. However, the ratios for the femoral canal were not constant. For instance, the ratio between the canal width 20 mm above lesser trochanter and the canal isthmus (canal flare index) was in the range of 2.37-5.35 (Rubin et al 1992). If the geometrical ratios of a stem does not match with that of canals, the stem will not fit with the canal either in the proximal or distal regions. Huiskes (1980) pointed out that the stability of the femoral stem depends on a balance of proximal and distal load transfer from the stem to the femur. This indicates that the stem which can only fit in the proximal or the distal region may not be adequate.

The proximal femur normally has a metaphyseal posterior curve and a diaphyseal anterior bow, with a wide variation. The posterior curve has a

range from 0 to 24 degrees, measured by the angle of intersection of the anterior and posterior axes. The anterior bow has a radius from 68.9 to 188.5 mm (Dorr 1986, Noble 1984 and Harper 1987). These two curvatures are sometimes responsible for the difficulty of inserting hip stems, especially for a long straight stem. In the diaphyseal region the canal shape is usually oval with a greater diameter anterior-posterior than medial-lateral. A stem with an oval shape in the distal region may have some advantages over the round shape to enhance rotational stability. However, the tooling for the oval shaped stem is difficult, since the canal can not be reamed into a oval shape.

2.2 Pathology of the hip

It is very difficult to design and assess femoral prostheses without understanding the pathology of hips. A wide variety of primary and secondary bone lesions and deformities arise in the hip joints. Some of the pathologies are best treated by conservative or alternative methods, but some have to be treated by total hip arthroplasty. Some canals which have less geometrical deformity may only require conventional stems, whereas in others with extensive deformities, custom stems may be necessary. In general, the following pathologies often require total hip replacements: osteoarthritis, juvenile rheumatoid arthritis and congenital dislocation of the hip.

2.2.1 Osteoarthritis

Osteoarthritis is the commonest variety of arthritis. It is a degenerative wear-and-tear process occurring in joints that are impaired secondary to previous disease, injury, vascular insufficiency and congenital defect.

The primary osteoarthritis of the hip was found to be extraordinarily rare (Harris 1986).

The hip joint is the commonest site for osteoarthritis. The articular cartilage is slowly worn away until eventually the underlying bone is exposed. This subchondral bone becomes hard and glossy, and the bone at the margins of the joint hypertrophies to form a rim of projecting spurs known as osteophytes. Meanwhile there is usually slight thickening in the capsule or synovial membrane. The onset of osteoarthritis is very gradual and most patients with osteoarthritis are past middle age. Pain, restricted movements and deformity of the hip joints are the common features for the osteoarthritis. The characteristics of the radiograph are the diminution of the cartilage space, sclerosis of the subchondral bone and osteophyte formation. There are many ways to treat osteoarthritis which depend on number of factors. However, if total hip arthroplasty is required, it gives excellent results in most of cases, with relief of pain and restoration of movement.

2.2.2 Juvenile rheumatoid arthritis

Rheumatoid arthritis is a chronic non-bacterial inflammation of joints. The precise cause is possibly due to a disorder of the auto-immune system. It usually affects several small joints at the same time, hands and feet are the commonest site. However, if the hip joints are affected, the consequence is serious. In the initial stage of the pathological process, the synovial membrane is thickened by chronic inflammation. Later the articular cartilage is gradually softened and eroded. Finally the subchondral bone may also be eroded, leaving a number of joints that are permanently damaged.

The patients are usually much younger than the osteoarthritis group, and more often girls than boys. The onset is gradual, associated with mild constitutional symptoms. The affected joints become increasingly painful and swollen. The movements of the joints are limited. The characteristics of the radiograph are diffuse rarefaction in the area of the joint, destruction of articular cartilage which leads to narrowing of the joint space, and the protrusion of the medial wall of the acetabulum. Constitutional treatment is always necessary and essential. If operative treatment is justified, total hip arthroplasty is often the method of choice.

2.2.3 Congenital dislocation of the hip

Congenital dislocation of the hip usually occurs either before or during birth or shortly afterwards. Its causes are probably a combination of genetic, hormone and breech malposition. But the relative significance of these various factors is not fully understood. Girls are affected 6-8 times more than boys, and in one third of all cases both hips are affected.

The femoral head is usually small and non-spherical, and often is dislocated or subluxed upwards and laterally from the original acetabulum. The original acetabulum is porotic and poorly developed. It is shallow and steep with a narrow opening and filled with fat and fibrous tissue. In the case of persistent dislocation, the femoral head can migrate a variable distance proximally and posteriorly to form and articulate with a false acetabulum, which is shallow, roofless with a thin medial wall and situated higher up on the thin dorsum of the ilium. The femoral neck is short, narrow, and can be anteverted as much as 90 degrees together with the proximal metaphysis. The greater trochanter is small and

attached far posteriorly along with the femoral neck anteversion. The lesser trochanter lies more anteriorly than normal.

In addition, the configuration of the intramedullary cavity is also distorted. The medullary cavity is usually narrow and straight, but the cortex of the femur usually is strong and thick. The femoral canal is wider in the anteroposterior dimension than mediolateral. Hypertrophy of the elongated capsule, and contracture and shortening of the muscles that cross the hip joint, especially the adductor and the iliopsoas, present another problem to regain the true length of the limb equal to the opposite normal leg. The sciatic and femoral nerves can also be contracted as a result of persistent dislocation. The neurovascular structures of the limb can be a hazard due to increase limb length and resulting in paralysis. If the patient is adult, the preliminary traction has little use in terms of leg length, but surgical soft tissue releases around the hip may be helpful.

In the late stage of progressive congenital dislocation, total hip replacement is often a treatment of choice. For the location of the acetabular cup, the greatest available amount of bone stock is at or near the level of the true acetabulum. If the seat of the acetabular component is above the level of the true acetabulum, the shortness of bone stock is a major problem. Therefore, the prosthesis should be placed at or near the level of the true acetabulum. The femoral component is usually small, with a straighter stem.

Fixed contractures of long standing must be overcome, particularly in flexor and abductor muscles. If the new cup is placed at the site of the true acetabulum, reduction of the hip may be impossible unless the

shortened abductors and flexors are released. There are two ways of releasing the muscles. Removal of the greater trochanter has commonly been used, which is reattached after reduction of the hip joint component with the leg in the position of 20 degrees abduction. But some surgeons consider that if the greater trochanter is removed it may not be possible to reattach successfully and thus the power of abduction will be lost (Fredin and Unander-Scharin 1980). In order to allow replacement of the hip at the true acetabular level, it may be necessary to shorten the femur by excising bone from its upper end, so that the femoral component locates in the shaft of the femur and the leg is short. The another new method which was described by Harley (Harley 1987) was to release the shortened abductors and flexors proximally by excising the upper third of the ilium and resuturing the released muscles in the cut edge of the ilium without tension. The advantages of this technique are maintenance of abductor power and restoration of normal leg length.

Total hip replacement provides an alternative method of treatment for CDH patients. However, the anatomical features of the femur in CDH patients, particularly the excessive anteversion of the femoral neck, present major problems. Originally, the conventional technique was to insert the femoral prosthesis in neutral version, overreaming the posterior margin of the neck to create a new opening, leaving a large space in the anterior prominence of the neck for cementing (Lazansky 1974). But this technique may not be applicable for cementless stem because the stem may not be stable. For this application, custom stems provide a better solution. The algorithm is that the proximal stem twists to fit with the twisted proximal metaphysis, while the stem neck is retroverted to match with the normal orientation of the acetabular cup. For cases with an extremely anteverted femoral neck, rotational osteotomy at the level of

the lesser trochanter was performed by Holtgrewe and Hungerford (1989), in which the anteverted neck was corrected by derotation of the proximal fragment.

2.3. Radiology of the femur

2.3.1 Plain radiograph

Until the 1970's, plain X-ray radiography was the only method to show bone and soft tissues. Even now the plain radiograph is still mostly widely used in orthopaedics for diagnosis and treatment follow-up. In total hip replacement, the plain radiograph has the particular values, for preoperatively selecting femoral and acetabular components and layout of surgical procedures, for postoperative follow-up and assessing the results.

The most common method for examining the hip joint includes an anteroposterior radiograph and a cross-table lateral film. A true anteroposterior view can be obtained by fifteen degrees internal rotation of the leg, maintained with a sandbag across the feet, thus the femoral head and neck are parallel to the cassette. However, sometimes this posture may be impossible to achieve due to fixed hip deformity and contractures. In this case, the X-ray beam can be adjusted to give the same result. The lateral radiograph of the hip can be performed in the cross-table method, accomplished with the patient in the supine position and the contralateral limb elevated above the patient. The lower extremity is internally rotated 10 to 15 degrees. The centre of the beam should be on the lesser trochanter. In another method called the Lauenstein technique, the patient is turned toward the affected side to a

nearly lateral position. The patient flexes the knee and draws up the thigh just short of ninety degrees. The opposite thigh is then extended. The beam is directed perpendicularly to the femur and table. These lateral films also give additional views of the acetabulum.

The femoral shaft appears smooth and cylindrical with a thick cortex. In the antero-posterior view the femoral shaft is usually straight. The narrowest part at the middle of the shaft is called the isthmus, where the cortex is thickest. In the lateral view the shaft shows a gentle convexity forwards, and the posterior contour may be slightly irregular. The diameter of the medullary cavity is usually wider in the lateral view than in the A-P view. The lesser trochanter presents a smooth round prominence, and normally points toward medial and posterior.

It is sometimes difficult to assess the rotation of a femur on a front view of a plain radiograph. However certain bony landmarks can be used to generally assess the femoral rotation. A prominent lesser trochanter with a foreshortened neck, the overlap of the greater trochanter and capital shadows indicate an externally rotated hip joint. The internal rotation of a hip joint can be indicated by complete overlap of the lesser trochanter with the femoral shaft. For a more accurate quantitative measurement of the neck anteversion, an additional lateral view of the radiograph can be useful by calculating the anteversion angle from the distances between the head centre and canal centre line in A-P and M-L views. However, this calculated anteversion angle does not account for the knee or ankle position. A CT scan can provide more precise measurement of the anteversion angle by overlapping the proximal femoral section with the femoral condylar section. In order to use plain X-ray for designing and

templating femoral stems, magnification scales are necessary in both A-P and lateral views, so that sizing errors can be minimized.

2.3.2 X-ray computed tomograph (CT)

The computer tomograph was introduced in the early 1970s (Hounsfield 1973). The basic principle of computed tomography is the use of a finely collimated beam of X-ray which is rotated around the patients while the radiation transmitted through the patient is recorded by sensitive scintillation detectors. This technique allows tomographic section to be obtained without overlap of different anatomical structures, with an efficient use of radiation dose and a high contrast sensitivity.

Computed tomograph was initially applied to the clinical investigation of intracranial pathology. This revolutionally development made diagnosis more accurate and precise. It soon became evident that CT had wider applications in other clinical fields. Scanners for the whole body came later with larger gantries. The advantage of CT in the investigation of skeletal and soft tissue disorders is the ability to clearly demonstrate areas of complex anatomy. Its particular value in total hip replacement is that it provides images of three-dimensional geometry of femoral and pelvic bones. The CT image can also more precisely define the inner-cortical boundary.

Standard CT provides a series of cross-sectional images of the femur. Each image is composed of a large number of picture (pixel) or volume (voxel) elements which can be ascribed a number on the Hounsfield scale according to the X-ray attenuation characteristics of the content of the voxel. On completion of the CT examination, a large block of digital

data is obtained, which is made up of multiple transverse sections. The CT data can be read into a computer with proper software. By using the technique of three-dimensional imaging, the femoral canal can then be three-dimensionally reconstructed from a series of contiguous transverse sections (Gillespie et al 1987c) and be redisplayed on the computer screen in any desired plane, or even as a 3-D a model of the femoral canal or pelvis.

In orthopaedic practice, CT has become an established and important investigation in the diagnosis and management of a range of musculoskeletal disorders. In total hip replacement, CT has played an important role in reconstructing the femoral canal for implant design, particularly for difficult cases, such as CDH, failed osteotomy and excessive bone remodelling.

CHAPTER THREE

INTRODUCTION (III) BIOMECHANICS OF THE HIP JOINT

Biomechanics is a basic science which applies engineering principles to the understanding of orthopaedic problems. In particular, biomechanics deals with motions and forces of the musculoskeletal system and the interrelationships between them. Stabilization of the hip joint is supplied by the balance of the body weight with the ligaments, joint capsule and muscles. Analysis of hip joint forces in a dynamic situation presents a problem due to the surrounding muscles acting as individual segments. The direction and magnitude of a single muscle force and its role in the hip motion is also difficult to determine. However, many orthopaedic problems can be simplified by a quasi-static or simple-static approach. Pauwels of Germany was the first to actually study the magnitude and direction of the force acting on the hip (Pauwels 1935, 1965). He pointed out that the centre of gravity lies eccentrically in relation to the longitudinal axes of the bones and this may provoke heavy bending moments. His work has led the way to a fuller investigation of the biomechanical environment of normal and reconstructed hips.

3.1. Basic concepts of biomechanics

Basically, joints have two functions, rotation and force transmission, which are acted by muscles. A force can be simply defined as a push (compressive) or a pull (tensile), and its nature has been summed up by Newton's laws. When a force applied to a fixed object, it will deform the object and will induce stresses in the material. If the object is free to move, it will accelerate in the direction of the force. A shear force tends to make one part of an object slide over an immediately adjacent part. A bone is subjected to a variety of forces in separated or in combined form. The intensity of the turning action about an axis between body segments is called the **moment** about the axis. The moment corresponds to the

product of the resultant force and the offset of the line of action of the resultant force. In order to produce linear acceleration of a body, an applied force is necessary where the force is equal to the product of mass and acceleration. To produce angular acceleration, a moment is required where the moment is equal to the product of a property of the body mass and the angular acceleration. **Stress** is the intermolecular resistance within an object to the action of an outside force which is applied to it, and is basically defined as the force per unit area on which it acts. But, in general, the stress varies across each cross section, and its general definition is the ratio of the infinitesimal force to the elementary area on which it acts. Stress can not be seen or measured directly, its magnitude can only be computed with an assumption that the object is composed of a homogeneous and isotropic material. This is not true for a bone structure, but with a modification of the mathematical formulas the results can be as close as possible. **Strain** can be measured, which is a change in the linear dimensions (compressive, tensile) or angle (shearing) of an object as the result of the application of a force.

The mechanical properties of materials describe their elasticity, their strength in tension and compression, and their resistance to wear. Isotropic materials are the simplest materials which have the same mechanical properties in all directions and require only two constants: Poisson's ratio and Modulus of Elasticity. Materials requiring more than two constants, and that are not completely symmetrical, are known as anisotropic materials. Cast metals, many polymers and simple biologic materials as costal cartilage are isotropic materials. Cancellous and cortical bone are anisotropic materials. For isotropic materials, a shear stress produces only a shear strain and does not change the volume of the material. Similarly, hydrostatic pressure produces a change in

volume but not in shape. **Friction** is defined as two loaded surfaces which are in relative motion and create resistance to each other. The friction forces are due to molecular adhesive, or plowing interactions at the localized contact points. **Wear** is defined as the removal of material from one or both surfaces. **Modulus of elasticity** represents a measure of the stiffness of the material under tension or compression stress, which can be calculated by the ratio of a stress to strain. A higher value of modulus of elasticity indicates a stiffer material. Modulus of rigidity represents a measure of the stiffness of a material under shear stress. **Viscoelasticity** is another property of a material, which is a combination of elastic and viscous. The characteristic of viscoelastic material is the time dependent stress relaxation and creep compliance. Soft tissue such as ligament, tendon and articular cartilage show high levels of viscoelastic behaviours. Wet bone or children's bone are less stiff and demonstrate more viscoelastic characteristics, and therefore are less easily broken under impact force. **Strain stiffening** is an increase in stiffness of the material with strain due to a reordering of the material structure. Ligament and tendon are strain stiffening material.

3.2. The contact force in the hip joint

The forces applied in the hip joints are the sum of body weight and muscle forces, expressed as a resultant force (R). The magnitude and distribution of the compressive stresses depend on three factors: 1) the magnitude of R which is affected by the body weight and balance of the muscle forces, 2) the area of the weight bearing surface which is basically determined by the size of the femoral head, 3) the orientation of R. The weight bearing areas of the contact surfaces in the hip joint were

found to range from 22.19 to 33.68 cm^2 with an average of 26.77 cm^2 under load, measured by Greenwald and Haynes (1972).

During the "single-legged stance" of gait, the centre of gravity moves towards the opposite side. The moment of the abductor (MA) balances the moment of partial body weight (MW) (full body weight excluding the swinging leg). The resultant force R intersects at the centre of the femoral head and diverges distally, divided into compressive, tensile, and shear forces (Fig.3.1). Because of the offset of the femoral head related to the long axis of the femur, it creates a bending moment which is function of the offset of the femoral head and the loading force. Since the force R acts to compress as well as to bend the femoral neck, the maximum compressive stresses on the medial side are always greater than the tensile stresses on the lateral side. The magnitude of the shearing component S depends on the inclination of the force R to the axis of the femoral neck. The torsion about the long axis of the femur increases in stair climbing and rising from a low chair, and is also affected by the anteversion of the femoral neck.

It has been observed that the force acting on the hip joint is greater than body weight due to the muscle forces surrounding the hip. However, because of the complexity and integrity of the hip joint, in the past, it was difficult to measure in vivo the forces transmitted by the hip joint and associated periarticular structures. Therefore a force plate has traditionally been used to mathematically determine the intersegmental force and moment resultants at the hip joint by modelling the body or parts as a rigid system. Because of the large number of load-carrying elements (muscles, ligaments) that act across the joint, it is unlikely to calculate the joint contact forces accurately and realistically. With the

development of advanced telemetry technique, it has been possible to measure in vivo the contact forces of the hip joint by using instrumented prostheses (Rydell 1965, English and Kilvington 1979, Davy et al 1988, Bergmann et al 1993). However, the hip forces which were measured directly in vivo were usually in the situation of post-operation, where the muscles surrounding the joint may have been weakened. Consequently the forces which were measured across the femoral head have not entirely agreed with the forces which were calculated.

Generally the predicted force by using analytical models is higher than that experimentally measured. These differences may be explained in part by the fact that mone of the experiments used subjects who had a normal pattern of gait. Paul (1965, 1976) predicted that the peak contact force of the hip joint is in the range of 3.5 to 6 times body weight. This was close to that calculated by Crowninshield (1978), whose result ranged from 3.3 to 5 times body weight. These results were also agreed by Hardt (1978), which were 5.7 times body weight. In 1965, Rydell used a strain gauged Austin Moore prostheses to directly measure the forces across the hip joint. The results showed three times body weight. Similar results were obtained by English and Kilvington (1979) with a telemeterized hip prosthesis. Davy et al (1988) recently used a telemeterized total hip prosthesis for a patient. They found that the peak resultant force during single-limb stance was 2.1 times body weight with the direction of force at 32 degrees respect to the axis of the neck of the prosthesis and 15 degrees towards posterior from the midplane of the prosthesis in the sagittal view. For ascending stairs, the peak force increased to 2.6 times body weight, and the orientation of the force changed to 70 degrees posteriorly. Bergmann et al (1992) used instrumented prostheses in two patients to measure the three-

dimensional hip forces acting on the head, and to calculate the torsional moments around the stem axis. The results varied between the two patients. Overall, the torsional moments for up-stairs were 50 % higher than that for the level walking, but there were no significant differences between down-stairs and level walking. The force also depended upon two other factors: time after operation and speed of walking. Bergmann et al (1993) measured two patients using a telemetrised total hip prostheses. The results showed that the loads stayed nearly constant for the first several months postoperatively, followed by an increase for another several months, then a succeeding decrease and remained constant. The force also had a linear relationship with the walking speed, the faster speed producing higher forces (English and Kilvington 1979, Bergmann et al 1993). However, Kotzar et al (1991) pointed out that in the range of walking speeds that are normal for a given individual, the peak joint contact forces are not strongly affected. Only when the walking speed exceeds the normal range does a pronounced speed effect become apparent.

3.3 Mechanical properties of implant and femoral bone

In general, the mechanical properties of prosthetic materials are readily defined. However for the mechanical properties of bone tissues, many investigators have reported different results. This is primarily because bone tissue is a heterogeneous, anisotropic material, and the experimental results depend on the location, shape and size of the specimen. Also, the mechanical properties of human bone tissue vary as a function of storage method, testing conditions, specimen orientation and its porosity, density, and ash content.

The Young's modulus of elasticity for bone cement is 3 GPa, for titanium alloy is 105 GPa and for cobalt chrome alloy is 210 GPa. Titanium alloy is a less stiff material which is suitable for used as femoral stem to transfer more bending force onto the bone. But on the other hand, titanium alloy is softer which is not suitable for the bearing surface. Cobalt chrome alloy is different to titanium alloy, which is stiffer and harder, and is suitable for used as the bearing surface. In order to obtain the advantages of these two material, a combination of a titanium femoral stem with a modular cobalt chrome head is widely used.

The elastic modulus for cortical bone varies according to the age, site, wet or dry status of the bone, and type of the force applied to the bone. It was found by Keller et al (1990) that the Young's modulus of elasticity was 13.5 Gpa for the proximal femur and 11.3 GPa for the distal femur. Knets et al (1980, 1987) observed that the elastic modulus of bone reached its peak at age of twenty to thirty, about 22 GPa, and then gradually reduced with age. Elastic modulus of bone is usually higher in tension (14.1 - 17.3 GPa) than in compression (8.69 - 10.46 GPa). Reilly and Burstein (1975) report 17.1 GPa with a standard deviation of 3.1 GPa for both tension and compression.

Trabecular cancellous bone is more sensitive to aging and certain pathological processes. It tends to undergo specific morphological and biomechanical changes, including alterations in density, changes in trabecular structures and contiguity, and variations in both strength and modulus. The reported compressive properties of trabecular bone were summarized by Goldstein (1987), which ranged from modulus values of 1.1 to 2942 MPa and ultimate strengths of 0.12 through 116 MPa. The tremendous variation in reported values is in part due to differences in

mechanical test methods, environmental conditions and possibly storage procedures. Recent work by Linde and Hvid (1987) suggests that preconditioning factors may play a major role in measurement consistency. Carter and Hayes (1977) reported that the strength of trabecular bone was proportional to the strain rate raised to the 0.06 power. A significant proportion of the variation, however, has been attributed to functional differences among the anatomic locations selected for study.

While there have been numerous studies on the compressive properties of trabecular bone, its tensile and shear properties have been reported by only a few investigators. Sonada in 1962 and Kaplan et al in 1985 reported that the tensile strength of trabecular bone was significantly less than its compressive strength. In contrast to these findings, several studies have reported no significant difference between the tensile and compressive properties of trabecular bone (Carter et al 1980, Neil et al 1983, Bensusan et al 1983). The shear strength of trabecular bone has been reported to range from 1 to 21 MPa (Melvin et al 1970, Halawa et al 1978, Saha and Gorman 1981, and Stone et al 1983). Similar to the compressive studies, these investigators found that the shear properties were dependent on anatomic location as well as the direction of testing, as would be expected from a highly anisotropic material.

3.4. Biomechanical basis for design of hip prosthesis

The essential function of a femoral component is to replace the femoral head and neck. However the implant fixation within the femoral canal becomes a key factor in long-term performance. Therefore the task of designing a femoral component is not only to restore the anatomic

position of the femoral head, but also to firmly fix the implant within the canal. For a cementless stem, there are two stages of fixation, the mechanical fixation (initial stability) and biological fixation (long-term stability). The initial stabilization of the stem is mostly dependent on the stem geometry. When bone tissue upgrowth occur, the stem stability can be further enhanced.

3.4.1 Stem neck design

Restoration of the centre of the femoral head is adjusted by two variables: the offset which is from the axis of the femoral shaft to the head centre, and the vertical height. Both determine the neck-shaft angle and neck-anteversion angle. Reconstruction of offset is important in balancing the abductor force with the centre of gravity of the body weight. If the offset is too short (neck is too vertical), the moment arm of the abductor will be shortened which demands greater force from the abductor muscles to balance the body and results in a greater resultant force across the artificial joint. At the other extreme, if the offset is too long (neck is too horizontal), the bending strains and stresses of the femoral shaft and stem will be increased that may lead to interface relative motion and loosening of the femoral stem. The correction of vertical height of the femoral neck can restore or readjust the equal leg length after total hip replacement. A radiographic study by Turula et al (1986) showed that mean leg discrepancies in 55 patients was 8.7 mm in unilateral and 11.6 mm in bilateral cemented total hip arthroplasty. This could disturb the equilibrium of the locomotor system, and cause low-back pain, limp or some other symptoms. Therefore, it is important to design a prosthesis with correct offset and vertical height of femoral neck. However, for a cementless stem, the offset and vertical height of the femoral head is

particularly difficult to adjust during surgery. In this regard, it seems that only a custom stem can consistently obtain the adequate neck length and orientation for every case.

3.4.2 Femoral head selection

It is not yet clear what size of femoral head is optimal. Currently the available head sizes range from 22 mm to 32 mm. The smaller size of head can produce lower frictional torque and stresses at the acetabular cement-bone interface (Charnley 1968), but higher contact stresses and greater linear wear, which the head can penetrate into the acetabular component (Charnley 1967, Gold BL and Walker PS, Livermore et al 1990). For the larger size of head, the greater frictional forces and larger quantities of wear debris can result (Dumbleton 1981). This debris is to some extent responsible for aseptic loosening of the prosthesis (Willert 1975). For the hip range of motion (ROM) after total hip replacement, it has been shown that a large neck diameter decreases ROM. In contrast, a larger head size increases ROM (Krushell et al 1991). Therefore, the choice of the size of head actually depends on the individual case to see which head size can mostly benefit the patient. In most cases, head sizes of 26 or 28 mm are used in an attempt to gain some of the advantages of each extreme. A study showed that with a 28 mm femoral head, the amount and rate of linear wear was the lowest, while the 22 mm femoral head showed the greatest amount and mean rate of linear wear, and the 32 mm femoral head showed the greatest amount and mean rate of volumetric wear (Livermore et al 1990). At present, femoral stem used with modular head have made the system more flexible. The modular heads have standard and ±6.0 mm or ±12 mm in neck length, which offer the possibility of selecting the head size or adjusting the neck length

during surgery by interchanging the femoral head. However, the corrosion between the femoral neck and head may be a long-term (Collier et al 1992).

3.4.3 Stem collar option

For many years, surgeons regarded the collar as an essential feature for any type of femoral prostheses (Harris 1980), because it can prevent stem sinkage and restore physiological stresses to the calcar region (Crowninshield 1980). Finite element analysis showed that the collar increased the stress in the medial cortex only in the most flexible prostheses, particularly those manufactured from titanium alloy (Tarr et al 1981). Markolf et al (1976) pointed out from their experimental observation that direct contact of a collar with the neck resection surface was difficult to achieve during surgery. However, laboratory studies evidently showed that a stem with a collar could produce more surface strains of bone by 36 % than that without a collar (Zhou and Walker 1990). This may be of benefit in reducing the bone remodelling process.

3.4.4 Optimal stem length

The optimum stem length depends upon a number of anatomic and mechanical considerations. Mechanically, a shorter stem, which has a shorter moment arm, produces a greater force in the distal contact region. While a longer stem can produce more bending and less distal compressive stresses. A theoretical study by Crowninshield (1980) showed that longer stems could reduce cement stresses. Anatomically, the stem length should be a function of the canal diameter and geometry. For a cementless prosthesis, if the proximal fit of an implant has been

achieved and the stability of the stem has been obtained, then the distal part of the stem has little function. While in a extremely varus or curved, or even more severely distorted canal, the stem may not be able to proximally fit with the canal. In this case, a longer stem with a distal taper to enhance stem stabilily may be necessary. The distal stem should not be so tightly fit as to carry axial load, which may reduce the proximal stresses. On the other hand, if the canal is straight (stovepipe type), the stem can be relatively shorter. The stem length is also based on the canal diameter, with a bigger diameter canal, the stem should be longer to balance the bending strains and stresses, while for a canal with smaller diameter, a longer stem may be prone to fracture. Therefore the stem length should vary according to each canal shape and size. The adequate length of the stem is vitally important which should not be compromised. For custom stems, all these design features and parameters can always be brought together for the individual stem, which include proximal fit, distal fit, stem length, neck length and neck orientation.

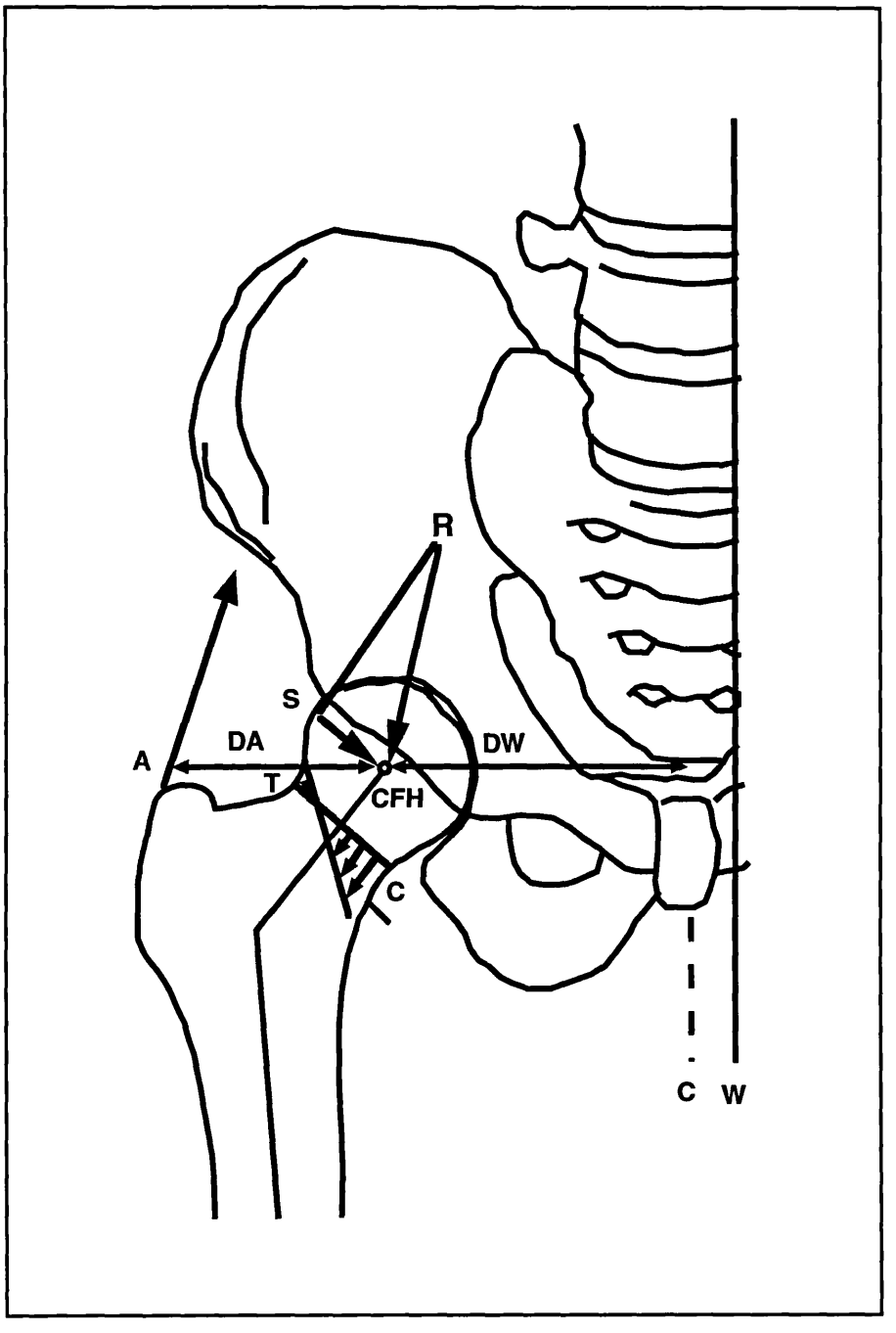

R - RESULTANT FORCE
C - COMPRESSIVE STRESS
T - TENSILE STRESS
CFH - CENTRE OF FEMORAL HEAD

S - SHEAR FORCE COMPONENT
A - ABDUCTOR FORCE
W - BODY WEIGHT
C - CENTRE OF BODY

DA - DISTANCE BETWEEN A AND CFH
DW - DISTANCE BETWEEN W AND CFH

$$A \times DA = W \times DW$$

FIG. 3.1 FORCES ACTING ACROSS THE HIP JOINT IN A SINGLE-LEGGED STANCE, DRAWN AS A "FREE BODY"

CHAPTER FOUR

RECONSTRUCTION OF FEMORAL CANAL AND DESIGN OF CUSTOM STEM

4.1 Establishment of a database of average shaped femoral canal

Twenty-six human cadaveric femurs in the 5th to 8th decades were clamped in a jig to a reproducible axis system based on the centre of the femoral head and the straight part of the shaft just below the lesser trochanter. The centre line of the shaft defined the vertical y-axis, the medial-lateral axis intersected the y-axis and the centre of the femoral head as the horizontal x-axis, and the anterior-posterior axis was mutually perpendicular to the other axis as the z-axis. The femurs were embedded and sectioned transversely, perpendicular to the y-axis. The section spacing was proportional to the length of the femur. For a bone length measured from the top of the femoral head to the distal medial condyle (L), the proximal twenty-one sections were spaced apart in $5 \times L$ / 500 mm (500 mm is a standard length of femur), and the distal four sections were $20 \times L$ / 500 mm apart. The sections were then photographed and the cortical cancellous interface of the femoral canal was identified for each section (Walker and Robertson, 1988). Proximally, the inner and outer contours were almost coincident due to the thin cortical wall, especially in the region of the greater trochanter.

The inner and outer contours were digitized into a Chromatics CGC 7900 computer using a Talos digitizer, to an accuracy of better than 0.25 mm. The boundary coordinates were then scaled according to the total length of the femur: $C2 = C1 \times L / 500$, where C2 = new coordinate, C1 = measured coordinate. The scaled contours of the corresponding sections of all bones were then superimposed in the computer and printed out. Average contours were then drawn repeatably with agreement to better than $\pm$ 1 mm in the region below neck cut. Above that level, there was

less correspondence due to the larger variation between the contours. The final average contours of each section were then used to reconstruct the three-dimensional average femur, which had forty points per section and twenty-five sections in total. This average femur had a natural appearance and each section was aligned smoothly to adjacent sections. Fig.4.1 shows the model of an average femur.

4.2 Three-dimensional reconstruction of an individual femoral canal

4.2.1 Digitizing the plain radiographs

In order to three-dimensionally reconstruct the shape of a given femur, A-P and M-L radiographs were taken including a scale marker beside the femur. Before the contour of the canal being digitized, seven points in the A-P view and six points in the M-L view were predefined (Fig. 4.2). These points were described as follows:

A. The centre line of the femoral canal in A-P and M-L views:

Each two points in A-P and M-L views of the X-rays were used for defining the centre line of the femoral canal. These are also used for defining the X- and Z- coordinate systems during reconstructing the femoral canal. In addition, these centre lines were used for determining and correcting the skew angles of radiographic films placed on the digitizing table.

B. Magnification scale marker in A-P and M-L views:

Two points on the A-P and M-L views were digitized on the magnification scale markers, which were 100 mm apart. The magnification factors were then used to adjust all of the dimensions in the system to normal, and thus the reconstructed canal was actual size.

C. Centre of the femoral head in A-P and M-L views:

The distance between the centre line of the canal and the centre of the femoral head were used to calculate the rotation of the femur by using a triangular algorithm. Also the centre of femoral head was used as the reference for the offset and height of the stem neck.

D. Trochanteric fossa (A-P views) and lesser trochanters:

The trochanteric fossa was defined as a top margin of the reconstructed canal. The distance between the intertrochanteric notch and lesser trochanter in A-P view was used to determine the stem length. The lesser trochanters both in A-P and M-L views have to be aligned at the same level on the digitizing table.

After all the above points had been defined, the contours of the femoral canals from A-P and M-L radiographs were then digitized. The data was then formatted and stored in the computer.

4.2.2 Coordinate transformations

The computer software carried out coordinate (x-, y-, and z- axis) transformations from each section of the average femoral canal to the individual reconstructed canal. The length of the reconstructed femur was

proportional to (3.5 times) the distance between the intertrochantric notch and lesser trochanter, and then divided into thirty-six spaces which had thirty-seven sections. The proximal twenty-one sections were at the same spacing, while the distal sixteen sections were grouped into four sections because of the relatively constant shape in the distal part of the femur. Forty points for each section were formatted and all the points were anti-clockwise, with point 1 always at the most medial side. The points on each section were proportionally adjusted according to the width of the individual canal in A-P and M-L views. In this way, the three-dimensional femoral canal was reconstructed with 40 points in each section and 25 sections in total.

4.2.3 Correction of femoral rotation in radiographs

The patient's femur could sometimes be rotated internally or externally when it was radiographed. This would occur especially in cases of severe fixed deformity. A gross rotation of the femoral bone could be easily determined by the radiographic appearance of the greater and lesser trochanter, and by the femoral condyle. However, for quantitative analysis, the angle of rotation could be calculated from the distances between the centre of femoral head and the central line of femoral canal in A-P and M-L views. For more precision, it could also be measured from CT scan by overlapping the proximal canal with the femoral condyle or some other reference lines. When the rotational angle was determined, software was used to transform the point in each section back to its normal position. The accuracy of the rotational correction was evaluated.

4.2.3.1 Correction of X-ray rotation in A-P view

On the radiographic film,when the femoral canal is rotated, the proximal medial curve is changed. This will affect the fit of the stem design in the actual canal curve. Usually the proximal medial contour is curved mostly when the femoral canal is in normal (neutral) position, and gradually straightens when the femoral canal was rotated either internally or externally. In order to determine the proximal medial canal curvature in different rotations, the average shaped canal was external rotated from 0 degrees to 60 degrees with 10 degrees increment. All the contours of the proximal canals with different rotations were overlapped and compared with the canal in the neutral position. The distances from the central line to the medial boundary were measured for all the canals from section 7-25, which ranged from 10 mm below the lower margin of the lesser trochanter to the trochanteric notch. It was found that the contours agreed closely between the normal canal and 20 degrees rotation, while from 30 degrees upwards, the medial line start to move in significantly (Fig. 4.3). The ratios of neutral canal over rotated canal were analysed from section 7 to section 25. The results are showed in Table 4.1. These ratios were then plotted by using computer graphics and a best fit line was drawn (Fig. 4.4). The formulas for the best fit line from 30 to 60 degrees were derived and used in the software for correcting the rotations in the A-P view.

4.2.3.2 Correction of X-ray rotation in the M-L view

Canal appearance is more sensitive to rotation in the M-L view of the radiograph. It can change the canal dimensions and the contour in anterior and posterior aspects. For accurately reconstructing the femoral canal by using plain radiographs, it is critical to correct the rotation. For

this purpose, software was developed which could correct the canal rotation.

The algorithm for correcting the canal rotation in M-L view is described as follows: Firstly, obtain the rotational angle which was calculated from the distance between the central line of the canal and the centre of the femoral head. Secondly, rotate the average canal to that angle. Thirdly, find the maximum diameters of each section in A-P and M-L views. Fourthly, calculate the ratios of diameters between the average canal and the individual canal in each section. Fifthly, each point on each section of the average canal was multiplied by the ratios, so that the average canal was transformed to the individual canal. Finally, the X-axis of the canal was shifted to align with the axis of the post-processed digitized contours.

For evaluating the results of correcting the canal rotation in the M-L view, a cadaveric femur without gross deformity was fixed in a jig and radiographed in the M-L view from 40 degrees internal rotation to 40 degrees external rotation, with 5 degrees increment. The contours of the inner cortical line for each canal rotation were digitized. The reconstructed canals with different rotation angles were compared with the neutral canal in each section. The results showed that the predicted canal in different rotations very closely matched with the neutral canal up to 30 degrees of internal and external rotation, particularly in the distal half of the canal. Beyond this range, the agreements were not so close. Fig.4.5 showed the cross-section geometries of the reconstructed canals with and without correction of rotation in 5, 15 and 30 degrees. The differences between the canals with and without correction of rotations

indicates that if the canal rotations are not corrected, plain X-rays were very inaccurate for designing custom stems.

4.3 Accuracy evaluation of the reconstructed femoral canal

The three-dimensionally reconstructed femoral canal from two views of plain radiographs was expected to have some geometry disagreements with the actual femoral canal. However, it was not clear in which areas there was the greatest mismatch and quantitatively how much difference existed between the two canals. Therefore, a study was conducted to compare the reconstructed femoral canals with the actual canals.

4.3.1 Materials and methods

Eleven proximal cadaveric femora with no gross abnormalities were radiographed in A-P and M-L views together with a scale marker. The radiographs were digitized and the predicted canals were reconstructed.

These femora were then embedded in a rectangular plastic block and transectioned to twenty-five slices on an Exotom Cut-Off Machine (Struers, Denmark). The transection levels were premarked on the plastic according to the predicted canal sections (Fig. 4.6), and thus the sections were cut at the same increment as the corresponding predicted canals. The slices were then micro-radiographed and the inner cortical walls were digitized. The femoral canals were reconstructed in the same coordinate system as the predicted canal, allowing a comparison to be made in the computer.

Software was developed to compare the reconstructed canal with the actual canal in each section. Each section was divided into four quadrants (medial, anterior, lateral and posterior). The technique was that a line was drawn from two adjacent points on the reconstructed canal (line A), and then a normal line (line B) was created from the middle of the line A to the boundary of the actual canal. The distance of the normal line was defined as fit (Fig. 4.7), and the angle between the line B and horizontal line was calculated and used to determine which quadrant the point belonged to. Fit in each quadrant was expressed as the mean distance of the normal lines in this quadrant. The area of cross-section of the actual canal was also compared with that of the reconstructed canal to find an area ratio.

4.3.2 Results

The reconstructed canals were compared with the actual canals at twenty-five sections in four quadrants. A typical comparison was shown in Fig. 4.8. There was loss of agreement in the trochanteric fossa regions, due to inaccuracy of the 'average femur', but this would not affect design of a femoral stem. Close peripheral agreement in the proximal third was obtained, the main errors being in the posterior border. Below that, agreement was close, especially in the distal region.

The overall differences between the reconstructed and the actual canals were less than 1 mm, while in the region below the lesser trochanter, the differences were closer to 0.5 mm (Fig. 4.9). The mean error obtained from the proximal medial region (section 18-25) was only 0.30±0.67 mm. In the middle region of medial side around the lesser trochanter (section 13-17), the error was 0.30±0.87 mm. The least error was observed in the

distal medial region (section 1-12), only 0.14±0.46 mm. The anterior and lateral sides showed similar results. While on the posterior side, the errors were slightly larger, 0.39±1.26 mm for the middle region and 0.55±1.29 mm for the proximal region.

For comparison of the cross-sectional areas between the reconstructed and actual canals (reconstructed canal over actual canal), an average ratio of 0.99±0.08 was observed (Fig 4.10), suggesting that the reconstructed canals were slightly smaller.

4.3.3 Discussion

In order to reconstruct the individual femoral canal, the A-P and M-L profiles of the canal were determined from plain radiographs. The accuracy of the canal profiles was previously studied by Rubin et al (1992). They determined a mean 'index of accuracy' (similar to our definition of 'fit') of 2.4 mm proximally and 1.3 mm distally. However, their data was obtained by using a contouring algorithm from video images of CT scans. This raises the question of the definition of the cortical boundary, especially in the proximal region, where an error can easily be introduced.

In order to define the inner 'cortical wall', the actual sections and their micrographs were presently studied. The defined cortical contours were referenced to where the bone would be reamed. Distortion of an 'average femur' model would clearly not allow for the prediction of the precise contours of a particular femur. However, as can be seen from a typical example (Fig 4.8), the overall outlines were accurate. The analysis showed that the mean peripheral error was less than 1 mm in all

regions, while in the majority the error was less than 0.5 mm. It was notable that the least errors occurred in the proximal medial and anterior regions as well as the distal region. These regions are regarded as being the most important for stem-bone force transfer.

4.4 Individual design of femoral stems

4.4.1 Canal preparation and stem generation in software

Having reconstructed the three dimensional femoral canal for an individual case, software was developed to design a custom stem. Surgical procedures for doing total hip replacement were simulated in software as follows:

A. Ream the distal canal:

The diameter of the reamer was determined by the average of the maximum and minimum canal diameter in section one, namely at the distal end. The reamer can be either parallel or conical depending on the canal geometry. The points from canal section 1 to section 7 were calculated and reorganised so that the reamer diameter was adjusted to the distal canal diameter. The reason for choosing the canal section up to section seven was that this region represented the distal part of the stem.

B. Femoral neck resection:

This part of the software was to regenerate the canal geometry in the proximal part, which was from section 15 to section 25. The proximal part of the canal was inclined to a given angle by using an algorithm of

generating and rearranging intersectional points. The given angle could either be input or by default which would be 25 degrees. The top section of the canal (section 25) had a slope of 25 degrees (by default), and then linearly reduced down to horizontal in section 15.

C. Best fit in proximal medial region:

The shape of the femoral canal in the proximal medial region resembles a half circle. Its smallest radius is usually above the lesser trochanter. The stem radius in the proximal medial region should match the canal radius. If the stem radius is too big, then the stem will likely be placed in valgus. If the stem radius is too small, then the stem will not be stable, particularly in torsion. In the computer design program, the proximal part of the stem is modelled as three circles, one for medial, one for lateral-anterior, and one for lateral-posterior. In order to obtain the best fit circle in the proximal medial region, the software searched the canal sections from 21 to 24, which were above the lesser trochanter, to determine the diameter of the medial circle. For producing the best fit medial curvature of the stem, a cubic fit was used. After testing the different combination of sections, sections 5, 19, 25 were choosen, which produced the best fit curve of the proximal medial stem for the canal.

D The curvature in the proximal anterior region:

The algorithm for producing the best fit curvature in the proximal anterior region was as same as that in the proximal medial region, only difference was that sections 5, 17, 25 were chosen for the cubic fit.

4.4.2 Stem design rationale

Soft cancellous bone cannot be relied upon to provide load transfer and initial stability. Therefore, the stem should be exactly fit to the inner cortical envelope. On the other hand, overreaming endosteal bone to achieve fit would resulting in weakening of the supporting bone. This will create stress concentrations and lead to adverse bone remodelling.

Theoretical and experimental studies have shown that cementless femoral stems result in more normal stress and strain transfer in the proximal medial femur than cemented stems (Huiskes 1989, Walker et al 1987, Zhou et al 1990). However, this optimal load transfer is very dependent on the stem with accurate fit. Finite element analyses have shown the load transfer between the stem and the bone occurs only in the proximal and distal thirds, with the middle third being relatively inactive. Furthermore, proximal stress protection is minimised if distal load transfer is limited. Therefore, the CAD-CAM stems were designed to achieve a close proximal medial and anterior fit and a sliding distal fit.

4.4.3 Stem design options

Apart from the essential design features of custom femoral stem, there are some other design options. These varieties of design options were used for designing stems for severely deformed geometries of femoral canal.

A. Stem neck anteversion angle:

This design feature is often for the case of Congenital Dislocation of the Hip (CDH), which the femoral neck is abnormally anteverted and the

head is dislocated upwards and laterally from the acetabulum (Coventry 1976). It was also found that the anteverted distortion usually started from the proximal metaphysis of the femur in an incremental version with the maximum distortion at the top.

Based on the anatomical distortion of CDH, the custom stem was designed so that the proximal part of the stem was twisted anteriorly to match the anterior curve of the canal, while the stem neck retroverted to retain the head in a normal position of the acetabular cup. Therefore the stem can fit in the anteriorly twisted canal with the stem neck pointed to the normal position of the acetabular cup (Fig. 4.11).

B. Femoral neck resection angle:

The custom stems had a default neck resection angle of twenty-five degrees, which preserved more femoral neck. Studies have shown that this part of the bone is stronger and ideal for load transfer and stem stabilization (Freeman 1986). However, in revision cases, the neck resection angle is different in each case due to the previous total hip replacement. Therefore, the custom stems have to change the stem neck angle to match with the previous resected neck angle. Fig. 4.12 showed the different neck angles of the stems.

C. Distal stem taper and lateral flare:

It was observed (Noble et al 1988) that there were three types of femoral canal shapes, which were 'stovepipe', 'champagne glass', and between them a "normal" canal shape. In order to design a custom stem to meet these variations, two design options were added — distal taper and

lateral flare. If a canal is narrow in the isthmus area but becomes wide towards proximal, then the distal tapered stem can be used, either by reducing the bottom part of the stem or expanding the middle part of the stem (Fig 4.13). If a canal diverges further upwards, the lateral flare option can be used, which produces a slope on lateral side by the algorithm of three points cubic fit. This slope can be extended up to section 55 (lower flare), section 60 (higher flare) and section 65 (higher flare). Then the lateral slope can be either linearly reduced down to align with the shoulder of the stem, or straight up to the shoulder of the stem (Fig 4.14).

These design options have greatly increased the varieties of the stems which can provide more accurate fit and stability with the different canal shapes.

4.4.4 Stem design for revision cases

Some of the commonest causes in revision total hip replacement are aseptic stem loosening and infection. When the stem needs to be revised, the bone structures usually become porotic or are sometimes absent. The loss of femoral bone stock has been classified into four grades (Engelbrecht and Heinert 1987), which was called the Endo-Klinik classification: Grade 1 — Radiolucent lines confined to the upper half of the cement mantle; clinical signs of loosening. Grade 2 — Generalised radiolucent zones and endosteal erosion of the upper femur leading to widening of the medullary cavity. Grade 3 — Widening of the medullary cavity by expansion of the upper femur. Grade 4 — Gross destruction of the upper third of the femur with involvement of the middle third, precluding the insertion of even a long-stemmed prosthesis. The

degree of destruction of the proximal region, whether by resorption or erosion, and the capacity of the bone for carrying bending and axial loading, results in the need for a progressive range of solution. Proximal bone preservation and stimulation of new bone are important considerations. The design principles for the revision cases are to transmit the force proximally as much as possible, especially in Grade 1 and 2. But in cases of severe upper femur destruction such as in Grade 3, the conical part of the stem between the upper and lower can be used for axial force transmission (Fig. 4.15). In this case, the main function of the upper femur is to transmit muscle forces, a situation much preferable functionally to proximal femoral replacement. For controlling the torsional rotation, the distal fluted stem for engaging into the normal cortical bone is a suitable option. After the upper part of the stem fills the proximal cavity, if there are any spaces between the stem and cortex due to bone erosion and cavity expansion, bone grafts are necessary to fill the gap and stabilize the stem. During load bearing, some evidence showed that the bone graft can be replaced by newly formed bone. A revision stem with the additional features of proximal grooves, together with HA coating, may further facilitate new bone growth and secure the stem.

4.5 Comparison of stem geometries designed from the reconstructed and the actual canals

It has been shown that the predicted canals have slight differences compared with the actual canals. The question is will these differences affect the design of the stem? In order to answer this question, a comparative study was conducted between two stems designed from the reconstructed canals and the actual canals.

4.5.1 Materials and methods

Eleven cadaveric femurs without gross deformity were used for the study. All the femurs were radiographed in A-P and M-L views with a scale marker. The femoral canals were reconstructed in twenty-five sections by the Hip Design workstation. After that, all the actual femoral bones were embedded in a plastic block and resected into twenty-five slices, at the same level as the predicted canals. The slices were then micro-radiographed, and the inner cortical walls were digitized. Finally the actual femoral canal shapes were produced. Stems were designed from both canals, and their coordinates were transformed to the same axes, so that the two stems could be compared by the software. Software was developed to compare the two stems in four quadrants (medial, anterior, lateral and posterior) and the areas of cross-sections.

4.5.2 Results

The stems which were designed from the reconstructed and the actual canals were compared at ten sections from stem tip to stem shoulder. Differences between these two stems were extremely small, especially in the distal region which showed only 0±0.22 mm difference in all four quadrants (Fig. 4.16). In the middle and proximal regions of the stem, the differences in the four quadrants were in the range of 0.09-0.29±0.25-0.5 mm. Comparison of cross-section areas of these two stems (actual/reconstructed) showed that in the distal region the stem designed from the reconstructed canal was slightly smaller (0.7±7.0 %) than that from the actual canal. While in the middle and proximal regions, the stems designed from the reconstructed canals were slightly bigger (2.5±6.0) than that from the actual canals (Fig. 4.17).

4.5.3 Discussion

The proximal medial fit is particularly important in stem design for load transfer (Huiskes et al 1991). While a close fit on the proximal anterior and posterior regions is necessary for rotational stability of the stem (Hua and Walker 1992). It has also been shown that distal fit plays an important role in eliminating thigh pain and in achieving stem stability (Campbell et al 1992; Engh et al 1987; Huiskes 1980; Whiteside 1989). From the present study, it was shown that the profiles of the canals reconstructed from the A-P and lateral X-ray films very accurately matched with the actual canals. Even if in some regions such as the greater and lesser trochanters, the two canal shapes were not the same, the stems designed from the two canals were virtually identical. This provides an indication that the canals reconstructed by the Hip Design Workstation were sufficiently accurate and reliable.

While CT is more accurate for determining overall canal geometries, plain radiographs provide an alternative method in reconstruction of femoral canals with sufficient accuracy in the key regions. The advantages of radiographs over CT are that they are easily obtainable, there is lower radiation exposure, and lower costs. However, in cases of very deformed canals, such as CDH, fracture and osteotomy, CT scan is still required to determine the canal shape.

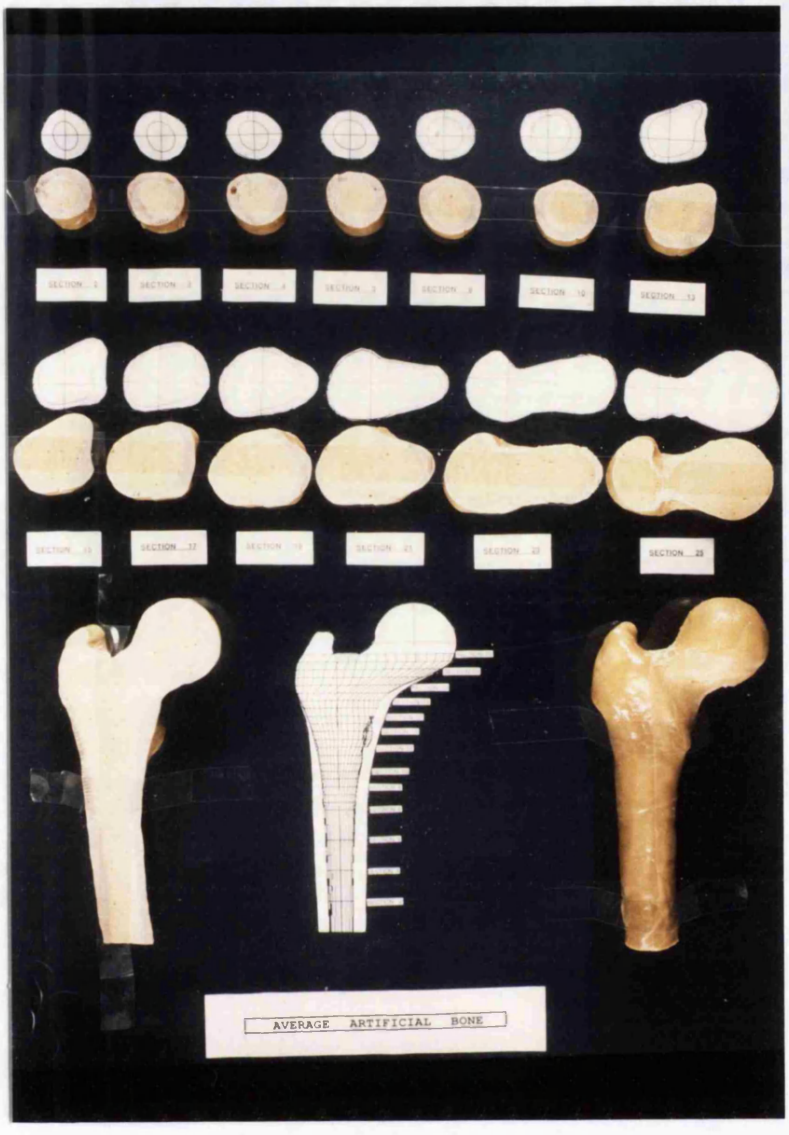

FIG. 4.1 THE MODEL OF A BONE AND CANAL IN AVERAGE GEOMETRY. TOP: CROSS-SECTION GEOMETRY. BOTTOM: GENERAL APPEARANCE

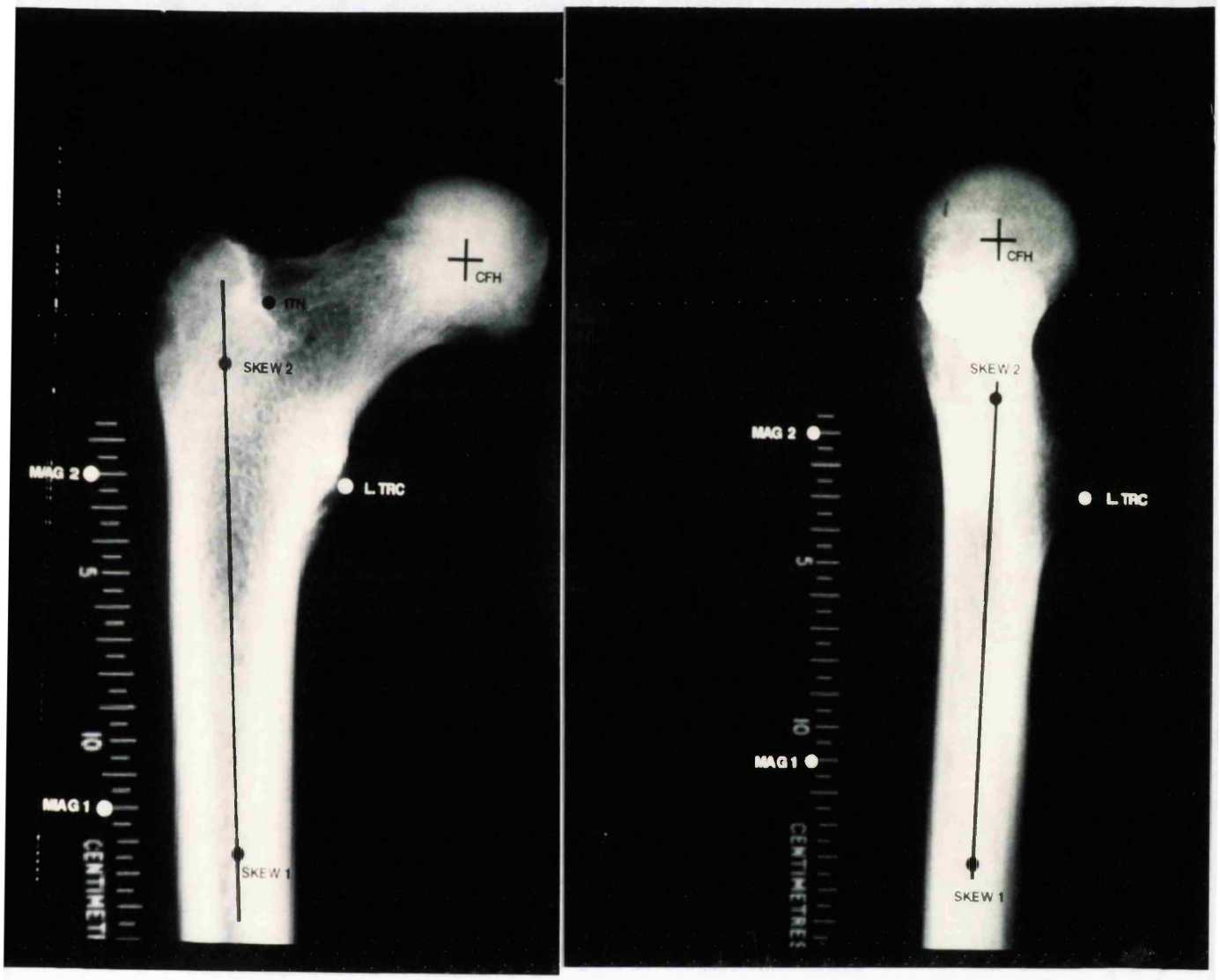

FIG. 4.2 DIGITIZATION OF REFERENCE POINTS ON A-P AND M-L VIEWS OF RADIOGRAPHS FOR RECONSTRUCTION OF FEMORAL CANAL

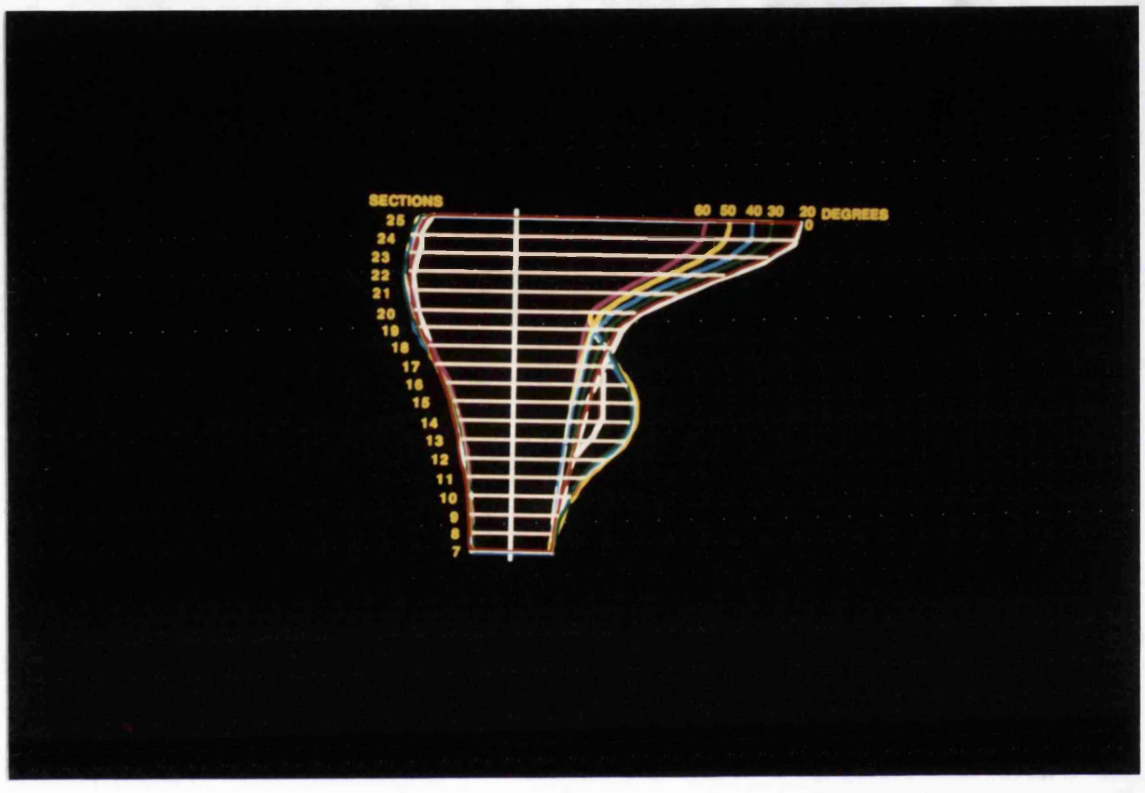

FIG. 4.3 RADIOGRAPHIC APPEARANCE OF THE PROXIMAL FEMORAL CANAL IN A-P VIEW WHEN THE FEMORAL CANAL IN NEUTRAL POSITION, 20, 30, 40, 50, AND 60 DEGREES OF ROTATION

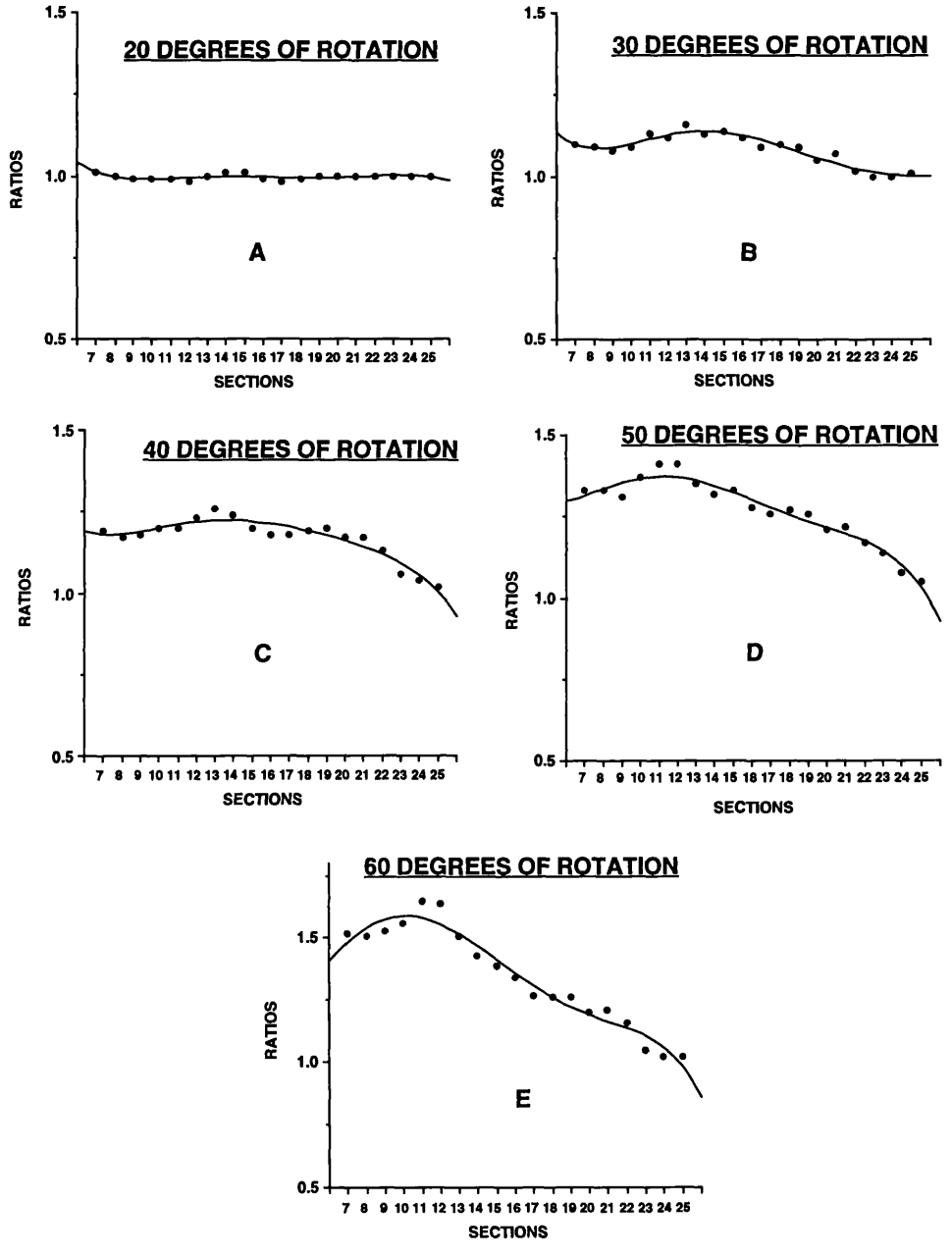

A $y = 1.0433 - 4.0927e\text{-}2x + 1.0854e\text{-}2x^2 - 1.2374e\text{-}3x^3 + 6.3429e\text{-}5x^4 - 1.1974e\text{-}6x^5$
$R^2 = 0.942$

B $y = 1.1331 - 5.0483e\text{-}2x + 1.7151e\text{-}2x^2 - 1.9688e\text{-}3x^3 + 8.9486e\text{-}5x^4 - 1.4218e\text{-}6x^5$
$R^2 = 0.922$

C $y = 1.1900 - 1.9110e\text{-}2x + 9.7208e\text{-}3x^2 - 1.3441e\text{-}3x^3 + 7.3568e\text{-}5x^4 - 1.4947e\text{-}6x^5$
$R^2 = 0.903$

D $y = 1.2974 + 1.3723e\text{-}2x + 5.3182e\text{-}3x^2 - 1.4620e\text{-}3x^3 + 1.0381e\text{-}4x^4 - 2.4005e\text{-}6x^5$
$R^2 = 0.953$

E $y = 1.4061 + 8.8955e\text{-}2x - 9.0170e\text{-}3x^2 - 7.9753e\text{-}4x^3 + 1.0472e\text{-}4x^4 - 2.8408e\text{-}6x^5$
$R^2 = 0.958$

FIG.4.4 THE RATIO OF THE NEUTRAL POSITION TO THE DIFFERENT ROTATION OF THE CANAL ON THE DISTANCE FROM THE CENTRE LINE TO MEDIAL PROFILE

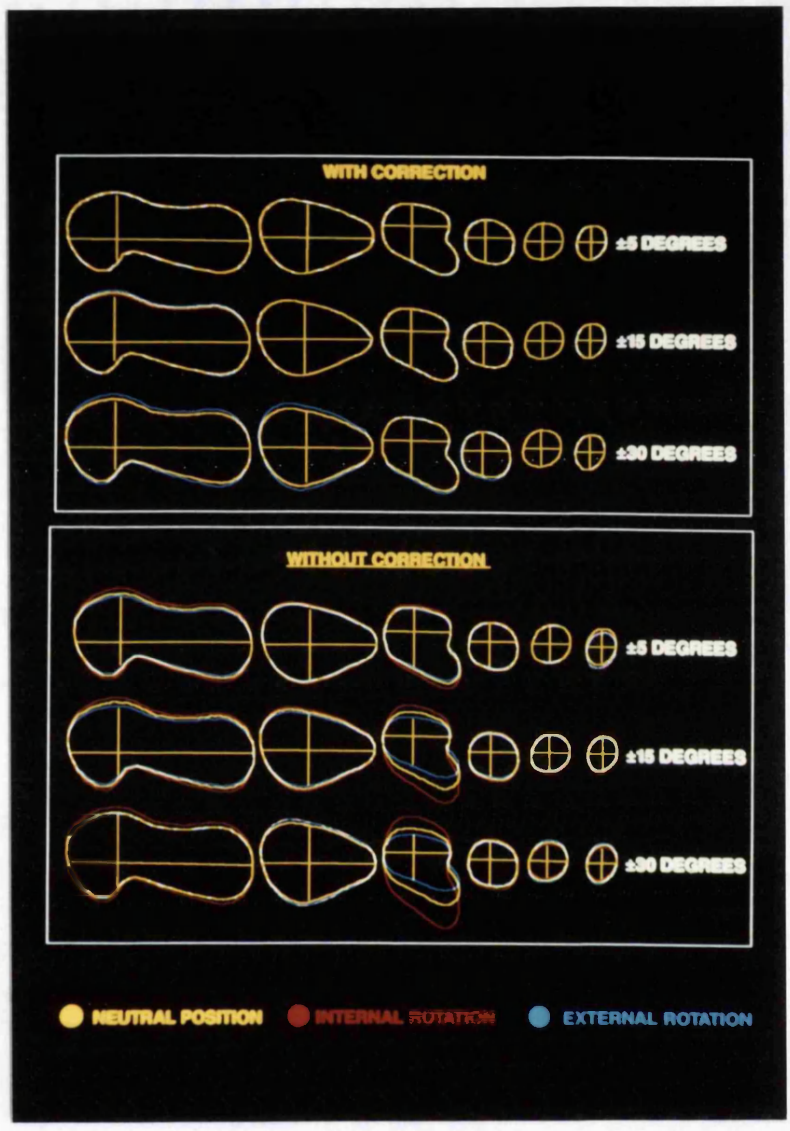

FIG. 4.5 COMPARISON OF CROSS-SECTION GEOMETRY OF PROXIMAL FEMORAL CANAL IN M-L VIEW OF THE RADIOGRAPH BETWEEN NEUTRAL POSITION AND ±5, ±15, ±30 DEGREES OF ROTATION: THE ROTATIONS WERE CORRECTED (TOP), THE ROTATIONS WERE NOT CORRECTED (BOTTOM)

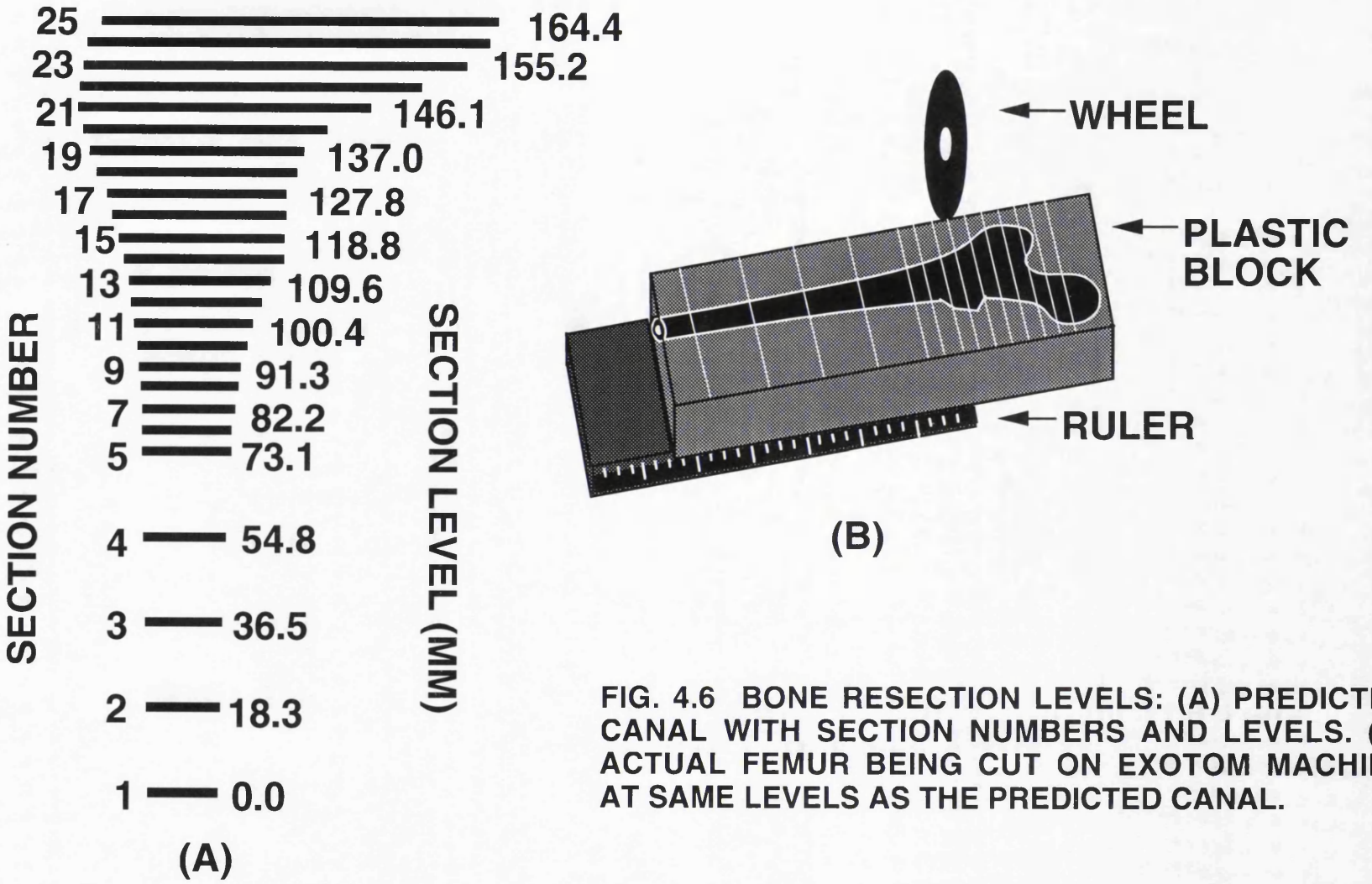

FIG. 4.6 BONE RESECTION LEVELS: (A) PREDICTED CANAL WITH SECTION NUMBERS AND LEVELS. (B) ACTUAL FEMUR BEING CUT ON EXOTOM MACHINE AT SAME LEVELS AS THE PREDICTED CANAL.

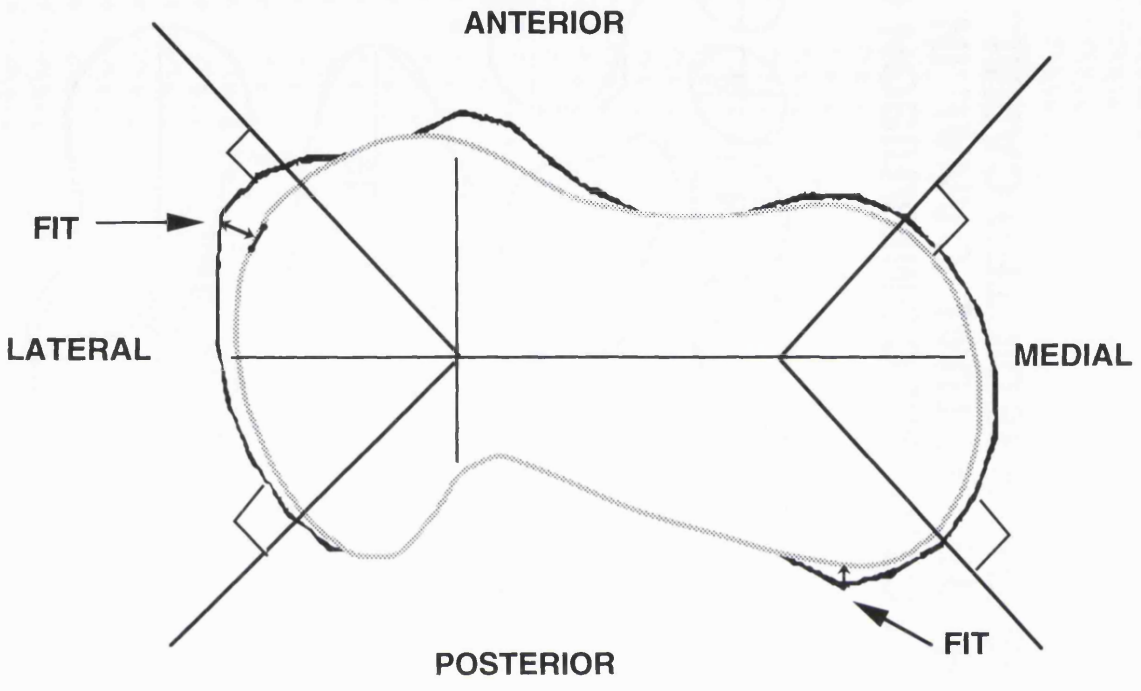

FIG. 4.7 LINE-TO-LINE COMPARISON OF THE PREDICTED CANAL WITH THE ACTUAL CANAL. FIT IS THE DISTANCE BETWEEN THE BOUNDARY OF TWO CANALS.

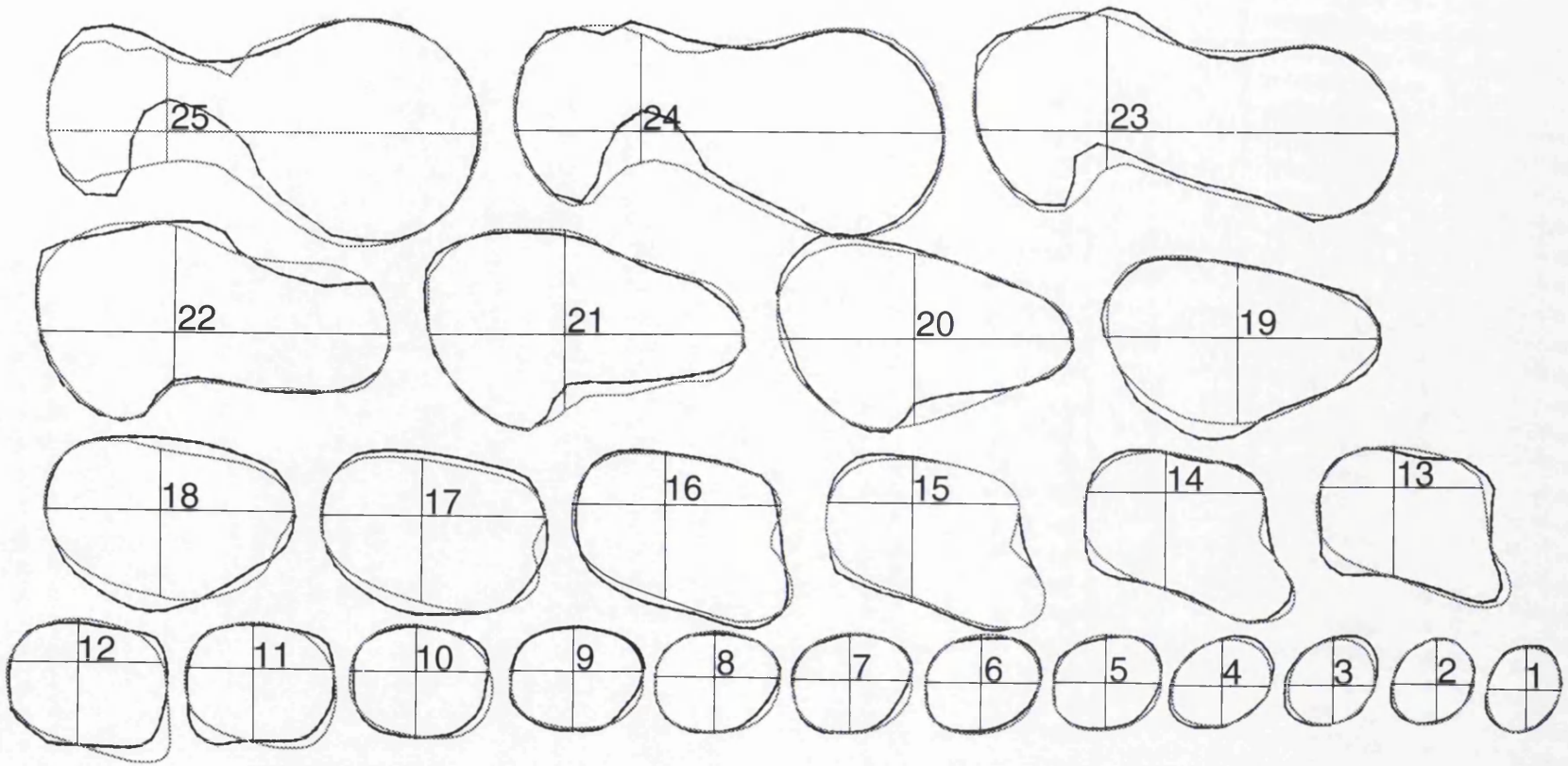

FIG. 4.8 A TYPICAL CROSS-SECTIONAL COMPARISON OF THE PREDICTED CANAL WITH THE ACTUAL CANAL IN 25 SECTIONS. THE DOTTED LINE IS THE PREDICTED CANAL.

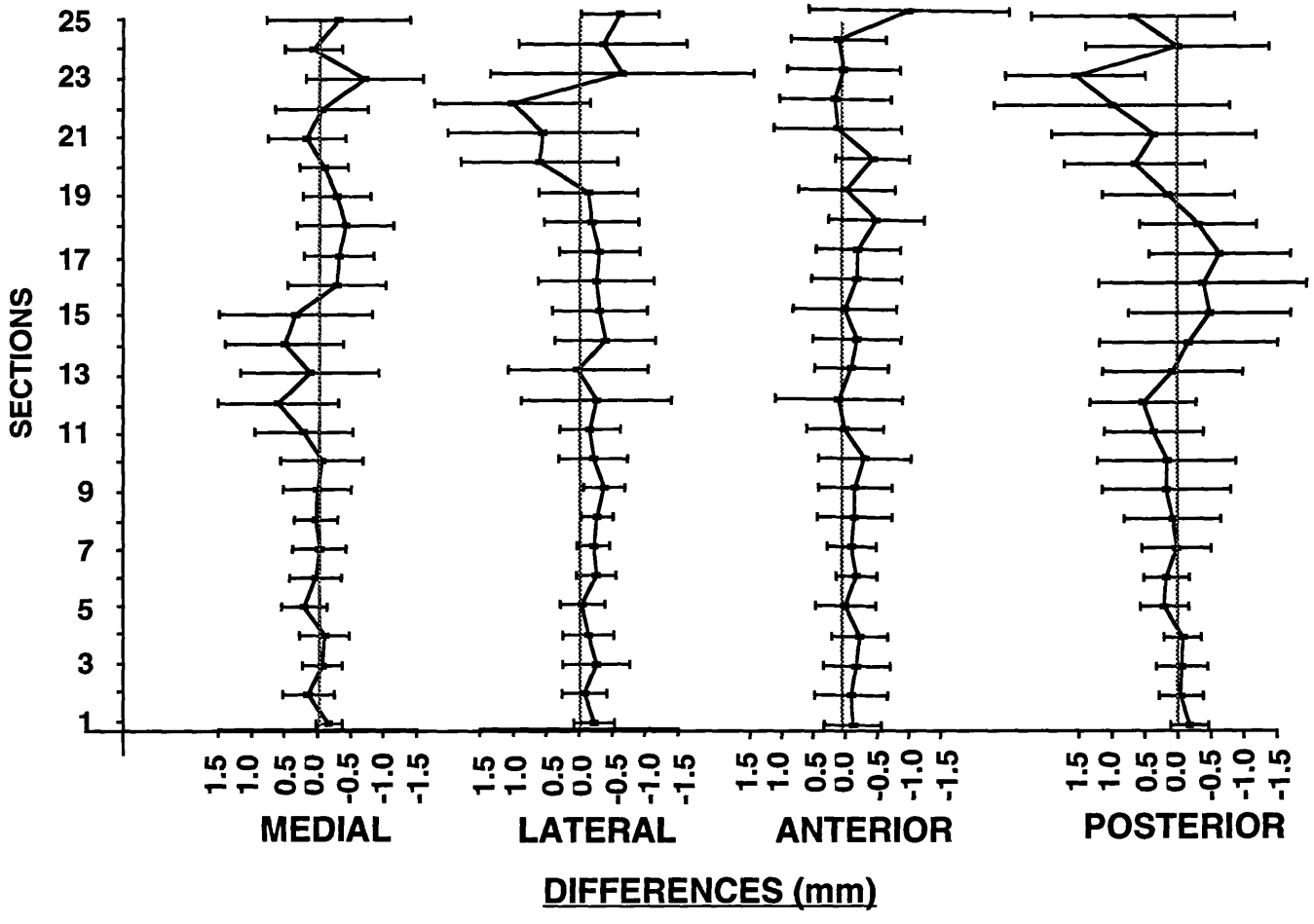

FIG. 4.9 COMPARISON OF THE PREDICTED CANALS WITH THE ACTUAL CANALS IN TWENTY-FIVE SECTIONS, WITH LINE-TO-LINE DIFFERENCES IN FOUR QUANDRALS (MINUS VALUE MEANS THE PREDICTED CANALS ARE SMALLER THAN THE ACTUAL CANALS).

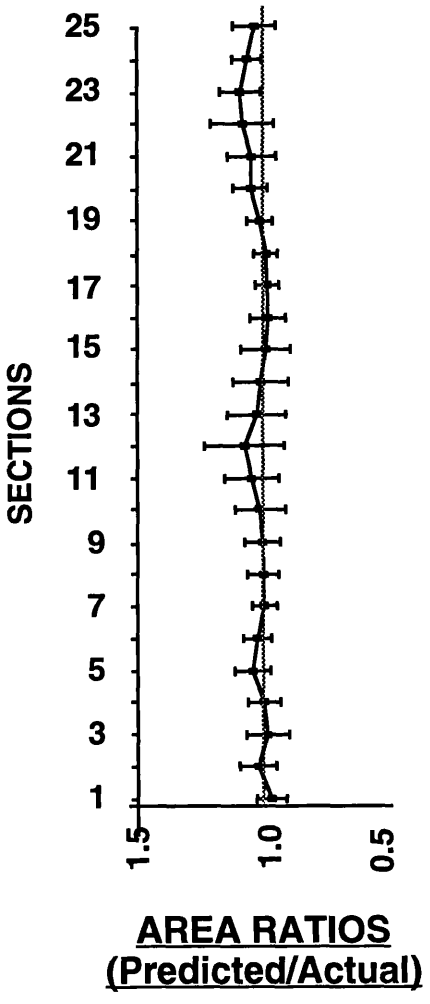

FIG. 4.10 COMPARISON OF THE DIFFERENCES IN CROSS-SECTIONAL AREA BETWEEN THE PREDICTED CANALS AND THE ACTUAL CANALS IN TWENTY-FIVE SECTIONS.

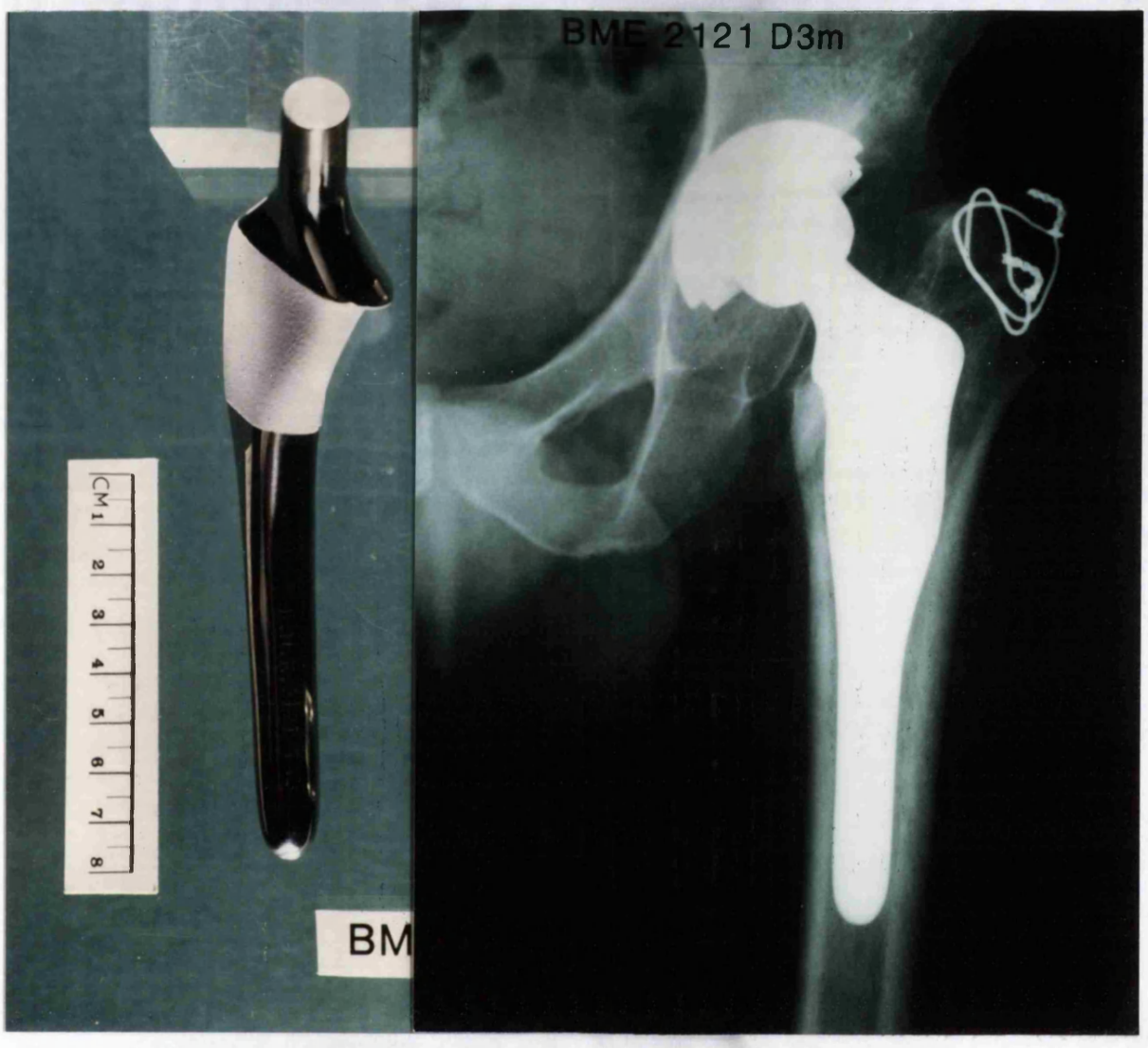

FIG. 4.11 THE FEMORAL STEM DESIGNED FOR THE CDH PATIENT: THE PROXIMAL PART OF THE STEM TWISTED ANTERIORLY, WHILE THE STEM NECK RETROVERTED TO REMAIN THE NORMAL POSITION OF THE ACETABULAR CUP

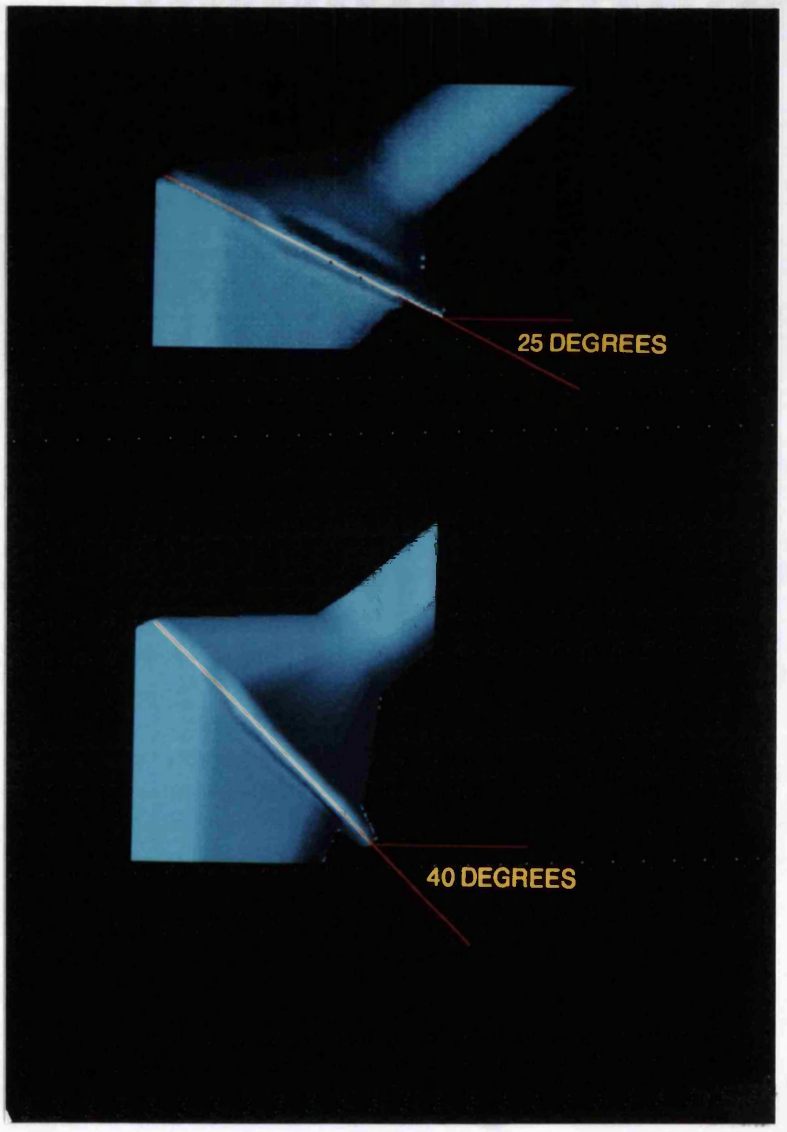

FIG. 4.12 CUSTOMIZED NECK RESECTION ANGLE FOR CAD-CAM STEM TO MEET INDIVIDUAL REQUIREMENT

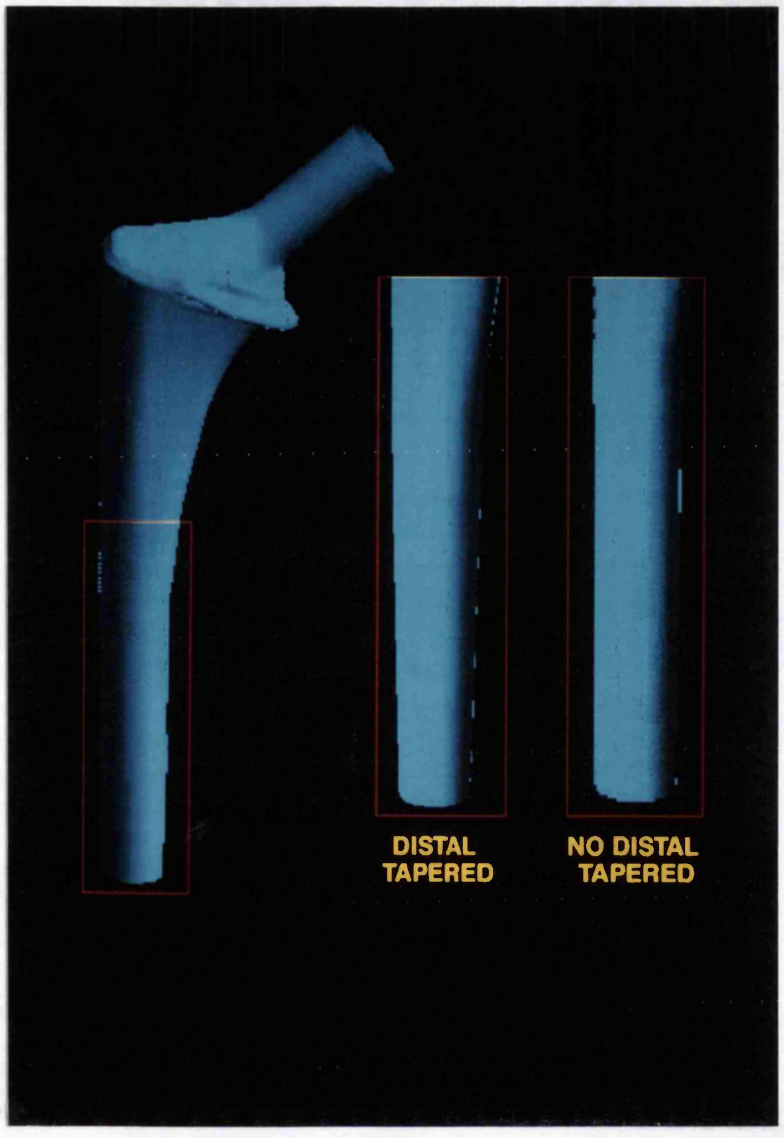

FIG. 4.13 DIFFERENT DESIGN (TAPERED OR NO TAPERED) IN DISTAL THIRD OF CAD-CAM STEM TO OPTIMALLY MATCH WITH THE INDIVIDUAL FEMORAL CANAL

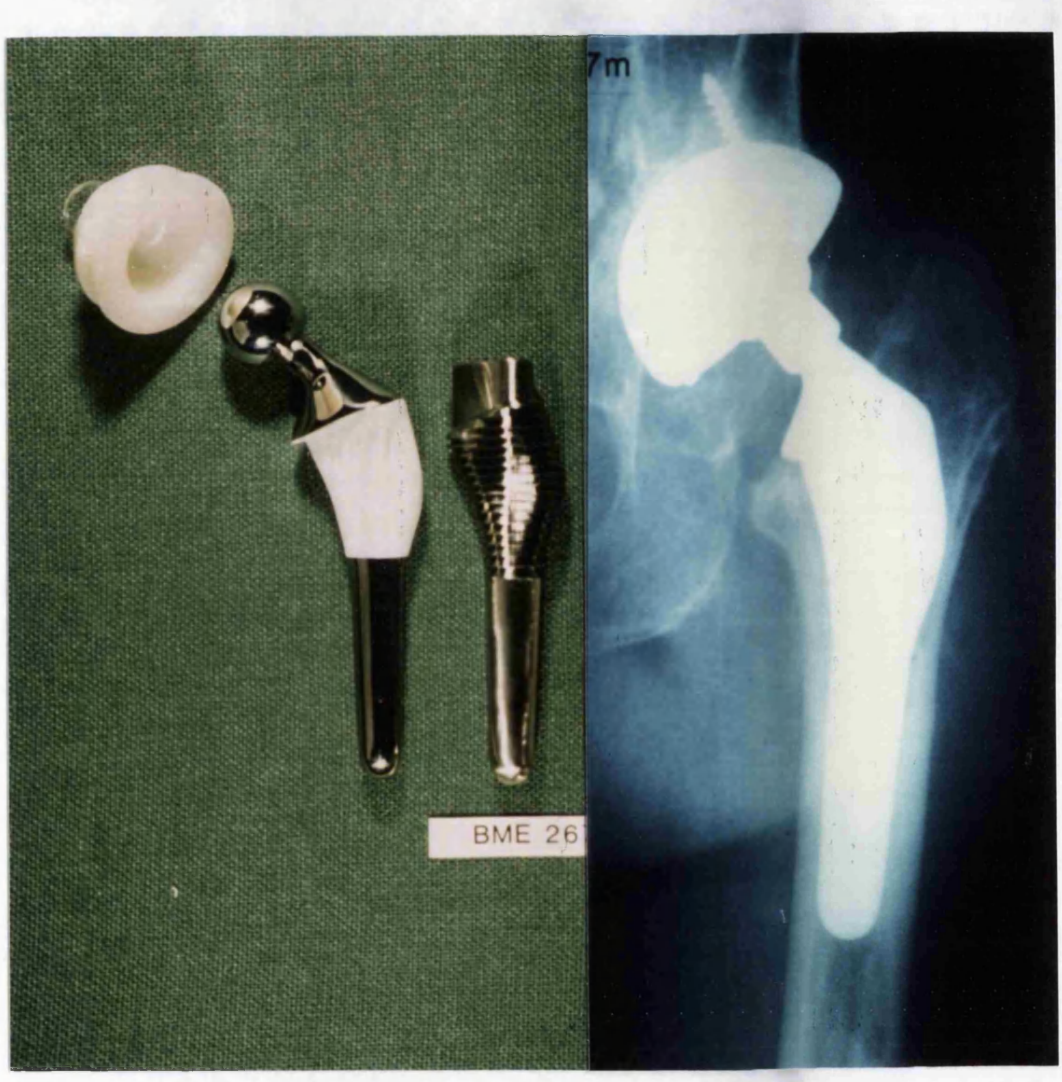

FIG. 4.14 LATERAL FLARE OF THE CAD-CAM STEM

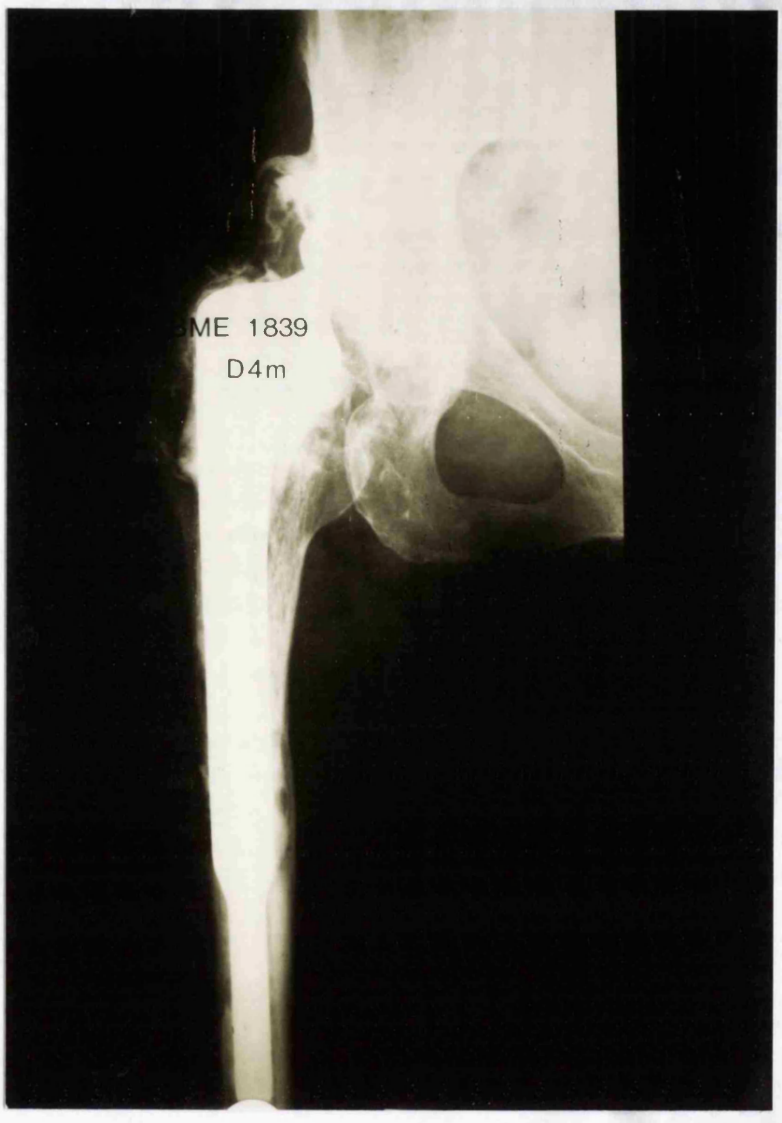

fig. 4.15 CAD-CAM STEM DESIGNED FOR REVISION CASE: THE CONICAL PART OF THE STEM BETWEEN THE UPPER AND LOWER WAS USED FOR AXIAL FORCE TRANSMISSION

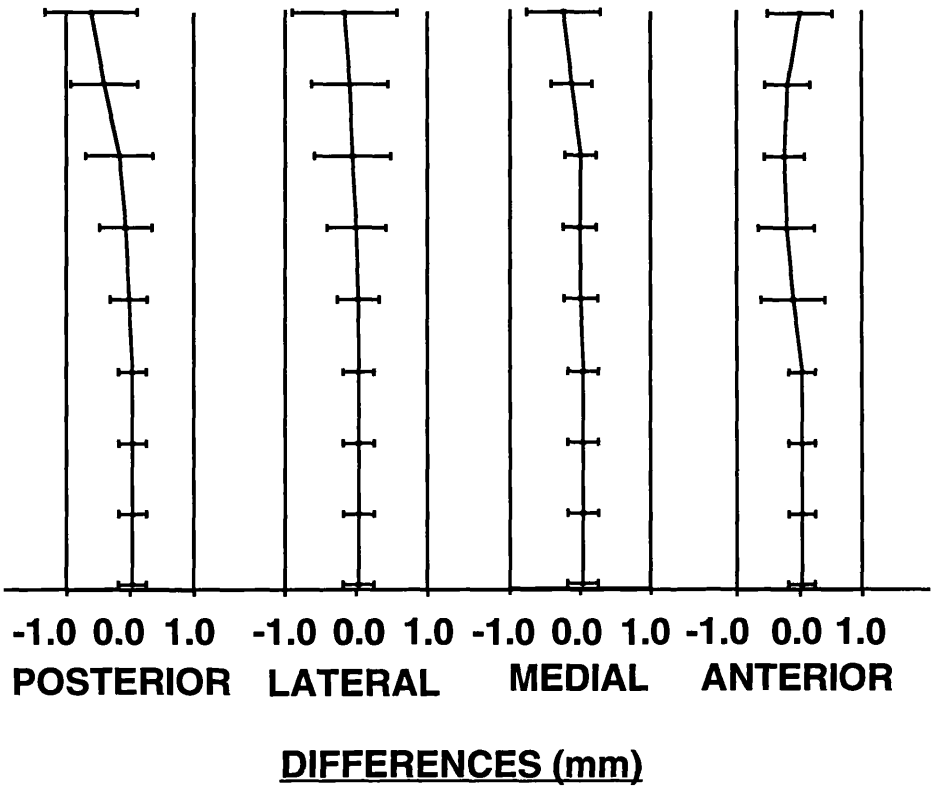

FIG. 4.16 LINE-TO-LINE COMPARISON OF THE STEMS DESIGNED FROM THE PREDICTED CANAL AND ACTUAL CANAL AT NINE LEVELS.

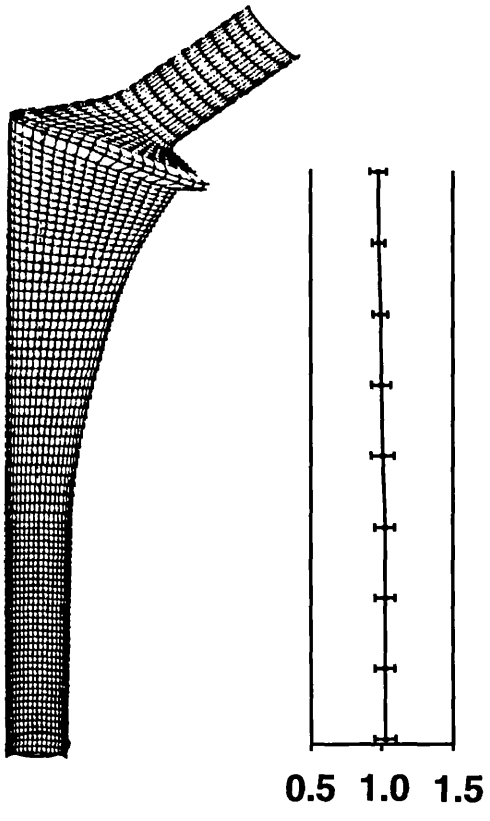

FIG. 4.17 COMPARISON OF THE DIFFERENCES IN CROSS-SECTIONAL AREA BETWEEN THE STEMS DESIGNED FROM THE PREDICTED AND THE ACTUAL CANALS IN NINE LEVELS

TABLE 4.1 RATIO OF THE DISTANCE BETWEEN CENTRAL LINE AND MEDIAL PROFILES OF EXTERNAL ROTATIONS IN NEUTRAL DEGREEOVER THAT IN VARIOUS POSITION

DEGREE / SECTION	0/20 RATIO	0/30 RATIO	0/40 RATIO	0/50 RATIO	0/60 RATIO
25	1.01	1.10	1.19	1.33	1.52
24	1.00	1.09	1.17	1.33	1.51
23	0.99	1.08	1.18	1.31	1.53
22	0.99	1.09	1.20	1.37	1.56
21	0.99	1.13	1.20	1.41	1.65
20	0.98	1.12	1.23	1.41	1.64
19	1.00	1.16	1.26	1.35	1.51
18	1.01	1.13	1.24	1.32	1.43
17	1.01	1.14	1.20	1.33	1.39
16	0.99	1.12	1.18	1.28	1.34
15	0.98	1.09	1.18	1.26	1.27
14	0.99	1.10	1.19	1.27	1.26
13	1.00	1.09	1.20	1.26	1.26
12	1.00	1.05	1.17	1.21	1.20
11	1.00	1.07	1.17	1.22	1.21
10	1.00	1.02	1.13	1.17	1.16
9	1.00	1.00	1.06	1.14	1.05
8	1.00	1.00	1.04	1.08	1.02
7	1.00	1.01	1.02	1.05	1.02

CHAPTER FIVE

EVALUATION OF THE STEMS FIT WITH THE FEMORAL CANALS

5.1 Introduction

Fit-and-fill describes the geometrical relations of the stem with the medullary cavity. Such relations are intended to provide indications of load transmission and stem-bone interface motion. Fit is a measure of the closeness of the stem to the cortical wall, which has usually been measured as gap distances around the periphery of transverse sections. Fill is a ratio of the area of the stem to the area of the canal across a transverse section (Fig 5.1).

It has been shown that a close fit of the stem in the proximal canal can achieve closer to normal stress distribution and less stem micromotion. However, if the stem is designed to fully fill the canal, then it will not be insertable due to the three-axis curvatures of the femur (Walker et al 1987). Therefore, the 'optimal fit' in proximal canal has always been a major concern during stem design. On the other hand, complete fill of a stem is not entirely justified by clinical results, as a large diameter stem could increase the stem stiffness, resulting in bone resorption, remodelling and thigh pain (Franks et al 1992). For this reason, stem fill should not be the only criterious for a stem. However, stem line-to-line fit with a canal directly reflects the stem-bone contact, which affects the stress distribution and stem stablization.

Therefore, a line-to-line fit of the CAD-CAM custom stems with the cortical bone was analysed in two categories. The stem fit predicted in the computer was compared with the actual stem fit obtained on bone specimens. The fit of the custom stems was also compared with that of standard stems in the same femur.

5.2 Materials and methods

5.2.1 Comparison between computer predicted fit and experimental fit

5.2.1.1 Stem designs and insertions

Ten cadaveric femora without gross abnormalities were used. All the soft tissues were removed and the femurs were fixed in formalin one week before the study. The femurs were radiographed in A-P and M-L views with the scale marker beside the femoral shaft. The radiographs were digitized and three-dimensional canals were reconstructed by using the Hip Design Workstation as described in detail in chapter 4.

The custom stems were individually designed for each bone to achieve close fit in the proximal-medial and proximal-anterior regions, and maximum fill in the distal region. The geometry of the custom stems and each canal were stored in the computer. The actual stems, which were made of Acetal, were then manufactured in the CNC machine. The stems had no grooves and the surfaces were polished.

The femoral necks were resected at twenty-five degrees. The canals were prepared with a matched-size reamer and identical rasps to make sure that each stem achieved a best fit.

5.2.1.2 Analysis of predicted fit

A software program was written to analyse the fit according to the geometrical data of the stems and canals. Firstly, the coordinate system of the stems and canals were transformed so that the stems were

correctly positioned into the canals. Secondly, the stems and canals were converted into one hundred sections from the neck resection level to the stem tip by using a linear interpolation algorithm. Finally, all the sections were mathematically transformed to the horizontal so that each canal section was aligned with the corresponding stem sections.

For analysis of the fit, a line was drawn between the two adjacent points on the stem section (line A), and a normal line was drawn from the middle of the line A to the canal periphery (line B). The distance of the line B was defined as " fit " between the stem and the canal (Fig. 5.2), and the angle between the line B and a horizontal line was calculated and used to determine which quadrant the point belonged to (medial, anterior, lateral and posterior). This process was repeated around the stem sections for every point.

5.2.1.3 Analysis of actual fit

The femoral bones together with the inserted custom stems were transversely CT scanned from neck resection to stem tip, seven slices in the proximal half and four in the distal half. The slice intervals were proportional to the stem-bone length. The boundaries of the inner cortex and the stems were digitized from the CT films and then formatted into forty points in each section with 100 sections from neck resection to stem tip, both for the stems and canals, by using linear interpolation. The stem-canal fit was calculated in the computer by the technique described in 5.2.1.2.

5.2.2 Comparison of fit between standard and custom femoral stems

5.2.2.1 Design and manufacture of custom and standard femoral stems

Ten cadaveric femora without gross abnormalities were used. The femurs were close to an average length (447 mm) to reduce the number of standard stems required. All the femoral bones were radiographed. The custom stems were designed and manufactured for each bone, while for the standard asymmetrical and symmetrical stems, the nearest size of the stem was selected for each bone. The details of the design of the custom and standard stems were described in chapter 4. The custom and standard stems had the same length, so that the comparison of the fit was made at same level. In order to perform CT scans, all the stems were made of acetal, manufactured in the CNC machine, and the surfaces were polished.

5.2.2.2 Stem insertion, CT scan and digitize

The standard surgical techniques were carried out for stem insertion. The femoral neck was resected at 25 degrees, and the distal canal was reamed to the approperiate diameter. Standard rasps were used for the symmetrical and asymmetrical stems, whereas the custom rasps identical to the stem shape were employed for the custom stems. The stem insertion sequence was symmetrical, asymmetrical and custom stems. Each stem-bone was CT scanned, including seven slices in the proximal half and four slices in the distal half. The inner cortical wall and stem boundary were digitized and the fit was analyzed as (5.2.1).

5.3 Results

5.3.1 Comparison between computer predicted fit and experimental fit

The stem-canals were divided into proximal, middle and distal regions (Fig. 5.3). Each section was then divided into medial, anterior, lateral and posterior quadrants (Fig. 5.4). For statistical analysis, a paired student t-test was used.

A. Proximal regions:

For the medial and anterior sides, the fit gaps were very small for both predicted and actual, only 0.48±0.48 (medial) and 1.46±0.31 (anterior) mm for predicted fit, 1.64±0.47(medial) and 2.19±0.6 (anterior) mm for actual fit. However, the differences between the predicted and actual fits were significant ($P<0.01$).

For the lateral and posterior sides, the fits were not so good for both the predicted and actual, 6.42±2.61 mm (lateral) and 7.75±1.98 mm (posterior) for the predicted fit, 5.95±2.05 mm (lateral) and 9.12±1.52 mm (posterior) for the actual fit (Fig 5.5 a). This was primarily because of the greater and lesser trochanters, where the stems could not fill in the canal adjacent to the cortical wall.

B. Middle and distal regions:

Overall, the predicted fit was 1.61±0.8 mm in the middle region and 1.09±0.65 mm in the distal region. The actual fit followed the same trend, but with larger values, 2.34±0.83 mm for the middle region and 1.29±0.74 mm for the distal region (Fig 5.5 b.c). Significant differences were found in the middle posterior and distal medial regions. The results showed that the predicted fit was, in general, better than the actual fit.

5.3.2 Comparison of fit between custom and standard stems

For statistical analysis, the variances of mean values for three types of stems were analysed by using the multivariate ANOVA (SYSTAT package). If the global analysis of variance was significant at 5 per cent level, a post-hoc pairwise comparison was carried out (Turkey HSD, Honest Significant Difference) to examine any differences between stem types.

A. Proximal region:

On the medial side, the fit for the custom, asymmetrical and symmetrical stems was 1.64±0.47, 2.74±0.87 and 2.92±1.12, respectively, suggesting that the custom stems were significantly better than the symmetrical and asymmetrical stems ($P<0.05$), but no difference was observed between the asymmetrical and the symmetrical stems ($P>0.05$) (Fig 5.6 a). On the lateral side, however, the fit for the custom stem (5.9±2.0) was only slightly better ($p>0.05$) than that for the asymmetrical stem (6.2±2.0) and symmetrical stem (6.2±2.4) (Fig 5.6 b). The fit on the posterior side was similar for the three types of stem ($P>0.05$), from 9.1 to 10.2 mm (Fig 5.6 c). Whereas, on the anterior side, the custom and asymmetrical stems showed a closer fit ($p<0.05$) than the symmetrical stems (Fig 5.6.d).

B. Middle region:

Overall, the custom stem showed smaller gaps (2,34±0.83) than the asymmetrical stem (2.98±0.8) and the symmetrical stem (2.99±0.95) (Fig. 5.7). However, such a difference was not statistically significant ($p>0.05$).

C. Distal region:

In the distal region, the results was similar to those obtained from the middle region. The custom stems showed a better fit (1.29±0.74) than the asymmetrical stem (2.22±1.06) and the symmetrical stem (2.04±0.88) (Fig. 5.8). However, no significant differences were obtained ($p>0.05$).

5.4 Discussion

5.4.1 Comparison between computer predicted fit and experimental fit

In the proximal region, on the lateral side, the actual fit had less value (5.95±2.05) than the predicted fit (6.42±2.61), while on the medial side the results were reversed. This indicated that the actual stems were placed in valgus. The overall differences of 0.3-1.3 mm between the predicted and the actual fit reflected that reaming and rasping in preparation of the cavity were not precise. The custom tooling system needs to be improved to insert the stem to the position of pre-operative planning. This phenomenon was also observed by other investigators (Bargar et al 1992), who obtained an average linear gap error of 1.2 mm, with only 21 percent of the implant periphery in contact with bone. They attributed this to tearing of the cavity by the rasp and put forward a method for machining the cavity using a milling cutter under robotic control.

5.4.2 Comparison of fit between custom and standard femoral stems

The results showed that the custom stems had a closer fit than the standard asymmetrical or symmetrical stems, particularly in the proximal medial region where the high forces are transmitted. The significance of this could be reflected by the stress and strain distribution of the bone, and could also be reflected by the bone remodelling process. Because the canal geometry is not standard, the standard stems can not provide a consistent fit, while the custom stems can fit with each individual canal.

In the proximal and middle regions, larger gaps were shown on the posterior side for all three types of stem. This was mainly because of the protrusion of the lesser trochanter. In the proximal anterior region, the custom and asymmetrical stem a showed closer fit than the symmetrical stem due to the anterior flare. This advantage might account for the rotational stabilities of the asymmetrical stems, especially under torsional loading.

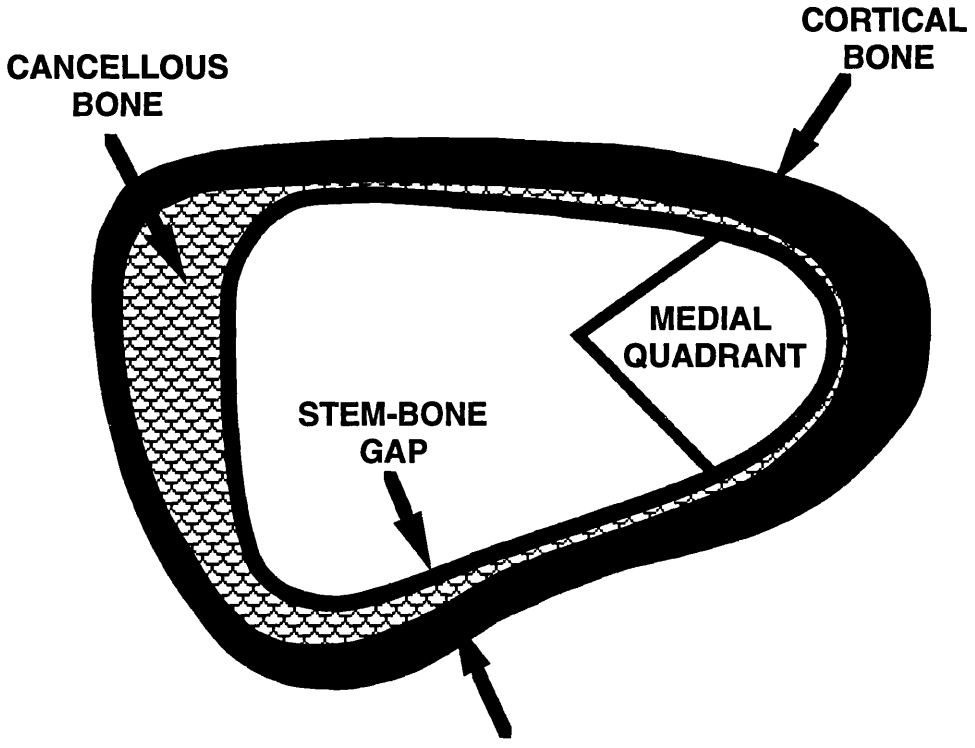

FIT = MEAN VALUE OF STEM -BONE GAP AROUND PERIPHERY OF INTEREST EG. ENTIRE PERIPHERY OR MEDIAL QUADRANT

$$\text{FILL} = \frac{\text{AREA OF STEM SECTION}}{\text{TOTAL AREA WITHIN CORTICAL PERIPHERY}}$$

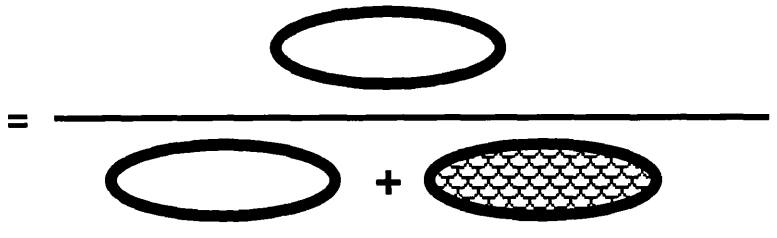

FIG. 5.1 DIFINITION OF FIT AND FILL

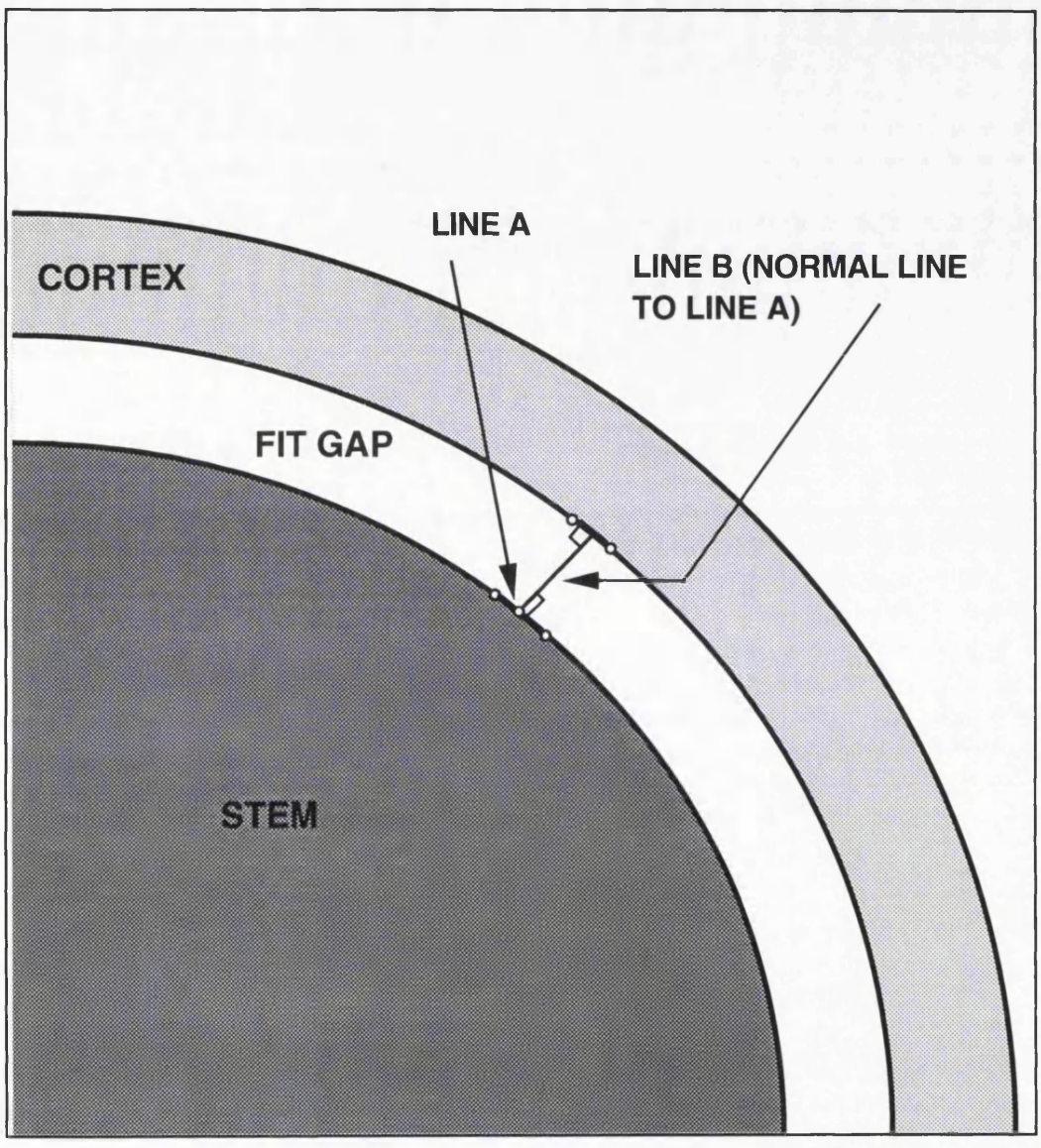

FIG.5.2 THE TECHNIQUES FOR COMPUTER PREDICTION OF FIT: LINE A IS A JOINT LINE OF TWO ADJACENT POINTS ON STEM PERIPHERY, LINE B IS THE NORMAL LINE TO THE LINE A. THE LENGTH OF THE LINE B IS THE FIT GAP.

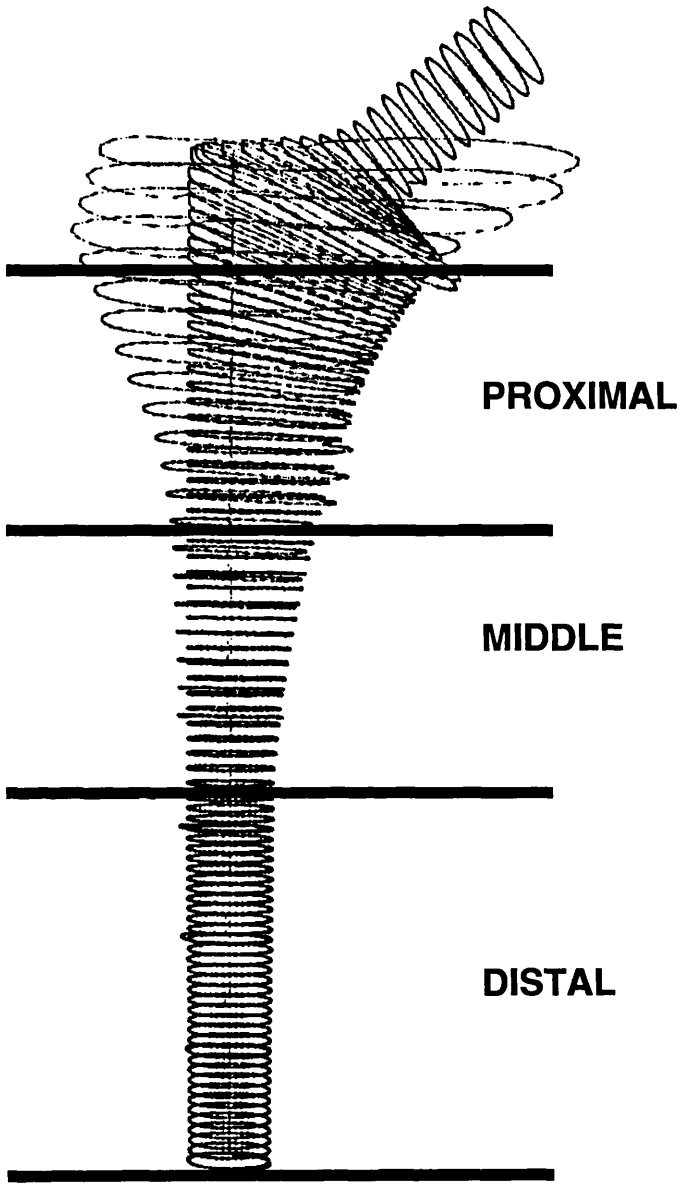

FIG.5.3 DEFINITION OF REGIONAL DIVISION OF CANAL- STEM: 71-100 % OF THE STEM LENGTH WAS DEFINED AS PROXIMAL REGION, 41-70 % WAS MIDDLE REGION, AND 1-40 % WAS DISTAL REGION

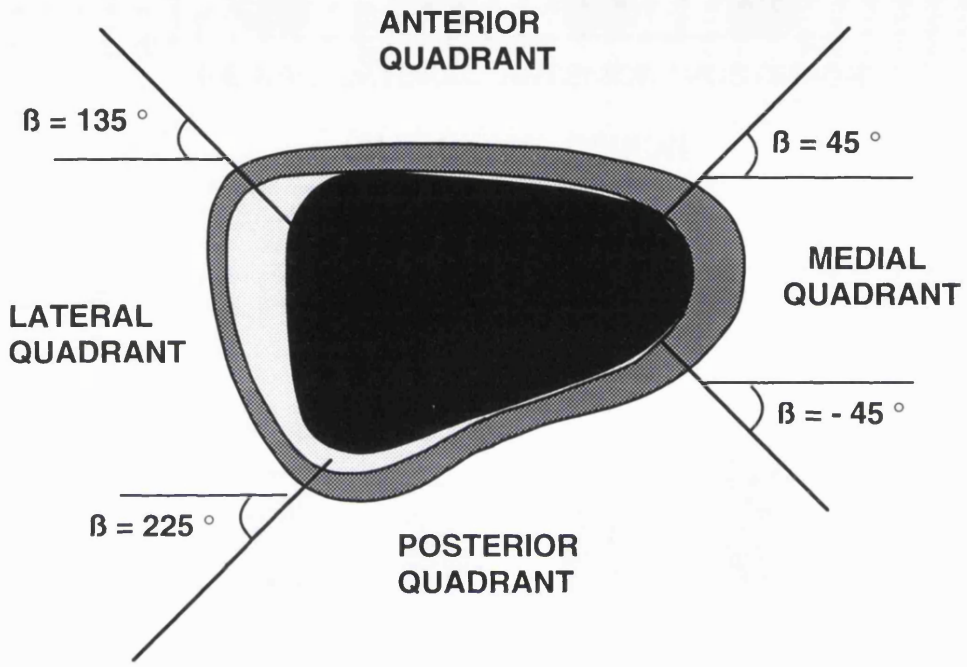

FIG.5.4 THE CROSS SECTION OF STEM-BONE WHICH DIVIDED INTO FOUR QUADRANTS: MEDIAL(45 ~- 45 DEGREES), ANTERIOR (45 ~135 DEGREES), LATERAL (135 ~225 DEGREES), AND POSTERIOR (225 ~- 45 DEGREES).

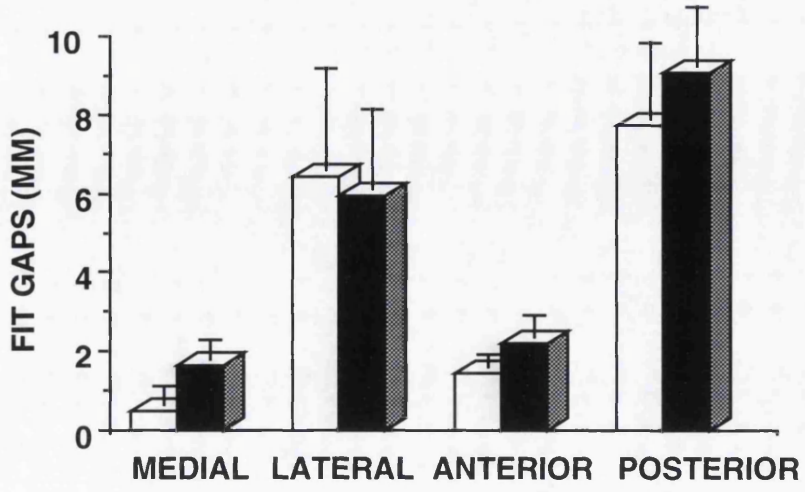

(A) PROXIMAL REGION

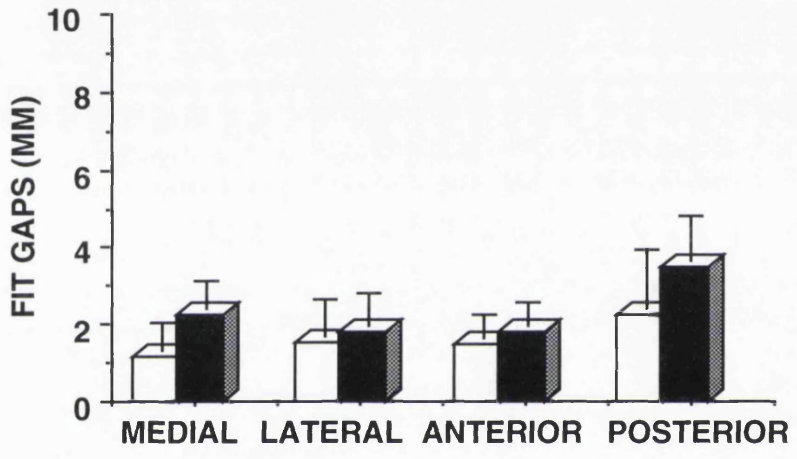

(B) MIDDLE REGION

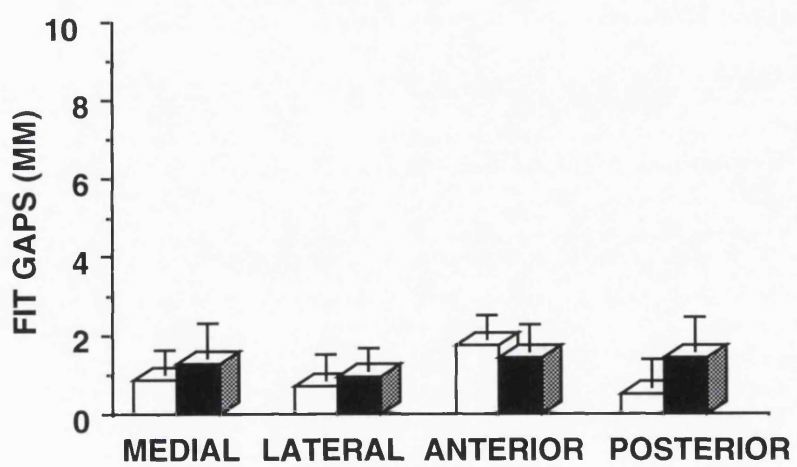

(C) DISTAL REGION

FIG. 5.5 COMPARISON OF THE PREDICTED FIT WITH THE ACTUAL FIT IN DIFFERENT REGIONS

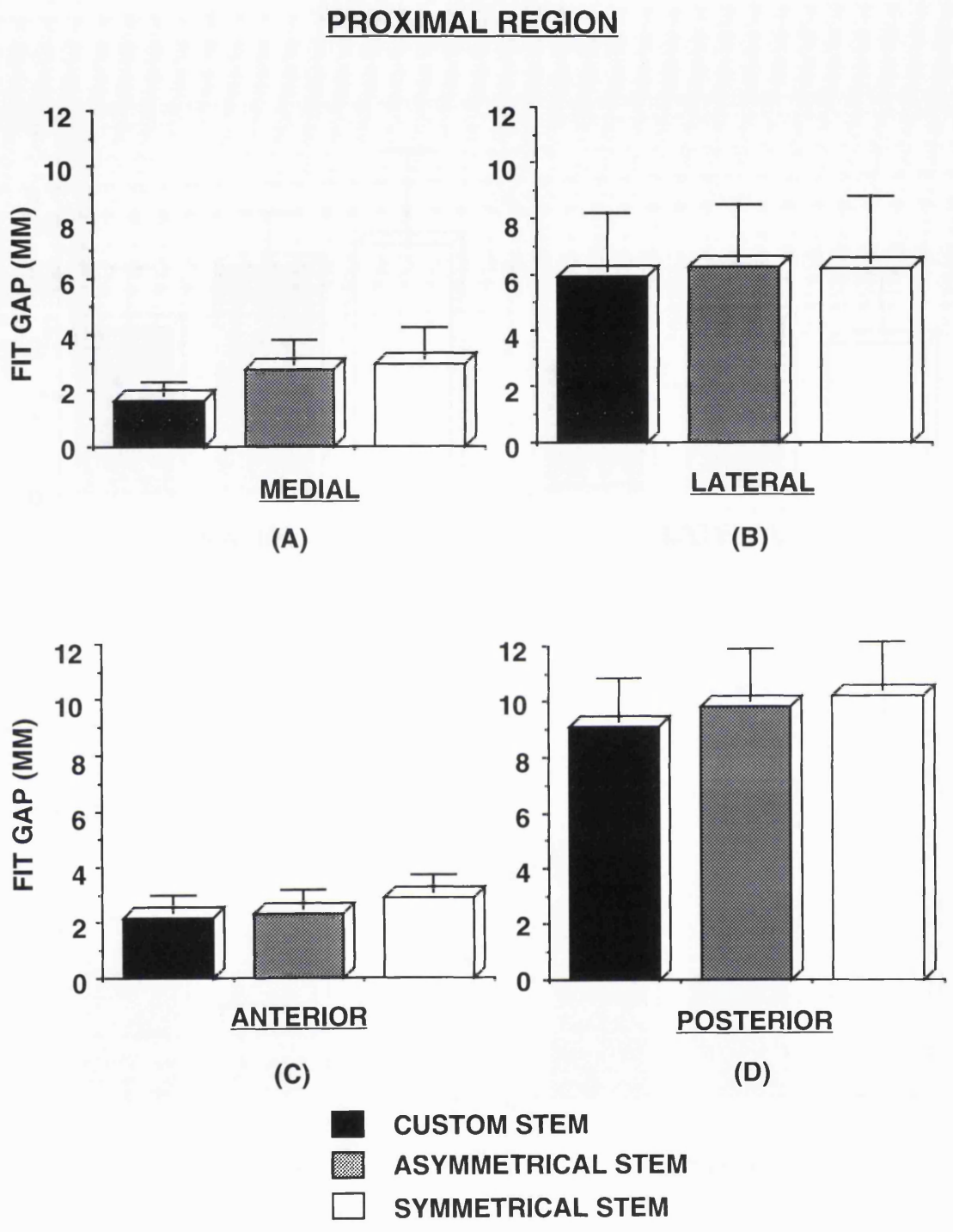

FIG.5.6 COMPARISON OF FIT IN FOUR QUADRANTS OF PROXIMAL REGION BETWEEN CUSTOM, ASYMMETRICAL AND SYMMETRICAL STEMS

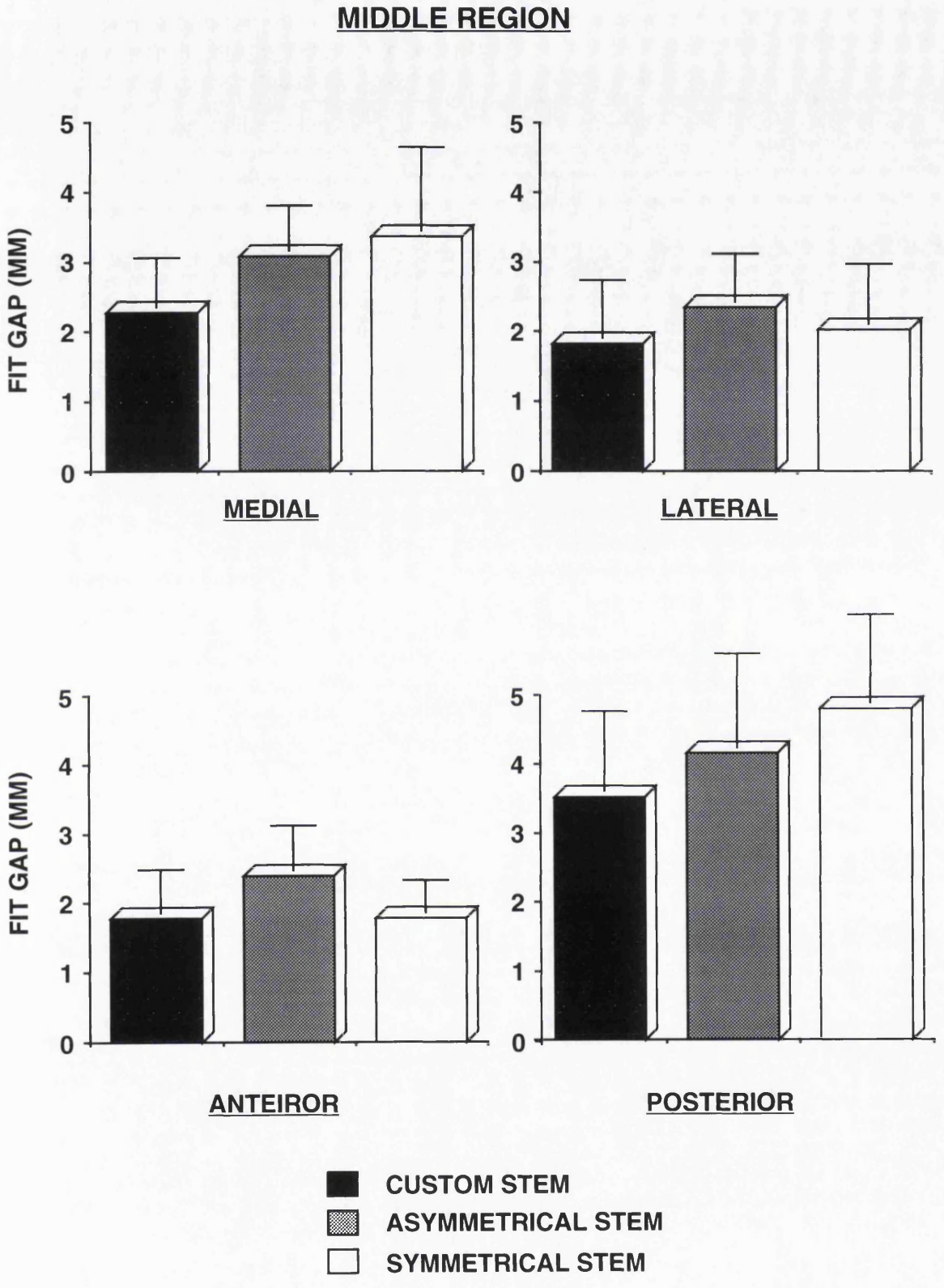

FIG. 5.7 COMPARISON OF FIT IN FOUR QUADRANTS OF MIDDLE REGION BETWEEN CUSTOM, ASYMMETRICAL AND SYMMETRICAL STEMS

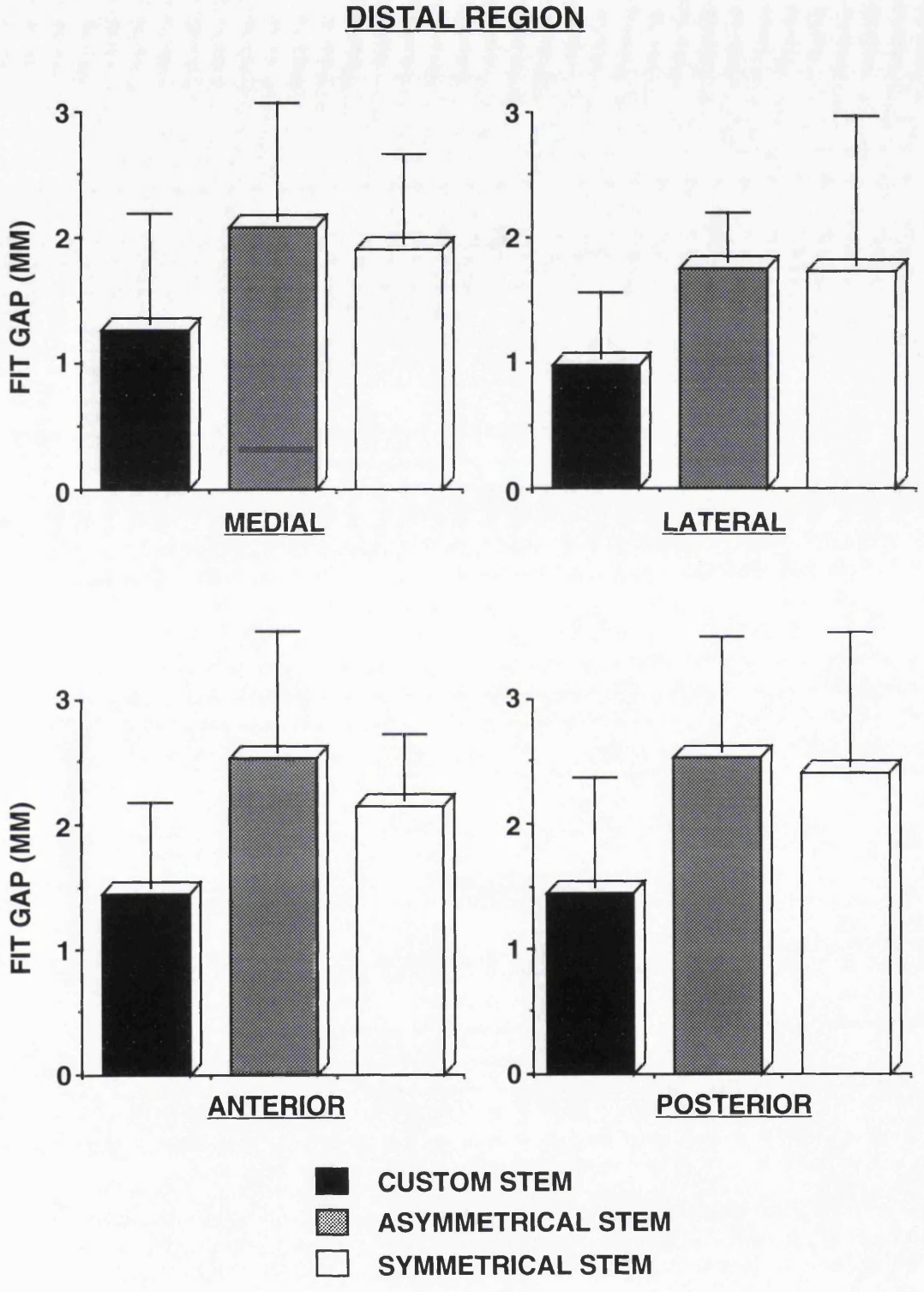

FIG. 5.8 COMPARISON OF FIT IN FOUR QUADRANTS OF DISTAL REGION BETWEEN CUSTOM, ASYMMETRICAL AND SYMMETRICAL STEMS

CHAPTER SIX

FEMORAL STRAIN DISTRIBUTION FOLLOWING CUSTOM AND STANDARD HIP REPLACEMENT

6.1 Introduction

It is clear that long-term clinical success of total hip replacement can be affected by the bone remodelling process. After stem insertion, bone remodelling can be affected by many factors, of which stress distribution is certainly important in respect of bone density changes. It has already been noted that the skeletal structures have the ability to adapt themselves to meet the functional demands placed upon them. Disuse atrophy and over-use hypertrophy are typical clinical examples. Several different theories have been postulated to explain the phenomenon of bone resorption and deposition. Wolff in 1870 had addressed his observation which been afterwards called Wolff's law, that is "...the law of bone remodelling is the law according to which alterations of the internal architecture clearly observed and following mathematical rules, as well as secondary alterations of the external form of the bones following the same mathematical rules, occur as a consequence of primary changes in the shape and stressing or in the stressing of the bones". Although there are some controversial issues about Wolff's law, it is the fact that implant-bone interface stresses, compressive, tensile and shear, can affect or moreover control the bone remodelling process, such as bone resorption at the interface, replacement by fibrous tissue, and unloading of the bone. On the other hand, bone-implant interface stresses can be affected by other factors. The fit of the implant geometry with the bone will determine the stress distribution of the bone. The surface of the implant, whether smooth, macro-grooved, porous or hydroxyapatite coated, will determine the extent to which shear, tensile and compressive stresses can be transmitted. Therefore it is vitally important to study the stresses and strains of the femoral bone and their alterations following total hip replacement. It is also necessary to study the changes in the stresses

and strains from the normal state, which is one criterior to evaluate different designs of hip stems.

6.2 Evaluation of the methodology of strain measurements

Many methods can be used to determine stresses and strains on the bone. These include brittle lacquers, holography, thermography, strain gauges, two-dimensional or three-dimensional photoelastic modelling and photoelastic coatings. In addition, finite element modelling is also widely used to analyse the stresses and strains. Each of these techniques has its strengths and limitations, but induvidually can yield valuable data.

6.2.1 Holography

Holography allows the reproduction of a wavefront of light, scattered by a three-dimensional object, and the photographically recorded interference patterns between two laser beams. The reference beam passed by a series of mirrors, from the laser to the photographic plate; the object beam is reflected from the object under study to impinge upon the photographic plate. The photographic plate is thus exposed to the reference and object beams simultaneously and the interference between the beams appears as a diffraction pattern which constitutes a hologram. Total absence of mechanical movement or vibration is essential during the exposure. Holographic interferometry permits the measurement of distortions on an object which has had a hologram recorded at one load and a separate hologram recorded at another load. This procedure is described as double-exposure holographic interferometry. The double-exposure of the two images produces a series

of interference fringes superimposed on the surface of the object. Properly interpreted, a hologram can thus be used for strain and stress analysis.

Holographic techniques provide non-contacting full-field displacement information. However, its extremely high sensitivity only allows small deformations to be recorded. Also, the direct comparison with associated local strain data is a formidable task. Therefore, the holographic techniques may not be suitable for comparison of strain distribution between a number of stems inserted in one femoral canal.

6.2.2 Strain gauge

Electric resistance strain gauges are commonly applied in biomedical engineering, especially in orthopaedics. The strain gauge utilizes the principle demonstrated by Lord Kelvin in 1856 that a conducting filament changes its electrical resistance as its length is changed. Strain sensitivity is defined as the ratio of the relative change in electrical resistance of a conductor to the relative change in its length. An applied load leads to a change in test piece geometry causing a change in gauge resistance, for a fixed voltage applied across the gauge, resulting in a change in the circuit current. The universally employed circuit with strain gauges is the Wheatstone Bridge. If the resistances change, the bridge becomes imbalanced and a connected galvanometer will obtain a reading which is proportional to the bridge imbalance. There are three types of strain gauges, wire gauge, semi-conductor gauge and foil gauge. The foil gauge is most suitable for biomedical applications on account of its low cross-sensitivity, the absence of stress concentrations

and the ease of obtaining excellent contact between gauge and test-piece even in highly contoured locations.

Although the strain gauge is a highly accurate device for recording strains on the surface of the object, invalid measurements can also be obtained. These influencing factors include inaccurate gauge position (Little et al 1990), gauge misalignment (Pople, 1980, Tuttle and Brinson 1984), and strain gradients when the gauge is mounted in an area of strain concentration producing a strain value unrepresentative of the true strain at a point (Perry 1984). In addition, selection of strain gauges is also important as some parameters can influence the measurement, such as foil, backing material, self temperature compensation, bridge voltage, protective coatings solders and lead wires (Window and Holister 1982).

In the past, strain gauge have often been used in analysing prostheses themselves (Weightman 1977), and prostheses which were implanted in cadaveric bone (Finlay et al 1986). However, because strain gauges only provide point information, the areas of interest must be identified prior to application of the gauge, otherwise misinterpretation can occur by inaccurate gauge positioning (Little et al 1990). For the femur, it was suggested that five rows of rosette gauges applied to the medial, lateral and anterior aspects were adequate. Finlay et al (Finlay et al 1982) recommend that 22 -25 rosette strain gauges could be arranged in five rows depending on the size of the bone. However, Carter et al (Carter et al 1981) have pointed out that for an accurate strain measurement the space between the rosette gauges around the bone circumference is very important, as greater gauge spacing yields less information of strain distribution. However, on the other hand, if too many strain gauges were

used, then the reinforcing effect of the gauges has to be considered. Therefore, for measuring the detail of stress distribution on the bone, there are practical limitations in the number of gauges applied.

6.2.3 Finite element analysis

The finite element method is essentially a process through which a continuum with infinite degrees of freedom can be approximated by an assemblage of subregions (or elements), each with a specified but now finite number of unknowns. The difference between the experimental and theoretical analysis is that, the experimental stress analysis uses a physical model, while the theoretical analysis uses a set of equations. The accuracy and realism of the mathematical model is based on number of assumptions and definitions, such as external loads, geometry, material properties and boundary conditions. The nature of these simplifications determines whether the model, and hence the result, are realistic in a quantitative, or only in a qualitative sense. The accuracy of the model can be checked with a convergency test, while the realism of the model can only be assessed by experimental verification or other direct means.

The Finite Element Model (FEM) was initiated in stress analysis of structures in engineering mechanics, and then introduced in the orthopaedic literature in 1972 (Brekelmans 1972). The use of the FEM has been reported during the last decade in an increasing number of orthopaedic research studies, which includes studies of stress related bone architecture and bone remodelling processes, design and optimization of artificial joints and fracture fixation devices. Many FEM

analyses are now focused on joint replacement, in particular the total hip prosthesis. Early studies using FEM used 2-D models, because mesh accuracy was easier to obtain in terms of cost efficiency. Anatomic 3-D models are more realistic and precise in geometrical descriptions, but practically numerical accuracy is sometimes difficult to obtain due to computer time requirements and memory space limitations. A major advantage of FEM is that it can carry out parametric analysis to study the effect of different variables, such as stem-bone interface bonding, stem geometry and material stiffness, regions of cortical or cancellous bone contact with stem. However, the complexity of the bone structures and their individual variability, particularly in precise descriptions of material properties and boundary connections, make finite element modelling very difficult, and need highly sophisticated and systemic experimental data to refine and evaluate FEM. Recently, with the development of advanced powerful computer technology, it is possible to construct realistic bone models in geometry and material properties by going direct from CT scan to the FEA model (Keyak et al 1993).

6.2.4 Photoelastic coating

6.2.4.1 Background

The method of birefringent photoelastic coating extends the classical procedures of two and three dimensional model photoelasticity. The concept of photoelastic coatings was first proposed by Mesnager of France in 1930, and the method was re-examined by Oppel of Germany in 1937. Mesnager tried to bond segments of glass to structures. The difficulties in machining glass, its high modulus which caused significant reinforcement, and the lack of a proper adhesive for bonding the

structure prevented this approach from being developed. Oppel used flat sheets of Bakelite. Here, the development of a severe "time-edge effect", lack of strong adhesives, and applicability only to flat surfaces prevented this method from being used industrially. With the availability of Epoxy resin in the 1950s, the required high-strength adhesive and a photoelastic sheet relatively free of time-edge effect could be produced. The development of the photoelastic coating method proceeded rapidly with contributions in materials, techniques, and instruments from Fleury and Zandman in France, D'Agostino, Drucker, and Liu in the United States, and Kawata in Japan.

However, at this time photoelastic coatings were still considered an academic curiosity by those in industry because a technique to apply coating surfaces with compound curvature had not been developed. Eventually, Zandman developed the contour sheet procedure for applying a constant thickness coating to curved surfaces without introducing residual birefringence. At the same time he developed a portable reflection polariscope, making the method practicable for quantitative measurements under industrial conditions. In the late 1950's Zandman, Redner, and Riegner treated the problem of reinforcement of the coating and developed techniques to account for reinforcing effects. Thus an obstacle was removed for obtaining quantitative data when coating thickness is not negligible with respect to the thickness of the part.

Following the developments of epoxy coating materials and adhesives, sheet-contouring techniques, and analysis procedures, the method was generally accepted. Considerable research was carried out to develop more sensitive and higher elongation coating materials. Several

instruments for laboratory and field use, particularly designed for photoelastic coatings were introduced. Methods were advanced for using the coatings in analysis of plasticity, thermoelasticity, vibrations, and wave and crack propagation. In addition, many engineers used the method to solve a wide variety of design problems.

Photoelastic coating has many advantages compared to the other methods of stress analysis. It provides point-by-point quantitative data or full-field stress patterns, which enable investigators to examine the complete strain distribution on an object and directly highlight areas of stress concentration. The method is non-destructive. Since the coatings can be applied directly to prototype parts and structures, it eliminates the need for elaborate and costly models. Both static and dynamic strains can be measured.

Photoelastic coatings have been used for a number of investigations in the field of biomechanics and orthopaedics. For example, a human skull was coated and then subjected to shock loading to simulate blows with sharp and dull instruments. In other examples, this strain measurement technique was applied for studying the biting action of the human jaw, fatigue failures in bone plates, and for evaluating the different designs of artificial legs and hip prostheses. For the purpose of comparing different designs of femoral stems, the photoelastic coating is particularly valuable.

6.2.4.2 Mechanism

A ray of ordinary monochromatic light (light of a single wave length between 400 and 800 nm) consists of a series of transverse wave

vibrations in random planes. As this ray passes through the polarising filter (which has its optical axis in the vertical plane), only the vertical vibration of the ray can pass through. This vibration is known as a plane polarised light wave and it is sinusoidal in character. As this plane polarised light wave passes through the coating, the wave splits up into two separate components, one of which vibrates in the direction of the algebraic maximum principal stress **s1**, and the other in the direction of the algebraic minimum principal stress **s2**. This is because the plastics becomes birefringent under strain. Also, each component wave passes through the plastic coating at a velocity which depend upon the magnitude of the particular principal stress and upon the optical properties of the plastics itself. The change in index of refraction is a function of the strain applied, similar to the resistance change in a strain gauge. If the magnitude of the two principal stresses are different, then there will be a phase difference in the emerging component waves which can be used as a measure of the magnitude of **s1-s2**. When these two component waves are reflected back by the bonding adhesive to the analyser, their horizontal components will pass through and the effect will be to produce two component waves of similar amplitude and retaining the phase difference. There are the essential ingredients for optical interference which gives rise to the fringe pattern called **isochromatics**.

Furthermore, if one of the principal stresses is parallel with the optical axis of the polariser, then the emerging plane polarised light wave enters the model in a direction parallel to a principal stress. Since there is no component in another direction, the plane polarised light wave passes through unchanged to meet the analyser. Since the optical axis of the analyser is perpendicular to the polariser, consequently no light can pass through the analyser. Thus a black spot will be observed. This black spot

lies with other black spots to form a constant inclination of principal stress directions which is termed an **isoclinic.**

6.2.4.3 Quarter wave

In using a plane polariscope, the isoclinic lines will be superimposed upon the fringe pattern and cause confusion when the stress magnitudes are analysed. In order to solve this problem, two quarter wave plates can be placed into the optical system. The plane polarised light emerging from the polariser will be changed into circularly polarised light on passing through the first quarter wave plate. The circularly polarised light does not have any directional property. When it enters the plastic coating, the circularly polarised light will be changed to the elliptically polarised light. The second quarter wave plate will then convert it back into two plane polarised component waves. Because of the non-directional character of circularly polarised light, the isoclinic fringes will not be produced in the plastic coating, only the isochromatic fringes will be seen which give information on the stress magnitudes.

When a photoelastically coated femoral bone is subjected to loads, the resulting stresses cause strains to exist generally throughout the bone and over its surface. The surface stresses and strains are commonly the largest compared with the interior of the bone. Because the photoelastic coating is intimately and uniformly bonded to the surface of the bone, the strains in the coating produce proportional optical effects which appear as isochromatic fringes when viewed with a reflection polariscope. This linear relationship is expressed as follows:

$$ex - ey = f \times N$$

where ex and ey are the principal strains in coating and bone surface; f is the fringe value of the coating (obtained by calibrating the coating); N is the fringe order.

6.2.4.4 Colour fringe and fringe order

White light is composed of all wavelengths in the visible spectrum. The relative retardation which causes extinction of one wavelength (colour) does not generally extinguish others. When, with increasing birefringence, each colour in the spectrum is extinguished in turn according to its wavelength (starting with violet, the shortest visible wavelength), the observer sees the complementary colour. It is these complementary colours which make up the visible fringe pattern viewed through analyser. The photoelastic fringe pattern appears as a series of successive and contiguous different-colored bands (isochromatics) in which each band represents a different degree of birefringence corresponding to the underlying strain. Thus the colour of each band uniquely identifies the birefringence, or fringe order. The complete sequence of fringe colours startes with black if the femoral bone has not been loaded, followed by yellow, red-purple, and blue-green. First integral-order fringe occurs between the red and blue, and the second fringe between red and blue-green, and the third between red and green. The colour fringes become narrower and closer as the strain gradient is steep.

6.2.4.5 Null-balance compensator

When the colour cycles increase, the fringe colour become paler and less distinctive. Also the ability to identify integral and fractional fringe

orders by colour depends primarily upon intimate familiarity with the fringe colours, even though it is still not easy to precisely distinguish the fringe colour. For this reason, a null-balance compensation technique is applied, which operates on the principle of introducing into the light path of the polariscope a calibrated variable birefringence of opposite sign to that induced in the photoelastic coating by the strain field. When the opposite-sign variable birefringence is adjusted to precisely match the magnitude of the strain-induced birefringence, complete cancellation will occur, and the net birefringence in the light path will be zero. The condition of zero net birefringence is easily recognized because it produces a black fringe in the isochromatic pattern. The device for synthesizing a calibrated variable birefringence is known as a null-balance compensator.

6.2.4.6 Disadvantages of photoelastic coating and their effects on the study

The main disadvantage of photoelastic coating technique is the reinforcement effect of the plastic coating in bending. The influence of the coating on a structural member is quite complex. Generally there are three factors of concern: **1.** For plates, beams or shells, the neutral axis of the coated member is shifted toward the coated side. However, for a circular shape, the neutral axis will not change. **2.** The coating increases the stiffness of the member, and decreases the deformation for a particular applied bending moment. **3.** There is a strain gradient through the thickness of the coating. The polariscope measures the average fringe order at the mid-plane of the coating, which is further from the neutral axis than the surface of the test member. The first two effects tend to depress the observed fringe order compared to the correct value, and

the third tends to exaggerate the fringe-order indication. All three effects operate simultaneously, but are influenced differently depending on the elastic-modulus and thickness of the coating material and tested specimen. There are some formulas which can be used to correct these errors, however these formulas are derived based on the homogeneous and isotropical materials, and may not be suitable for structures like bone.

Femoral bone is basically a circular and symmetrical shape. When it is coated, the neutral axis should not be shifted. For the second factor, the modulus of the coating (PL-1) and adhesive (PC-1) materials are 2.9 GPa and 3.1 GPa respectively, which is similar in general to cancellous bone (3 GPa), but six times smaller than for cortical bone (15-20 GPa) and much smaller than for femoral stem. For an average size of femoral bone, the stiffness is calculated to be increased by 15% with the coating. However for a comparative study of femoral stems, the last two inherent errors are equally built into the strain measurement system. Also, when comparing the results of the different stems, it is not only comparing the strain value itself, but also comparing the percentage of the strain values to the correspondent intact bone. In this case, the error caused by the reinforcement effect of the coating should not affect the comparative results.

Another disadvantage of the photoelastic coating method is that it only measures the difference in the principal strains, namely shear strain. It does not give the magnitude of the principal strains separately. On the other hand, a 3-element strain gauge (rosette strain gauge) will give the principal strains and their directions. If the surface of bone had equal

longitudinal and circumferential strains, this would show as zero by the photoelastic coating method.

6.2.4.7 Parasitic birefringence

Any initial colour pattern in a photoelastic coating with no load will cause an error in subsequent fringe-order measurement. This initial colour can be caused by mishandling of the plastic during coating, by a difference between the temperatures at which the coating is bonded in place and the subject in test, by the contraction of the bonding cement caused by its continuous polymerizing, and finally by the edges not protected against humidity. The cement contraction may occur after a period of a month which should not effect the results if the test is finished soon. Unprotected edges can be avoided by carefully applying a layer of cement along the edges. The last three factors usually cause the parasitic birefringe along the edges of the coating, while the mishandling can induce the parasitic birefringe at any place. If the initial birefringe happens, the correction is always required, which can use the equation provided by Measurements Group:

$$N = Nf^2 + Ni^2 - 2 \times Nf \times Ni \times \cos 2(\beta f - \beta i)$$

Where Ni is the initial fringe order and ßi is the initial isoclinic angle, while Nf is the final fringe order and ßf is the final isoclinic angle. N is the corrected fringe order, which is due only to the test load. The corrected isoclinic angle of the principal stress can also be calculated in another equation.

6.2.4.8 Orthopaedic application

Since the 1970's, there were several reports of applications of photoelastic coatings in the orthopaedic field. Frankel and Burstein (1970) showed an example of a photoelastic coating on a loaded femur with two drill-holes in it. DiNovo (1985) reported the use of the material on a fibre-composite model of bone fitted with a fracture-fixation plate. Finlay et al (1986, 1989) have reported the use of photoelastic coatings as preliminary full-field strain analyses before subsequent detailed strain gauge investigations of total hip replacements in the pelvis and femur. Walker et al (1988) and Zhou and Walker (1988) used the technique in studying the changes in femoral strains associated with hip implants.

It has been demonstrated that the strains of the bone change rapidly from one point to another, and the location of the maximum strain can also change after the insertion of different stems. In addition, there are discrete patches of high strain concentration on the loaded bone (Zhou 1990). Therefore a full-field strain distribution pattern for a complete analysis and defining many points for quantitative recording may be ideal. To take these aspects into account, photoelastic coating technique is an ideal choice of the study.

6.3 Comparison of strain distribution following custom and standard stems replacement

6.3.1 Introduction

The strains and stresses in the bone of the femur change considerably after total hip replacement. These altered stresses and strains will gradually induce femoral remodelling (Brown 1985, Hill 1988 and Huiskes 1989), which can lead to stem loosening and clinical failure.

Studies on retrieved femoral specimens revealed that these altered strains and stresses may or may not resume to normal after several years of physiological loading (Murphy et al 1984, Maloney et al 1989). Among the many factors involved, the geometry of the stem played an important role in the load transfer to the femur, especially for cementless stems (Morscher 1983, Schimmel 1988, Walker et al 1990). In addition, the amount of bony ingrowth onto the HA coated stem depends considerably on the stem geometry and load transfer between the stem and the canal (Heimke 1981). Therefore, measuring and analysing stress magnitudes and distributions can be of paramount importance in evaluating stem design. One of the hypotheses is that a close proximal fit can produce the stresses and strains closer to normal, whereas a distal tight fit will reduce proximal strains (Walker et al 1988). Also, a current controversy in cementless hip design is that whether an anatomic design, where the proximal region is designed to fit the anatomic shape, has an advantage over a symmetrical design, and whether custom stems provide the optimal solution. Further, do uncemented stems have an advantage over cemented, at least from a strain point of view? A study has therefore been conducted in an attempt to produce some laboratory evidence to answer these questions by measuring the principal shear strains of femoral bone for the different stem designs.

6.3.2 Materials and methods

6.3.2.1 Cadaveric femurs

Eight right-sided adult cadaveric femurs were obtained from autopsies, selected on the basis of lack of deformity and porosis, and on being reasonably close to average size to minimise the number of different

stem sizes required. The femurs were radiographed in A-P and lateral views with a scale marker and fixed in formalin prior to test. The formalin fixation has been shown to have little effect on the modulus of elasticity of the bone, producing only 1.3% reduction in tension and 6.2% in compression (McElhaney et al 1964, Finlay et al 1989) The bone surfaces were cleaned and degreased several times using methylene spirits and acetone to provide a satisfactory surface for bonding of the photoelastic coating.

6.3.2.2 Photoelastic coating

The birefringe coating materials of type PL-1 resin and PC-1 adhesive (The Measurements Group Inc, Raleigh, NC) were used according to the instruction manual. The fringe values were calibrated for each femoral coating. The coating thickness was 2.3 mm. On the medial side, the coating extended from the neck resection line down to the femoral shaft with a length of 160 mm, while on the lateral side, the coating started at the top of the greater trochanter, down to the same level as on the medial side. The coating, in two parts, was divided longitudinally into medial and lateral halves with the joining lines at the anterior and posterior. Fifteen measuring points spaced 10 mm apart were premarked on the coating along medial, lateral and anterior lines, the upper medial points being 5 mm below the neck resection.

6.3.2.3.Measurement

A 030-series reflection polariscope consisting of a white light source (The Measurements Group Inc, Raleigh, NC) was used. Colour fringes on the surface of the coating were viewed through the Analyser when the

specimen was loaded, showing the overall patterns of shear strain distribution. The direction of the principal shear strains could be measured relative to the vertical loading axis by rotating the Analyser, so that the optic axes of the quarter-wave plates aligned with those of the polarizer and analyzer, converting the unit to a plane-polariscope. For measuring strain magnitudes, the quarter-wave plates were oriented with their optic axes at 45 degrees to the polarizer and analyzer axes, and the unit is restored to the circular polariscope condition. A Model 232 Null-Balance Compensator (The Measurements Group Inc, Raleigh, NC) was then attached to the Analyser to precisely quantify the magnitude of the shear strains at the selected test points.

The strains of the intact femur were firstly measured, and the femoral head was then resected and the stems were inserted in the sequence of symmetrical, asymmetrical, custom and cemented symmetrical. The surgery was carried out with extreme care to achieve the closest possible fit for each stem. After canal preparation, in most cases there were regions of residual strain as shown by the colour patterns. Although these residual strains were only a few per cent of the values after loading to 1000 N, they were quantified before insertion of the stems and accounted for afterwards.

6.3.2.4 Calibration of fringe value for coating material

In reflection photoelasticity, the basic relationship between strain and fringe order is:

$$ex - ey = N\,l / 2\,t\,K = f \times N$$

where: **ex** and **ey** are the principal strains; **N** is number of fringe order; **l** is the wavelength of tint of passage in white light, taken as 575nm; **t** is the

coating thickness; **K** is the strain-optical coefficient of the photoelastic plastic and **f** is the fringe value of the plastic coating (m/m) per fringe. In order to translate measured fringe orders in a photoelastic coating into strains or stresses in the coated part, it is necessary to introduce the strain-optic sensitivity of the coating, which is similar to the gauge factor in strain gauges. The fringe value, specifies the strain-optic sensitivity of a particular photoelastic coating, and can be calculated from the nominal values of K and the known thickness t. However, for the greatest accuracy, a specimen from each sheet of photoelastic plastic should be calibrated for strain-optic sensitivity.

The calibration procedure was referenced to the instruction from the technical manual by the Strain Measurement Group. A Photoelastic Model of 010-B cantilever Calibration fixture (The Strain Measurement Group, Inc, Raleigh) was used, which consists of a rigid cast frame for mounting and deflecting a cantilever beam. An aluminum-alloy beam with the dimension of 6.35×25×305 mm was loaded at its free end by a precision micrometer, a known state of strain imposed upon the coating permitting accurate measurement of the deflection. A calibration strip dimensioned 25×76 mm from the same sheet as the one coated on the bone was cut and placed on the calibration beam, with a cross marked on the centre of the strip. Rotating the micrometer head slowly, until the spindle of micrometer contacts the beam, and continue rotating until the micrometer reading reaches a round number. The fringe order at the premarked centre of strip was measured for the initial setting. The micrometer head was then rotated four full turns and another fringe order was measured, continuing for five increments to obtain a total of six readings, including the pre-load measurement at the initial micrometer setting.

The deflection values were then plotted versus the fringe order. The best fit straight line was drawn through the data to determine the slope of the line, $\Delta N / \Delta D$, in fringes per inch of deflection, and then obtain the fringe value f from Calibration Chart. Fig 6.1 showed one example of calibrations.

6.3.2.5 Femoral stem design and manufacture

Femoral stems were designed and manufactured by using the Hip Design Workstation. The symmetrical and asymmetrical stems were designed from an average-shaped femoral canal, whose geometry was obtained by measuring twenty-six American adult femurs (Walker & Robertson 1988). For the custom stems, they were designed from eight individual femoral canals, which were reconstructed by the Hip Design Workstation. Stem design was divided into two stages. First of all, the distal portion of the stem was reconstructed. It was straight and its diameter was determined from the average value of the A-P and lateral diameter of the canal. After that, the proximal portion of the stem was reconstructed by a best-fit cubic curve algorithm, which was matched to the medial endosteal cortex. For the anatomic and custom stem, another cubic curve was matched to the anterior flare of the canal, while for the symmetrical stem, the anterior part of the stem was straight.

Because of the general shape of the femoral canal, the resulting stems were a sliding fit distally, a close-fit proximally, but with clearance in the mid-stem region. The difference between the custom and anatomic stems was that the custom stem had medial and anterior curves to match each individual canal. Both the symmetrical and the anatomic stems were

selected for each femur from a seven-size system. The stem size was chosen so that the canal cortex would not be overreamed, particularly in the proximal-medial region. In order to make the prostheses comparable, the three stems tested in the same femur had the same stem length and neck cutting angle and were all made of Titanium-6 Aluminium-4 Vanadium alloy with a polished surface. The orientation and offset of the stem neck were adjusted to match each femoral head. The stems were also collarless, so that the stability of the stems was entirely dependent on the stem shape.

6.3.2.6 Loading

The distal femurs were resected just above the femoral condyles and potted into a metal tube. The pot was fixed firmly onto the base. The femoral shafts were oriented at 17 degrees laterally and 10 degrees posteriorly, so that the force applied vertically on the head of the prosthesis would produce forces and moments resembling a single leg stance. A load of 1000 N was applied using an Instron Universal Testing Machine (Fig. 6.2).

6.3.2.7 Testing procedures

The intact femur was firstly measured at the marked points for direction and magnitude of the principal shear strains. The femoral neck was then resected and the stems were inserted in the sequence of symmetrical, anatomic, custom and cemented symmetrical. The surgery was carried out with extreme care. For the symmetrical and anatomic stems the standard rasps were used to prepare the femoral canal. For the custom stems, the rasps being used were identical to the stem shapes with

cutting teeth on the upper half only. After the canal was prepared, in most cases there were regions of residual strain as shown by concentrated colour patterns. These residual strains were quantified before insertion of the stems and accounted for afterwards.

6.3.2.8 Statistical analysis

The variances of mean strain values for four type of stems were analysed by using the multivariate ANOVA (SYSTAT package). The strain values were used as "variances" and the stem types were used as "group" variables. If the global analysis of variance was significant at 5 percent level, a post hoc pairwise comparisons was carried out (Turkey HSD (Honest Significant Difference)) to examine any differences between stem types.

6.3.2.9 Abductor simulator and strain gauges

In addition, another formalin-fixed femur without gross abnormality was used to compare the surface strain with and without the abductor, measured by the techniques of photoelastic coating and strain gauges. A nylon strap was used to simulate the abductor muscles, fixed on the greater trochanter by two screws 20 degrees from the vertical axis. The femur was thoroughly cleaned and degreased, and potted in the metal tube with the same orientation described above. Four rossette strain gauges, with alignment of 45 degrees to each other, were glued on the surface of the bone in the proximal medial and lateral, and distal medial and lateral regions. The abductor, strain gauge and photoelastic coatings positions are shown in Fig.6 2. Each time before loading, the strain gauges were readjusted to zero. The femur was loaded to 1000 Newton,

and the strain values were recorded for each channel. After that, the photoelastic coating was applied to the surface of the bone on top of the strain gauges. Finally when the readings from the photoelastic coating were completed, another four rosette strain gauges were glued on to the surface of the coating at the same locations as the previous strain gauges The values from the strain gauges, underneath and above the photoelastic coating, were all recorded. The values from the strain gauges were calculated as differences in the principal strains, namely shear strains, in order to be comparable with the photoelastic coating results.

6.3.3 Results

There were three criteria for comparing the shear strains of each stem: the maximum shear strains and their locations (described by point number) on each side (medial, lateral and anterior); the proximal shear strains (average value of top three points) on the medial side; the shear strain distribution patterns on medial and lateral sides. The strain-optic sensitivity of a particular coating (fringe value f) was calibrated for each bone, which ranged from 900 to 1100 μm/m per fringe.

In general, the shear strain distribution patterns for eight intact femurs were similar and consistent, only the strain magnitudes differed from one bone to another. The shear strains after insertion of different stems were changed considerably compared with the intact femur.

6.3.3.1 Maximum shear strains

On the medial side, Table 6.1 showed that the symmetrical and the asymmetrical stems produced maximum shear strains just below the neck resection, whereas the maximum shear strains produced by the custom stems were similar to the normal position, which were 20-30 mm below neck resection. However for cemented stems, the maximum shear strains were located 60 mm below the neck resection. The magnitude of maximum shear strains produced by symmetrical stems, custom stems and asymmetrical stems was 1035±244 (94% of intact bone), 957±244 (86% of intact bone) and 831±246 (75% of intact bone) microstrains respectively. Cemented stems only produced average 609±112 microstrains (56% of intact bone).

The values of maximum shear strain on the anterior side varied considerably from one stem to another in reference to the intact bone, especially for the asymmetrical stems. Fig. 6.3 showed that the maximum shear strains for the symmetrical, custom, asymmetrical and cemented stems were 421±94 (103% of intact bone), 434±104 (116% of intact bone), 599±129 (148% of intact bone), and 325±102 (81% of intact bone) microstrains, respectively. The asymmetrical stems produced significant higher shear strains ($p<0.05$) than the other stems.

On the lateral side, four types of the stems showed no differences in the maximum shear strains ($p>0.05$). The symmetrical, custom, asymmetrical and cemented stems produced 488±121 (92% of intact bone), 481±99 (91% of intact bone), 475±68 (91% of intact bone) and 429±92 (80% of intact bone) microstrains respectively (Fig. 6.6).

6.3.3.2 Proximal shear strains

The proximal shear strain values were considerably changed after insertion of any type of stem compared with the intact bone. In average, the proximal shear strains on the medial side were close to normal for the symmetrical and custom stems, which were 921 and 875 microstrains, only 6% and 11% lower than normal, and there were no statistical differences between these two. The asymmetrical stems gave slightly lower values at 750 microstrains, which was 24% lower than normal strain. However the strains for the cemented stem were only 238 microstrains, which was 75% lower than normal (Fig. 6.4). The differences between the custom and asymmetrical stems were significant ($p<0.05$). The cemented stem showed a significant difference with all other cementless stems ($p<0.05$).

6.3.3.3 Shear strain distributions

The proximal shear strain values alone were not representative of the overall strain status. Figure 6.5 shows a typical example of the strain distribution on the medial side. The strains with the symmetrical stem rapidly diminished below the level of the neck resection, and similarly but to a less extent with the asymmetrical, whereas, the shear strain distribution patterns for the custom stems were closer to that of the normal bone. These characteristics of the strain distribution patterns were observed for all of the eight femurs. The mean data obtained on the medial side for the eight femurs (Table 6.3) showed the diminution of the strain values below the level of the neck resection. The highest values for the symmetrical and asymmetrical stems were only 5 and 15 mm below the neck, but there was a large reduction beyond that. For the custom stems, only a small reduction (from 94 to 78% of normal strain) was observed from the neck down to 55 mm below. The cemented stems

showed a reverse pattern. The lowest strain (20% of normal bone) was just below the neck resection, then slightly increased at 55 mm below, but still only 64% of normal strain was reached.

6.3.3.4 Abductor simulator and strain gauges

There were significant strain changes with and without the abductor. In the proximal-lateral, distal-lateral and distal-medial sites, the strains were increased from 44 to 101% with the abductor active (Fig 6.7). However, in the proximal-medial region, there was a decrease of 14% with the abductor acting. The possible reinforcing effect of the photoelastic layer was analysed by comparing the results of strain gauges and photoelastic coating at the same sites. The reductions in strain after application of the coating ranged from 9 to 14%, the largest value being proximal-medial and the smallest distal-lateral (Table 6.2). It was noted that a close agreement of the strain values was obtained from the strain gauges on top of the coating and from the photoelastic coating itself.

6.3.4 Discussion

6.3.4.1 Photoelastic coating technique

The photoelastic coating technique is an effective method to analyse the strain patterns on the bone surface and evaluate the variables in stem design. It provides a complete strain distribution pattern and comparative strain magnitudes between different stems.

The effect of the photoelastic coating layer in stiffening the system and reducing the strain magnitudes is of great concern. In present study, a

14% reduction of the strain was observed in the proximal-medial region and 9% below the level of the lesser trochanter. However with absence of an abductor force, it was observed that there was a 14% increase in strain magnitude. Therefore the proximal-medial values measured by the photoelastic coating without abductor force would be close to the actual bone surface values measured by strain gauges with an abductor force, whereas, the strain values in other regions could be underestimated by using the photoelastic coating technique. However, for the purpose of comparing different stems, the photoelastic coating provides the relative strain value on the bone surface, and these strain values changed after insertion of different stem. The amount of strains on the bone surface were the function of the stem geometry.

6.3.4.2 Abductor simulator

The presence of the abductor muscles has been regarded as a very important factor in determining the realistic strain status on the surface of the bone. Finlay et al found that with the abductor simulator, the strain magnitude was increased both on the medial surface, by 32%, and on the lateral surface, by 53%. In present study, quantitatively similar results were observed on the lateral side and at the distal-medial location. However in the proximal-medial, the strain value was decreased by 14 % instead of increased. Different orientation of the abductor strap may affect the results. In addition, with the abductor simulator, the location of the maximum strain on the proximal medial region was moved downwards.

6.3.4.3 Stem design

The introduction of the stems altered the shear strains on the surface of the femur in both magnitude and distribution. The magnitudes for the cemented stems in the proximal-medial region, considered to be an important region for load support and fixation, were considerably reduced. On the other hand, the strains for all of the uncemented stems were much closer to normal, but the strains were sensitive to the type of uncemented stem, notably to the fit. The symmetrical stems produced a concentration of strain on the medial side but low strain anteriorly due to lack of contact. The standard asymmetrical stem showed a variable strain pattern depending on the relative fit along anterior-posterior and medial-lateral directions. This variation resulted in high anterior strains in some femurs, as well as higher standard deviations in both the medial and anterior values, compared with the other stems. The most reproducible pattern and the one closest to normal was produced by the custom stems. Hence it can be proposed that stems with a close proximal fit are advantageous, assuming that the attainment of normal strains is ideal. Also assuming the strain patterns can be maintained over time, the 'stress protection' and hence bone resorption, may be less with uncemented than with cemented stems because of the much lower strains produced with the latter.

Concerning reaming the canal to fit the stem, local residual strain patches could be generated. This phenomenon was observed by using the photoelastic coating technique, especially on the anterior side of the bone for fitting the asymmetrical stems. Therefore, overreaming the cortical bone in order to fit the stem may not be an ideal approach.

The custom stems were designed for the individual canal and the advantage of this approach was reflected in present study by the

consistently uniform strain distribution from eight femurs. The strain values measured can only represent those in the early stages of post-operation. In clinical practice, no matter what type of cementless stem is used, including a porous or hydroxyapatite coated stem, a modified load transfer pattern is, to some extent, likely to take place after a period of stem resettling, which may affect the subsequent bone remodelling. In order to minimize the bone remodelling, it is suggested that a cementless stem which is intended to produce strains approaching those of the normal femur, should load the femur proximally, physiologically and uniformly, and should maintain stable with minimal micromotion at the interface allowing maximum proximal bone apposition .

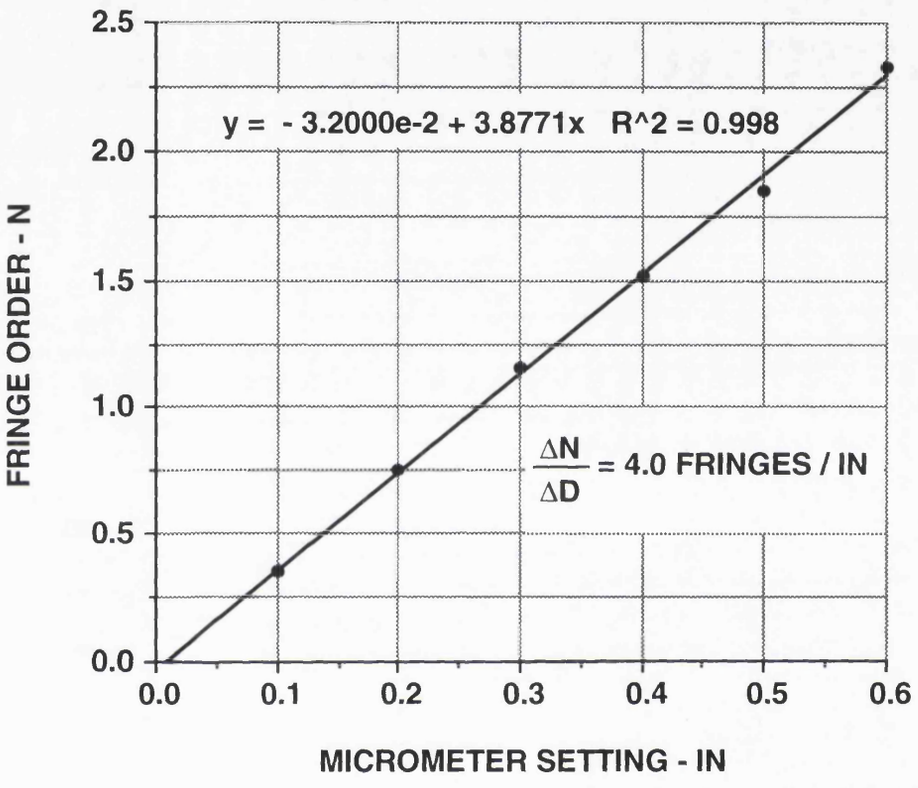

FIG. 6.1 GRAPH OF FRINGE ORDER VERSUS MICROMETER SETTING FOR DETERMINING ΔN / ΔD, WHICH FOR OBTAINING A FRINGE VALUE FROM CALIBRATION CHART.

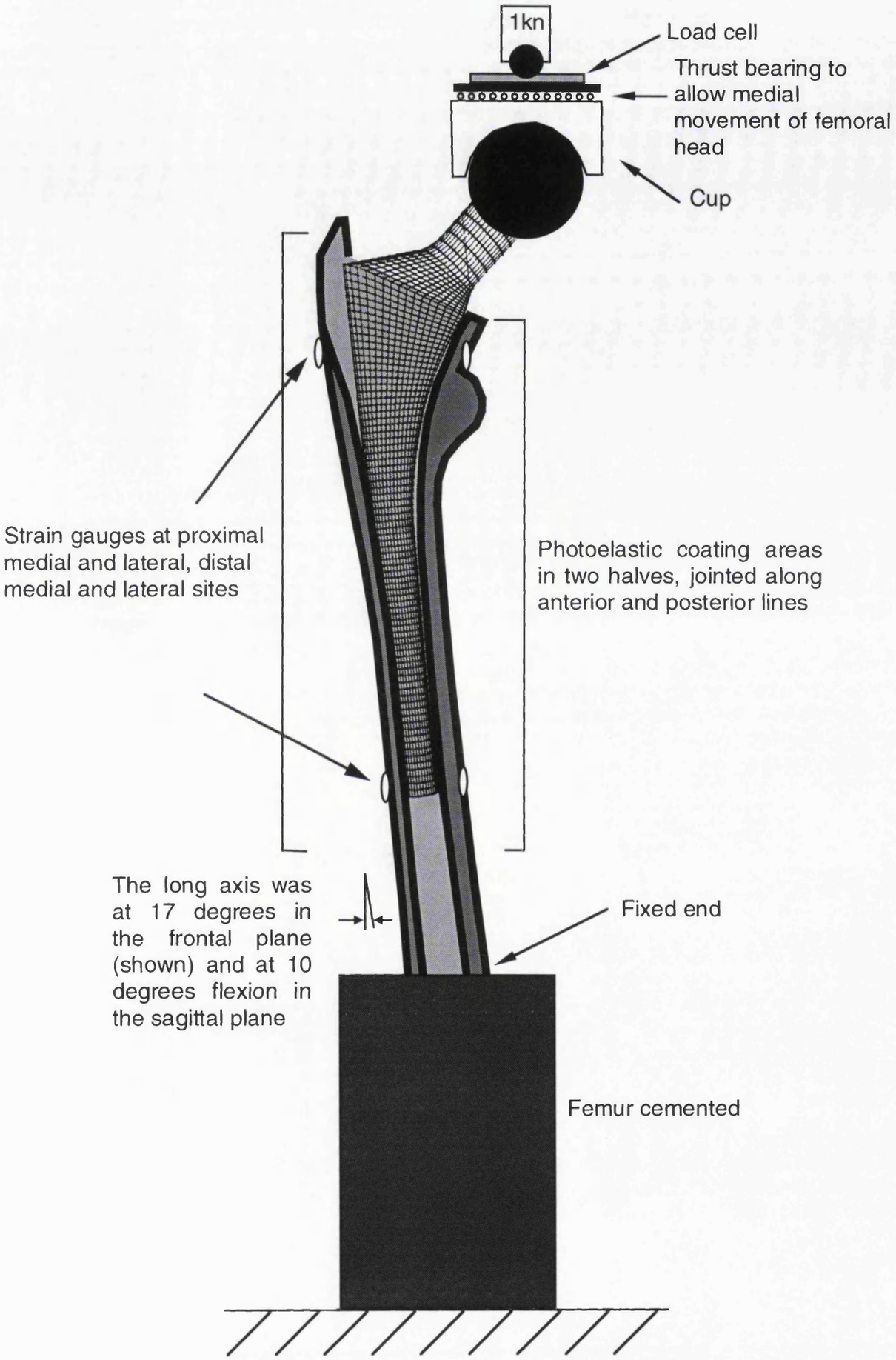

FIG. 6.2 THE EXPERIMENTAL SET-UP, SHOWING THE LOADING CONFIGURATIONS, FEMORAL ORIENTATION, PHOTOELASTIC COATING AREAS AND STRAIN GAUGE LOCATIONS

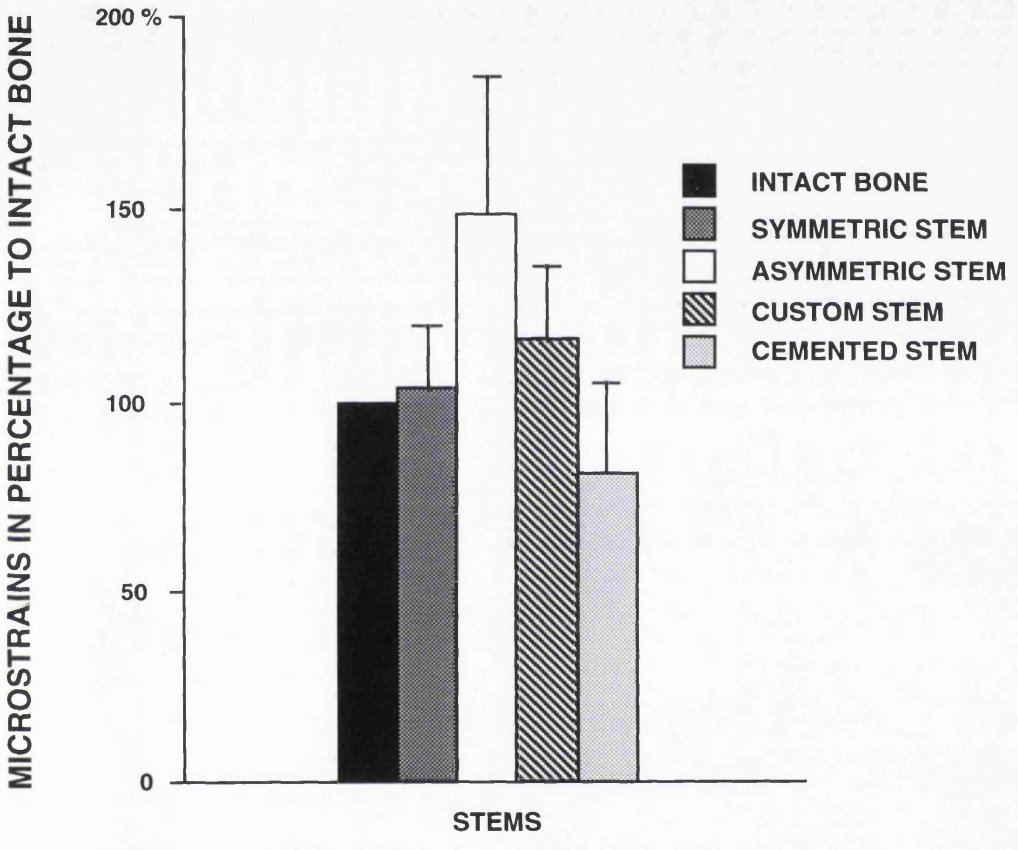

FIG.6.3 COMPARISON OF THE MAXIMUM STRAIN VALUES ON ANTERIOR SIDE BETWEEN DIFFERENT TYPES OF STEMS

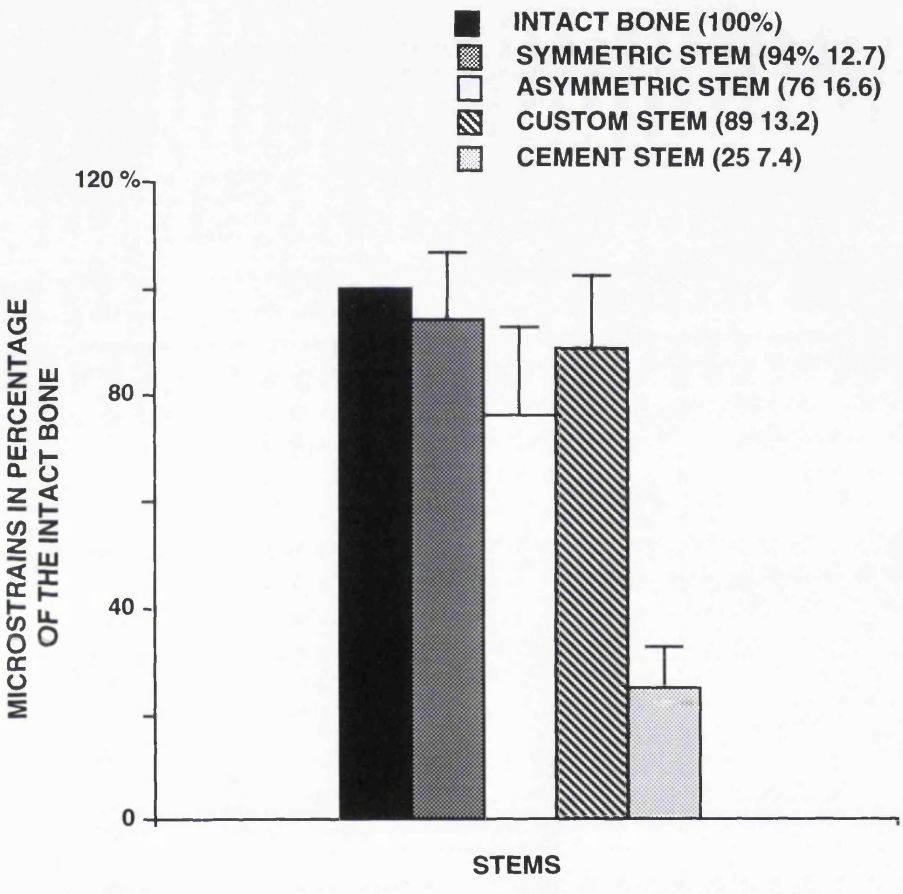

FIG. 6.4 COMPARISON OF THE PROXIMAL STRAINS ON MEDIAL SIDE BETWEEN DIFFERENT TYPES OF STEMS.

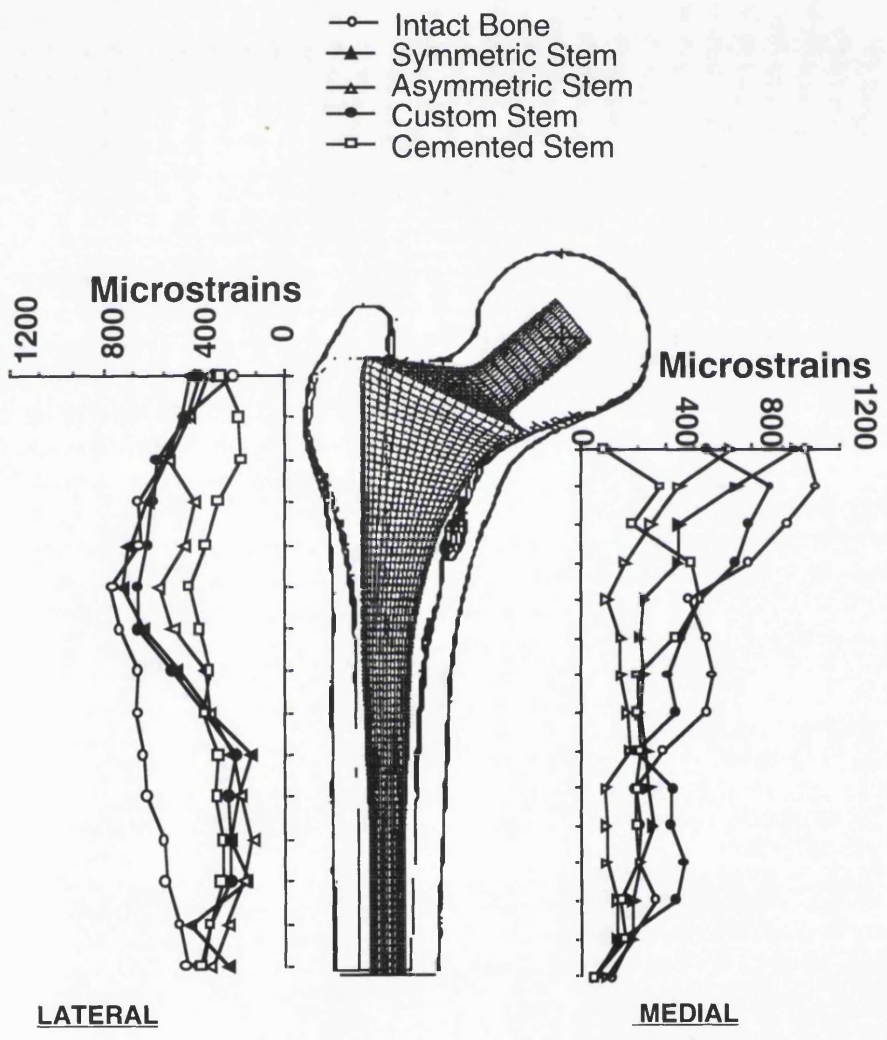

FIG.6.5 A TYPICAL PATTERN OF STRAIN DISTRIBUTION

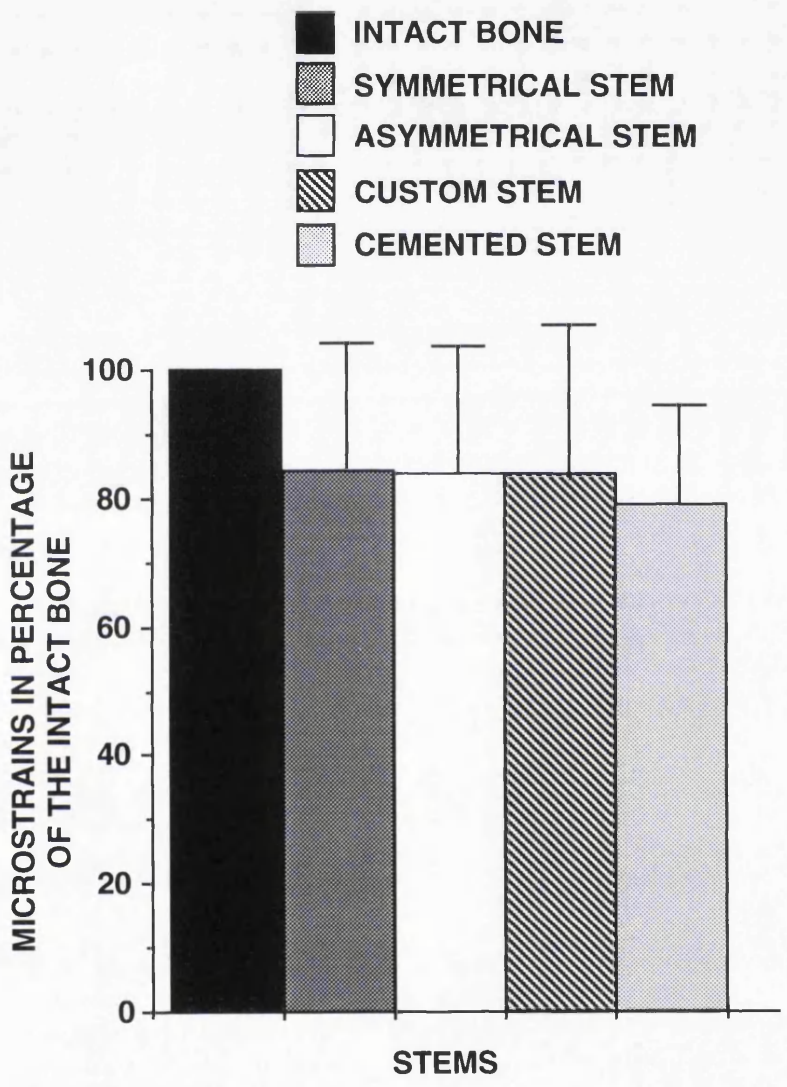

FIG. 6.6 COMPARISON OF THE MEAN STRAINS ON LATERAL SIDE BETWEEN DIFFERENT TYPES OF STEMS

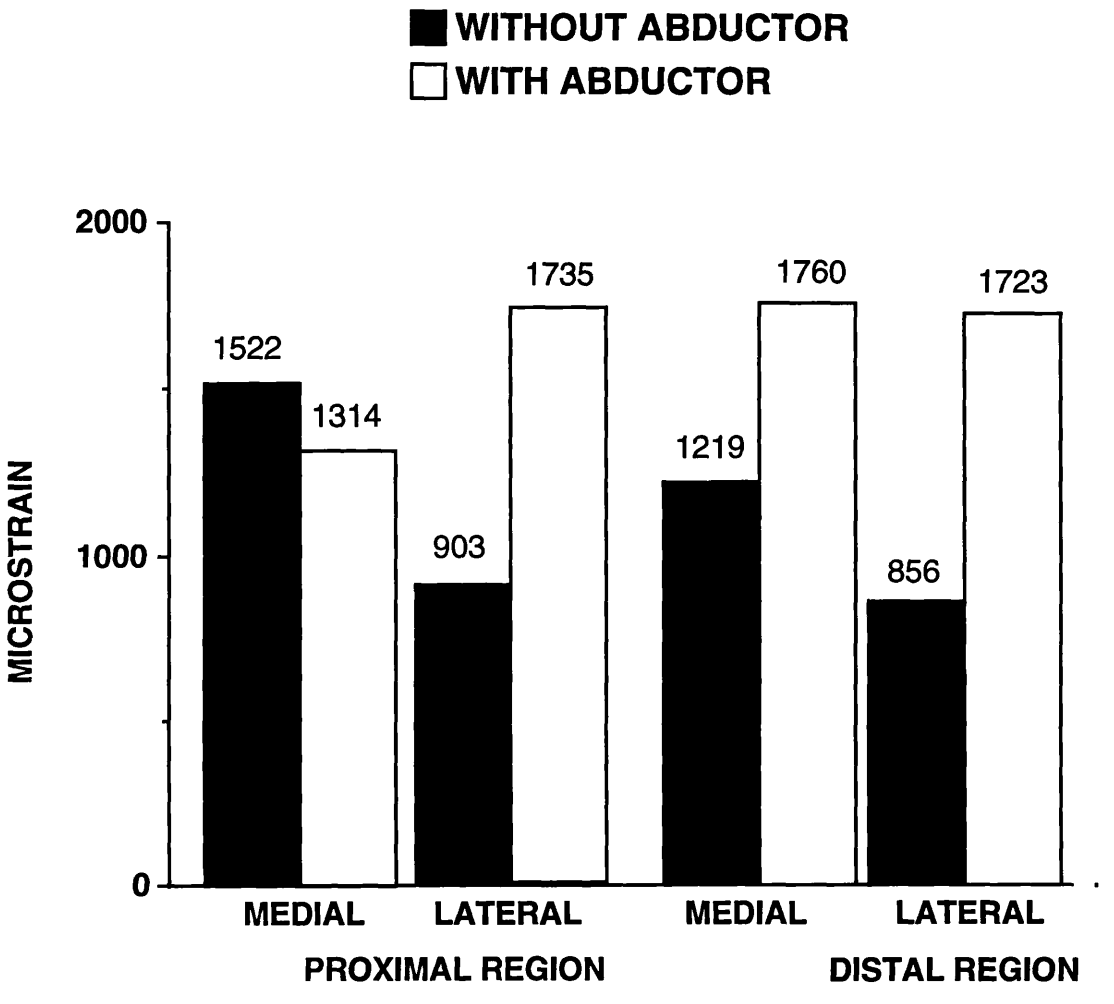

FIG. 6.7 STRAIN CHANGES WITH AND WITHOUT ABDUCTOR SIMULATOR MEASURED BY STRAIN GAUGE IN FOUR REGIONS

TABLE 6.1 COMPARISON OF THE PEAK STRAIN VALUES AND LOCATIONS BETWEEN DIFFERENT TYPES OF STEMS ON MEDIAL SIDES. (PTS 1 IS THE LOCATION OF THE MOST TOP LEVEL AND PTS 15 IS THE MOST BOTTOM LEVEL)

Bone		Bone			Sym			Asym			Custom			Cement		
No.	Strain	Pts*	%	Strain	Pts	%	Strain	Pts	%	Strain	Pts	%	Strain	Pts	%
1	1048	3	100	891	2	85	808	2	77	975	3	93	487	3	46
2	1094	2	100	996	1	91	697	1	64	881	2	81	556	5	51
3	907	3	100	971	2	107	697	3	77	735	2	81	546	8	60
4	884	3	100	782	2	88	580	2	66	720	3	81	512	5	58
5	814	3	100	728	2	89	579	2	71	672	2	83	557	6	68
6	1345	3	100	1283	2	95	932	2	69	1204	2	90	690	5	51
7	1222	4	100	1223	2	100	1096	3	90	1160	2	95	789	7	65
8	1510	3	100	1403	2	93	1255	1	83	1308	2	87	733	9	49
Mean			100			94			75			86			56
SD						7.1			8.9			6			8

* PTS IS AN ABBREVIATION OF POINTS

TABLE 6.2 COMPARISON OF THE STRAIN VALUES BEFORE AND AFTER PHOTOELASTIC COATING, MEASURED BY STRAIN GAUGES AND PHOTOELASTIC COATING TECHNIQUE

	Strain Gauge Without Coating	Photoelastic Coating	Strain Gauge Above Coating
Medial Proximal	1522	1303 (14.3%)	1312 (13.8%)
Medial Distal	1219	1083 (11.1%)	1162 (4.6%)
Lateral Proximal	903	812 (10.1%)	791 (12.4%)
Lateral Distal	856	776 (9.4%)	810 (5.4%)

TABLE 6.3 THE MEAN STRAIN VALUES AND STANDARD DEVIATIONS (N=8) FOR THE STEMS AT THE DIFFERENT DISTANCES BELOW THE NECK RESECTION (EXPRESSED AS A PERCENT OF THE STRAIN IN THE INTACT FEMURS)

	DISTANCE FROM NECK RESECTION (mm)					
STEM TYPE	**5**	**15**	**25**	**35**	**45**	**55**
SYMMETRIC	113±23	100±16	75±19	72±25	73±21	66±18
ASYMMETRIC	88±27	78±17	64±18	61±23	64±25	63±19
CUSTOM	94±31	93±10	81±11	80±14	83±22	78±18
CEMENTED	20±8	28±12	26±9	45±13	66±24	64±20

CHAPTER SEVEN

RELATIVE MOTION OF HIP STEMS UNDER LOAD: AN *IN VITRO* STUDY OF STRAIGHT, ANATOMIC AND CUSTOM DESIGNS

7.1 Introduction

The relative motion between an uncemented femoral stem and the surrounding medullary canal has important implications to the interface response and the clinical success of the prosthesis in total hip replacement. Earlier studies showed that cemented stems had less relative motion between the stem and the bone than cementless stems (Nunn and Freeman 1989, Phillips et al 1990, Rothman and Cohn 1990, Schneider et al 1989). However, microfracture of the cement mantle under torsional load (Sugiyama et al 1989) and major stress shielding of the cemented stem (Zhou et al 1990) have been observed. Such events are likely to contribute to a deterioration of results with time (Harris et al 1991). Therefore cemented stems are generally considered not to be ideal for the young and active patients. Clinical and animal studies have showed that uncemented stems with hydroxyapatite or porous coating can induce bone apposition to the stem (Oonishi et al 1989, Bloebaum et al 1991). This may achieve longer survival of the femoral prosthesis. However, achieving 'osseointegration' will rely on the stability of the femoral stem in the canal (Soballe et al 1992). The initial stabilities of cementless hip prostheses have previously been studied (Walker and Robertson 1988, Schneider et al 1989, Burke et al 1991, McKellop et al 1991). The results suggested that the relative motion between the stem and the bone varied considerably between different designs. Anatomically shaped stems generally showed less rotational motion than straight stems. Recently, a test of stem-bone relative motion has been recommended as an important criteria to evaluate initial fixation of a femoral stem both intraoperatively and laboratorily (Harris et al 1991).

It is generally believed that stem-canal fit and cross-sectional fill are important factors in controlling relative motions (Walker and Robertson 1988) and in relieving thigh pain (Whiteside 1989). Due to wide variations in the geometry of femoral canals, an off-the-shelf femoral stem may not be able to consistently produce minimal relative motion when compared with a custom stem (Hua et al 1991). The hypothesis of the present study was that a custom stem would produce the least relative motion, whereas a standard symmetrical stem the most, with a standard asymmetrical stem being intermediate. In order to test this hypothesis, a comparative study between the three types of stem was conducted.

7.2 Materials and methods

7.2.1 Stem design and manufacture

Eight non-paired adult cadaver femurs from older subjects, three right and five left, were radiographed and fixed in formalin prior to testing. The individual canal shapes were obtained by digitizing the internal cortical line of the A-P and lateral views of the radiographs, and then the Hip Design Workstation software predicted and reconstructed the three-dimensional canal shape.

Femoral stems were designed by using an algorithm which was a sliding fit distally with 0.5 mm clearance gap, a close-fit proximally, and with clearance in the mid-stem region. The standard symmetrical and asymmetrical stems were designed from an average-shaped femoral canal whose geometry was obtained by measuring twenty-six American adult femurs (Walker and Robertson 1988), while the custom stems were designed for each individual femoral canal. The differences between the

standard symmetrical and asymmetrical stems were that the asymmetrical stem had anterior curves. Both the symmetrical and the asymmetrical stems were selected for each femur from a seven-size system. The criteria for choosing the size of femoral stem was that the femoral canal should not be overreamed particularly in the proximal-medial region, but also in the distal region if possible.

In order to make the prostheses comparable, the three stems tested in the same femur had the same stem length and neck cutting angle, and were all made of Titanium-6 Aluminium-4 Vanadium alloy with a polished surface. The neck offset of the stems was adjusted to match the centre of the femoral head for each femur, so that the bending moment for all three type of stems was the same. The stems were collarless, so that the stability of the stems was entirely dependent on the stem shape. The standard rasps were used for the symmetrical and asymmetrical stems, whereas for the custom stems, individual rasps which were identical to the stem shape were used. All of the stems and rasps were automatically manufactured on a four-axis CNC machine.

7.2.2 Loading

The femurs were resected just above the femoral condyles and potted in a metal tube at 12 degrees laterally and 10 degrees posteriorly, so that the force applied vertically on the head of the prosthesis would produce forces and moments resembling a single leg stance (Fig. 7.3). After each stem was tested using the simulated single leg stance loading, the femur was repositioned at seventy degrees from the vertical with the anterior side facing upwards. A plastic pillar was used posteriorly to support the proximal part of the femur. The transducer readings were set to zero. A

single force of 150 Newtons was applied to the prosthetic head, which produced torsional loading through the prosthesis. This loading configuration was used to simulate stair climbing and chair rising (Fig. 7.4). The transducer readings were then taken to obtain the amount of stem-bone relative rotation under torsional loading.

7.2.3 Measurement

In order to measure the relative motion between the stem and the bone in a direction parallel to the long axis of the bone, a hole was drilled in the bone twenty millimeters below the lesser trochanter in the A-P plane. A smaller hole was drilled at the same location through the stem of the prosthesis. After the stem was inserted into the femur, a metal rod was tightly fitted into the stem with enough clearance within the hole in the bone so as not to impede any motion of the rod or stem during cyclic loading. Onto each end of the rod, fifteen millimeter plastic cube targets were screwed and glued, against which the transducers were located. A plastic fixture holding two LVDTs (Sangamo, a division of Solartron Transducers) parallel to the femoral stem was fixed to the proximal femur using four pointed screws. The transducers were located anteriorly and posteriorly. The average displacement reading of the two transducers was used as the measure of relative motion. The relative horizontal motions in the A-P and M-L planes were measured only at the tip of the implant. One hole was drilled through the bone laterally and another posteriorly. A plastic fixture holding the transducers perpendicular to the femoral shaft was fixed to the femur at the level of the tip of the implant by three pointed screws. The position of the transducers was shown in Fig. 7.1.

Relative rotational motion was determined at the level of the neck cut by two transducers placed anteriorly and posteriorly. These two transducers were held by a plastic plate which was screwed tightly onto the vertical medial face of the greater trochanter. A small hole was drilled at the base of the neck of the stem, and a metal rod aligned anterior-posterior was fixed through the hole. Plastic cube targets with a smooth surface were screwed and glued onto the ends of the rod. Relative rotational motion between the stem and bone was calculated from the anterior and posterior transducer readings (Fig. 7.2).

7.2.4 Data acquisition

The femoral stems were inserted and tested in the sequence of symmetrical, asymmetrical and custom. Insertion was carried out by templating the X-ray to determine the level of neck cut, resecting the neck, reaming the distal canal through an entry point in the trochanteric fossa, followed by rasping to shape the proximal part of the canal. A force of 1,000 Newton was applied vertically to the head of prosthesis at three single load to seat the stem into the canal by using a Dynamic Hydraulic Test Machine (R.D.P. - Howden Ltd, Leamington Spa, Works. England). The transducers were then set to zero. The readings were monitored simultaneously by a linked computerized data acquisition system (Labview, National Instruments). A cyclic force between 0 and 1000 Newton was then applied at a frequency of 1 Hz. The readings were recorded at the end of every 500 cycles, up to 2500 cycles. The difference in the displacement with and without applied load was defined as the relative motion, and the differences between the initial position of the stem (after three single load) and the position after cyclic loading was defined as migration (Fig. 7.5).

7.3 Results

The relative motion data from eight femurs for the symmetrical, asymmetrical and custom stems were analysed and compared by using SYSTAT statistical analysis package. Multivariate ANOVA was used for statistical analysis. If the null hypothesis was rejected at 0.05 level of significance, a multiple comparisons procedure was carried out (using Turkey HSD, a conservative algorithm) to examine any differences between stem types.

7.3.1 Axial relative motion

In the initial stage of loading (0 cycle of loading), there occurred only small differences between the three types of stems with a micromotion range from 80-100μm (Fig. 7.6). After 500 cyclic loading, the motion for all the prostheses were again similar, but the range of the motion was now reduced to 20-30μm. The motion continued to reduce up to 2500 cycles when the migration values were only 6±6μm, 19±13μm and 11±12μm for symmetrical, asymmetrical and custom stems. No differences were observed between three types of stems ($p=0.083$).

7.3.2 Rotational relative motion

Overall, the angular displacement for the symmetrical stems was higher than that for the asymmetrical and custom stems (Fig. 7.7). However significant differences were observed only at 500 cycles of loading with the asymmetrical stems ($p=0.044$) and with the custom stems ($p=0.017$). The corresponding relative angular motions were 0.063±0.056,

0.018±0.022 and 0.009±0.013 degrees for the symmetrical, asymmetrical and custom stems. No differences were observed between three types of stems for the remainder of the test.

7.3.3 Lateral relative motion at the stem tip

For most of the stems, the tip moved laterally during cyclic loading, but in a few stems, the tip moved medially at certain stages of cyclic loading. Overall, the lateral motion for all the categories was very small and the differences were not significant (Fig. 7.8).

7.3.4 Posterior motion at the stem tip

On average, the stem tip of the symmetrical and the custom stems moved posteriorly, whereas most of the asymmetrical stems moved anteriorly (Fig. 7.9). Except for the first loading, the custom stems produced less motion than the asymmetrical stems ($p<0.05$). The symmetrical and asymmetrical stems generally produced similar results, only at the first loading, symmetrical stems had less motion than the asymmetrical stems ($p<0.05$). No differences were observed between the custom and the symmetrical stems.

7.3.5 Axial migration

The migrations was approximately 150 μm after 2500 cycles of simulated single-limb-stance loading. Most of the migration had occurred by 1000 cycles of loading. No significant differences were observed between the stems (Fig. 7.10).

7.3.6 Torsion

These data refer to the test in which the femur was located at 70 degrees to the vertical axis. The stems rotated a great deal more than in the previous test, even though the loading force was very small (150 newtons). Compared with the asymmetrical and the custom stems, the symmetrical stems had a greater relative angular motion (Table 7.1), and the differences were significant both with the asymmetrical stems ($p=0.008$), and with the custom stems ($p=0.007$). The custom stems produced the least motion but no difference was observed when compared with the asymmetrical stems ($p>0.05$).

7.4 Discussion

Pre-clinical testing methods can provide valuable comparative data with regard to different stem designs. Since actual femora vary in shape, size and quality of bone, each type of stem should be tested in several femora. Also comparisons between different types of stems should ideally be made by testing each stem in the same femur. McKellop et al (1991) used synthetic composite model femora to compare three different uncemented stems with a cemented stem. The advantage of the method was that, because the different stems were compared in separate femora, optimum preparation of the canal was possible for each stem, whereas the disadvantage was that, because all of the stems were tested in one particular femoral model only, there was the possibility of preferential shape-matching of some stems compared with others. Also, the elastic modulus of the epoxy reinforced with fiberglass powder (7-10 GPa) was lower than for human cortical bone (15-20 GPa), which may have affected the magnitude of the interface motion between the implant and

the cortical wall of the femur. Phillips et al (1990) used thirteen pairs of femurs to compare two types of uncemented stems and another five pairs to determine the differences between the uncemented and cemented stems. This seems to be ideal if an adequate numbers of femurs can be obtained.

Other investigators have reinserted different types of stems into the same femoral canal as was carried out in the present study (Walker et al 1987, Nunn et al 1989, Burke et al 1991). The advantage of this method was that it allows each type of stem to be tested in the same femoral canal, as well as in several canals with different geometries. However, the previous reaming of the canal may have affected the fit of the stems that followed if the stem geometries were substantially different. Also, the cyclic loading may alter the quality of the femoral bone at certain locations if the stresses were beyond the elastic limit. The method used in the present study can be considered valid only if a small number of stem designs are to be tested and if each successive stem require progressive removal of bone.

In the present experiments, the asymmetrical stem fitted exactly into the cavity left by the symmetrical stem after reaming the anterior bone of the proximal anterior flare. The custom stem required further reaming of residual cancellous bone as well as small local regions of cortical bone. Each stem had the same length and required the same proximal bone cuts; this eliminated the need for changes in the bone cuts and made the results more comparable. The fixation of a specimen in formalin and the postmortem changes that occur before fixation in formalin have been shown to produce only slight reductions in the elastic properties of bone (McElhaney et al 1964, Ashman et al 1982). Finlay et al (1989) reviewed

the literature on the effects of embalming on the mechanical testing of bone and concluded that embalmed specimens provide a suitable model for a comparative evaluation of prostheses.

The measurement of relative motions (displacements and rotations) at discrete locations has its limitations, because such measurements made at various locations are likely to differ. Recently, some investigators have produced a full-field representation of relative motion by displaying stem motion relative to the femur (Gilbert et al 1992). This representation required an assumption of a rigid body, which did not account for local elastic deformations, especially those of the bone. However, in a study where measurements at discrete points will be taken, the choice of those points in areas of special interest is advantageous.

In order to detect rotational movement of the femoral prosthesis, some previous investigators have mounted one transducer in the proximal-medial part of the prosthesis. Although the femoral prosthesis in these previous studies rotated posteriorly, the actual rotatory centre of the cross-section of the prosthesis can not be predetermined. Transducers mounted in different positions, therefore, will record different displacements. If these displacements are interpreted as rotations, the results will not be reproducible. In the present study, two transducers were used to detect rotational motion wherever the rotatory centre was located. By calculating and presenting the relative angle of rotation, the results can be compared with those of other experiments that also measure this angle.

Attention has been drawn to the importance of the torsional stability of femoral components when these are large force components acting on

the anterior of the femoral head. Wroblewski (1979) and Harris et al (1991) postulated that torsional loading and rotational instability of the stem were the critical factor in failure of total hip arthroplasty both for cemented and cementless prostheses. However even in situations in which torsional loading can be applied, such as stair climbing and chair rising, different data has been given for the position and force applied to the femoral head (Rydell 1966, Williams 1968, Paul and McGrouther 1975, English and Kilvington 1978, Berme and Paul 1979, Crowninshield and Brand 1981). Davy et al (1988) obtained data from a telemeterized total hip prosthesis that had been implanted in one patient. After thirty-one days postoperatively, they found that in the single-limb stance, the joint contact force was 1160 Newtons (2.1 times body weight), with the resultant force located on the anterosuperior portion of the ball. During stair-climbing, a joint contact force of 1450 Newtons (2.6 times body weight) was oriented at a maximum of 70 degrees anteriorly.

The present study used this data to simulate physiological loading with the exception that a load of 150 newtons was used as a torsional force to avoid overstressing the bone. All of the tests (with the exception of the torsion test), demonstrated the importance of taking readings of relative motion after periods of cyclic loading. After only 500 cycles, the relative motions were significantly less than they had been at the start of the test. The fact that there were only small changes after 1000 cycles suggests that 1000 cycles is a sufficient duration for the test.

Under axial loading, the stabilities were achieved primarily by the wedging of the femoral stem into the canal, mostly in the medial-lateral plane. This was evidenced by the fact that the results of axial motion of the symmetrical stem were similar to those of the custom or asymmetrical

stems. On the other hand, the symmetrical stems showed more rotational motion, especially under the torsional loading, than did either of the other two types of stem. In contrast, the asymmetrical stems and the custom stems were much more stable in rotation, both under simulated single leg stance and during simulated stair climbing. These data suggest that an important factor in rotational stability is the close contact of the stem with the cortical bone in the proximal region, especially in the medial and anterior aspects. An additional advantage of the asymmetrical and custom stems compared with the symmetrical stem was the reduced in 'toggle' in the A-P and M-L planes, again possibly due to the better proximal fit and fill. In theory, the main advantage of the custom stem is its greater consistency of close fit and fill. In the present study, this theoretical advantage did not result in a significant reduction of relative motions compared with the asymmetrical stems, although a trend has been observed that the custom stems did produce lower values of relative motion than the asymmetrical stems in every catogory. By increasing the number of bones being studied, statistical differences of the custom stems with the asymmetrical stems could likely be demonstrated. In addition, if the study was carried out in bones with severe deformity, then the custom stems could show significant differences with the standard asymmetrical stems.

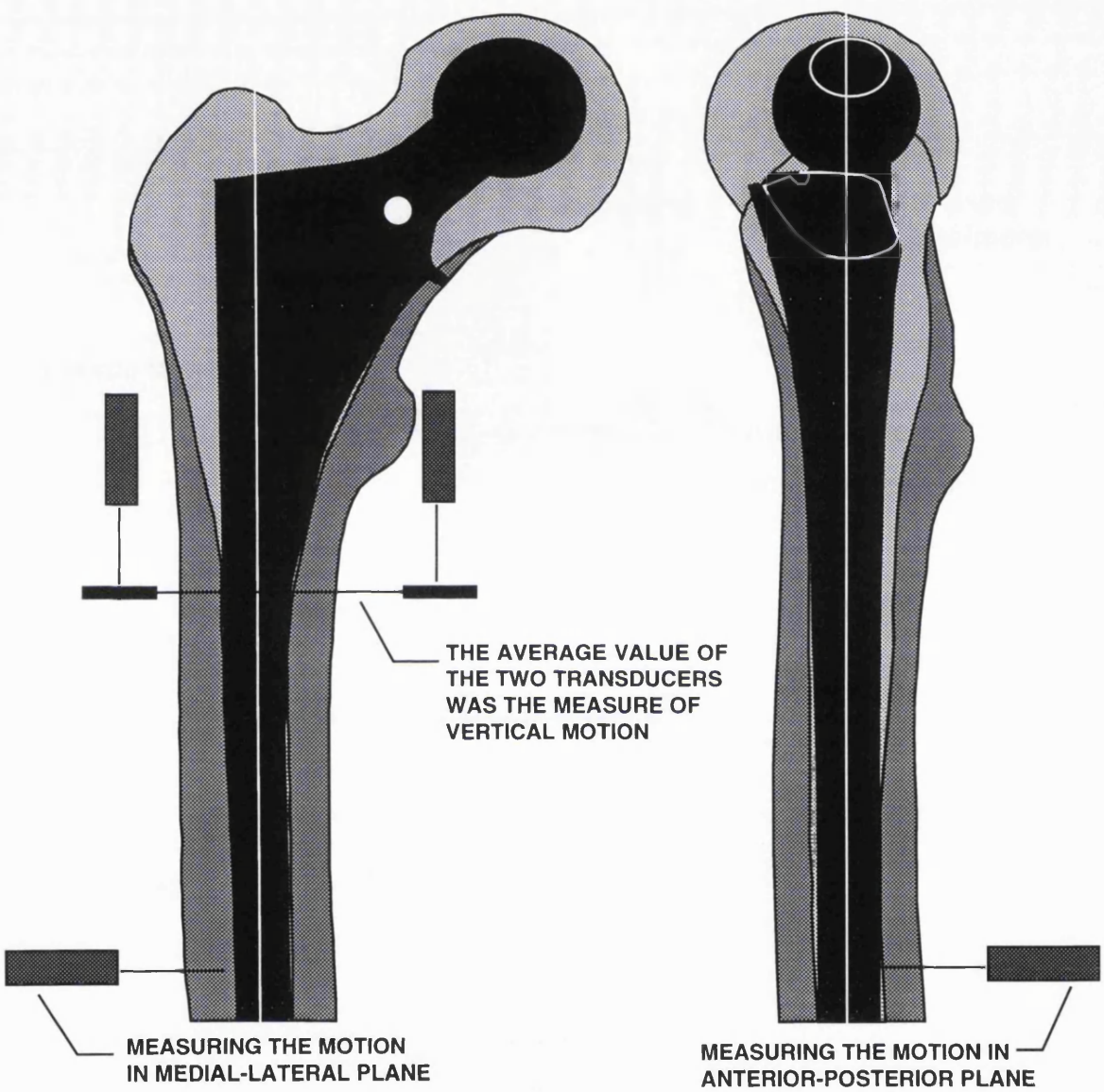

FIG. 7.1 THE POSITION OF THE TRANDUCERS IN MEASURING VERTICAL, MEDIAL-LATERAL AND ANTERIOR-POSTERIOR MICROMOTIONS

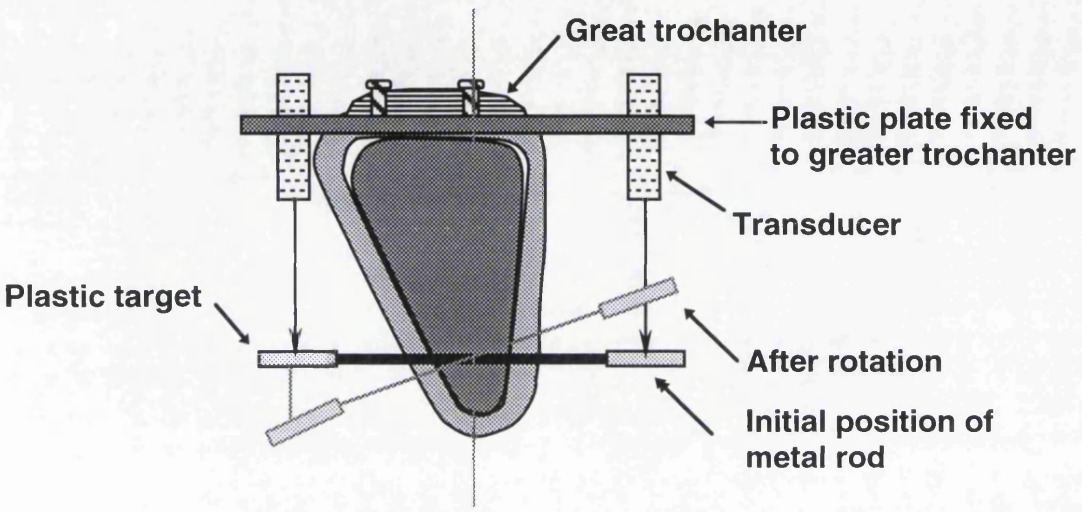

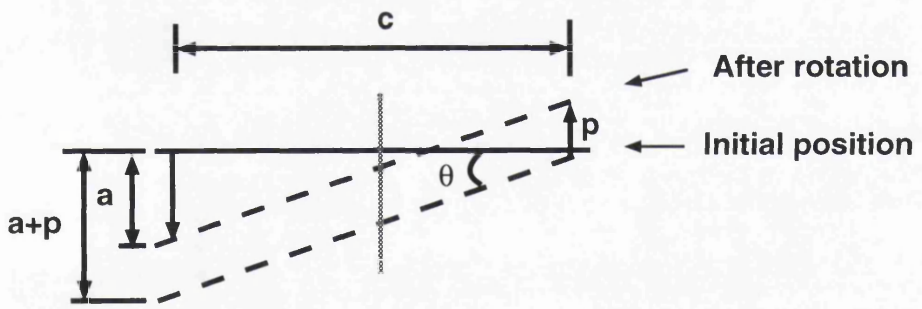

$$\tan\theta = \frac{a + p}{c}$$

FIG. 7.2 AN OVERHEAD VIEW OF THE STEM AND FEMUR ALONG THE VERTICAL AXIS OF THE FEMUR, WITH THE MEASUREMENT AND CALCULATION OF THE ROTATION OF THE STEM RELATIVE TO THE BONE (ANGLE θ)

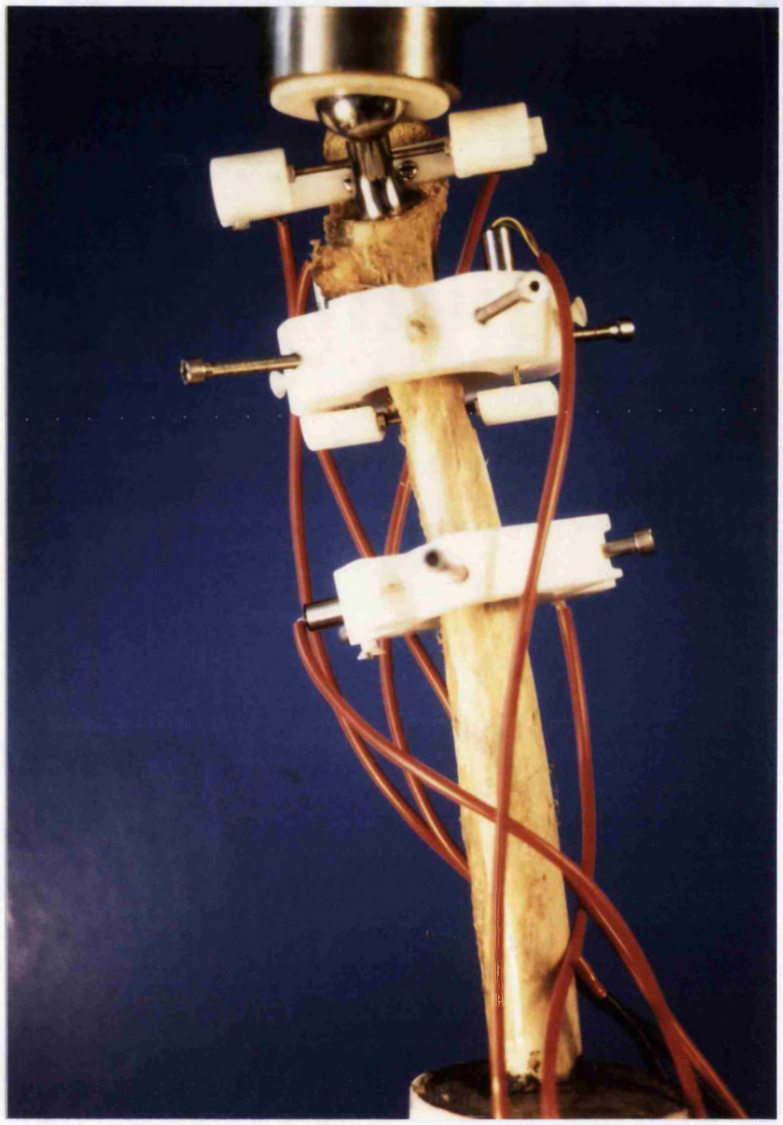

FIG. 7.3 EXPERIMENTAL SETUP FOR MEASUREMENT OF VERTICAL, LATERAL AND POSTERIOR RELATIVE MOTIONS BETWEEN THE STEM AND THE BONE

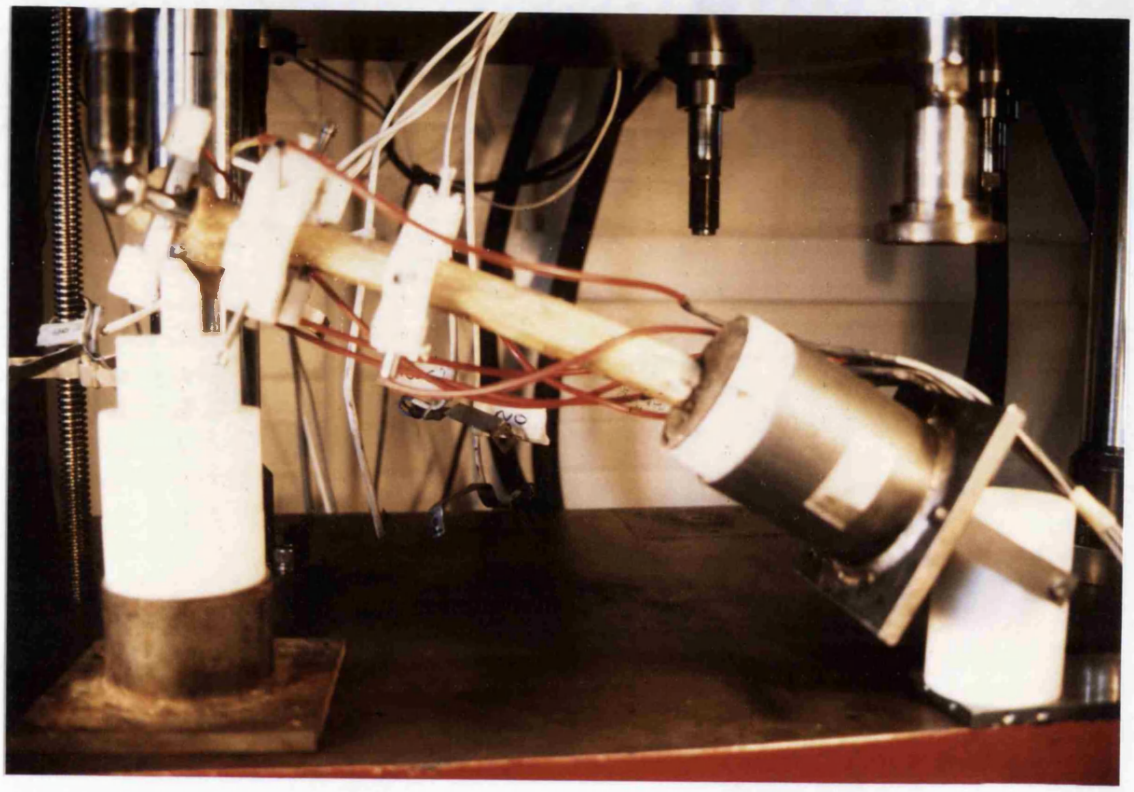

FIG. 7.4 EXPERIMENTAL SETUP FOR MEASUREMENT OF THE RELATIVE ROTATIONAL MOTION UNDER TORSIONAL LOADING

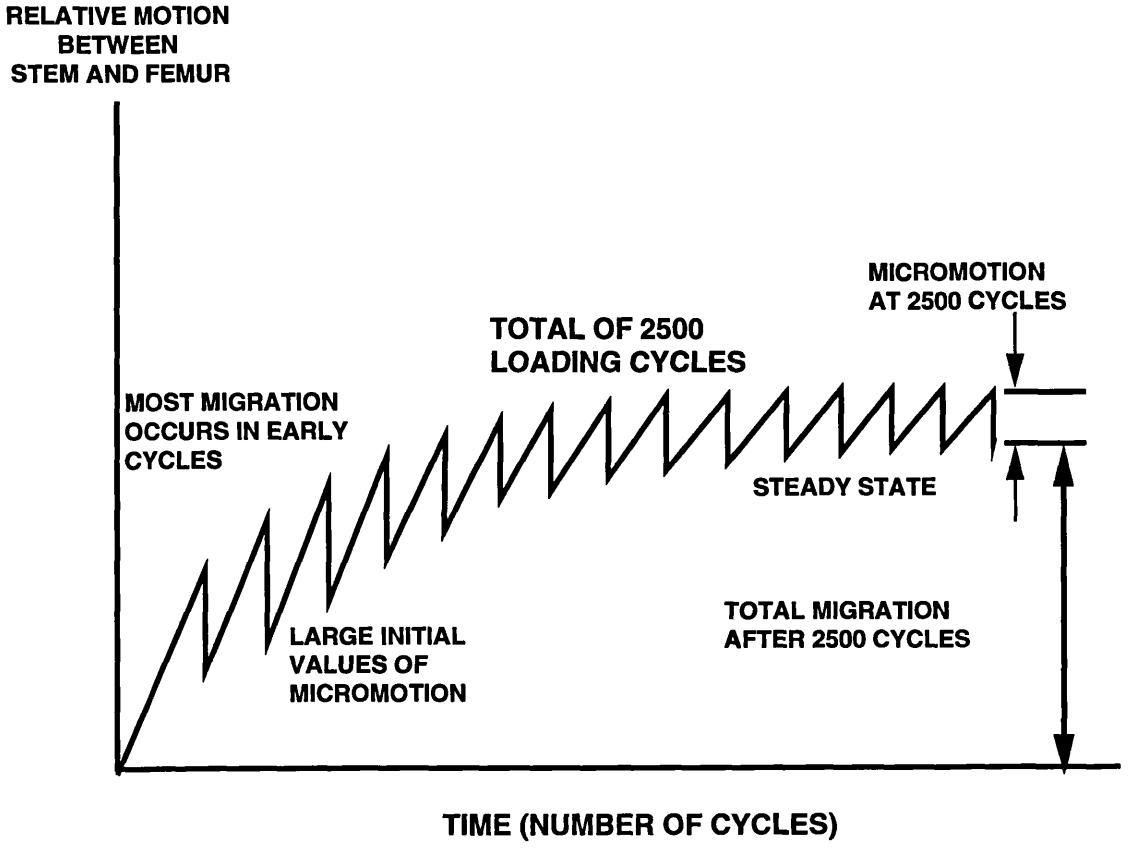

FIG. 7.5 DEFINITION OF RELATIVE MOTION AND MIGRATION OF THE STEM RELATIVE TO THE BONE.

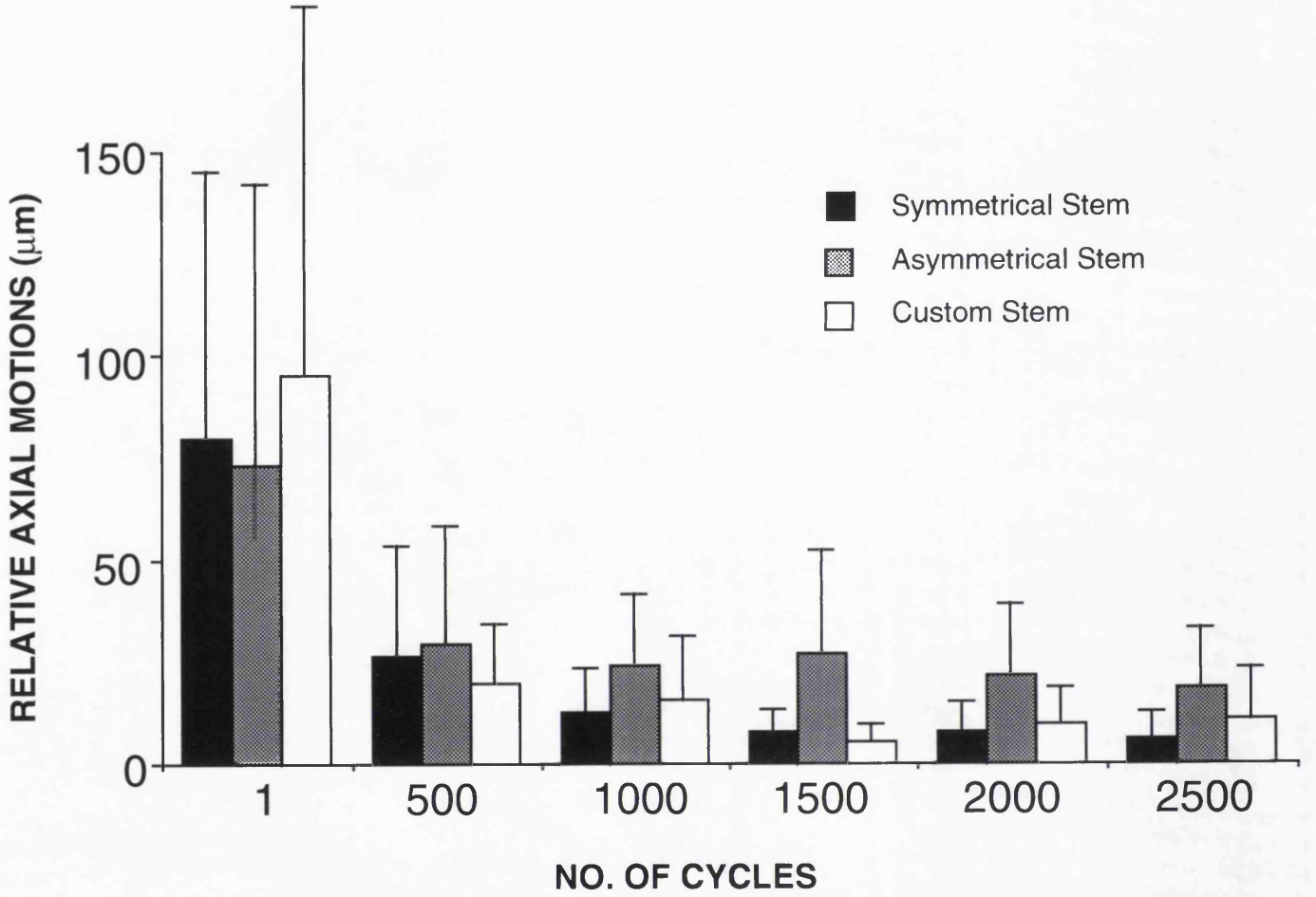

FIG. 7.6 COMPARISON OF RELATIVE AXIAL MOTION AFTER CYCLIC LOADING BETWEEN SYMMETRICAL, ASYMMETRICAL AND CUSTOM STEMS

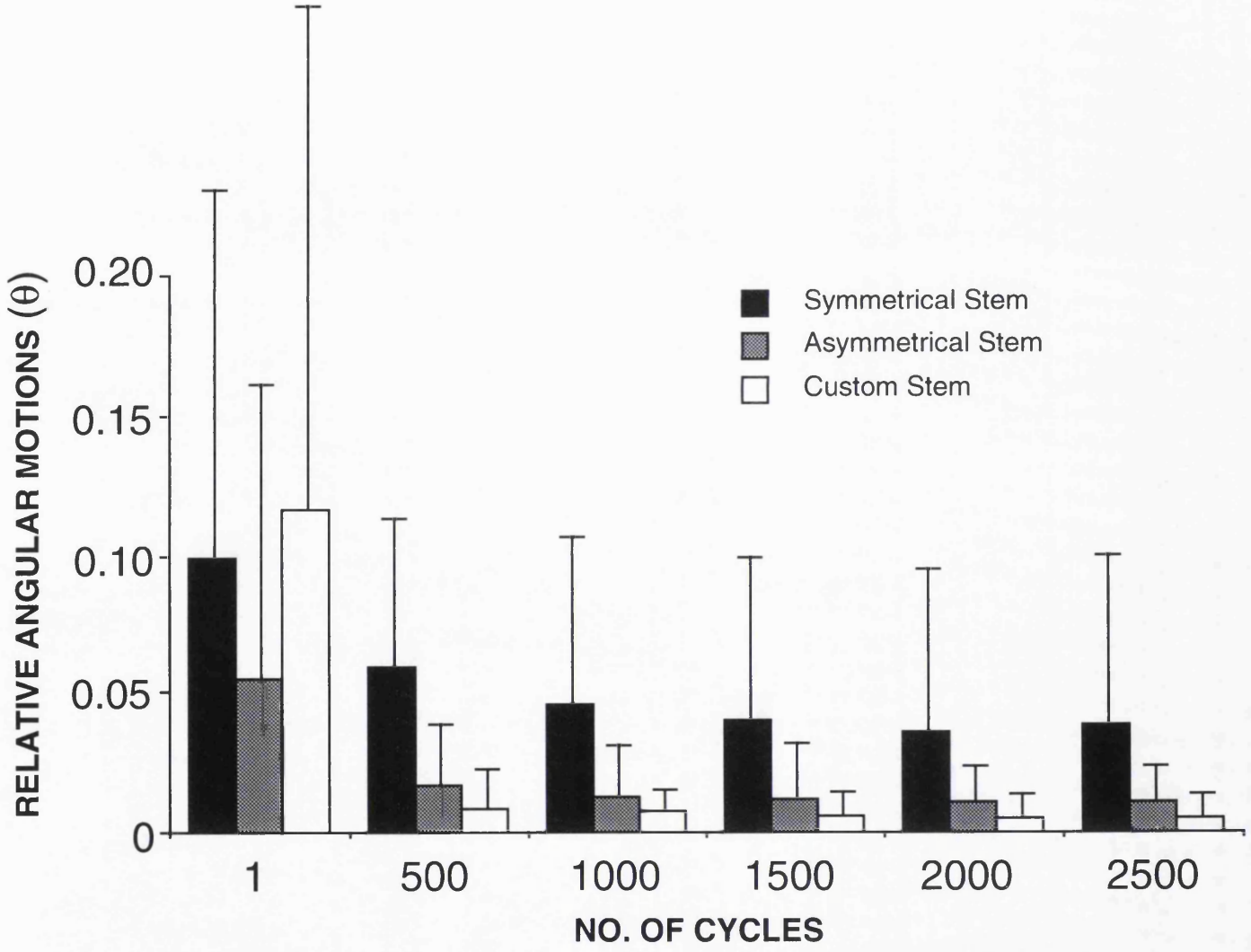

FIG.7.7 COMPARISON OF RELATIVE ROTATIONAL MOTION AFTER CYCLIC LOADING BETWEEN SYMMETRICAL, ASYMMETRICAL AND CUSTOM STEMS

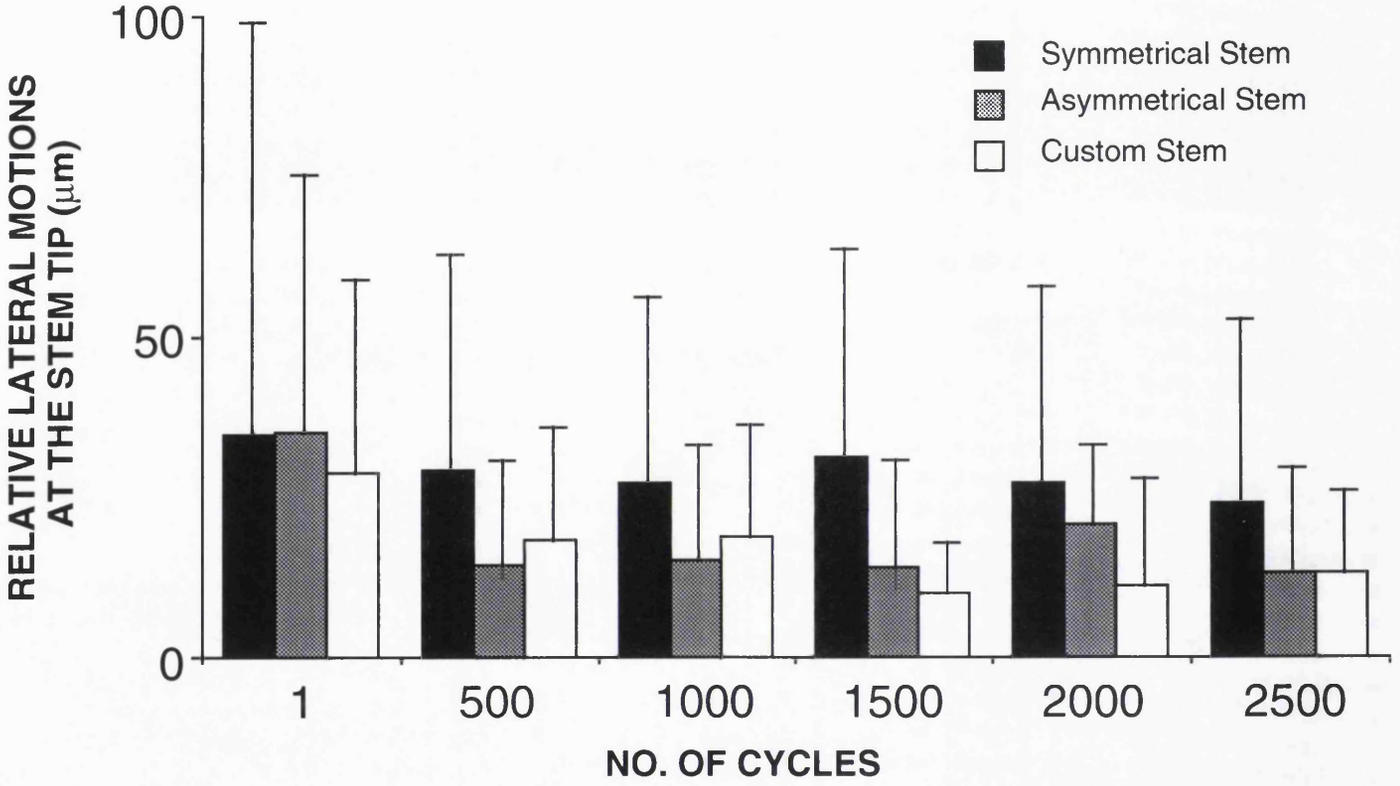

FIG.7.8 COMPARISON OF RELATIVE LATERAL MOTION AT THE STEM TIP AFTER CYCLIC LOADING BETWEEN SYMMETRICAL, ASYMMETRICAL AND CUSTOM STEMS

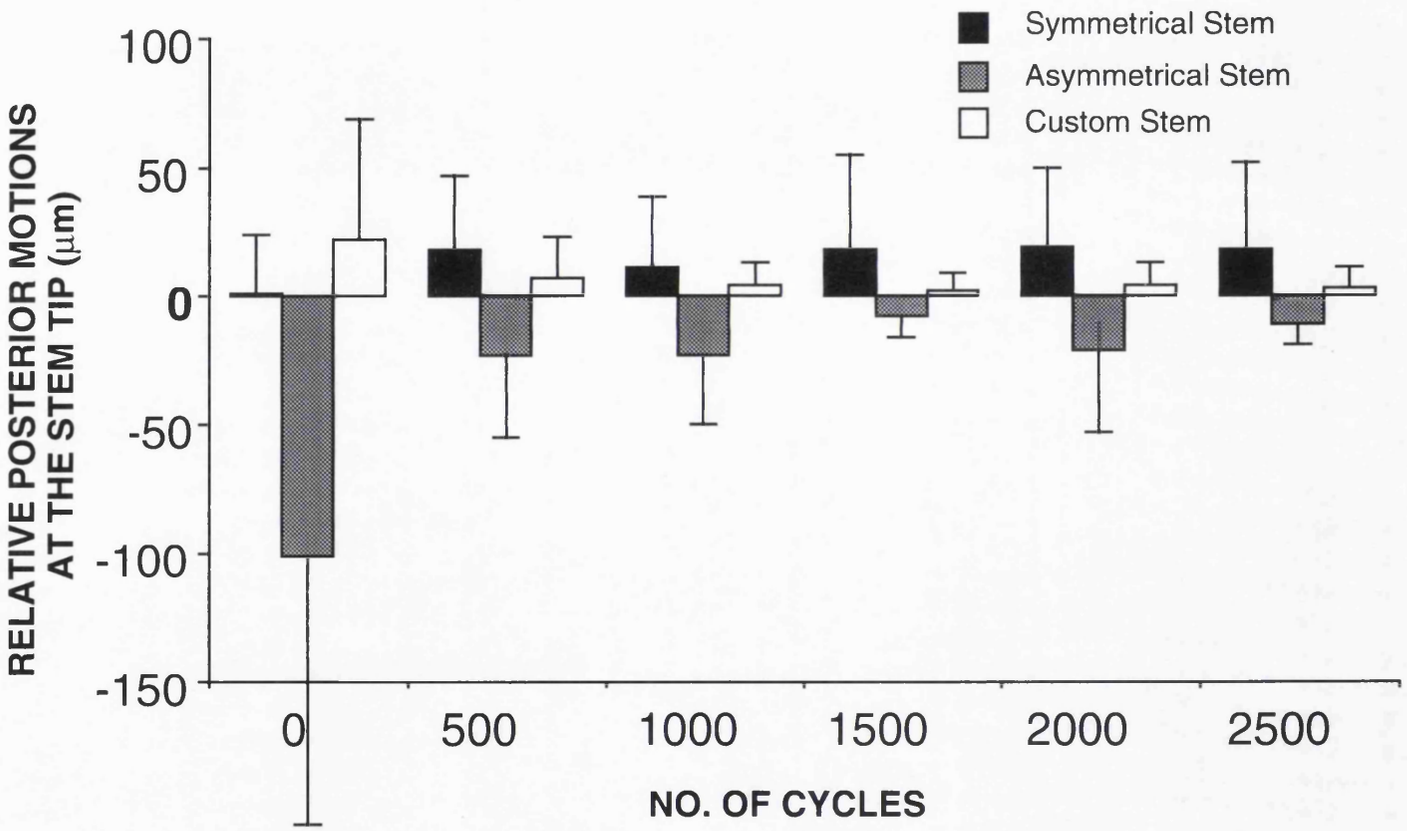

FIG. 7.9 COMPARISON OF RELATIVE POSTERIOR MOTION AT THE STEM TIP AFTER CYCLIC LOADING BETWEEN SYMMETRICAL, ASYMMETRICAL AND CUSTOM STEMS (MINUS VALUES INDICATE THAT THE TIP OF THE STEM MOVES ANTERIORLY)

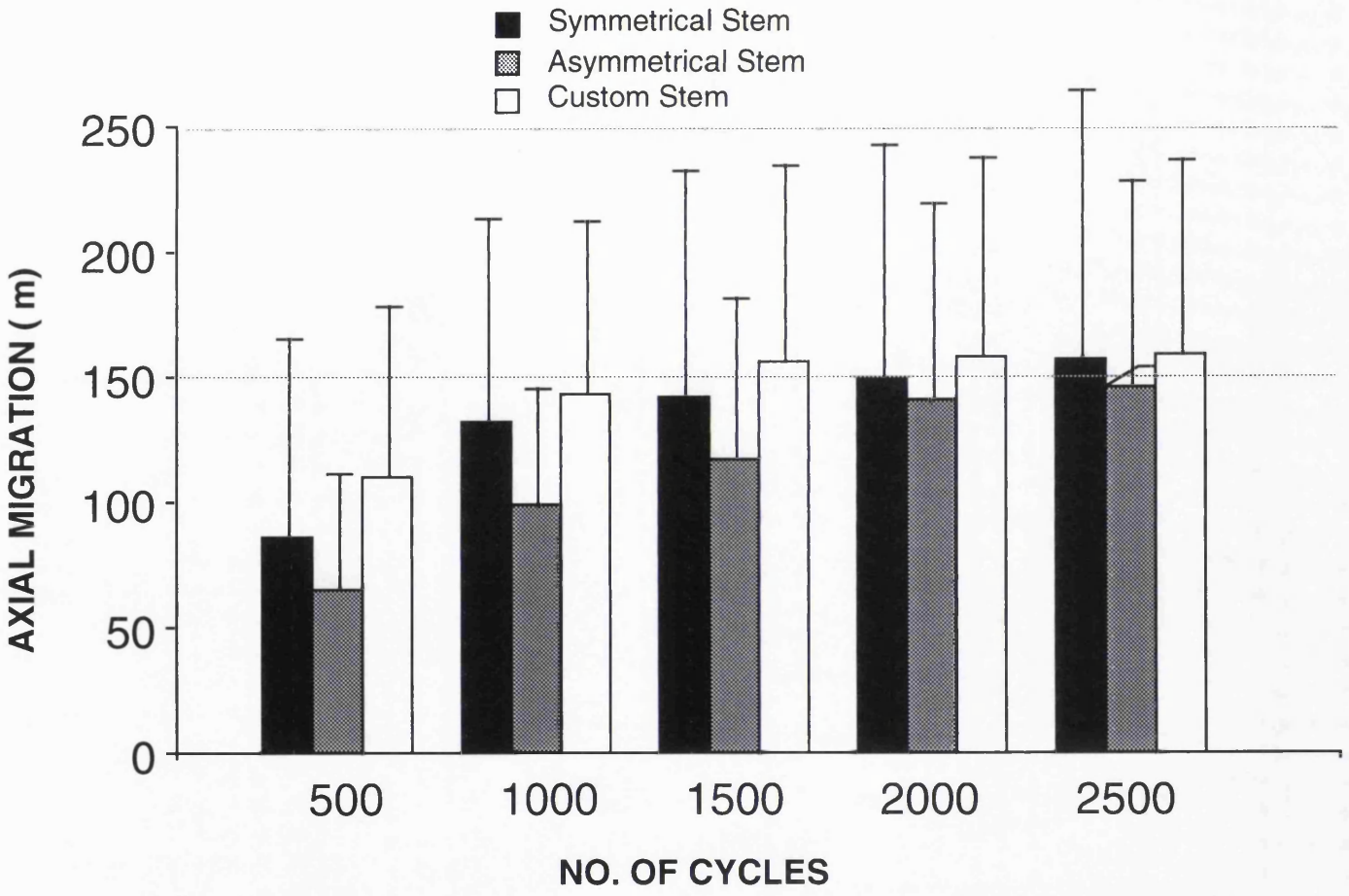

FIG. 7.10 COMPARISON OF AXIAL MIGRATIONS OF THE STEMS AFTER CYCLIC LOADING BETWEEN SYMMETRICAL, ASYMMETRICAL AND CUSTOM STEMS

TABLE 7.1 RELATIVE ANGULAR MOTION UNDER TORSIONAL LOADING

Bone No.	Symmetrical	Asymmetrical	Custom
	θ	θ	θ
1	0.183	0.024	0.029
2	0.118	0.022	0.011
3	0.051	0.016	0.029
4	0.192	0.043	0.012
5	0.123	0.004	0.022
6	0.068	0.009	0.001
7	0.030	0.007	0.007
8	0.568	0.031	0.018
Mean	**0.167**	**0.019**	**0.016**
SD	**0.172**	**0.013**	**0.010**

CHAPTER EIGHT

CLINICAL FOLLOW UP OF CUSTOM HIP STEMS

8.1 Hip stem migrations over time

8.1.1 Introduction

Total hip replacement (THR) is now well recognized as a method of relieving pain and restoring mobility in the dysfunctional joint. However, the main limitation of THR is the tendency of loosening of the stems over time, which is even more likely to occur in the younger, active and heavier patients (Cornell and Ranawat 1986). Among the many factors involved, aseptic loosening is the most common cause for prosthetic failure. It was found that stem migration was associated with stem loosening and other radiographic signs such as bone resorption and cement fracture, and it was also associated with long term clinical results (Loudon 1989, Freeman et al 1994). Therefore, it is very important to measure stem migrations over time, especially in the early stages, in order to provide the indication of stem performance in the long-term. However, the critical problem in measuring migration of femoral stems from plain radiographs is the reproducibility of the femoral position in subsequent X-ray films. If the femoral bone is rotated or flexed when compared with the previous X-ray film, accurate comparison may be invalid. Previous studies have focused on this problem and several techniques have been developed. All of these techniques have their own strengths and disadvantages, which are reviewed as follows.

8.1.1.1 Roentgen Stereophotogrammetric Analysis (RSA)

Roentgen stereophotogrammetric analysis is a reliable technique of obtaining accurate three-dimensional measurements from radiographic images in order to determine the spatial position of skeletal landmarks

and structural displacements within the musculoskeletal system. RSA overcomes the shortcomings of single plane radiographs which may yield a magnified and distorted image (Selvik 1989, Wykman et al 1988). This is because X-ray tubes act essentially as point sources emitting energy in a radial manner. As a result, any object not coplanar with the X-ray film plane produces a nonlinear image larger than itself. In total hip replacement, two techniques of roentgen stereophotogrammetry has been used to measure implant alignment, migration and loosening.

A. Bi-plane roentgen photogrammetry technique

In bi-plane roentgen photogrammetry, an object point is imaged on two radiographic films at right angle to each other. The orientation of the two films must be known in a coordinate system and the projected object point on each of the films must be determined in this coordinate system. In addition, the location of the two points sources (X-ray anode perspective centres) must be known in the same coordinate system. The coordinate system is established by two reference frames, each containing orthogonal wires. Two reference frames are placed at right angles to each other on the top of cassettes to construct the three-dimensional coordinate system. In this way, the spatial position of the object point can then be determined. The calibration markers are placed parallel to the film and reference planes to provide control for the multi-line spatial intersections which determine the coordinate system of the two anode perspective centres. The principal axes of the two X-ray anodes are orthogonal.

After data acquisition, the image coordinates are transformed to the reference frame coordinate system. Then the common reference system

coordinates of the anode perspective centres are determined, followed by the calculation of the coordinates of all object points via space intersections. Subsequent computations are needed including points distances which are used in the determination of relative prosthetic motion.

B. Convergent roentgen photogrammetry

Another roentgen photogrammetry system is composed of a single film plane and two radiographic tubes, each tube having a 20 degrees angle from the vertical, convergent to the object. A reseau plate containing fiducial marks is placed on the top of the film cassette. The reseau plate projects a calibrated pattern onto the x-ray film which can be used to detect the presence of any film distortion.

The imaging process of the roentgenographic stereophotogrammetry is executed in two phases. First is the anode resection phase. This is a calibration process in which two X-ray photographs are made from the reseaus and calibration plates. From these two films the spatial position of the anodes are determined by a resection computation. For the second phase, the calibration plate is removed from the frame, and the test subject is positioned in front of the reseau plate. The two X-ray anodes are activated simultaneously to obtain the images of the markers at the same instant of time. Thus, the coordinates of the image points can be determined on a coordinatograph. To determine the spatial position of the measured points, complicated mathematical calculations and coordinate transformations are involved.

C. Comparison of the two techniques

Overall, the accuracy of the two photogrammetry systems are very similar and very high (Lipper and Harrington 1982). However, regarding attainable precision, the geometric strength of the bi-plane configuration in the determination of the spatial position of object is more desirable than the 40 degree of convergent configuration. In addition, the bi-plane radiographic technique can use simultaneous exposure of A-P and lateral views, whereas the convergent radiographic technique requires two seperate exposures. With respect to the calibration process however, the bi-plane radiographic technique needs individual calibration for each patient whereas the convergent radiographic technique only requires one calibration for a group of patients. Based on the clinical criteria and accuracy, both systems meet the requirements for evaluation of loosening and migration of prostheses.

8.1.1.2 Conventional radiographic techniques

A. Grid radiograph

Although the roentgen photogrammetry techniques provide high accuracy of repositioning the femur for evaluating the migration of the stem in the subsequent radiographs, it is relatively complex, time consuming, and expensive. It also requires implantation of multiple metal beads in the femur as the fixed reference point. Therefore, the application of these techniques has not been widely accepted. Amstutz et al (1986) recommended superimposing a grid on the plain radiograph, with the centre of the grid-coordinate system over the pubic symphysis which has to be accurately reproducible. The patients are supine on the radiographic table, with the hips being fully extended and the feet being

held in neutral position by a foot-holder. The X-ray tube is centred over the femoral head, and the position of the centre of the beam is marked on the plexiglass grid and recorded in the file. In order to superimpose one X-ray onto another X-ray film, the magnification of these film has to be the same.

Amstutz et al (1986) studied forty-six surface replacements and twenty cemented total hip replacements with one year interval. The results showed that the magnification scale was 18±2% comparing with the actual size. In forty-one surface replacements (89%) and eighteen total hip replacements (90%), the images of the subsequent X-ray films could be exactly superimposed. However, there occured two surface replacement and two total hip replacements where the images could not be superimposed because of the differences in flexion and rotation of the hip at the time of the serial examinations. It appears that although this technique, together with other techniques such as using a chariot device (Kirkpatrick et al 1983) and using a metal slug placed in the femur as a fixed reference point (Paterson et al 1986), has improved the accuracy of measuring stem migration, it is still less than fully satisfactory.

B. Radiographic image analysis

The above techniques are only suitable for a prospective study, where the patients will receive X-rays with the specified techniques. However, an accurate technique for retrospective study of series of X-ray is necessary, which enable analysis of large number of past cases with long-term follow-up. A number of methods have been investigated to measure the migration of stems from ordinary plain X-rays.

Jones et al (1988) and Hardinge et al (1991) employed the technique of radiographic image analysis to measure the stem migration. The image analysis system consists of a personal computer, a light box, a video camera and a high resolution television monitor. The heart of the system is a frame grabber card contained within the computer. The video camera scans the back-lit radiographic film, then outputs into the frame grabber which, under software control, converts it into a digital image. This image is held in the computer memory and used to reconstruct an analog signal for simultaneous display on the TV monitor. The system can improve the quality of the image and quantify predefined parameters. A poor radiographic image can be manipulated to enhance its intensity, contrast or consistency of exposure by filtering the image mathematically. In addition, areas of specific interest can be selectively enhanced. However, the actual accuracy of measuring stem migration depends on the reference points selected in bone and stem, and depends on the magnification determined from the X-ray .

The present study has therefore been conducted for the purpose of developing and evaluating a new technique for measuring stem migration by digitizing standard plain A-P radiographs. By using this technique, migrations of CAD-CAM custom stems have been measured. In addition, bone-stem interface resorption and remodelling were radiographically studied.

8.1.2 Materials and methods

8.1.2.1 Methodology study of digitizing X-ray

A study on the methodology of digitizing X-ray was carried out to determine the accuracy of the technique used for measuring the migration of the stems. Six cadaveric femurs with four types of femoral stem (Charnley, Stanmore, Norwich and Ring) were used. Each of four stems was inserted tightly into three different femoral canals, resulted in totally twelve stem-bone combinations. In order to account for different radiographic views taken in a series of X-rays over a long period of time, the stem-bone was fixed in a jig so that the angle of flexion-extension and internal-external rotation could be adjusted (Fig.8.1). Radiographs were taken with the tested stem-bones in neutral, ten degrees of flexion-extension, and ten degrees of internal-external rotation. A number of reference points on the bone and stem were selected and digitized (described in detail below). The magnification scale, as well as the distances between the stem and bone were measured in the different orientations to determine whether or not the magnification scale and the stem migration would be affected. The position of the reference points were also studied to determine which reference points could produce consistent and reliable results.

A. Reference points on femoral bone and stem

Twenty-three reference points were selected and digitized on the bone and the stem. Points 1, 3, 5 and 2, 4, 6 were digitized on the circumference of the femoral head from which the centres of two circles were calculated. If the diameter and centres of these two circles matched to each other with a difference of less than 0.2 mm, further analysis would continue. Otherwise it was assumed that the digitizing was not accurate enough, and a prompt would be given to repeat the digitizing. The diameter of the circle was compared with the actual diameter of the head

to determine the magnification scale in that location. Points 7-10 were digitized on the stem neck or collar to calculate the magnification scale at that location. It has been observed that the magnifications could be different if the head was anterverted. Therefore the neck or collar was used to represent the plane of the proximal stem. Points 11-12 at 50 percent of stem length and points 13-14 at 10 percent of stem length from bottom were used to define the coordinate system of the stem. A stem centre line was drawn through the middle of point 11-12 and points 13-14, then point 15 was defined at the centre of the stem tip.

For the femoral bone, point 16, 17, 18 represents the top of the greater trochanter, the most lateral point of the greater trochanter, and the most medial point of the lesser trochanter. Points 19-22 were digitized on the outer cortex at the same level as the stem (points 11-14) to define the coordinate system of the femoral canal. Finally one free point (point 23) was digitized on any distinguished landmark for the particular femur, such as a wire or screw (Fig.8.2).

After the reference points were digitized, the coordinates of all points were divided by the neck magnification so that all the measurements were actual size. The femoral coordinate was determined from the centre line of the canal, and the stem coordinates were determined from the centre line of the distal part of stem. Subsequently, all the reference points were transformed according to the femoral coordinate system so that the distance between the stem and bone could be measured in the same coordinate system. The distances between the reference points on the stem and bone were calculated and recorded in the direction of the y-axis of the femur. Any distance changes in the subsequent radiographs were defined as migration of the stem. The varus-valgus angle of the

stem relative to the femur was calculated from the changes of the angle between the stem mid-line and the canal mid-line. The internal and external rotations of the stem were not considered in this study because the technique could not accurately detect the rotational position of the stem.

B. Comparison of two magnification scales (head vs neck)

In order to compare the magnification scale from the stem head and neck, a CAD-CAM hip stem which inserted in the femur was radiographed. A radio-opaque ruler placed alongside the stem served as a control. The magnification of the radiographs were calculated from the known diameters of the head and neck. The radiographs were taken with the stem-bone in neutral, 10 degrees internal and external rotation and 10 degrees flexion and extension.

Six points on the outline of the femoral head were digitized to calculate the head diameter, which was divided by the actual head diameter to provide the head magnification. A line crossing to the neck was drawn at the base of the neck, and the two crossed points were digitized. The distance between the two points was calculated and divided by the actual diameter of the neck to produce the neck magnification. These two magnifications were then compared with the magnification calculated from the ruler to determine which method was more accurate.

When the magnification scale was determined, it was used to calibrate all the reference points on the femur and stem, so that the measurements between the stem-bone were actual size. Any differences of the

magnification in the subsequent radiographs were corrected and therefore should not influence the results.

C. Accuracy of the digitization

The accuracy and repeatability of the digitization were evaluated. Each radiograph with twenty-three reference points were repeatedly digitized ten times. Totally ten different radiographs were studied to determine the accuracy of the digitization.

8.1.2.2 Radiographic evaluation of CAD-CAM stems

From September of 1989 to July of 1993, two hundred and thirty-seven CAD-CAM custom stems were inserted. The diagnosis categories were revision (30%), JRA (28%), CDH (15%), OA(8%) and other abnormal morphology (19%). Among them, forty-eight cases were radiographically followed up in immediate post-operation, six months, one and two year intervals. Thirty female patients and seventeen male patients had average age of thirty-three (from fifteen to eighty-one years old). All the prostheses were uncemented (press-fit).

The migration of thirty-six Charnley stems and thirty-nine Stanmore stems were analysed, which served as a comparison with the CAD-CAM stems.

8.1.3 Results

8.1.3.1 Methodology evaluation

A. Comparison of two magnification scales (head vs neck)

The results obtained clearly showed that the neck magnification was closer to the ruler when compared with the head magnification (Table 8.1). The difference between the ruler and the neck and between the ruler and the head was 0.22±0.58% and 2.8±0.93% respectively. The magnification scales measured from the femoral head changed significantly from the minimum of 111.5% when the stem was in flexion to the maximum of 116.5% when the stem was in extension, whereas the results measured from the stem neck were slightly stable, ranged from 108.8% in minimum when the stem was in flexion to 113.1% in maximum when the stem was in extension. Fig. 8.3 showed the comparison of the magnification scales taken from the ruler, stem head and stem neck.

B. Reference points on bone and stem

The reference point on the most prominent part of the lesser trochanter (point 18) was not stable when the bone was in different orientations, especially in rotation. The distance between the lesser trochanter and stem collar changed within the range of 1.71-6.23 mm, averaging 3.59 mm (Fig. 8.4). The correlation between the position of the lesser trochanter and the bone orientation was not constant, which depended mostly on the profile of the lesser trochanter of the particular bone. However in general, when the bone was in flexion, the point on the lesser trochanter moved distally which increased the stem-bone distance, whereas in extension, the point moved proximally which decreased the stem-bone distance. When the stem-bone was in internal-external rotation, the point on the lesser trochanter also moved.

The reference point on top of the greater trochanter was relatively stable. The change of the distance between the greater trochanter and the stem collar was only 0.24 mm (from 0.1 to 0.32mm) when the stem-bone was in different orientations (Fig.8.5).

The stem tip as a reference point was not stable, the difference could be as much as 7.62 mm when the stem orientation changed (Fig. 8.6), whereas the stem collar or the proximal-lateral corner of the stem was observed to be relatively stable (Fig. 8.5).

C. Varus and valgus angles of stem-bone

The varus and valgus angle between the stem and bone were defined as the angle between the long axes of the stem shaft and the femoral shaft. It was observed that the error in varus-valgus angle was 1.2 degrees (from 0.72 to 1.74 degrees).

D. Accuracy of the digitization

The twenty-three reference points of an X-ray were repeatedly digitized ten times. The differences between the maximum and minimum values on each points were averaged. The results showed that the accuracy of the digitization was 0.07±0.03 mm in the x-axis and 0.06±0.02 mm in the y-axis. Instead of repeatedly digitizing on a single spot, this repeatability study was taken on the actual radiographs with the same reference points as the one used for the migration studies, therefore the results were more realistic.

8.1.3.2 Radiographic evaluation of the CAD-CAM stems

A. Radiolucent line

Radiolucent lines were found in ten hips (21%). Most of them occured in six months and were less than 1 mm in width. The most common place for the radiolucent lines was at top lateral part of the prostheses (Fig.8.7). These lines may be caused by stem migration in the early stage, which were particularly true for the cementless stems.

B. Bone formation and bone resorption

The formation of new bone was observed in eight cases (17%). It usually occurred at the stem tips which contacted with the cortex (Fig.8.8). Such bone formation occurred more commonly on the lateral than on the medial cortex. There was no sign of bone resorption.

C. Migration of CAD-CAM stems

Most of the stems migrated in the first six months. During this period (N=48), 58% of the stems migrated less than 1 mm, 21% from 1-2 mm, 17% from 2-5 mm and 4% was more than 5 mm. The results obtained from six month to one year (N=40) suggested that the stems were more stable, 83% less than 1 mm, 13% from 1-2 mm, 2% from 2-5 mm and 2% more than 5 mm. The stems were even more stable during one to two years (N=5) in that all the stems migrated less than 1 mm (Fig.8.9). In two cases, the stems migrated 4.26 mm and 7.06 mm during the first six months, but both were stable (<1.47 mm) in one year. Clinical follow-up suggested that relief of thigh pain and restoration of hip function were almost universal.

D. Other complications

One femur fractured six weeks after total hip replacement and the stem migrated 10 mm, although the stem was found rigidly stable during revision. This case was not included in the migration study.

8.1.3.3 Radiographic migration of the cemented stems

The migration which occurred with the Charnley stems during first six months was <1 mm, 1 - 2 mm, and 2 - 5 mm in 66%, 22% and 12% of the cases respectively (N=36). From 6 months to 1 year, the stems were more stable as such that 80% and 20 % of cases migrated less than 1 mm and 1 - 2 mm respectively. No stems migrated more than 2 mm during this period. From one to two years, 82% migrated less than 1 mm and 14% from in 1 - 2 mm. However, another 4% of stems were observed to have a migration of 2 - 5 mm.

The migration pattern of the Stanmore stems was similar to that of the Charnley stem. During the first six months, the stem migrated less than 1 mm, 1 - 2 mm, and 2 - 5 mm in 67%, 21% and 12% of cases (N=39). From six months to one year, 84% migrated less than 1 mm, 16% from 1 - 2 mm, and no stems migrated more than 2 mm. During one to two years, the stem migrated less than 1 mm, 1 - 2 mm, and 2 - 5 mm in.79%, 19% and 2% of the cases.

8.1.4 Discussion

8.1.4.1 Magnification scale

In order to accurately measure stem migration, it is very important to obtain a precise magnification scale of the X-ray film. The femoral head has previously been employed to calculate the magnification since it has a circular profile on the X-ray (Hardinge et al 1991). However, because of the neck anteversion and inconsistent rotation of femur in the subsequent X-rays, the femoral head can be positioned anteriorly (away from the film) or posteriorly (close to the X-ray) with respect to the stem axis, which will lead to an inconsistency in the magnification. The amount of error depends on the offset of the femoral head. When the stem collar or the neck is close to the stem axis, the magnification error is therefore be reduced. In addition, if a metal backed acetabular cup is used, the femoral head will be covered so that the circular profile can not be defined. The present study used the neck or collar of the stem to determine the magnification scale.

8.1.4.2 Reference points

Selection of a stable point for reference of the femoral bone is of paramount importance in accurately measuring stem migration. Some anatomic landmarks are sensitive to the orientation of the femora in radiographs, which are thus not suitable as a reference. The present study suggests that the lesser trochanter is sensitive to the rotation of the femora, whereas the greater trochanter is relatively stable. Although additional marks can enhance the definition, such as Herbert screw, beads or staples implanted into the greater trochanter along the plane of the femoral stem (Mulroy et al 1991), this may not be available in a retrospective study. The present study used the greater trochanter as a bone reference.

The point for the stem reference is even more difficult to define, which mostly depends on the geometry of a particular stem. The present study suggests that the stem reference should in principle be selected in the proximal part of the stem close to the bone reference, so that the effect of stem-bone orientation on the distance between the stem and the bone can be minimized. The stem tip is not stable, therefore can not be used as a stem reference. Mulroy et al (1991) used a transverse hole through A-P plane in the proximal portion of the stem to define the position of the implant. The position of the hole on radiographs was found consistent, and the orientation of the stem could be detected according to the shape of the hole. However, if the stem is thick enough in the anterior-posterior axis, the hole can then be shadowed by the metal and lose its image. Jones et al (1988) used a cross point of the centre of the femoral head perpendicular to the centre line of the stem shaft as a stem reference. It was observed that this point could also be affected by the orientations of the stem. Additional features of the stem can also be used as reference and improve the accuracy, such as the tip of upward extension of the Freeman stem. The present study employed the collar or proximal lateral corner of the stem as a stem reference, which provided relatively accurate and reliable results. Although the error of only 1.2 degrees of varus-valgus angle was obtained in the study by using present technique, it is recognized that the accuracy depends on the stem position within the canal. The varus-valgus angle can be affected by the rotation if the stem has not been placed in the centre of the canal. This is agreed in other studies (Goodman et al 1987, Albert et al 1991). Therefore, the present study did not measure the varus-valgus angle of the CAD-CAM stems.

8.1.4.3 The technique of measuring stem migration

Although other methods are more accurate and reproducible in measuring stem migration (Kirkpatrick et al 1983, Chandler et al 1984, Amstutz et al 1986, Harding et al 1991, and Mulroy et al 1991), most of them are technically complicated and time-consuming, while some can only be used for prospective studies. The present technique of measuring stem migration by digitizing A-P X-ray is simple, and relatively accurate. It can be used for retrospective studies to determine the correlation of the early migration with the long-term clinical survival.

The present technique can only measure axial migration. In order to measure stem migrations in three coordinates (Vertical, varus-valgus, internal-external rotation), more advanced and reliable techniques are needed.

8.1.4.4 Comparison of migration between CAD-CAM stems and cemented stems

Overall, the cemented stem is stable initially and deteriorates over time, whereas the cementless stem will migrate initially and then stablize or further migrate. In the present study, the short-term results of CAD-CAM stem are comparable to the cemented Charnley and Stanmore, and slightly better after one year.

Most of the CAD-CAM stems which migrated more than 2 mm were designed in the early stages. The stem was basically straight and the surface was polished. The design was improved afterwards so that the stem has lateral flare, proximal grooves and HA coating. By analysing

fifteen stems with the improved design, all the stems migrated less than 1 mm in a six month period. The long-term results of the CAD-CAM stems are to be studied in the future.

8.2 Bone density changes over time following CAD-CAM hip replacement

8.2.1 Introduction

Adverse bone remodelling and bone resorption following total hip replacement has been a major concern in the long term stability of a femoral prosthesis. Bone remodelling may correlate with stem geometry, material properties and remaining bone quality. If bone loss occurs continuously and significantly, it may indicate the failure of the stem. Therefore, it is very important to follow up the changes of the bone mineral density after total hip replacement. Bone mineral density can be measured with several techniques, such as quantitative digital radiography, quantitative computer tomography, dual photon absorptiometry (Dunn et al 1980, Bohr and Schaadt 1985, Wahner et al 1985), and dual energy radiographic absorptiometry.

8.2.1.1 Plain film radiography

Conventional radiography is the most readily available and frequently used method for studying bone pathology in clinical practice. This technique may visually assess the overall osteopenia. However, it is often not able to differentiate between radioluscent pathology until changes in excess of 30% have occurred (Ardran 1951, Vose 1966, Renton 1990). Therefore, such techniques have been superseded by more accurate quantitative techniques.

8.2.1.2 Ultrasound

Ultrasound is currently used for a wide range of diagnostic investigations with a precision of 2-5% (Parfitt 1990), and is the only imaging technique that does not use ionising radiation. Ultrasound calculates the velocity and the attenuation of bone, then predicts bone mineral density. The broadband ultrasound attenuation (BUA) has been compared with the DEXA scan on the changes of bone mineral density (BMD) of spine and femoral neck, the results suggested that the prediction of BMD from BUA is not good enough in the individual.

8.2.1.3 Quantitative computer tomography (QCT)

This technique utilises a conventional CT scanner with an additional computer software package capable of measuring the bone mineral density of the trabecular component of the bone skeletal. It is the only technique which gives a true density measure in mass per unit volume and is able to differentiate between trabecular and cortical bone. While the sensitivity of the technique is high and the accuracy and precision is acceptable, its significant radiation exposure at approximately 18 mGy for routine BMD assessment has precluded such a technique from being used in screening procedures. However, recently developed Peripheral Computerised Tomography (pQCT) seems promising, as it has high sensitivity and extremely low dosage. The particular strength of pQCT is its ability of three-dimensional measurement of bone density in grams/cm^3.

8.2.1.4 Absorptiometry

A. Single photon absorptiometry

When a beam of photons is passed through the body, hard tissues such as bone absorb more photons than soft tissues. By using this principle, bone mineral content was measured. In the early 1960's, single photon absorptiometry with low energy source was used. The photon beam was directed through the skeletal (forearm) positioned in a waterbath and detected on exit by a scintillation counter. The waterbath was used to make soft tissue factor constant. Repositioning the patient in this technique was critical and the half life of the isotope required regular calibration and adjustment.

B. Dual photon absorptiometry

Dual photon absorptiometry was developed in 1970's, which allowed the bone mineral content of deeper skeletal sites to be measured. Two photon energies were used, primarily from gadolinium 153, which emits energy peaks at 44 and 100 keV. At these energy levels, there is good separation between soft tissue and bone. The dual photon absorptiometers were calibrated against known standards, often a solution of hydroxyapatite within a step wedge container.

C. Dual energy X-ray absorptiometry (DEXA)

Dual energy X-ray absorptiometry (DEXA) is the most recent development in bone densitometry (Sartoris and Resnick 1990). This technique uses X-ray absorption to determine the amount of bone in specified skeletal regions. An X-ray source has a number of advantages

over radionuclides such as increased source intensity, flexibility in the selection of the energy spectral and no source decay. Basically, there are three fundamental different system in dual energy generation, which are K-edge filtration to produce two narrow energy bands, rotary calibration filtration by switching source voltages and rotating calibration wheel, and samarium filter to optimise the energy distribution. By comparing with the older, widely used dual photon absorptiometry, DEXA is considered to be superior in terms of less radiation dose (<5 mRem), enhanced image resolution, precision and reduced scanning time (Kelly et al 1988, Wahner et al 1988, Pacifici et al 1990, Sartoris and Resnick 1990). By improving system resolution and increased efficiency from the usage of a fan shaped X-ray beam, a precision of less than 1% has been reported (Kiratli et al 1992).

DEXA scan has widely been employed in clinical to analyse the changes of bone mineral density following total hip arthroplasty (Kiratli et al 1992, Kilgus et al 1993). In the present study, the CAD-CAM hip stems were also followed up by DEXA scan.

8.2.2 Materials and methods

8.2.2.1 DEXA scanner

The DEXA scanner (QDR-1000, Hologic Inc), which used for the present study, produces two energies by switching source voltages, and a rotating calibration wheel. The X-ray beam passes through two filters to provide the dual energies required and a third calibration plate of known constant material. The precision of the scanner is better than 0.01 g/cm^2, and the accuracy is 0.5%. The scanning time for the hip is 6.0 min. The

radiation dose to the patient is less than 5.0 mRem per scan, which allows repeat measurements with little hazard.

The software package for data analysis was provided by the manufacturer (Hologic Inc) for both acquisition and analysis of data. This software allows the measurement of BMD adjacent to metal implants, and allows to scan the entire femoral component, the surrounding femur, and the soft tissue to be scanned. Bone mineral content (BMC, in grams) and area (cm^2) were measured, and the BMD was calculated within each region of interest, using an automated algorithm which included a software-driven edge detection algorithm. Areas of the scan in which the X-ray beams were attenuated by the metal implant were automatically subtracted from the scan results. In addition, a standardised soft tissue region around the implant was defined which, in the analyses, was also subtracted from all regions of interest to give bone-density values independent of local soft tissue inhomogeneities. Seven Gruen zones are definable and are used for the analysis.

8.2.2.2 CAD-CAM patients

Eleven male and ten female patients with CAD-CAM hip replacement (Sixteen right and five left) were DEXA scanned during 1992-1993. The average age, height and **body weight** of the patients were 54yrs (21-48), 166cm (142-180) and 74kg (40-97) respectively. During scanning, the patient was in a supine position, and the leg was parallel to the long axis of the table so that the transverse beam path would be perpendicular to the femoral shaft. The feet were positioned on a triangular frame which resulted in reproducible hip positions in a series of scanning. The patient was asked to remain immobile during the scan

(6 minutes). Twenty-one cases were scanned over a six month period, which five cases were scanned at one year. The analysis of bone mineral density was based on the seven Gruen zones.

The changes of bone mineral density in a period of 0-6 months and 6-12 months were statistically analysed (paired t-test) by using SYSTAT package. The difference between the age groups (younger and older than 50 years old) was also analysed (Student's t-test).

8.2.3 Results

Bone mineral density varied considerably from region to region, and from patient to patient. Overall, bone mineral density was higher in the mid-shaft of the femur than in the proximal femur (Fig. 8.10). Compared with immediate post-op, bone mineral density was reduced by 5% on average during the first six months, with maximum loss of 12% in zone 2 and no changes in zone 4 (Fig 8.11). Compared with six month, bone mineral density at one year was further reduced by 1.4% on average, with a maximum loss of 12% in zone 7 and a maximum gain of 5% in zone 4 (Fig. 8.12). However, statistical differences were only observed in zone 2 and 3 ($p=0.001$) during the first six month .

No differences were observed in sex, side, height and weight ($P>0.05$). However, the bone mineral density was less changed in the older group (>50's) than in the younger group (<50's) (Fig. 8.13). Although similar results of BMD were obtained after the immediate post-op, 1.29 g/cm^2 for the younger and 1.30 g/cm^2 for the older, after six months, the younger group lost 10% of bone density, but the older group gained 1.6% of bone. Such a difference was significant in zone 7 ($p=0.043$).

8.2.4 Discussion

The changes in bone mineral density following total hip replacement reflect the stem design and predict the clinical results. By increasing scan resolution and eliminating metal artifact by means of a special segmentation algorithm, DEXA scan can now accurately measure BMD *in vivo* . However, the disadvantage of the A-P DEXA measurements is in that it can only provide two-dimensional information of BMD without considering the depth of the measurement. A more sophisticated multiple DEXA technique has recently been developed, which has the ability to combine A-P and lateral scan together while the patient remains still on the X-ray couch. This provides three-dimensional measurements and the results are expressed as grams of bone per cube. This later technique enhances the accuracy and precision of the unit compared with the A-P DEXA.

The previous study observed that the bone loss in the distal region was less than that in the proximal region following total hip replacement (Kilgus et al 1993), which agreed with present results. It has also been observed from the present study that BMD increases with time in the distal region, but continues to decrease in the proximal region within a year. McCarthy et al (1991) presented a result with loss of 38.1±17.9% of BMD in the proximal medial regions after 1-3 years of cemented total hip replacement.CAD-CAM stems showed a similar pattern of bone loss but of a much less quantity. It has been reported that the reduction of BMD will cease after the second postoperative year (Engh and Bobyn 1988). However, progressive bone loss even after 7-14 years was also

observed (McMarthy et al 1991). The different observation suggest that changes of BMD depend on the stem design.

A change with age in increase of higher density bone and decrease of lower density bone has been oberved (Simmons 1991). This may explain the observation from present study that the older group has less change in BMD, whereas the younger group with a substantial amount of recently formed, lower-density bone is more accessible to bone remodelling. The significance of the observation is that comparision of BMD change following total hip replacement has to be in age-matched groups.

The early results of DEXA scan of the CAD-CAM stems were encouraging, and the bone mineral density only changed in a small range. This could be associated with a closer fit and better stress distribution of the CAD-CAM stems, which has been shown in the laboratory studies.

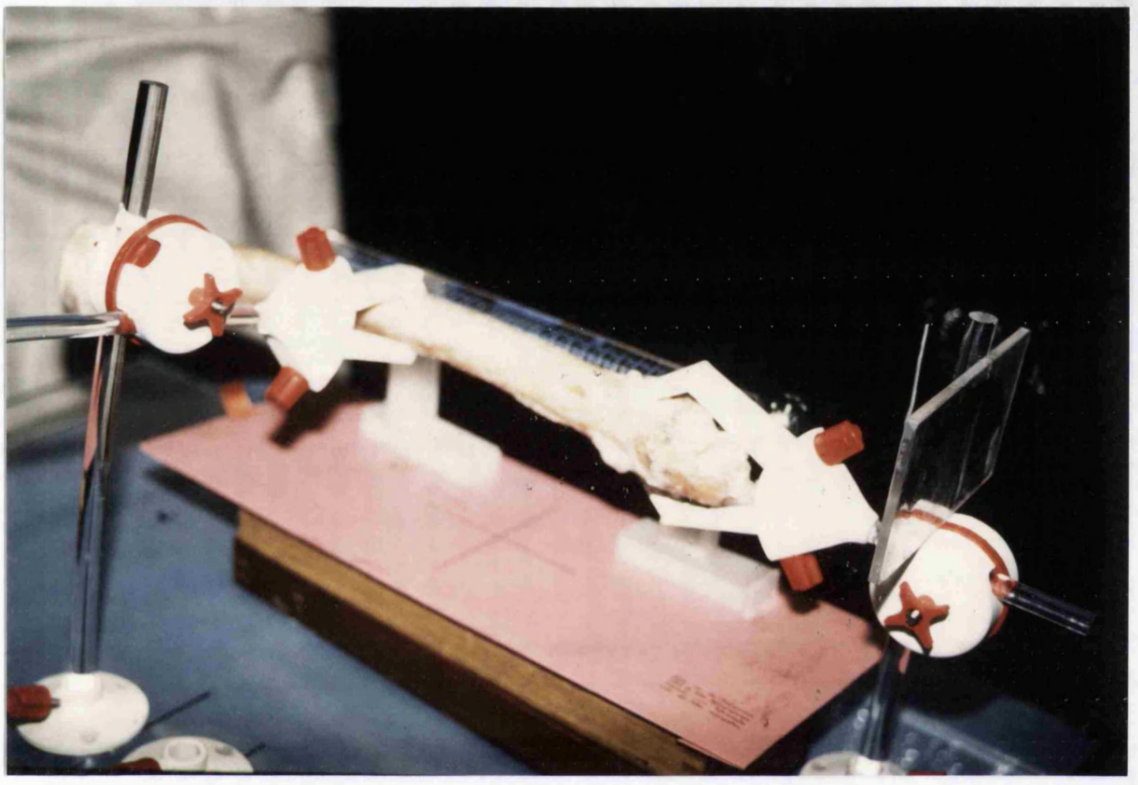

FIG. 8.1 DEVICE FOR HOLDING THE STEM-BONE IN A KNOWN ANGLE OF ROTATION AND ORIENTATION DURING RADIOGRAPH

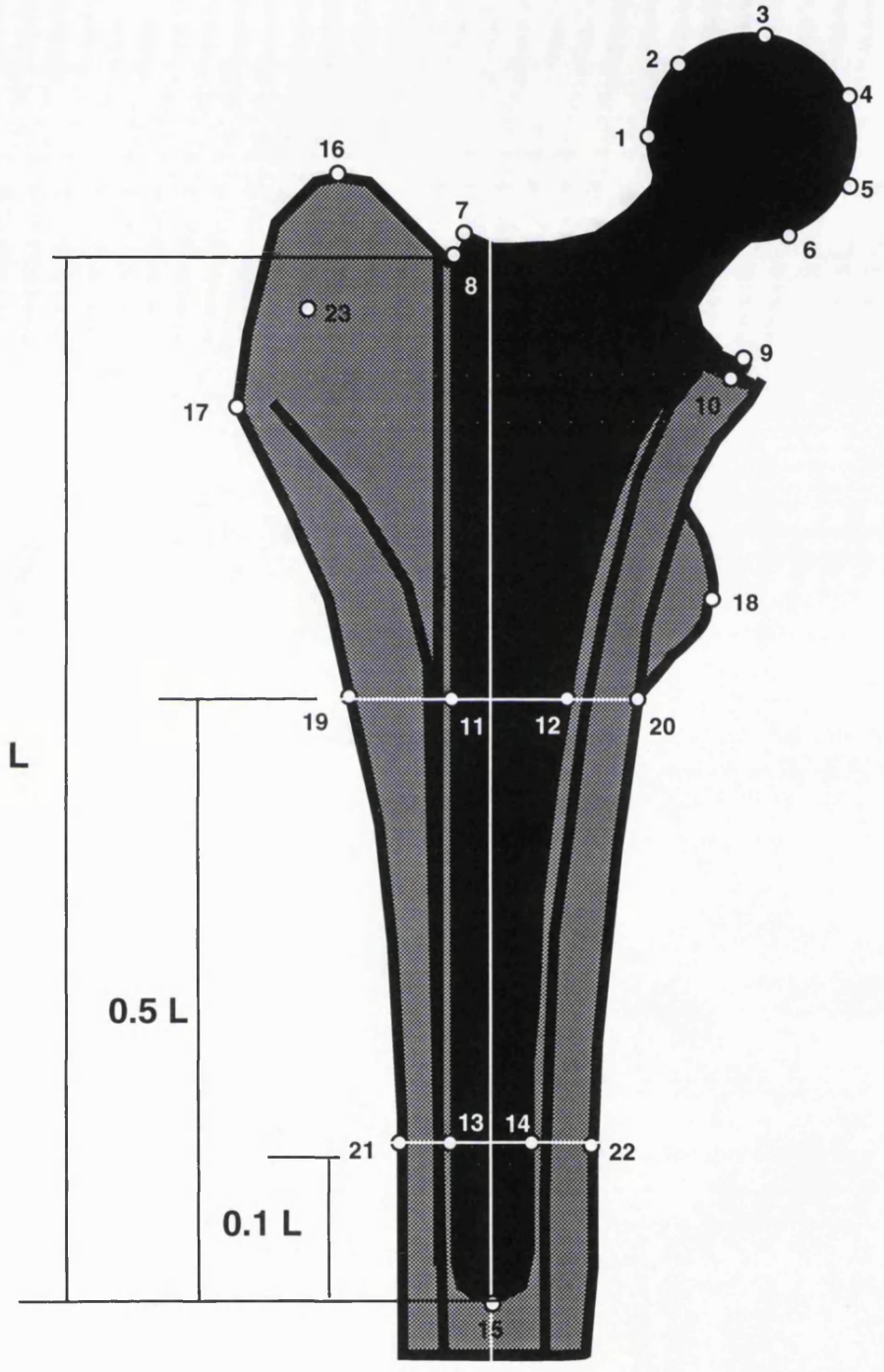

FIG. 8.2 RETROSPECTIVE MEASUREMENT OF STEM MIGRATION FROM PLAIN A-P RADIOGRAPHS: REFERENCE POINTS ON STEM AND BONE FOR DIGITIZATION

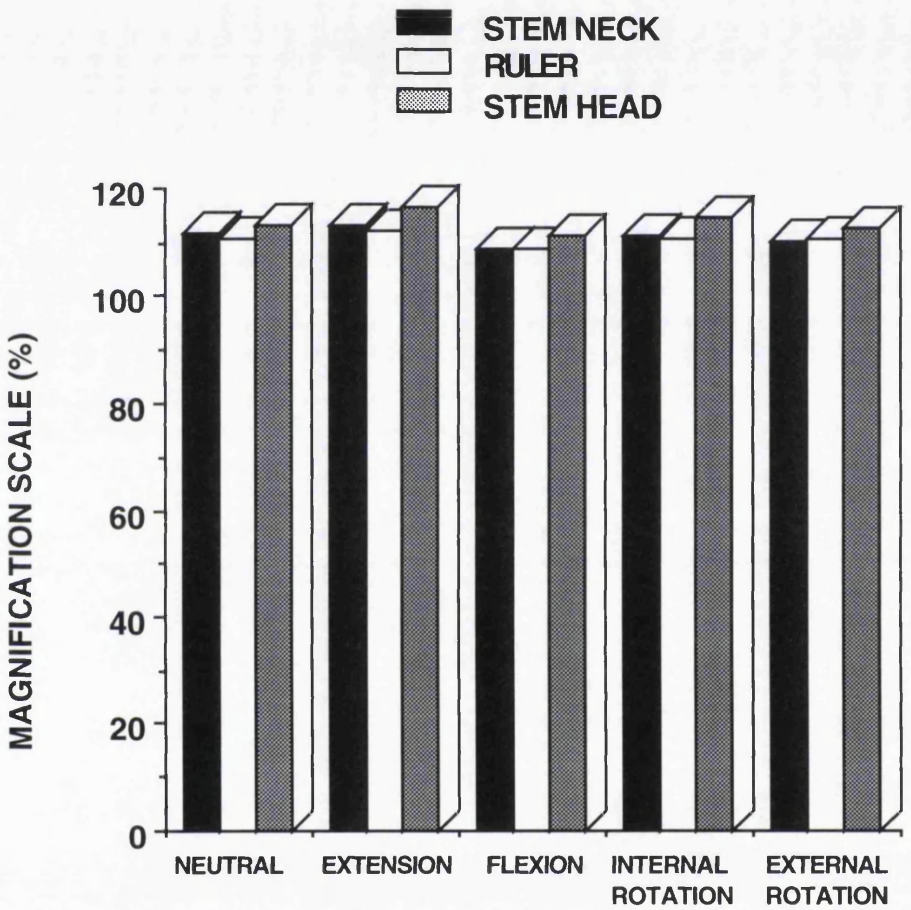

FIG. 8.3 COMPARISON OF MAGNIFICATION SCALES MEASURED FROM RULER, NECK OF STEM AND FEMORAL HEAD

N=NEUTRAL, F=FLEXION, E=EXTENSION, IR=INTERNAL ROTATION, ER=EXTERNAL ROTATION

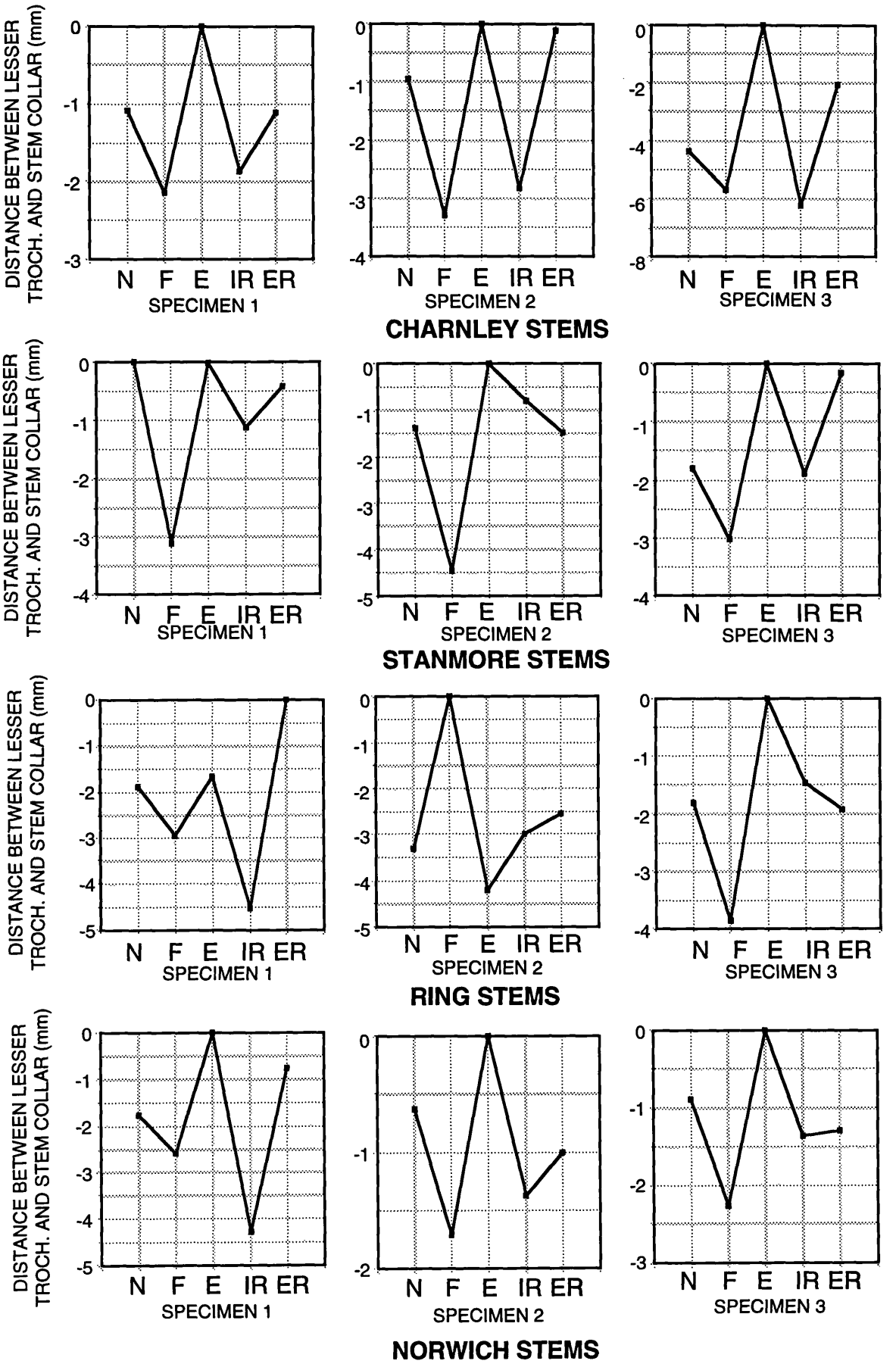

FIG. 8.4 EFFECT OF DIFFERENT RADIOGRAPHIC ORIENTATION ON THE STEM MIGRATION WHEN USING LESSER TROCHANTER AS A REFERENCE POINT

N=NEUTRAL, F=FLEXION, E=EXTENSION, IR=INTERNAL ROTATION, ER=EXTERNAL ROTATION

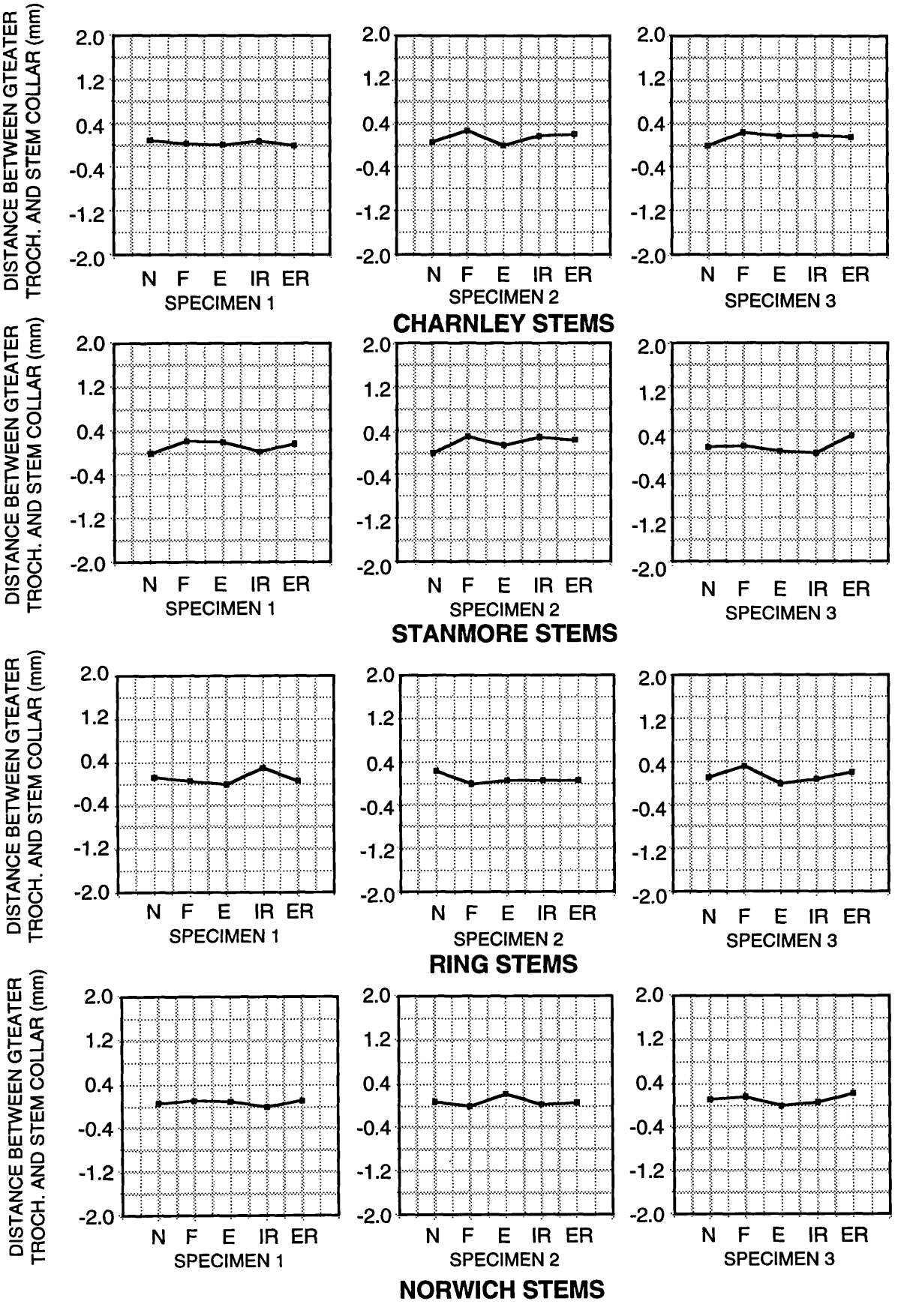

FIG. 8.5 EFFECT OF DIFFERENT RADIOGRAPHIC ORIENTATION ON THE STEM MIGRATION WHEN USING GREATER TROCHANTER AND STEM COLLAR AS A REFERENCE POINT

N=NEUTRAL, F=FLEXION, E=EXTENSION, IR=INTERNAL ROTATION, ER=EXTERNAL ROTATION

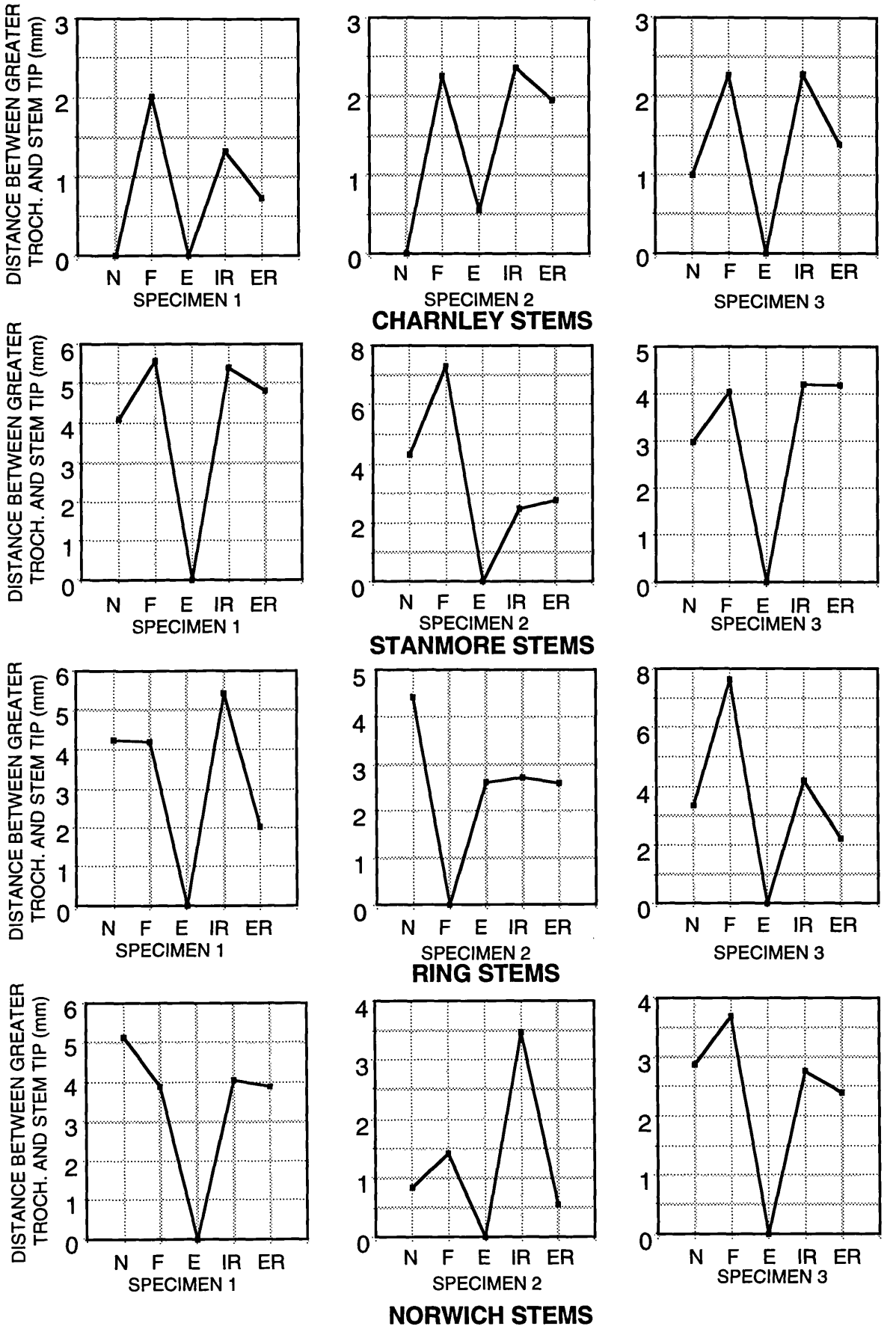

FIG. 8.6 EFFECT OF DIFFERENT RADIOGRAPHIC ORIENTATION ON THE STEM MIGRATION WHEN USING STEM TIP AS A REFERENCE POINT

FIG. 8.7 RADIOLUCENT LINE AT TOP LATERAL REGION OF THE CAD-CAM STEM

FIG. 8.8 BONE FORMATION AT BOTTOM OF THE CAD-CAM STEM

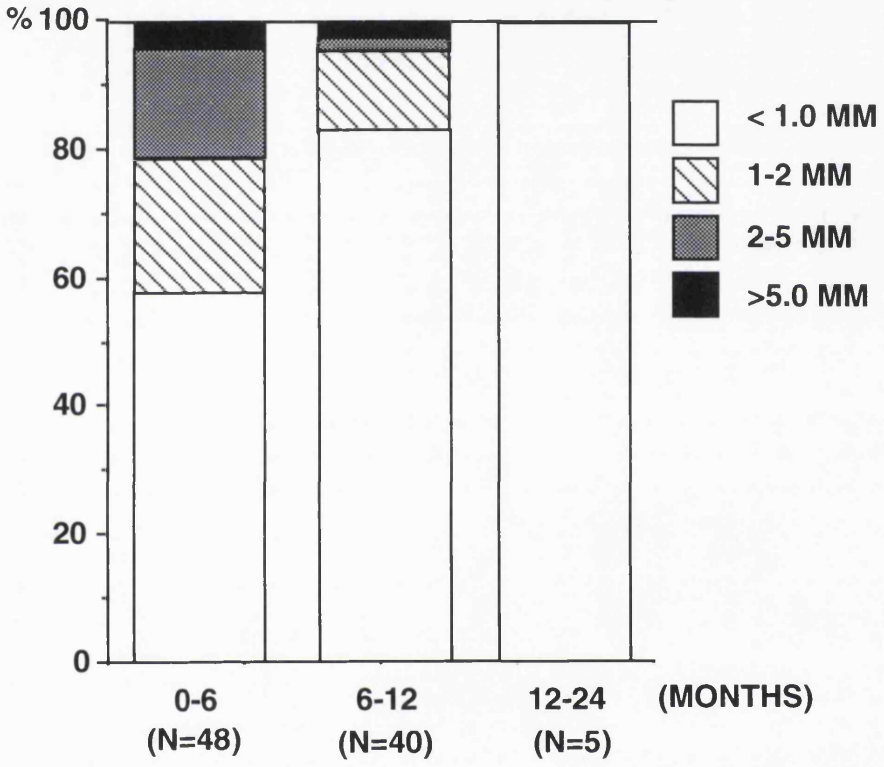

FIG. 8.9 EARLY RESULTS OF RADIOGRAPHIC MIGRATIONS OF CAD-CAM STEMS

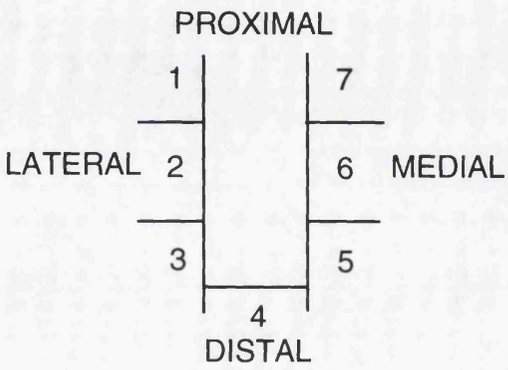

GRUEN ZONES DIAGRAM

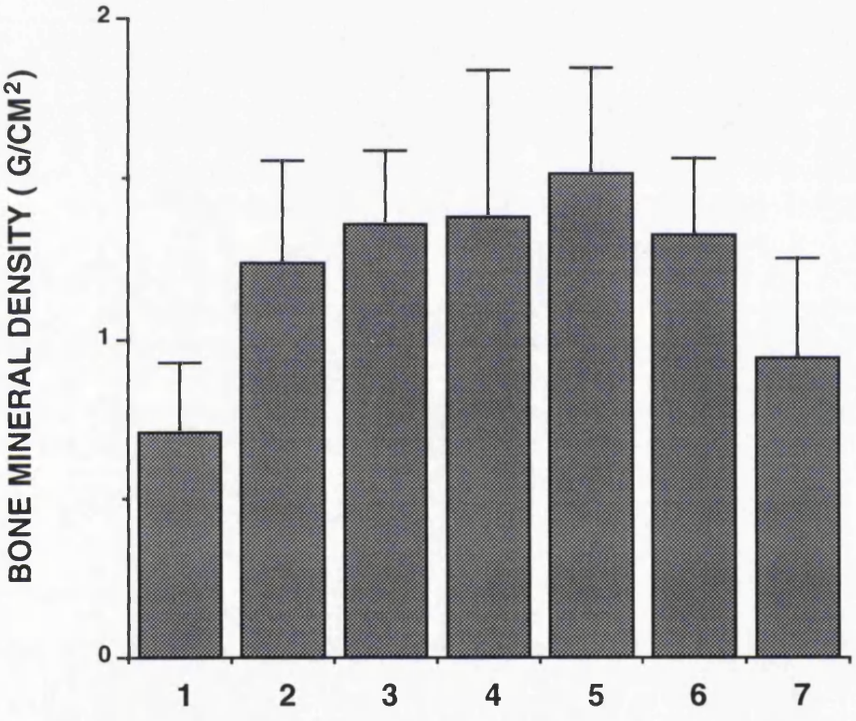

FIG. 8.10 BONE MINERAL DENSITIES AT DIFFERENT GRUEN ZONES

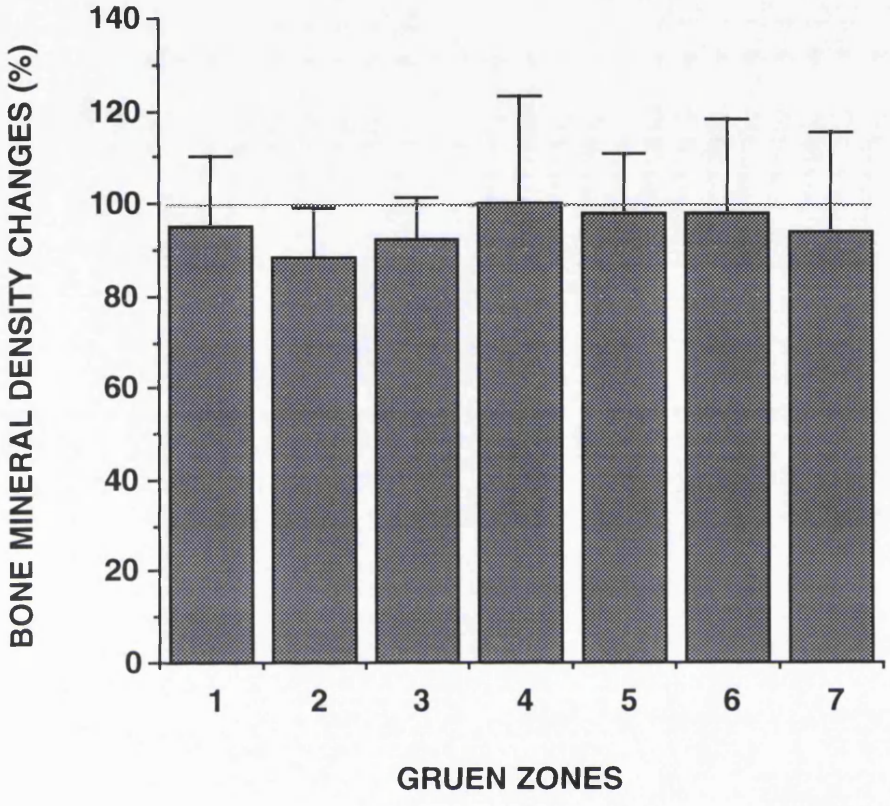

FIG. 8.11 BONE MINERAL DENSITY CHANGES IN PERCENTAGE BETWEEN IMMEDIATE AND SIX MONTHS POST-OPERATION

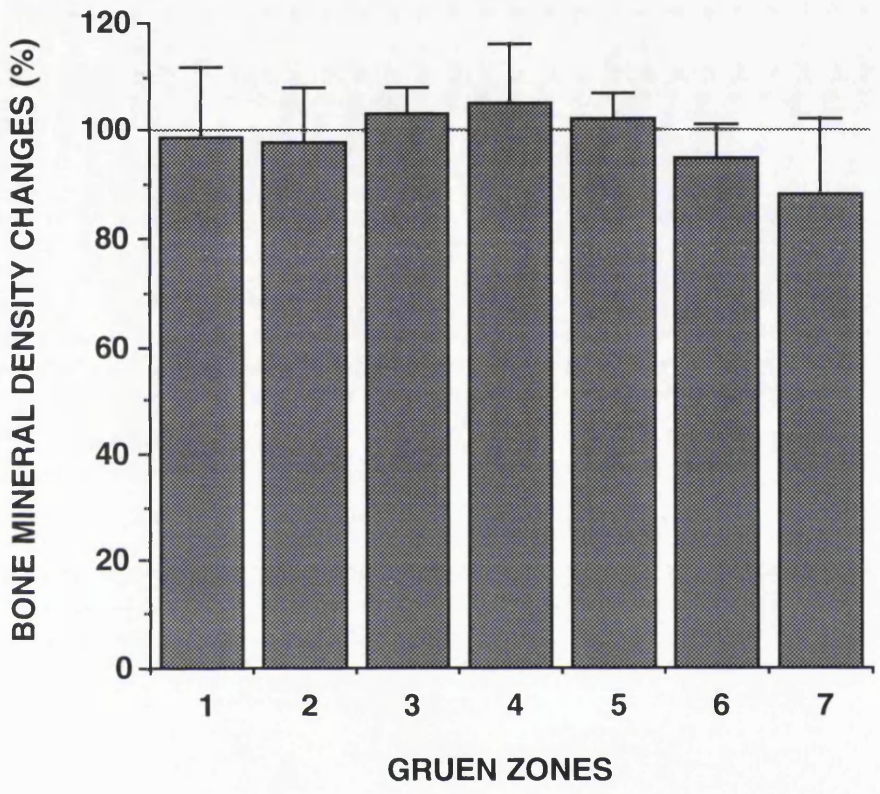

FIG. 8.12 BONE MINERAL DENSITY CHANGES IN PERCENTAGE BETWEEN SIX AND TWELVE MONTHS POST-OPERATIONS

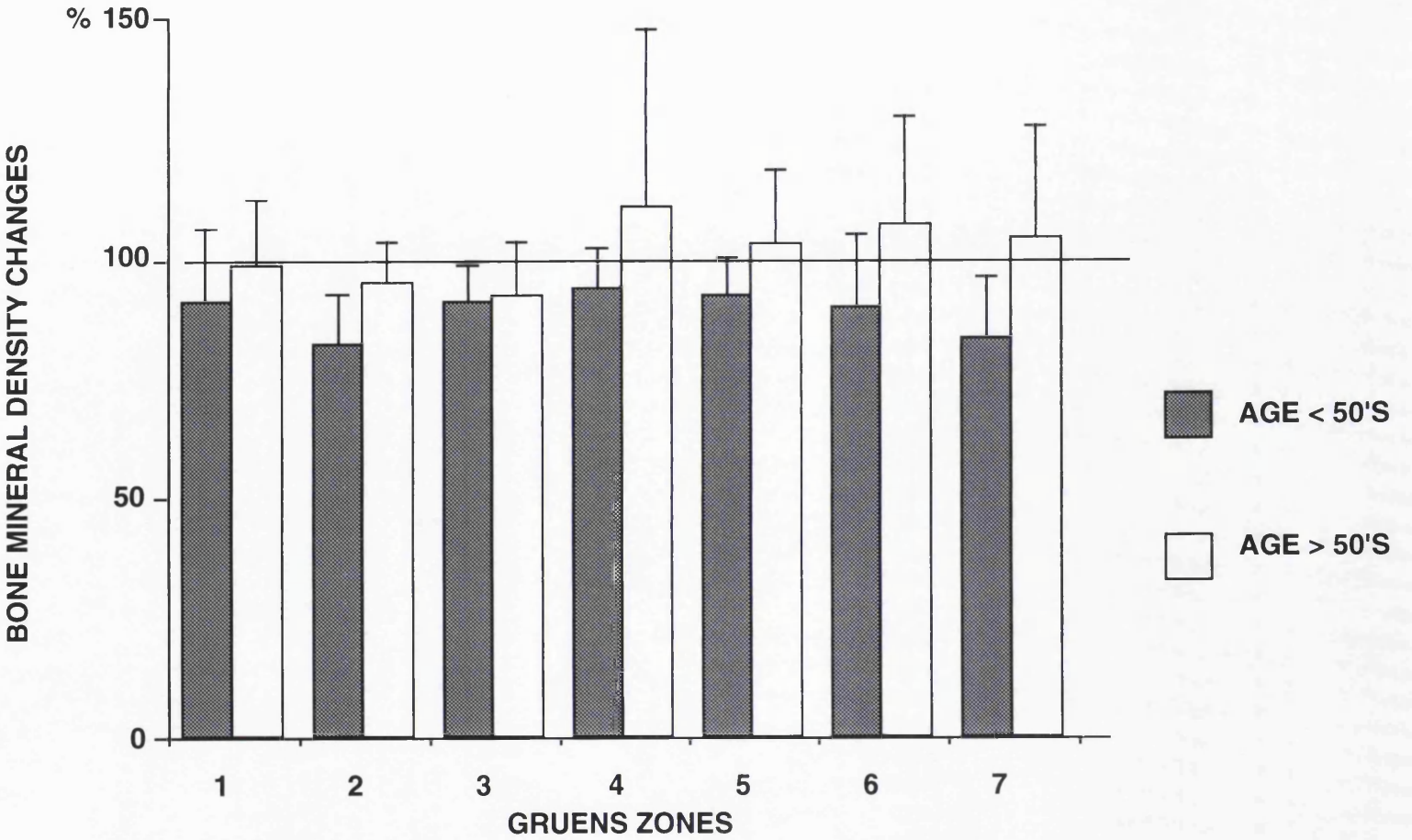

FIG. 8.13 DIFFERENCES IN CHANGE OF BONE MINERAL DENSITY BETWEEN OLDER (>50 YRS) AND YOUNGER (<50 YRS) PATIENTS AFTER SIX MONTHS POST-OPERATION

TABLE. 8.1 COMPARISON OF MAGNIFICATION MEASURED FROM FEMORAL HEAD, NECK AND RULER (RULER SERVED AS CONTROL)

	MAGNIFICATION			DIFFERENCE	
STEM ORIENTATION	HEAD (%)	NECK (%)	RULER (%)	HEAD VS RULER	NECK VS RULER
NEUTRAL	113.4	111.8	111	2.4	0.8
EXTENSION	116.5	113.1	112.5	4	0.6
FLEXSION	111.5	108.8	109.1	2.4	-0.3
EXTERNAL ROTATION	114.5	111.5	111	3.5	0.5
INTERNAL ROTATION	112.7	110.5	111	1.7	-0.5
			AVERAGE	**2.8**	**0.22**
			SD	**0.93**	**0.58**

CHAPTER NINE

BIOLOGICAL FIXATION OF THE HIP STEMS

9.1 Introduction

The concept of biological fixation of total hip prostheses has evolved in an attempt to decrease the incidence of long-term aseptic loosening, which is one of the primary problems of cemented fixation. Although it has been demonstrated by Malcolm et al (1991) that direct attachment of bone to cemented femoral stems does occur, it is widely believed that the commonest interface between the cement and bone is a fibrous soft tissue layer which contains of foreign body giant cells, fibroblasts and macrophages. However for cementless fixation, the particular advantage of biological fixation lies in its potential for direct attachment of the implant to bone without an interposed fibrous tissue layer, and even more importantly, for remodelling with time of the interface between the stem and the ingrowing bone and maintaining stability (Bobyn et al 1981, Pilliar et al 1983 Spector et al 1987, Whiteside et al 1993). Biological fixation can be affected by many factors, such as initial stem stability, the gap between the stem and the femoral cavity, the surface finish of stem, and the stiffness of the stem geometry and material.

The effect of the stem-canal gap and the initial stability of the stem on biological fixation has previously been studied (Engh et al 1987, Soballe et al 1993). It has been observed in porous coated stems that gaps of 1.5-2 mm were bridged by bone in twelve weeks (Bobyn et al 1981 and Cameron et al 1976). The deposition of bone was most prominent on the HA coated prosthesis that was close to the endosteal of the bone, especially in areas where the force was transmitted (Bauer et al 1991).

In recent years, the surface finish of stem has received great attention. Such surface coatings include titanium sintered meshes, sintered porous

titanium and cobalt chromium beads, and sintered or plasma-sprayed hydroxyapatite coating.

9.1.1 Bonding of bone to porous-coated implants

The earliest use of a porous implant was to fill and repair soft tissue defects with polyvinyl sponge material (Grindlay and Waugh 1951). Observations on the bone defect replaced by the porous implant suggested that new bone had grown into the scaffolding offered by the polyninyl sponge (Struthers 1955). Applications of porous biomaterials for the fixation of a surgical implant through tissue ingrowth have offered a tremendous improvement in the strength of the metal--bone attachment.

Attention initially focused on ceramics and polymers, partly because of concerns about the corrosion of porous metals (Lucas et al 1987). The intrinsic brittleness of the ceramics and the weakness of the polymers have limited their use in porous form. However, porous-coated metallic implants have shown promise for load-bearing orthopaedic applications, the PCA, AML and Harris-Galante being examples of these hip implants.

Techniques involved in the coating of porous materials onto the substrate include sintering heat treatment (Cook et al 1984, Kohn et al 1990, Yue et al 1984), diffusion bonding (Sumner and Galante 1990) and plasma spraying (usually titanium) (Kelman et al 1991). Madreporic finish of the Lord Hip is another technique which is a beaded finish with cast cobalt chrome beads (Load and Bancel 1983). It is suggested that a pore size of 50-200 μm is appropriate for the optimal amount of bone ingrowth, the fastest ingrowth rate, and the maximum attachment strength. (Klawitter

and Hulbert 1971, Bobyn et al 1980, and Robertson et al 1976). However, it was observed that majority of the porous coating could contain fibrous tissue (Cook et al 1988 and Thomas et al 1986).

Static and cyclic fatigue shear strengths of cobalt-based alloy bead coatings and titanium-fibre coatings are stronger than the shear strength of the stem-bone interface, but delamination of the porous coatings has been documented clinically (Callaghan et al 1988). Separation of beads from a porous coated implant has also been observed (Buchert et al 1986, Davey and Harris 1988, Engh and Bobyn 1985), which bead loosening increases with time (Maloney et al 1992). In addition, the potential for toxicity or even carcinogenicity of metal ion exists (Heath et al 1971, Sunderman Jr 1971, Woodman et al 1984). In addition to corrosion, there is a release of metal debris due to wear or fretting or fretting-corrosion mechanisms, and material released by wear or fretting is more susceptible to corrosion because the protective effect of the passive oxide film is reduced.

Clinical observation suggested that the amount of bone ingrowth was associated with stem fit and stability, and thigh pain was lower when the stem was extensively coated (Engh et al 1990). Other extensive studies on the PCA stem and the Harris-Galante porous titanium-fibre coated prosthesis revealed the improvement of clinical results (Heekin et al 1993 and Martel et al 1993) and the occurrence of bone ingrowth (Sumner et al 1988).

9.1.2 Bonding of bone to hydroxyapatite coated implant

Hydroxyapatite has the same chemical and crystallographic structure as the apatite of living bone (Jarcho 1981), which are biocompatible and have osteoconductive properties that promote apposition of bone to a metal implant (de Groot et al 1987, Geesink et al 1987, Geesink et al 1988). Hydroxyapatite-coated stem can form a chemical bond with the bone with a strength comparable to that of cortical bone itself (Geesink et al 1988). This fixation is far stronger than that provided by current cemented or uncemented techniques. Push-out tests demonstrated failure at the metal-HA interface before failure at the HA-bone interface. Once chemical fixation has taken place, there is no significant biodegradation (Klein 1983, 1984, Hoogendoorn et al 1984). However, most recent results suggest that the coating resorbs or delaminates after a period of time but the amount of resorption is not directly correlated with the duration of the stem in vivo (Bauer et al 1991).

Hydroxyapatite is a very brittle material with a high modulus of elasticity, so there is a risk of coating separation from more elastic materials such as polyethylene and metal alloys when the composite is subjected to bending. It has been reported that 10 to 15 micron thickness of coating may dissolve during the process of bone union during the first few months, whereas delamination of the coating occured on a stem with 200 microns (Kester et al 1991) If the hydroxyapatite coating flakes off, small but very hard particles are produced, which can scratch the stem and generate metallic particles. Metallic particles together with other particles can then migrate into the bearing surfaces and cause additional polyethylene wear (Cambell 1993). All these particles can be phagocytosed by macrophages. Macrophages then become activated and produce prostoglandins and interlukins which recruit further macrophages into the interface. Prostoglandins and interlukins also

recruit osteoclasts within this interface which lead to bone resorption and subsequent loosening. It was therefore suggested that a coating of 50 microns was optimal.

Sintered apatite can form very tight bonds with living bone (Denissen et al 1980, de Groot 1980 Jarcho 1981 and Winter et al 1981), but its mechanical properties are poor(de Groot et al 1981), whereas plasma-sprayed hydroxyapatite provide a bond between titanium and hydroxyapatite with the same maximum shear strength as cortical bone. Push-out studies on transcortical plugs inserted into the femora of dogs have demonstrated that hydroxyapatite coated stems produced tight bonds between the stem and bone (Ducheyne et al 1980, Geesink et al 1987, Thomas et al 1987, Cook et al 1988b).

Histological studies on retrieved hydroxyapatite coated prosthesis showed that the bone tissue ingrowth could occur as early as ten days (Furlong and Osborn 1991). Where the newly formed immature bone overlay the hydroxyapatite coating with new trabeculae bridging to the endosteal bone. There was no evidence of an inflammatory reaction or of fibrous tissue formation (Thomas KA et al 1989, Hardy et al 1991, Furlong and Osborn 1991). However, It was also noted that the HA coated stem contained significantly higher amounts of bone ingrowth at three weeks post-implantation than the one without coating, but no difference at six weeks (Jasty et al 1992), which suggested that plasma-sprayed HA coating may be useful in enhancing the early ingrowth of bone into porous-surfaced stem, but may lack long-term effectiveness. In clinical and radiographic follow-up, a minimum follow up of two years on 238 proximal HA coated stems revealed very encouraging results (Capello et al 1992).

9.1.3 The effect of implant stiffness on the osseointegration of titanium alloy

Implant materials for total hip replacements are much stiffer than natural bone. Titanium alloy (6% aluminium, 4% vanadium) which is the least stiff of the alloys, has a modulus 5 times higher than the cortical bone. The mismatch in the modulus between bone and alloy indicates that the load transmitted by the implant to the bone will not be in a physiological range, and stress protection induced bone remodelling can be expected. Moreover, because of the mismatch of the material modulus, relative motion at the bone-stem interface may occur when the implant is cyclically loaded. To solve the problems, many trials on various materials have been conducted, such as use of composite polymeric hip stems which have a significantly reduced modulus when compared with metallic alloys, thus such stem can be expected to transfer load more physiologically and preserve the density of the proximal femur. In experimental studies using canine models it has been shown that use of these composite stems reduces cortical porosis in the proximal femur when compared with the porosis induced by metallic stems (Galante 1991).

The stem stiffness is not only determined by the material, but also closely related to stem diameter and geometry. Large and relatively stiff stems are often needed for revising of a previously cemented stem, where the medullary cavity is usually porotic and enlarged. However, little was known about effects of reduced stem stiffness by altering stem geometry on the tissue ingrowth and bone remodelling. Therefore, in order to investigate effect of stem stiffness on the osseointegration of titanium

alloy, titanium stems with various stiffness were inserted in the distal portion of femora of the rat.

9.2 Materials and methods

9.2.1 Implant design

The implant, which was made of titanium-6-alumium-4-vanadium, was designed as an intramedullary rod with small groove in A-P plane. The rod had 20 mm in length and 2.5 mm in diameter. A 15 mm slot was machined proximally or distally in the frontal plane to reduce stiffness. The solid implant was served as control (Fig. 9.1).

9.2.2 Rat selection

Twenty-four Wistar male rats, aged 9-12 months old and weighing 500 gram, were selected. Three or four rats were kept in the same cage before and after surgery, and all the rats were sacrificed three months after surgery.

9.2.3 Surgical procedure

All the rats were operated on the shaved right hind limb. There were three groups of eight rats, the groups implanted with the proximally slotted ,distally slotted and the solid rod. The anaesthetic procedure used an atmosphere of CO_2 which was maintained using a mixture of oxygen and halothane. The area around the right knee was thoroughly cleaned and scrubbed, using benodine solution. A 6 mm long medial incision was made, the patella and patella tendon being retracted laterally to expose

the knee. The knee was not dislocated and no ligaments were resected. The intramedullary cavity of the distal femora was located by gouging a small starter hole through the intercondylar notch. This hole and the intramedullary cavity were gradually enlarged by using consecutively-sized drill until a final drills of 2.5 mm in diameter was used. The intramedullary rod was then inserted and press fitted into place using a sterile pin punch. The wound was closed, using Dexon 30 sutures, an antibiotic was administered into the the neck, and the animal was allowed to recover. The rod was recessed below the patella-bearing area. The procedure was repeatable and consistent, and each intramedullary rod achieved a line to line fit (Fig. 9.2). The operation took approximately 10 minutes and no problems occurred.

9.2.4 Histological preparation

The rats were sacrificed after three months, and the right femora removed, fixed in formalin, dehydrated and embedded in acrylic resin. The sections were polished and mounted on an SEM (Scanning Electron Microscope) stub and viewed under Back Scatter Electron detection (BSE) in a JEOL 35c scanning electron microscope. The amount of bone upgrowth to the implants was measured in the distal, middle and proximal sections by using a line intercept method.

9.3 Results

BSE detection distinguishes between bone, soft tissue and titanium alloy through differences in atomic number of the constituent elements that compose these materials. Materials composed of higher atomic numbers show stronger emission of electrons than those materials with lower

atomic numbers. Titanium alloy emits more electrons and appears brighter than bone which in turn appears brighter than soft tissue.

The osseointergration in the bone-stem interface had occurred at various locations. The differences in the amount of bone upgrowth on to the distally, proximally slotted and solid stems in the distal, middle and proximal regions of femur suggested that the modulus of the stem has the greatest affect on the amount of osseointegration. Significant differences ($P < 0.05$) were observed between the proximally slotted and the solid titanium stems in the proximal sections, whereas no difference was noted in the distal sections between the three types of stems.

In addition, there was also a difference in the amount of bone upgrowth onto solid stems in the proximal and distal sections ($P<0.05$). In the distal area, bone formed a ring around the implant (Fig.9.4), this ring of bone being often less than 100 μm in width with small islands of soft tissue occuring between the implant and the bone (Fig.9.5). In contrast, bone contact in the proximal femur was minimal for the solid implant (Fig.9.6), and a gap of 30 μm was observed between the surrounding bone and the implant surface (Fig.9.7).

Close apposition of bone to the circumference of the rod was observed at the middle sections for the slotted stems, with a thin layer of bone adjacent to the slot of the stem (Fig.9.8).

9.4 Discussion

By slotting the titanium stem and reducing the stiffness of the implant, an alteration in the amount of bone upgrowth on to the alloy surface

occured. The amount of bone upgrowth in the proximal region appeared to be significantly higher for the proximally slotted stem than that for the solid stem, but no difference was obtained in the middle and distal region. This is because the proximal region is subjected to a higher bending force than distal, so that the effect of the flexible stem on transferring more local force becomes significant.

The solid stem had less bone upgrowth proximally than distally which can be explained by the fact that the distal portions of the implant are positioned within cancellous bone where bone remodelling is more active, whereas the proximal portions are within cortical bone.

Although this model employs stems which are press-fitted into the femora, load must be transferred through the implant to the bone when the femora are in bending. It has previously been shown that the mechanical loading conditions at the bone implant interface influences the amount and site of bone in contact with stem surfaces (Heinke 1989). It was observed from present study that the use of a low modulus stem may not only reduce the problems of stress protection but also increase the amount of biological fixation of the implants.

The clinical relevance of the present study is that, in order to achieve line-to-line contact between the stem and bone so that osteointegration can take place, stem stiffness has to be reduced to avoid stress protection. To achieve this, a stem with a large diameter but slotted in the middle can be designed. This is particularly useful in revision situations where the medullary cavity is usually enlarged after removing the cement mantle. Such slotted stems have been designed for several revision cases. One of the examples is showed in Fig.9.9, which the distal

diameter of the implant was 20 mm in order to fit with the canal, whereas a 3 mm distal slot was produced in the A-P plane to reduce stem stiffness. The long-term clinical results, together with bone remodelling and osseointegration of the slotted stem will be evaluated.

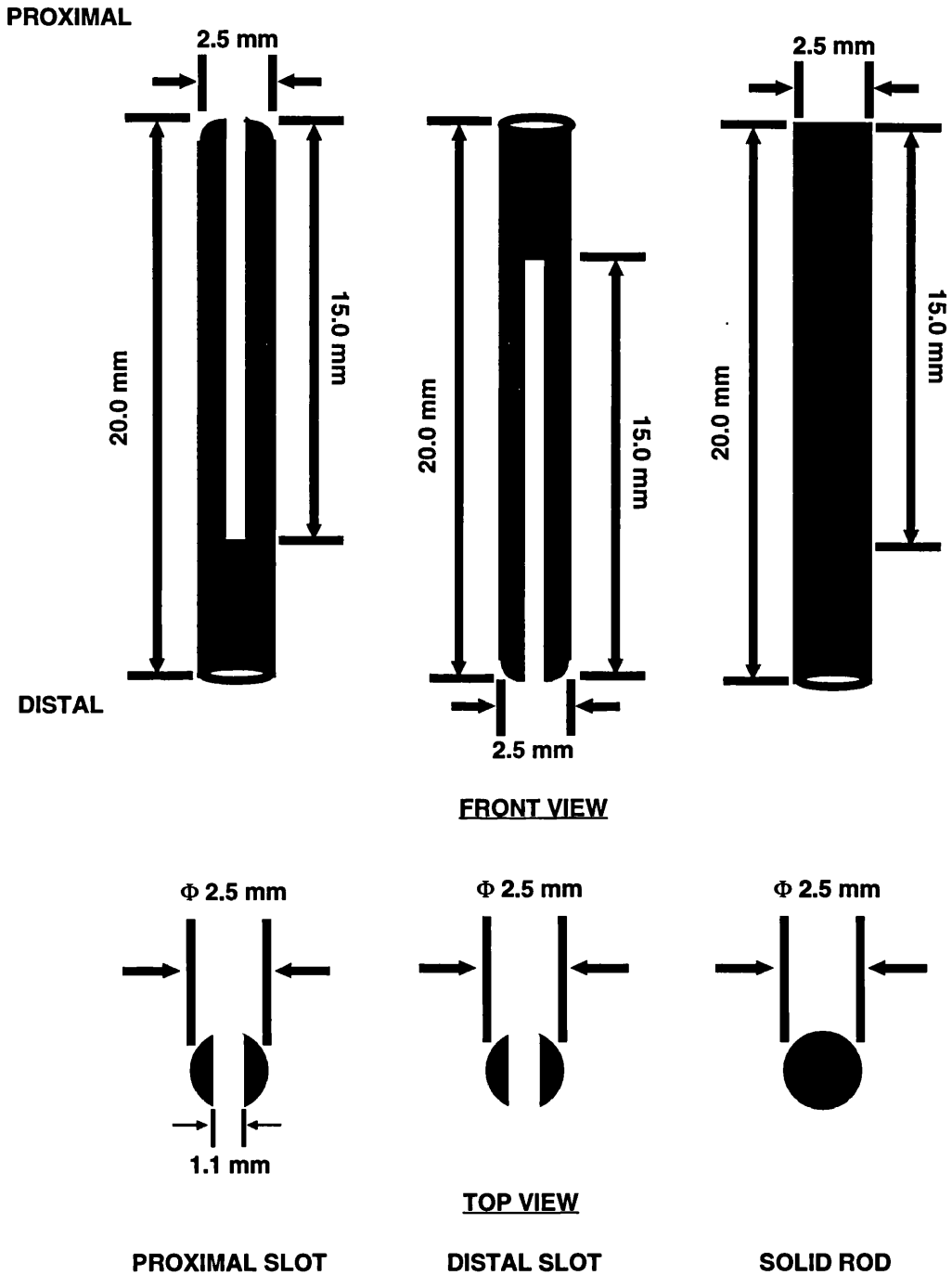

FIG. 9.1 DESIGN OF INTRAMEDULLARY ROD WITH AND WITHOUT PROXIMAL AND DISTAL SLOT (MAGNIFICATION $\times$ 5.0)

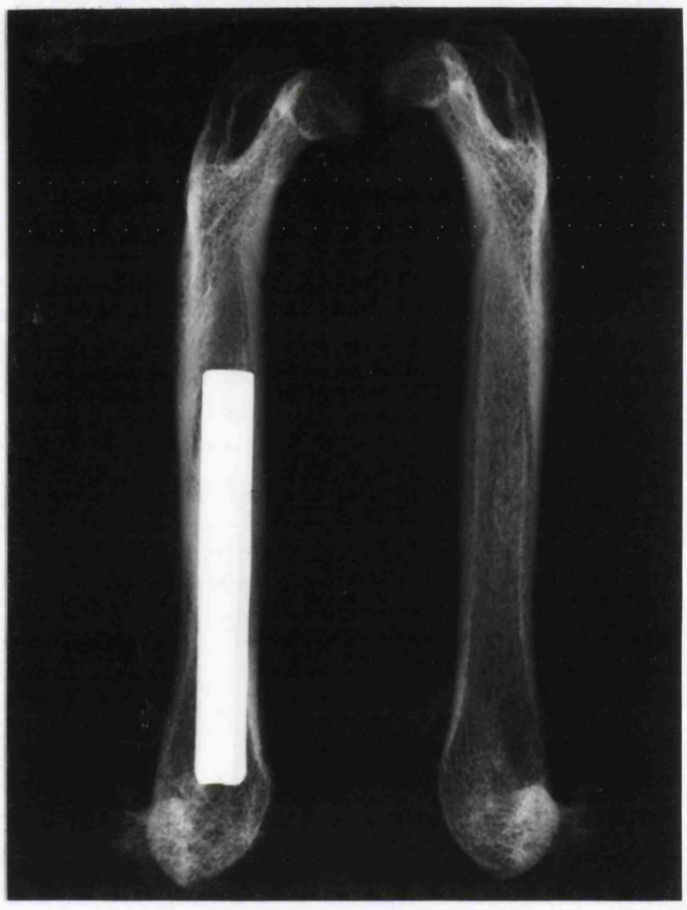

FIG. 9.2 RADIOGRAPH OF IMPLANT WITHIN RAT FEMORA. MAG. = x2.7

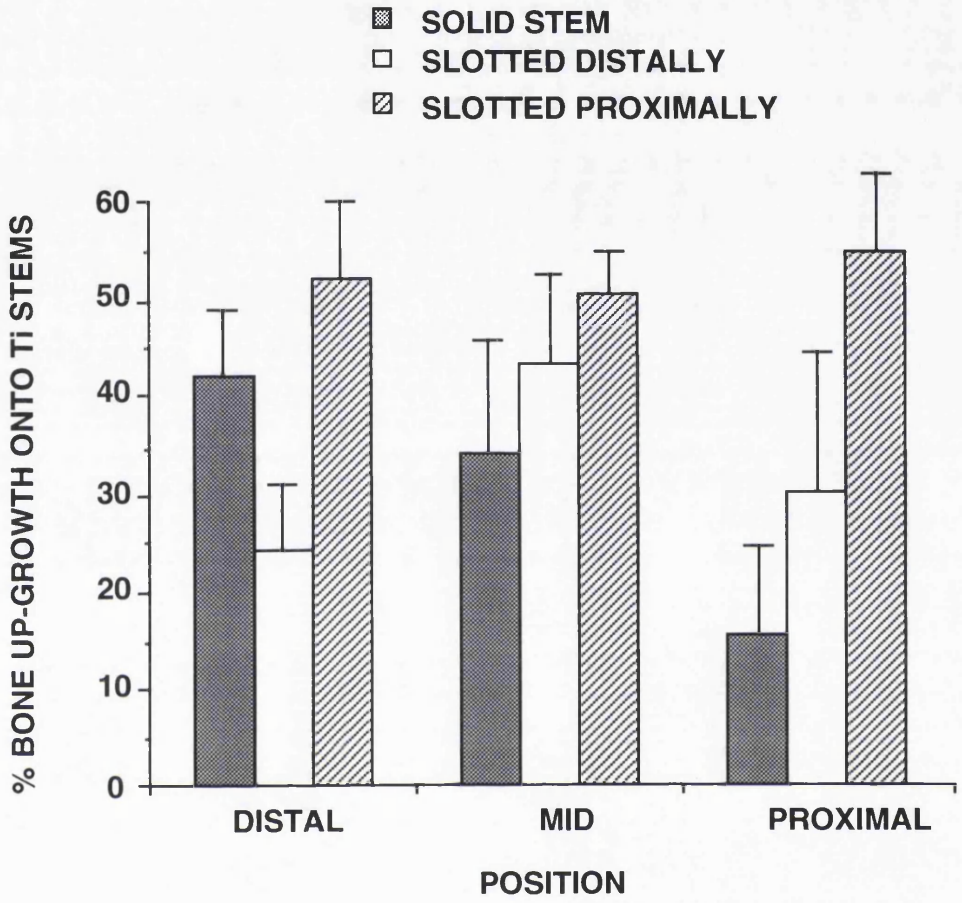

FIG. 9.3 HISTOGRAM SHOWING DIFFERENCES IN BONE UPGROWTH ON TO PROXIMALLY SLOTTED, DISTALLY SLOTTED AND SOLID TITANIUM RODS AT THE DISTAL, MIDDLE AND PROXIMAL POSITIONS.

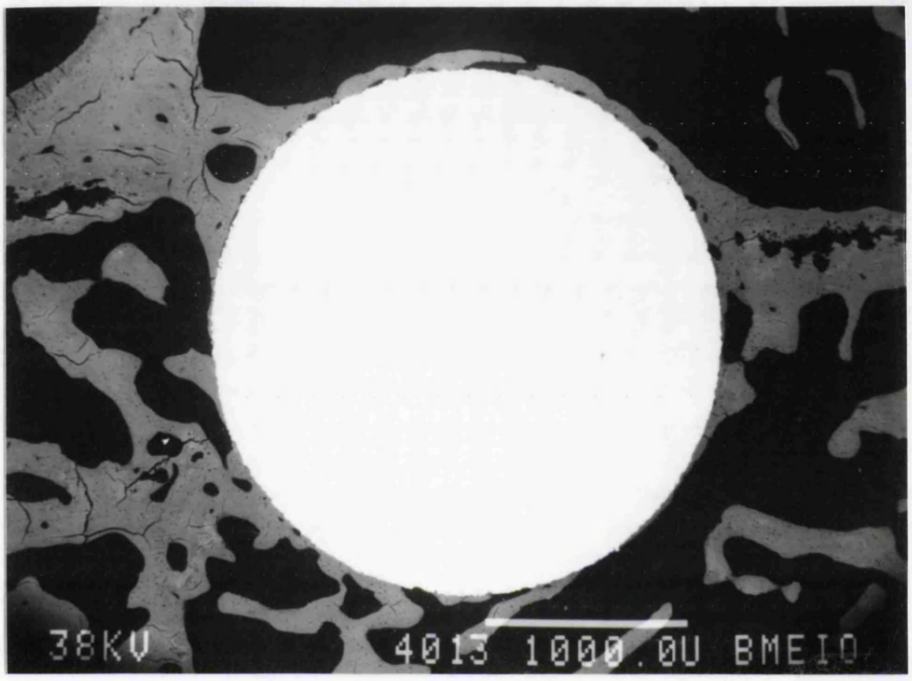

FIG. 9.4 BSE MICROGRAPH OF STEM IN DISTAL REGION OF FEMUR SHOWING THE FORMATION OF A RING OF BONE AROUND THE IMPLANT. MAG. = x30

FIG. 9.5 BSE MICROGRAPH OF IMPLANT IN DISTAL REGION OF FEMUR SHOWING THE RING OF BONE AND SMALL ISLANDS OF SOFT TISSUE BETWEEN THE IMPLANT AND BONE. MAG. = x227

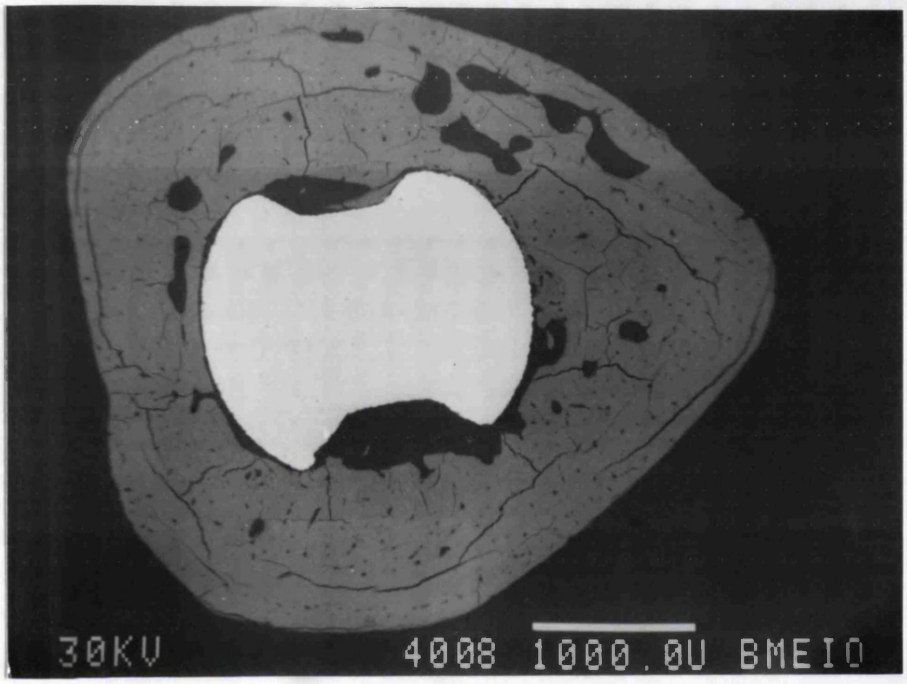

FIG. 9.6 BSE MICROGRAPH OF SOLID IMPLANT IN PROXIMAL PART OF FEMUR. MAG. = x24

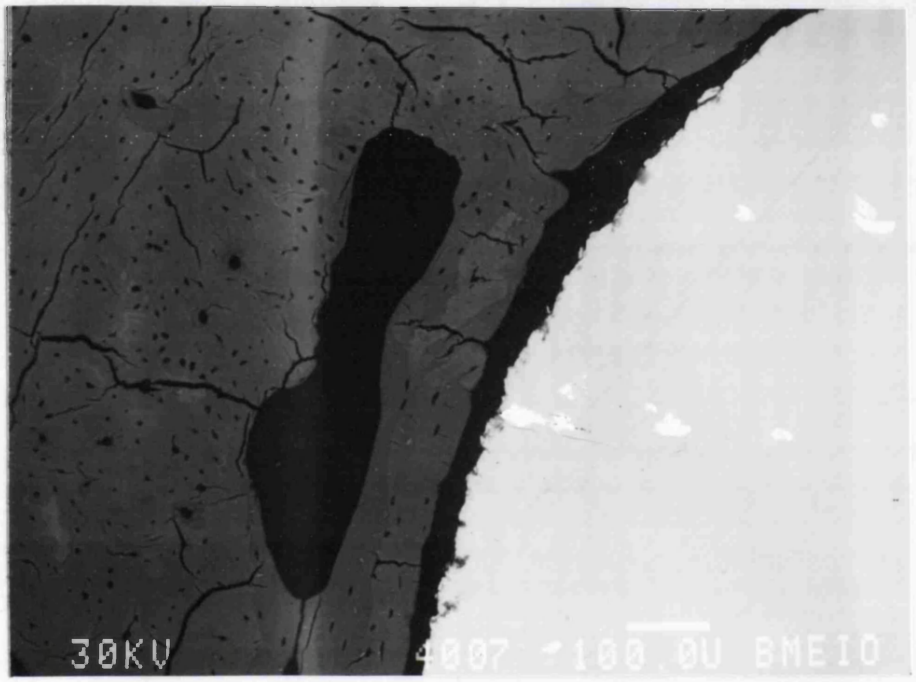

FIG. 9.7 BSE MICROGRAPH OF SOFT TISSUE BETWEEN THE IMPLANT AND BONE AROUND A SOLID ROD IN PROXIMAL PART OF FEMUR. MAG. = x120

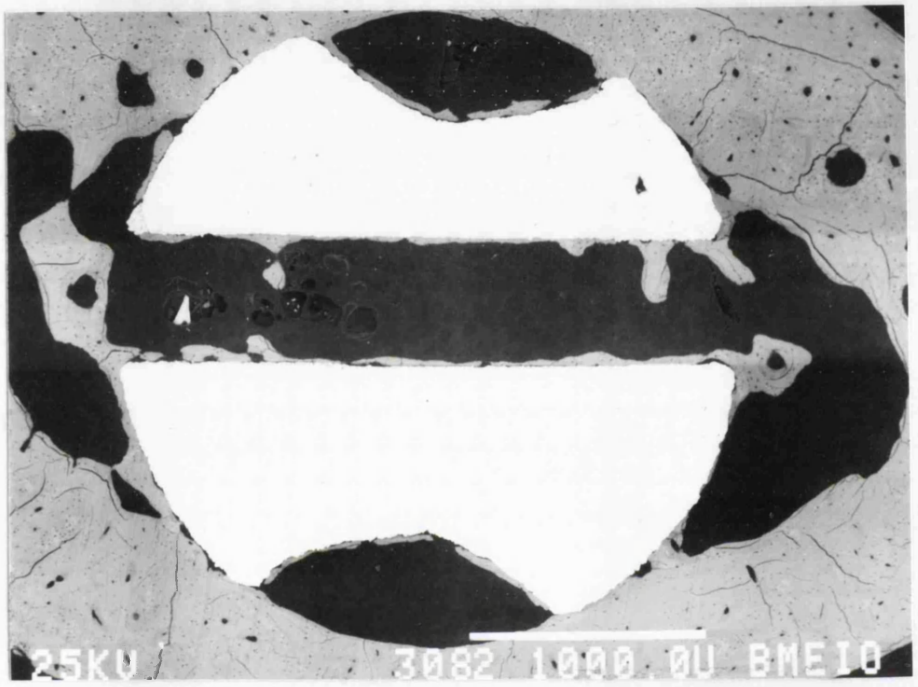

FIG. 9.8 SLOTTED IMPLANT IN PROXIMAL PART OF FEMUR SHOWING UPGROWTH OF BONE AROUND THE ROD AND ALSO WITHIN THE SLOT. MAG. = x35

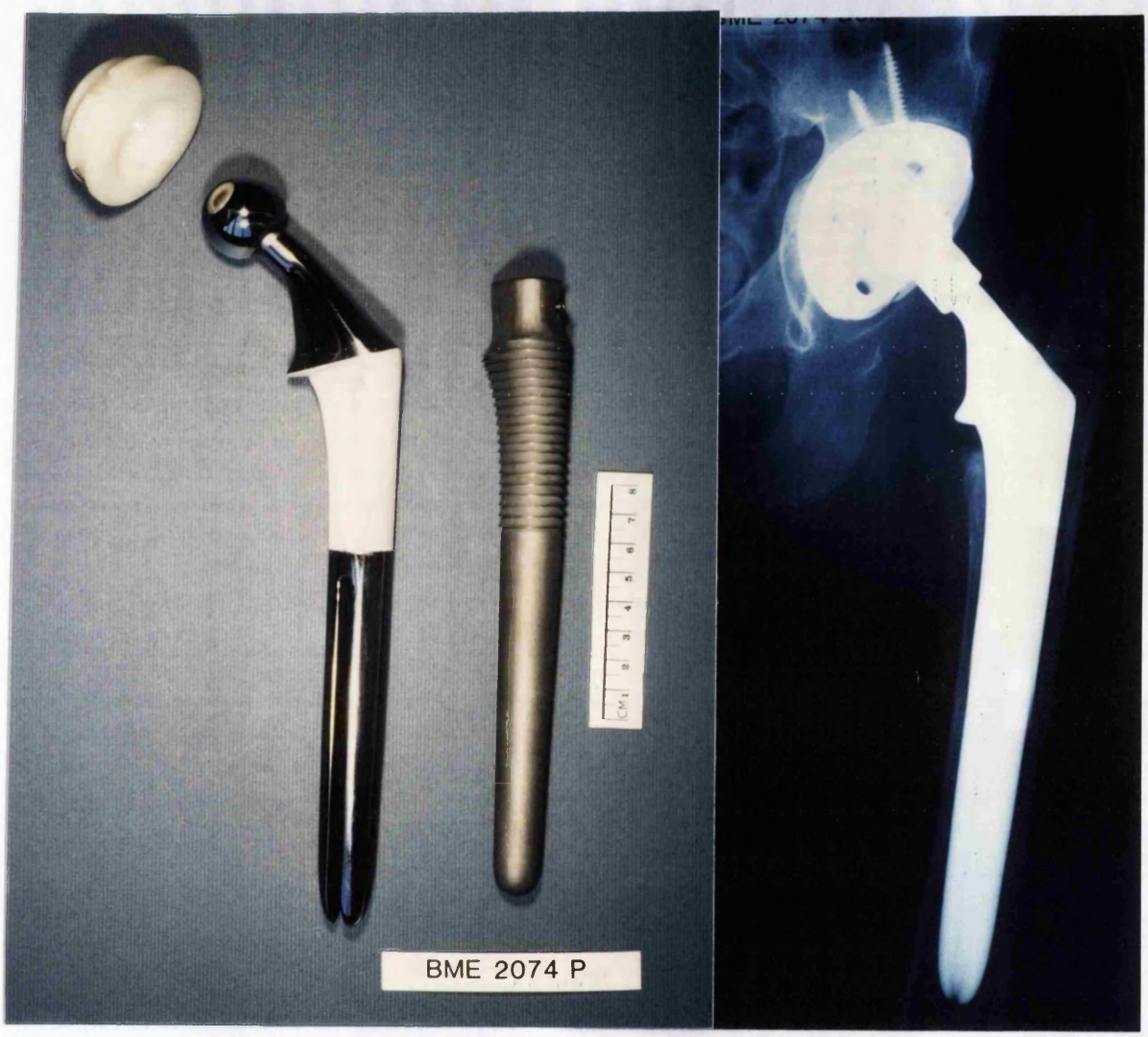

FIG. 9.9 REDUCING STEM STIFFNESS BY MAKING DISTAL SLOT WHILE LINE-TO-LINE CONTACT OF THE STEM WITH THE BONE WERE STILL ACHIEVED

CHAPTER TEN

SUMMARY AND FUTURE PROSPECTIVE

10.1 Evaluation of hip stem geometry

In total hip replacement, the geometry of the stem, particularly in the proximal region, influences the stem performance and clinical results. Therefore many previous studies have been undertaken in order to improve the design of stem geometry . The work presented in this thesis has further demonstated the importance of stem geometry, and the results obtained showed that different stem geometries will produce different results, both in laboratory testing and in clinical practice. CAD-CAM custom stems consistently achieved a good fit with the canal as compared with other standard stems, so that custom stems showed a better results in stress distribution and stem-bone relative motion.

A number of comparative studies have been previously conducted to evaluate the stem geometry by using the stem under investigation versus a control. The limitation of such a comparison is that the conclusion can only be drawn as to which stem as a whole is better. The purpose of the present study is to investigate only the proximal geometry of the stem (custom vs standard), therefore the material, stem length, distal diameter, offset and surface finish were all kept same as a control.

10.2 The design algorithm of CAD-CAM custom stems

It is widely recognized that stem fit with the canal in the proximal medial and anterior regions are of the most importance in terms of load transfer and stem stability. The CAD-CAM custom stems were therefore designed to consistently achieve the proximal fit with each individual canals. The results presented in the thesis have confirmed the design algorithm.

The major advantage of the custom stem is in its accurate fit and versatile design for each individual as well as for difficult cases, for which the standard stem can not consistently achieve. However, the higher cost of a single custom stem limits its widely use. But if a large inventory of standard stems necessary for each hospital is accounted for, the whole cost may not be very much different between the standard and custom stems. Moreover, from a long-term point of view, if the CAD-CAM custom stem can more effectively improve the quality of patients' life and can survive longer, then it can be more cost effective. In addition, with the advance of the technology, it is possible to reduce the cost of the custom stems so that it can be used more extensively.

10.3 The significance of pre-clinical evaluation on stem design

Since the laboratory testing can produce various information, such as stem fit, stress and strain distribution, stem-bone relative motion, and biological fixation with an animal model, pre-clinical evaluation of a newly designed prosthesis is therefore very important in predicting clinical results and improving stem design. However, such a pre-clinical evaluation has to be based as a whole on the different aspects of test, because a particular stem can produce better stress distribution but less stability. Currently, it has strongly been recommended that measurement of stem fit, strain distribution and relative stem-bone motion are the most effective techniques for pre-clinical evaluation of a newly designed hip stem, and histological analysis with an animal model is a valuable method for investigating biological response to different materials and types of stems. Therefore, in order to systemically evaluate CAD-CAM custom stems and draw a more reliable conclusion, the present work has employed all the above mentioned methods.

10.4 Current problems and future study

Although CAD-CAM custom stem can achieve a precise fit with the femoral canal, the surgical techniques and instrumentation currently used for preparing canals have limited its accuracy in clinical practice. In order to solve this problem, geometrically identical rasp and diameter-matched tapered reamer have therefore been provided, for which the surgical results were improved. However, it may still not be sufficient for achieving an accurate and repeatable surgical fit. In order to produce a more consistent and controllable results, the guilding devices for neck-cutting and the entry hole have to be customized as well in the future.

Early stem migration is associated with long-term clinical results, therefore a technique has been developed in the present work to measure the axial migration of the CAD-CAM custom stem by digitizing A-P plain X-ray film. Although the method is simple, easy and cheap to use for a retrospective study with reasonable accuracy, the major disavantage, is that it can not measure varus-valgus and rotational angle. Since rotational stability of a stem is more critical for achieving long-term success, development of such a method to measure multiple axes is necessary in the future.

10.5 Concluding remarks

The Hip Design Workstation provides an effective and accurate technique in designing custom stems to tackle individual hip problems. The results presented in this thesis have evidently showed that the CAD-CAM custom stems consistently achieved superior results than the standard stems based on a better fit with the proximal canal, better stress distribution on the medial side of the bone, and less stem-bone relative motion. The particular inherent

value of the CAD-CAM custom stem is not only in its accurate fit but also in its versatile design, so that the patient can always receive the best possible stem for their hip replacement.

BIBLIOGRAPHY

Albert TJ, Sharkey PF, Chao W, Hume E and Rothman RH (1991): Rotation affects apparent radiographic positioning of femoral components in total hip arthroplasty. J Arthroplasty 6:S67-S71

Alkire MJ, Dabezies EJ and Hastings PR (1987): High vacuum as a method of reducing porosity of polymethylmethacrylate. Orthopaedics, 10:1533-1539

Amaranath L, Cascorbi HF, Singh-Amaranath AV (1975): Relation of anaesthesia to total hip replacement and control of operative blood loss. Anesth Analg 54:641

Amstutz HC, Markolf KL, McNeice GM and Gruen TA (1976): Loosening of total hip components: cause and prevention. In The Hip (Proceedings of the Hip Society). 102. St. Louis. C. V. Mosby Co.

Amstutz HC, Ouzounian T, and Grauer D et al (1986): The grid radiograph: a simple technique for consistent high-resolution visualization of the hip. J Bone Joint Surg 68A: 1052

Andersen P and Levine DL (1987): Adhesion of fibre metal coatings. In Quantitative characterization and performance of porous implants for hard tissue applications, Ed: Lemons JE, PP: 7-15

Anderson LD, Hanisa WR Jr and Waring TL (1964): Femoral head prostheses. J Bone Joint Surg., 46A:1049

Andriacchi TP, Galante JO, Belytschko TB and Hampton S (1976): A stress analysis of the femoral stem in total hip prosthesis. J. Bone Joint Surg. 58A:618

Anthony PP, Gie GA, Howie CR and LIng RSM (1990): Localised endosteal bone lysis in relation to the femoral components of cemented total hip arthroplasties. J Bone Joint Surg 72-B: 971-979

Armstrong DL, Cook SD, Enis JE and Lisecki EL (1993)Experimental and clinical experience with HA-coated porous implants. Proc. in 1st European congress of orthopaedics. 20-23 April, pp:S7-2

Ashman RB, Donofrio M, Cowin SC and Von Buskirk, WC (1982): Postmortem changes in the elastic properties of bone. Orthop Trans 6: 223-4

Averill RG, Pachtman N and Jaffe WL (1980): A basic dimensional analysis of normal human proximal femora. In Proceedings of the 8th Annual Northeast Bioengineering Conference, Cambridge, MA, PP: 352

Bansusan JS, Davy DT, Heiple KG and Verdin PJ (1983): Tensile, compressive and torsional testing of cancellous bone. Transaction of the Orthopaedic Research Society. PP:132

Bargar WL (1989): Custom-fit cementless total hip replacement. Proc. 56th Annual meeting, AAOS, Las Vegas.

Bargar WL (1989): Shape the implant to the patient: A rationale for the use of custom-fit cementless total hip implant. Clin. Orthop. 249:73-78

Bargar (1992): Accuracy of implant interface preparation: Hand-held broach vs robot machine tool. Proc. Orthop. Res. Soc. Washington D. C. PP: 374

Barrack RL, Mulroy Jr RD and Harris WH (1992): Improved cementing techniques and femoral component loosening in youg patients with Hip arthroplasty: A 12-year radiographic review. J Bone Joint Surg. 74-B: 385-389

Barton JR (1827): On the treatment of ankylosis by the formation of artificial joints, North Am. Med. Surg. J. 3:279-292.

Bauer JA, Conzen P, Wurster K (1988): The effect of BW 755C on wound healing in a scald burn injury pig model - Morphological and biochemical findings. In: Paubert-Braquet M editor: Lipid mediators in the immunology of shock. Plenum press, New York, London, P519

Bauer TW, Geesink RT, Zimmerman R and McMahon JT (1991): Hydroxyapatite-coated femoral stems: Histological analysis of components retrieved at autopsy. J Bone Joint Surg. 73-A: 1439-1452

Beckenbaugh RD and Ilstrup DM (1978): Total hip arthroplasty. A review of three hundred and thirty-three cases with long follow-up. J. Bone Joint Surg. 60A:306

Bergmann G, Graichen F and Rohlmann A (1993): Hip joint loading during walking and running, measured in two patients. J Biomechanics 26: 969-990

Berme N, and Paul JP (1979): Load actions transmitted by implants. J. Biomed. Eng., 1: 268-72

Bloebaum RD, Merrell M, Gustke K and Simmons M (1991): Retrieval analysis of a hydroxyapatite-coated hip prosthesis. Clin Orthop, 267:97-102

Bobyn JD, Pilliar RM, Cameron HU and Weatherly GC (1980): The optimum pore size for the fixation of porous-surfaced metal implants by the ingrowth of bone. Clin. Orthop. 150:263-270

Bobyn JD, Pilliar RM, Cameron HU and Weatherly GC (1981): Osteogenic phenomena across endosteal bone-implant spaces with porous surfaced intramedullary implants. Acta Orthop. Scandinavica, 52: 145-153

Bohr H, Schaadt O (1985): Bone mineral content of the femoral neck and shaft: relation between cortical and trabecular bone. Calcif Tissue Int 37: 340-344

Bombelli R, Gerundini M, Aronson J (1984): Early results of the EM isoelastic cementless total hip prosthesis: 300 consecutive cases with 2-year follow-up. Hip 33, 1984

Bosco JA, Lachiewicz PF and DeMasi R (1993): Survivorship analysis of cemented high modulus total hip arthroplasty. Clin Orthop. 294: 131-139

Brackett EG (1925): Fractured neck of the femur-operation of transplantation of the femoral head to trochanter, Boston Med. Surg. J. 192:1118-1120

Brekelmans WAM, Poort HN and Slooff TJJH (1992): A new method to analyse the mechanical behaviour of skeletal parts. Acta Orthop. Scand. 43:301-317

Brown JW and Ring PA (1985): Osteolytic changes in the upper femoral shaft following porous-coated hip replacement. J Bone Joint Surg. 67B:218

Buchert PK, Vaughan BK, Mallory TH, Engh CA and Bobyn JB (1986): Excessive metal release due to loosening and fretting of sintered particles on porous-coated hip prostheses. J. Bone Joint Surg. 68A: 606

Burke DW, Gates EI and Harris WH (1984): Centrifugation as a method of improving tensile and fatigue properties of acrylic bone cement. J Bone and Joint Surg, 66A: 1265-1273

Burke DW, O'Connor D, Zalenski EB, Jasty M and Harris WH (1991): Micromotion of cemented and uncemented femoral components. J Bone Joint Surg [Br], 73B:33-7

Callaghan JJ, Salvati EA, Pellicci PM, Wilson PD Jr and Ranawat CS (1985): Results of revision for mechanical failure after cemented total hip replacement. 1979-1982. A two to five-year follow-up. J Bone Joint Surg 67A-1074-1085

Cameron HU, Pilliar RM and Macnab I (1973): The effect of movement on the bonding of porous metal to bone. J Biomed Mater Res 7:301-311

Cameron HU, Pilliar RM and Macnab I (1976): The rate of bone ingrowth into porous metal. J. Biomed. Mater. Res. 10:295-302

Capello WN (1989): Fit the patients to the prosthesis. Clin Orthop 249:56

Carlsson AS, Gentz CF, and Lindberg HO (1979): Thirty-two non-infected total hip arthroplasties. J Bone Joint Surg. 61B: 419

Carnochan JM (1860): Archives of Medicine 284. Cited in Thompson FR: An essay on the development of arthroplasty of the hip. Clin. Orthop. 44:79-82, 1966

Carter DR, Caler WE and Harris WH (1981): Resultant loads and elastic modulus calibration of long bone cross sections. J. Biomech. 14:739-745

Carter DR, Hayes WC (1977): The compressive behavior of bone as a two phase porous structure. J Bone and Joint Surg., 59A(7): 954-962

Carter DR, Schwab GH, and Spengler DM (1980): Tensile fracture of cancellous bone. Acta. orthop. scand. 51:733-741

Chandler DR, Tarr RR, Gruen TA and Sarmiento A (1984): Radiographic assessment of acetabular cup orientation: a new design concept. Clin Orthop 186:60

Chandler HP, Reineck FT, Wixson RL and McCarthy JC (1981): Total hip replacement in patients younger than thirty years old: A five year follow up study. J. Bone and Joint Surg. 63-A: 1426-1434

Charnley J (1953): Compression arthrodesis, including central dislocation as a principle in hip surgery, Edinburgh and London, E&S Livingstone, 242-255

Charnley J (1960): Anchorage of the femoral head prosthesis to the shaft of the femur. J. Bone Joint Surg 42B:28

Charnley J (1967): Factors in the design of an artificial hip joint. Proc Inst Mech Eng 181:104-111

Charnley J (1975): Fracture of femoral prostheses in total hip replacement. A clinical study. Clin. Orthop. 111: 105

Charnley J and Longfield K A (1968): The optimum size of prosthetic heads in relation to the wear of plastic sockets in total hip replacement of the hip. Internal publication No. 15. Wrightinton hospital, Wigan, England, Centre for hip surgery

Charnley J (1970): Total hip replacement by low-friction arthroplasty. Clin Orthop Rel Res 72:7

Charnley J (1975): Fracture of femoral prostheses in total hip replacement. A clinical study. Clin. Orthop. 111:105

Charnley J (1982): Evolution of total hip replacement. Faltin lecture. Ann Chir Gynaecol 71:103

Clark JM, Freeman MAR and Witham D (1987): The relationship of neck orientation to the shape of the proximal femur. J Arthroplasty 2:99

Collier JP, Mayor MB, Chal JC, et al (1988): Macroscopic and microscopic evidence of prosthetic fixation with porous coated materials. Clin Orthop 235:173

Collier JP, Surprenant VA, Jensen R, Mayor MB and Surprenant HP (1992): Corrosion between the components of modular femoral hip prostheses. J Bone Joint Surg [Br] 74b: 511-7

Collis DK (1977): Femoral stem fracture in total hip replacement. J. Bone Joint Surg. 59A:1033

Collis DK (1991): Long-term (twelve to eighteen-year) follow up of cemented total hip replacements in patients who were less than fifty years old: a follow-up note. J Bone Joint Surg. 73-A: 593-597

Cook SD, Thomas KA and Haddad RJ (1988a): Histologic analysis of retrieved human porous coated total joint components. Clin. Orthop. 234:90-101

Cook SD, Thomas KA, Kay JR, Jarcho M (1988b): Hydroxyapatite-coated titanium for orthopaedic implant applications. Clin Orthop. 232:225-43

Cornell CN, Ranawat CS (1986): Survivorship analysis of total hip replacements: results in a series of active patients who were less than 55 years old. J Bone Joint Surg 68-A: 1430-1434

Coventry MB (1976): Total hip arthroplasty in the adult with complete congenital dislocation. Proc Sci Meet Hip Soc 4:77

Crowninshield RD and Brand RA (1981): A physiologically based criterion of muscle force prediction in locomotion. J. Biomech. 14:793-801

Crowninshield RD and Brand RA (1981): The prediction of forces in joint structures: Distribution of intersegmental resultants. Exer. and Sport Sci. Rev., 9: 159-81

Crowninshield RD, Brand RA, Johnston RC and Milroy JC (1980): An analysis of femoral component stem design in total hip arthroplasty. J Bone Joint Surg. 62A: 68-78

Dai KR, An KN and Hein T, et al (1985): Geometric and biomechanical analysis of the femur. Trans Orthop Res Soc 10:99

Davey JR and Harris WH (1988): Loosening of cobalt chrome beads from a porous-coated acetabular component. A report of ten cases. Clin. Orthop. 231:97

Davies JP, Burke DW, O'Connor DO and Harris WH (1987): Comparison of the fatigue characteristics of centrifuged and uncentrifuged simplex P bone cement. J. Orthop. Res. 5: 366-371

Davy DT, Kotzar GM, Brown RH, Heiple KG, Goldberg VM, Heiple Jr KG, Berilla J and Burstein AH (1988): Telemetric force measurements across the hip after total arthroplasty. J Bone Joint Surg. 70A: 45-50

de Groot K (1980): Bioceramics consisting of calcium phosphate salts Biomaterials 1:47-50

de Groot K, de Putter C, Sillevis Smitt PAE and Driessen AA (1981): Mechanical failure of artificial teeth made of dense calciumhydroxylapatite. Science of Ceramics 11:433-7

de Groot K, Geesink R, Klein CPAT and Seekian P (1987): Plasma sprayed coatings of hydroxyapatite. J. Biomed. Mater. Res., 21: 1375-1381

Denissen HW, de Groot K, Makkes PCh, van den Hooff and Klopper PJ (1980): Tissue response to dense apatite implants in rats. J Biomed Mat Res 5:713-21

Delbet P (1919): Resultat eloigne d'un vissage pour fracture transcervicale du femur, Bull. Mem. Soc Chir. Paris 45:434

Diegel PD (1989): Initial effect of collarless stem stiffness on femoral bone strain. J Arthroplasty 4(2):173-178

DiNovo JA (1985): A photoelastic coating technique for studying surface stress in bone plates. J. Clin. Engng., 10(2):149-156

Dorr LD (1986): Total hip replacement using APR system. Tech Orthop 1(3):22

Dorr LD, Takei GK and Conaty JP (1983): Total hip arthroplasties in patients less than forty-five years old. J. Bone and Joint Surg. 65-A: 474-479

Dorre E (1989): Hydroxyapatitkeramik-beschichtungen fur verankerungsteile von huftgelenkprothesen (technische aspekte). Biomed. Technik. 34:46-52

Ducheyne P, Hench LL, Kagan A et al (1980): Effect of hydroxyapatite impregnation on skeletal bonding of porous coated implants. J. Biomed. Mater. Res. 14:225-37

Dumbleton JH (1981): Tribology of natural and artificial joints. Amsterdam, Elsevier, PP 325-380

Dunn WL, Wahner WH, Riggs BL (1980): Measurement of bone mineral content in human vertebrae and hip by dual photon absorptiometry. Radiology 136: 485-487

Engelbrecht E and Heinert K (1987): Klassifikation und behandlungsrichtlinien von knochensubstanzverlusten bei revisionsoperationen am huftgelenk - mittelfristige ergebnisse. Primare

und revisionsalloarthroplastik Hrsg - Endo - Klinik, Hamburg.Berlin, etc: Springer-Verlag, pp: 189-201

Engelhardt JA, Saha S (1988): Effect of femoral component section modulus on the stress distribution in the proximal human femur. Med. & Biol. Eng. & Comput. 26:38-45

Engh CA, Bobyn JD (1985): Biological fixation in total hip arthroplasty. Thorofare, New Jersey Slack, pp: 7-8

Engh CA, Bobyn JD (1988): Results of porous coated hip replacement using the AML prosthesis. In Fitzgarald R (Ed): Non-cemented total hip arthroplasty. New Yourk, Reven Press. PP: 393-406

Engh CA, Bobyn JD, Glassman AH (1987): Porous-coated hip replacement. The factors governing bone ingrowth, stress shielding, and clinical results. J Bone Joint Surg 69-B: 45

Engh CA, Massin P and Suthers KE (1990): Roentgenographic assessment of the biologic fixation of porous-surfaced femoral components. Clin Orthop 257: 107-128

English TA and Kilvington M (1979): In vivo records of hip loads using a femoral implant with telemetric output (a preliminary report). J. Biomed. Eng.,1: 111-115

Euler E, Bauer J, Jonck LM and Kreusser Th (1989): Thermotoxicity of palacos cement. Unfallchirurg 92:606-610

Fabry G, MacEwen GD and Shands AR (1973): Torsional of the femur: A follow-up study in normal and abnormal conditions. J Bone Joint Surg 55A: 1726

Finlay JB, Bourne RB and McLean J (1982): A technique for the in vitro measurement of principal strains in human tibia. J. Biomech., 15:723-739

Finlay JB, Rorabeck CH, Bourne RB, and Tew WM (1989): In vitro analysis of proximal femoral strains using PCA femoral implants and a hip-abductor muscle simulator. J. Arthroplasty, 4: 335-45

Frankel, VH and Burstein AH (1970): Elasticity, in Orthopaedic biomechanics . The applications of engineering to the musculoskeletal system. Lea & Febiger, Pholadelphia, PA, pp. 40-76

Franks E, Mont MA, Maar DC, Jones LC and Hungerford DS (1992): Thigh pain as related to bending rigidity of the femoral prosthesis and bone. Proc Orthop Res Soc, Washington DC. PP: 296

Freeman MAR (1986): Why resect the neck? J Bone Joint Surg. 68-B: 346-349

Freeman MAR, Plante-Bordeneuve P (1994): Early migration and late aseptic failure of proximal femoral prostheses. J Bone Joint Surg. 76-B: 432-438

Fredin HO, Unander-Scharin LE (1980): Total hip replacement in congenital dislocation of the hip. Acta Orthop. Scand. 51: 799-802

Furlong RJ, Osborn JF (1991): Fixation of hip prostheses by hydroxyapatite ceramic coatings. J Bone Joint Surg 73-B:741-5

Fyhrie DP (1988): Effects of ingrowth, geometry, and material on stress transfer under porous-coated hip surface replacement. J Orthop Res 6(3):425-433

Geesink RT, de Groot K and Klein CPAT (1987): Chemical implant fixation using hydroxyapatite coatings. The development of a human total hip prosthesis for chemical fixation to bone using hydroxyapatite coatings on titanium substrates. Clin. Orthop. 225: 147-170

Geesink RT, de Groot K and Klein CPAT (1988): Bonding of bone to apatite-coating implants. J Bone Joint Surg. 70-B:17-22

Gilbert JL, Bloomfield RS, Lautenschlager EP and Wixson RL (1992): A computer-based biomechanical analysis of the three-dimensional motion of cementless hip prostheses. J Biomechanics, 25: 329-340

Girdlestone GR (1928) : Arthrodesis and other operations for tuberculosis of the hip. In Girdlestone GR, editor: The robert jones birthday volume, cambridge, Mass., Oxford University Press.

Gluck T (1891): Referat uber die durch das moderne chirurgische experiment gewonnenen positiven resultate, betreffend die naht und den ersatz. von defecten hoherer gewebe, sowie uber die verwerthung resorbirbbarer und lebendiger tampons in der chirurgie, Arch. Klin. Chir. (Berl.) 41:187-239

Gold BL and Walker PS (1974): Variables affecting the friction and wear of metal on plastic total hip joints. Clin Orthop 100: 270

Goldstein SA (1987): The mechanical properties of trabecular bone: Dependency on anatomical location and function. J Biomech. 20: 1055-1061

Goodman S, Rubenstein J, Schatzker J et al (1987): Apparent changes in the alignment of the femoral component in hip arthroplasties associated with limb positioning. Clin Orthop 221:242

Greenwald AS, Haynes DW (1972): Weight-bearing areas in the human hip joint. J Bone Joint Surg. 54-B: 157-163

Grindlay JH and Waugh JM (1951): Plastic spinge which acts as a framework for living tissue. Experimental studies and preliminary report of use to reinforce abdominal aneurysms. Arch. Surg., 63: 288-297

Grove EWH (1927): Some contributions to the reconstructive surgery of the hip. Br. J. Surg. 14:486-517, 1927

Gruen TA, McNeice GM and Amstutz HC (1979): "Modes of failure" of cemented stem-type femoral components. Clin Orthop 141:17-27

Haboush EJ: A new operation for arthroplasty of the hip based on biomechanics, photoelasticity, fast-setting dental acrylic, and other considerations. Bull Hosp Jt Dis 14:242

Halawa M, Lee AJC, Ling RSM and Vangala SS (1978): The shear strength of trabecular bone from the femur and some factors affecting the shear strength of the cement-bone interface. Arch. Orthop. Traum. Surg. 92: 19-20

Hardinge K, Porter ML, Jones PR, Hukins DWL and Taylor CJ (1991): Measurement of hip prostheses using image analysis: The maxima hip technique. J Bone Joint Surg (Br) 73-B:724-728

Hardt DE (1978): Determining muscle forces in the leg during normal human walking — An application and evaluation of optimization methods J. Biomech. Eng., 100: 72-78

Hardy DC, Frayssinet P, Guilhem A, Lafortaine MA and Delince PE (1991): Bonding of hydroxyapatite-coated femoral prostheses J Bone Joint Surg 73-B:732-40

Harley JM, Wilkinson JA (1987): Hip replacement for adults with unreduced congenital dislocation. J Bone Joint Surg. 69-B: 752-755

Harper MC, Carson WL (1987): Curvature of the femur and the proximal entry point of an intramedullary rod. Clin Orthop 220:155

Harris WH (1986): Etiology of osteoarthritis of the hip. Clin Orthop 213:20-33

Harris WH, McCarthy JC, O'Neill OA (1982): Femoral component loosening using contemporary techniques of femoral cement fixation. J Bone Joint Surg 64A: 1063

Harris WH, Mulroy RD, Maloney WJ, Burke DW, Chandler HP and Zalenski EB (1991): Intraoperative measurement of rotational stability of femoral components of total hip arthroplasty. Clin Orthop 266: 119-26

Heekin RD, Callaghan JC, Hopkinson W, Savory CG and Xenos JS (1993): The porous-coated anatomic total hip prosthesis, inserted without cement: Results after five to seven years in a prospective study. J Bone Joint Surg., 75A: 77-91

Heimke G (1981): The effects of mechanical factors on biocompatibility tests. J Biomed Engng 3:209

Herman JH, Sowder WG, Anderson D, Appel AM and Hopson CN (1989): Polymethylmethacrylate-induced release of bone-resorbing factors, J Bone Joint Surg 71A:1530-1541

Hille E (1988): Experimental stress-induced changes in growing long bones. Int Orthop 12(4):309-315

Holtgrewe JL and Hungerford DS (1989): Primary and revision total hip replacement without cement and with associated femoral osteotomy. J Bone Joint Surg 71-A: 1487-1495

Hoogendoorn HA, Renooij W, Akkermans LMA, Visser W and Wittebol P (1984): Long-term study of large ceramic implants (porous hydroxyapatite) in dog femora. Clin Orthop 187:281-8

Hozack WJ, Rothman RH, Booth RE and Balderston RA (1993): Cemented versus cementless total hip arthroplasty: A comparative study of equivalent patient populations. Clin. Orthop. 289:161-165

Hua, J.; Iguchi, H.; and Walker, P. S.: Comparison of fit and fill between custom stems and standard stems. Procs of the ISSCP. San Francisco, PP. 65, 1991

Huiskes R (1989): Adaptive bone remodelling and biomechanical design considerations for non-cemented total hip arthroplasty. Clin Orthop. 12:1255

Hunter G, Welsh R, Camepan HV and Bailey W (1979): The results of revision total hip arthroplasty. J Bone Joint Surg. 61B:419

Izquierdo RJ and Northmore-Ball MD (1994): Long-term results of revision hip arthroplasty. J Bone Joint Surg 76-B: 34-39

Jarcho M (1981): Calcium phosphate ceramics as hard tissue prosthetics. Clin Orthop 157:259-78

Jasty M, Jensen JF, Burke DW, Harrigan TP and Harris WH (1985): Porosity measurement in commercial bone cement preparation and the effect of centrifugation of porosity reduction. Trans. Orthop. Res. Soc., 10: 239

Jasty M, Maloney WJ, Bragdon CR, O'Connor DO, Haire T and Harris WH (1991): The initiation of failure in cemented femoral components of hip arthroplasties. J Bone Joint Surg 73-B: 551-558

Jasty M, Rubash HE, Paiement GD, Bragdon CR, Parr J and Harris WH (1992): Porous-coated uncemented components in experimental total hip arthroplasty in dogs: Effect of plasma-sprayed calcium phosphate coatings on bone ingrowth. Clin. Orthop. 280:300-309

Jayson M.(1971), Editor: Total hip replacement, Philadelphia, J. B. Lippincott Co, P11.

Jones LC and Hungerford DS (1991): Cement disease. Clin. Orthop. 225: 192-206

Jones R, editor: Orthopaedic surgery of injuries, London, 1921, Frowde, 2 Vols.

Jones PR, Taylor CJ and Hukins DWL (1988): Prosthetic hip failure: preliminary findings of retrospective radiograph image analysis. MEP Ltd 17:119-125

Judet J and Judet R (1950): The use of an artificial femoral head for arthroplasty of the hip joint. J. Bone Joint Surg. 32B:166-173

Kaplan SJ, Hayes WC, Stone JL and Beaupre GS (1985): Tensile strength of bovine trabecular bone. J Biomech. 18: 723-727

Kavanagh BF, Dewitz MA, Ilstrup DM, Stauffer RN and Coventry MB (1989): Charnley total hip arthroplasty with cement: fifteen year results. J. Bone and Joint Surg. 71-A 1496-1503

Kavanagh BF, Ilstrup DM and Fitzgerald RH Jr (1985): Revision total hip arthroplasty. J Bone Joint Surg 67A: 517-526

Kelly TL, Slovik DM, Schoenfeld DA, Neer RM (1988): Quantitative digital radiography versus dual photon absorptiometry of the lumbar spine. J Clin Endocrin Metab 67:839-844

Kelman DC, Takeuchi MJ and Smith TS (1991): Effect of metallic plasma sprayed coatings on high cycle fatigue. Trans. Soc. Biomater., 14: 290

Kester MA, Manley MT, Taylor SK and Cohen RC (1991): Influence of thickness on the mechanical properties and bond strength of HA coatings applied to orthopaedic implants. Trans. Orthop. Res. Soc., 16:95

Keyak JH, Fourkas MG, Meagher JM and Skinner HB (1993): Validation of an automated method of three-dimensional finite element modelling of bone. J Biomed. Eng. 15: 505-509

Kilgus DJ, Shimaoka EE, Tipton JS and Eberle RW (1993): Dual-energy X-ray absorptiometry measurement of bone mineral density around porous-coated cementless femoral implants: Methods and preliminary results. J Bone Joint Surg. 75-B: 279-287

Kingsley PC, Olmsted KL (1948): A study to determine the angle of anteversion of the neck of the femur. J Bone Joint Surg 30A: 745

Kiratli BJ, Heiner JP, McBeath AA and Wilson MA (1992): Determination of bone mineral density by dual X-ray absorptiometry in patients with uncemented total hip arthroplasty. J Orthop Res 10:836-844

Kirkpatrick JS, Clarke IC, Amstutz HC and Jinnah RH (1983): Radiographic techniques for consistent visualization of total hip arthroplasties. Clin Orthop 174:158-163

Klawitter JJ and Hulbert SF (1971): Application of porous ceramics for the attachment of load bearing internal orthopaedic applications J Biomed. Mater. Res. Sympos. 2(1): 161-229

Klein CP, Driessen AA and de Groot K (1984): relationship between degradation behaviour of calcium phosphate ceramics and their physical

chemical characteristics and ultrastructural geometry. Biomaterials 5:157-60

Knessl J, Gschwend N, Scheier H and Munzinger U (1989): Comparative study of cemented and cementless hip prostheses in the same patient. Arch Orthop Trauma Surg. 108: 276-278

Kotzar, G. M.; Davy, D. T.; Goldberg, V. M.; Heiple, K. G.; Berilla, J.; Heiple, Jr K. G.; Brown, R. H.; and Burstein, A. H.: Telemeterized in vivo hip joint force data: A report on two patients after total hip surgery. J Orthop. Res., 9: 621-33, 1991

Krushell RJ, Burke DW and Harris WH (1991): Range of motion in contemporary total hip arthroplasty. J Arthroplasty Vol. 6 No. 2: 97-101

Last RJ (1959): Anatomy, Regional and applied, 2nd ed. Boston, Little, Brown & Co.

Lazansky MG (1974): Low-friction arthroplasty for the sequelae of congenital and developmental hip disease. In: Total hip replacement in young patients. AAOS: Instructional course lectures 23:194-200

Letournel E (1986): Failures of biologically fixed devices: Causes and treatment. In Brand, RA (ed): The Hip: Proceedings of the Fourteenth Open Scientific Meeting of The Hip Society. St. Louis, C. V. Mosby, P318

Lexer E (1908): Uber Gelenktransplantation. Med Klin. Berlin 4:817-820

Linde F and Hvid I (1987): Stiffness behavior of trabecular bone specimens. J Biomech. 20: 83-89

Little EG (1990): Three dimensional strain rosettes from an analysis of the Geomedic Knee prosthesis and underlying cement fixation, in Appplied Stress Analysis. Eds: T.E. Hyde and E. Ollerton, Elsevier, Barking.

Little EG, Tocher D and O'Donnell P (1990): Strain gauge reinforcement of plastics. Strain, 26(3): 91-98

Livermore J, Ilstrup D and Morrey B (1990): Effect of femoral head size on wear of the polyethylene acetabular component. J Bone Joint Surg. 72-A: 518-528

Lord G and Bancel P (1983): The madreporic cementless total hip arthroplassty. New experimental data and a seven year clinical follow-up study. Clin Orthop 176: 67-76

Loudon JR and Older MW (1989): Subsidence of the femoral component related to long-term outcome of hip replacement. J Bone Joint Surg. 71-B: 624-628

Lucas LC, Lemons JE, Lee J and Dale P (1987): In vitro corrosion of porous alloys. In Quantitative characterization and performance of porous implants for hard tissue applications. Ed: Lemons JE, PP: 124-136

Malcolm AJ (1991): The bone-cement interface in long-standing prosthetic implants. in: Limb salvage — Major reconstructions in oncologic and nontumoral conditions. Eds: F. Langlais, B. Tomeno. Springer-Verlag Berlin Heidelberg.

Maloney WJ, Jasty M, Burke DW, O'Connor DO, Zalenski EB, Bragdon C and Harris WH (1989): Biomechanical and histological investigation of cemented total hip arthroplasties. Clin. Orthop 249:129

Maloney WJ, Davey JR and Harris WH (1992): Bead loosening from a porous-coated acetabular component: A follow-up note. Clin. Orthop. 176: 112-114

Markolf KL and Amstutz HC (1976): A comparative experimental study of stresses in femoral total hip replacement components: the effects of prostheses orientation and acrylic fixation. J. Biomech 9:73

Martin RB, Pickett JC, Zinaich S (1980): Studies of skeletal remodelling in aging men. Clin Orthop Rel Res 149:268-282

McCarthy CK, Steinberg GG, Agren M, Leahey D, Wyman E and Baran DT (1991): Quantifying bone loss from the proximal femur after total hip arthroplasty. J Bone Joint Surg. 73-B: 744-748

McElhaney J; Fogle J; Byars E and Weaver G (1964): Effect of embalming on the mechanical properties of beef bone. J. Appl. Physiol., 19: 1234-6.

McKee GK (1951): Artificial hip joint. J. Bone Joint Surg. 33B: 465

McKee GK and Watson-Farrar J (1966): Replacement of arthritic hips by the McKee-Farrar prosthesis. J. Bone Joint Surg. 48B: 245-259

McKellop H; Ebramzadeh E; Niederer PG and Sarmiento A (1991): Comparison of the stability of press-fit hip prosthesis femoral stems using a synthetic model femur. J. Orthop. Res., 9: 297-305.

Melvin JW, McElhaney JH and Roberts VL (1970): Development of a mechanical model of the human head. Determination of tissue properties and synthetic substitute materials. Soc. Automotive Engineers Trans. 79: 700-703

Mesnager M (1930): Sur la determination optique des tensions interieures dans les solides a trois dimensions. Comptes Reendus, Paris, 190:1249

Moore AT (1952): Metal hip joint-new self-locking Vitallium prosthesis, South. Med. J. 45:1015-1019

Moore AT (1957): The self-locking metal hip prosthesis. J. Bone Joint Surg. 39A:811-827

Moore AT and Bohlman HR (1943): Metal hip joint-a case report. J. Bone Joint Surg. 25:688-692

Morscher EW and Dick W (1983): Cementless fixation of "isoelastic" hip endoprosthesis manufactured from plastic materials. Clin Orthop 176:77

Muller ME (1957): Die Hufnahen femurosteotomien, Stuttgart, Georg Thieme Verlag

Mulroy Jr RD, Seklacek RC, O'Connor DO, Estok DM and Harris WH (1991): Technique to detect migration of femoral components of total hip arthroplasties on conventional radiographs. J Arthroplasty 6:S1-S4

Mulroy Jr RD and Harris WH (1990): The effect of improved cementing techniques on component loosening in total hip replacement: An 11-year radiographic review. J Bone Joint Surg. 72-B: 757-760

Murphy JB (1905): Ankylosis: arthroplasty-clinical and experimental, J. A. M. A. 44: 1573-1582; 1671-1678, 1749-1766.

Murphy SB, Walker PS and Schiller AL (1984): Adaptive changes in the femur after implantation of an Austin-Moore prosthesis. J Bone Joint Surg 66A:437

Neil JL, Demas TC, Stone JL and Hayes WC (1983): Tensile and compression properties of vertebral trabecular bone. Transactions of the Orthopaedic Research Society, PP:344

Noble PC, Alexander JW, Lindahl LJ, et al (1988): The anatomic basis of femoral component design. Clin Orthop 235:148

Nunn D, Freeman MAR, Tanner KE and Bonfield W (1989): Torsional stability of the femoral component of hip arthroplasty. J Bone Joint Surg. [Br] 71B: 452-5

Oh I, Bourne RB and Harris WH (1983): The femoral cement compacter: an improvement in cementing technique in total hip replacement. J Bone Joint Surg 65A: 1335

Oh I and Harris WH (1978): Proximal strain distribution in the loaded femur: An in vivo comparison of the distribution in the intact femur and after insertion of different hip replacement femoral components. J Bone Joint Surg 60A:75

Ollier LXEL: Traite des resection et des operations conservatrices qu'on peut practiquer sur le systeme osseus, Paris, 1885, Masson et cie, Editeurs.

Oonishi, H.; Yamamoto, M.; Ishimaru, H.; Tsuji, E.; Kushitani, S.; Aono, M.; and Ukon, Y.: The effect of hydroxyapatite coating on bone growth into porous titanium alloy implants. J Bone Joint Surg [Br], 71-B: 213-6, 1989

Oppel G (1937): Das polarisationsoptische schichtverfaren zur messung der oberflachenspannungen am beanspruchten bauteil ohne model. Zeitschrift des vereines deutscher ingenieure, 81:638

Pacifici R, Rupich R, Griffin M et al (1990): Dual energy radiography versus quantitative computer tomography for the diagnosis of osteoporosis. J Clin Endocrinol Metab 70:705-10

Parfitt AM (1990): The compling of bone formation to bone resorption: a critical analysis of concept and of its relevance to the pathogensis of osteoporosis. Metabolic Bone Disease, 4:1-6

Paterson M, Fulford P and Denham R (1986): Loosening of the femoral component after total hip replacement: the thin black line and the sinking hip. J. Bone and Joint Surg. 68-B: 392-397

Paul JP (1965): Bio-engineering studies of the forces transmitted by joints. (II) Engineering analysis. In Biomechanics and related bio-engineering topics Edited by R. M. Kenedi. Oxford, Pergamon Press PP: 369-380

Paul JP (1976): Approaches to design. Force actions transmitted by joints in the human body. Proc. Roy. Soc. London, B, 192: 163-172

Paul JP and McGrouther DA (1975): Forces transmitted at the hip and knee joint of normal and disabled persons during a range of activities. Acta Orthop. Belgica, 41(supplement 1): 78-88

Pauwels F (1935): Der schenkelhalsbruch ein mechanisches problem. Ferdinand Enke Verlage, Stuttgart

Pauewls F (1965): The importance of biomechanics in orthopaedics. Ninth congress of the society internationale de chirurgie orthopaedique et de traumatologies, Wien, Wiener medizinischen akademie, Wien.

Payr E (1910): Blutige mobilisierung versteifter Gelenke, Zentrabl. Chir. 37:1227

Perry CC (1984): The electric resistance strain gauge revisited. Exptl. Mech., 24(4): 286-299

Phillips TW, Messieh SS and McDonald PD (1990): Femoral stem fixation in hip replacement. A biomechanical comparison of cementless and cemented prostheses. J. Bone Joint Surg. 72B:431-4

Phillips TW, Nguyen LT and Munro SD (1991): Loosening of cementless femoral stems. A biomechanical analysis of immediate fixation with loading vertical; femur horizontal. J. Biomechanics, 24: 37-48

Pierson JL and Harris W (1994): Cemented revision for femoral osteolysis in cemented arthroplasties. J Bone Joint Surg. 76-B: 40-44

Pilliar RM (1983): Powder metal-made orthopaedic implants with porous surface for fixation by tissue ingrowth. Clin. Orthop. 176:42-51

Pople J (1980): DIY strain gauge transducers. Strain, 16(1): 23-36

Reickeras O, Bjerkreim I, Kolberstevedt A (1983): Anteversion of the acetabulum and femoral neck in normals and in patients with osteoarthritis of the hip. Acta Orthop Scand 54:18

Reilly DT, Burstein AH and Frankel VH (1974): The elastic modulus for bone. J. Biomechanics 7:271-275

Ring PA (1968): Complete replacement arthroplasty of the hip by the Ring prothesis, J. Bone Joint Surg. 50B:720-731

Ring PA (1988): Long term results of uncemented hip replacement. In: Recent developments in orthopaedic surgery. Editors J.Noble, CSB Galasko, Manchester University Press. PP: 214-221

Robertson DM, St Pierre L and Chahal R (1976): Preliminary observations of bone ingrowth into porous materials. J Biomed. Mater. Res. 10:335-344

Rothman, R. H.; Cohn, J. C.: Cemented versus cementless total hip arthroplasty. Clin. Orthop., 254: 153-69, 1990

Rubin PJ, Leyvraz PF and Aubaniac JM, Argenson JN, Esteve P and DERoguin B (1992): The Morphology of the proximal femur: A three-dimensional radiographic analysis. J Bone Joint Surg [Br] 74-B: 28-32

Ruff CB, Hayes WC (1988): Sex differences in age-related remodelling of the femur and tibia. J Orthop Res 6:886-896

Rydell NW (1966): Forces acting on the femoral head-prosthesis. A study on strain gauge supplied prostheses in living persons. Acta Orthop. Scand, Supple 88

Saejong S, Hirano S, Granholm JW and Walker PS (1987): The influence of the interface on bone strains and stem-bone micromotion in press-fit total hip stems. Orthop. Trans. 12:484

Saha S and Gorman PH (1981): Strength of human cancellous bone in shear and its relationship to bone mineral content. Trans. Orthop. Res. Soc. PP:217

Sartoris DJ and Resnick D (1990): Current and innovative methods for noninvasive bone densitometry. Radiol Clin N Am 28: 257-279

Schimmel JW (1988): Primary fit of the lord cementless total hip: A geometric study in cadavers. Acta Orthop Scand 59(6):638-642

Schneider, E.; Eulenberger, J.; Steiner, W.; Wyder, D.; Friedman, R. J.; and Perren, S. M.: Experimental method for the in vitro testing of the initial stability of cementless hip prostheses. J. Biomechanics, 22: 735-44, 1989

Schneider E, Kinast C, Eulenberger J, Wyder D, Eskilsson G and Perren SM (1989): A comparative study of the initial stability of cementless hip prostheses. Clin Orthop 248:200-209

Schurman DJ, Bloch DA, Segal MR and Tanner CM (1989): Conventional cemented total hip arthroplasty: Assessment of clinical factors associated with revision for mechanical failure. Clin Orthop 240:173-180

Selvik G (1989): Roentgen stereophotogrammetry. A method for the study of the kinematics of the skeletal system. Thesis, Lund University 1974. Acta Orthop Scand, suppl no 232.

Simmons Jr ED, Prizker KPH and Grynpas MD (1991): Age-related changes in the human femoral cortex. J Orthop. Res. 9: 155-167

Smith-petersen MN (1917): A new supra-articular subperiosteal approach to the hip joint, Am. J. Orthop. Surg. 15:592-595

Smith-petersen MN (1939): Arthroplasty of the hip—a new method, J. Bone Joint Surg. 21:269-288

Smith RW and Walker RR (1964): Femoral expansion in aging women: implications for osteoporosis and fractures. Science 145:156

Smith-petersen MN (1948): Evolution of mould arthroplasty of the hip joint, J. Bone Joint Surg. 30B: 59-75

Sonoda T (1962): Studies on the strength for compression, tension, and torsion of the human vertebral columns. J Kyoto Pref. Med. Univ. 71:659

Spector M (1987): Historical review of porous coated implants. J Arthroplasty. 2: 163-177

Spector M, Davis RJ, Lunceford EM, Harmon SL (1983): Porous polysulfone coatings for fixation of femoral stems by bony ingrowth. Clin Orthop 176: 34-41

Stone JL, Beaupre G and Hayes WC (1983): Multiaxial strength characteristics of trabecular bone. J Biomechanics 16: 743-752

Struthers AM (1955): An experimental study of polyvinyl sponge as a substitute for bone. Plast. and Reconstr. Surg., 15: 274-287

Stulberg SD (1989): Custom-made primary total hip replacements. Orthopaedics 12-9: 1245-1252

Sugiyama H, Whiteside LA and Kaiser AD (1989): Examination of rotational fixation of the femoral component in total hip arthroplasty. Clin Orthop. 249:122-128

Sumner DR Jr and Galante JO (1990): Bone ingrowth. In: Surgery of the musculoskeletal system. Eds: C. McC. Evarts. Ed. 2: 151-176. New York. Churchill Livingstone

Sumner DR, Turner TM, Urban RM, Galante JO (1988): Long-term femoral remodelling as a function of the presence, type and location of the porous coating in cementless THA. Trans. Orthop Res Soc, 13: 310

Swanson SAV, Freeman MAR and Day WH (1971): The fatigue properties of human cortical bone. Med & biol Engng, 9: 23-32

Thomas KA, Cook SD, Thomas KL and Haddad RJ (1986): Tissue growth into retrieved noncemented human hip and knee components In Biomedical Engineering V, Recent Developments pp 198-203 Edited by S Saha New York, Pergamon Press

Thomas KA, Cook SD, Haddad RJ, Kay JF and Jarcho M (1989): Biologic response to hydroxyapatite-coated titanium hips: A preliminary study in dogs. J. Arthroplasty 4:43-53

Thomas KA, Kay JF, Cook SD, Jarcho M (1987): The effect of surface macrotexture and hydroxyapatite coating on the mechanical strengths and histologic profiles of titanium implant materials. J. Biomed. Mater. Res. 21:1395-414

Thompson FR (1952): Vitallium intramedullary hip prosthesis-preliminary report, N.Y. State J. Med. 52:3011-3020

Thompson DD (1980): Age changes in bone mineralization, cortical thickness, and haversian canal area. Calcif Tiss Int 31:5-11

Turula KB, Friberg O, Lindholm S, Tallroth K and Vankka E (1986): Leg length inequality after total hip arthroplasty. Clin Orthop 202:163-168

Tuttle ME and Brinson HF (1984): Resistance foil strain gauge technology as applied to composite materials. Exptl. Mech., 24:54-65

Vannier MW, Conroy GC, Marsh JL and Knapp RH (1985): Three dimensional cranial surface reconstructions using high resolution computer tomography. Am. J. Phys. Anthropol.

Wahner HW, Dunn WL, Mazess RB, et al (1985): Dual-photon Gd-153 absorptiometry of bone. Radiology 156:203-206

Walker PS, Poss R, Robertson DD, Reilly DT, Ewald FC, Thomas WH and Sledge CB (1990): Design analysis of press-fit hip stems. Orthop Rel Sci., 1: 75-85

Walker PS and Robertson DD (1988): Design and fabrication of cementless hip stems. Clin. Orthop. 235:25-34

Walker PS, Schneeweis D, Murphy S and Nelson P (1987): Strains and micromotions of press-fit femoral stem prostheses. J. Biomechanics 20:693-702

Weber FA and Charnley J (1975): A radiological study of fracture of acrylic cement in relation to the stem of a femoral head prosthesis. J. Bone Joint Surg. 57B:297

Weightman B (1977): Stress analysis, in The scientific basis of joint replacement (eds S. A. V. Swanson and M. A. R. Freeman), Pitman, Tonbridge Wells

Whiteside LA (1989): The effect of stem fit on bone hypertrophy and pain relief in cementless total hip arthroplasty. Clin Orthop., 247:138-47

Whiteside LA, White SE, Engh CA and Head W (1993): Mechanical evaluation of cadaver retrieval specimens of cementless bone-ingrown total hip arthroplasty femoral components. J Arthroplasty 8:147-155

Whitman R (1904): A new treatment for fracture of the neck of the femur, Med. Rec. 65:441-447, 1904

Wiles PW (1958): The surgery of the osteoarthritic hip. Br. J. Surg. 45:488-497

Willert HG and Semlitsch M (1975): Reaction of the articular capsule to plastic and metal wear products from joint endoprostheses. Sulzer Tech Rev 2:1-15

Williams JF and Svensson NL (1968): A force analysis of the hip joint. Bio-Med Eng., 3: 365-70

Williams RP and McQueen DA (1992): A histopathologic study of late aseptic loosening of cemented total hip prostheses. Clin Orthop 275:174-186

Wilson JN and Scale JT (1970): Loosening of total hip replacements with cement fixation. Clinical finding and laboratory studies. Clin Orthop. 72:145

Wiltse LL, Hall RH, Stenehjem JC (1957): Experimental studies regarding the possible use of self-curing acrylic in orthopaedic surgery. J. Bone Joint Surg. 39A: 961

Window AL and Holister GS (eds) (1982): Strain gauge technology, Applied science publishers, Barking.

Winter M, Griss P, de Groot K, et al (1981): Comparative histocompatibility testing of seven calcium phosphate ceramics. Biomaterials 2: 159-60

Wixson RL, Lautenschlager EP and Novak MA (1987): Vacuum mixing of acrylic bone cement. J. Arthroplasty, 2: 141-149

Woolson ST, Dev P, Fellingham LL and Vassiliadis A (1986): Three dimansional imaging of bone from computerized tomography. Clin. Orthop. 202: 239

Wroblewski BM (1979): The mechanism of failure of the femoral prosthesis in total hip replacement. Int Orthop., 3:137-9

Wykman A, Selvik G and Goldie I (1988): Subsidence of the femoral component in the noncemented total hip: A roentgen stereophotogrammetric analysis. Acta Orthop Scand 59(6): 635-637

Zhou XM, Walker PS and Robertson DD (1990): Effect of press-fit stems on strains in the femur -- A photoelastic coating study. J. Arthroplasty. 5:71

PUBLICATIONS

1. J. Hua and P. S. Walker: Differences in femoral strains following custom, anatomic, and symmetrical hip replacements. Proceeding of 37th Annual Meeting, Orthopaedic Research Society, March 4-7, 1991, Anaheim, California

2. J Hua, H. Iguchi and P. S. Walker: Comparison of fit between custom stems and standard stems. Proceeding of 4th Annual International Symposium on Custom Prostheses, San Francisco, 1991

3. H. Iguchi, J. Hua and P. S. walker: Fit-and-Fill prediction in the custom hip prosthesis design. Proceeding of Fourth Annual International Symposium on Custom Prostheses, San Francisco, 1991

4. J. Hua and P. S. Walker: A comparison of cortical strain following cemented and uncemented proximal and distal femoral replacement. Trans. 6th International Symposium on Limb Salvage. Sept. 1991, Montreal, Canada.

5. G.W. Blunn, J. Hua, A. Hunter, M.E. Wait and P.S. Walker: The effect of implant stiffness on the osseointegration of Titanium alloy. In: 9th European Conference of Biomaterials, Chester, U.K., 9-11 September 1991

6. J. Hua, H. Iguchi and P. S. Walker: Accuracy of prediction of 3-D femoral canal shape and custom stem design from plain X-ray. Proceeding of 38th Annual Meeting, Orthopaedic Research Society, February 17-20, 1992, Washington, D.C.

7. J. Hua, G. W. Blunn, M. E. Wait and P. S. Walker: correlation of stress distribution with bony remodelling in retrieved femora with proximal femoral replacements. Proceeding of 38th Annual Meeting, Orthopaedic Research Society, February 17-20, 1992, Washington, D.C.

8. J. Hua and P. S. Walker: Stabilities of standard and custom hip stems under axial and torsional loading.In: Turner-Smith (Ed): Micromovement in Orthopaedics, 1993, PP: 64-76

9. J Hua and P. S. Walker: A comparison of cortical strain following cemented and press-fit proximal and distal femoral replacement. J Orthop Res. 10:739-744, 1992

10. J. Hua and P. S. Walker: A versatile hip design workstation — Scientific rationale. Proceeding of Fifth Annual International Symposium on Custom Prostheses, Windsor, United Kingdom, 1-3 Oct, 1992

11. J. Hua and P. S. Walker: Relative motion of Hip stems under load: An in vitro study of straight, anatomic and custom designs. J Bone Joint Surg. 76-A: 95-103, 1994

12. J. Hua and P. S. Walker: Closeness of fit of noncemented stems improves the strain distribution in the femur. J Orthop. Res., 1994, in press

13. H. Iguchi, J. Hua and P.S. Walker: The accuracy of using radiographs for custom hip stem design. J Arthroplasty, 1994, in press.

14. J. Hua and P.S. Walker: CAD-CAM custom hip stem — The inherent values of accuracy and versatility. Hip International, 1994, in press